16+

ISSN 1028-4427 (Print)
ISSN 2542-131X (Online)

Гений Ортопедии
Orthopaedic Genius

Том 31
№ 6
2025

Научно-теоретический и практический журнал
Основан в память академика Г.А. Илизарова

Курган

Учредитель и издатель журнала:

федеральное государственное бюджетное учреждение «Национальный медицинский исследовательский центр травматологии и ортопедии имени академика Г.А. Илизарова» Министерства здравоохранения Российской Федерации

Издание журнала осуществляется при поддержке Ассоциации по изучению и применению метода Илизарова России (A.S.A.M.I. Россия)

Журнал включен в перечень научных специализированных изданий ВАК, в которых могут публиковаться основные результаты диссертационных работ на соискание ученой степени кандидата наук, ученой степени доктора наук (3.1.8 – травматология и ортопедия)

Журнал включен в Реферативный журнал и Базы данных ВИНИТИ

Сведения о журнале ежегодно публикуются в международной справочной системе по периодическим и продолжающимся изданиям «Ulrich's Periodicals Directory»

Журнал включен в библиографические и реферативные базы данных РИНЦ и SCOPUS

Журнал включен в электронные информационные ресурсы базы данных EBSCO

Электронная версия журнала размещена на сайтах

https://ilizarov-journal.com
https://elibrary.ru
https://cyberleninka.ru

Адрес: 640021, Россия, г. Курган, ул. М. Ульяновой, 6
Телефоны: (3522) 43-06-94 – редакция
(3522) 23-42-60 – реклама
Интернет: https://ilizarov-journal.com/
Email: genius@ilizarov.ru

Оригинал-макет изготовлен ОИАиВР ФГБУ «НМИЦ ТО имени академика Г.А. Илизарова» Минздрава России

Журнал зарегистрирован Федеральной службой по надзору в сфере связи, информационных технологий и массовых коммуникаций ПИ № ФС77-68207 от 30 декабря 2016 года

Территория распространения: Российская Федерация, зарубежные страны

Язык: русский, английский

Издается 6 раз в год

Цена свободная

Original Articles

New technologies

Clinical Cases

Review Article

Оригинальные статьи

Новые технологии

Клинические случаи

Обзорная статья

Original article
https://doi.org/10.18019/1028-4427-2025-31-6-695-706

Comparison of bone transport and acute shortening methods in the treatment of gunshot defects of the tibial diaphysis

D.V. Davydov[1], M.N. Nelin[1]✉, A.A. Artemiev[2], A.A. Kerimov[1], A.A. Maksimov[1], N.I. Nelin[1], P.A. Radaev[1]

[1] Burdenko Main Military Clinical Hospital, Moscow, Russian Federation
[2] National Diagnostic Center, Moscow, Russian Federation

Corresponding author: Maksim N. Nelin, email nelinmaksimdoc@gmail.com

Abstract

Introduction The use of high-precision, high-yield munitions in modern warfare has led to an increase in the number of wounded personnel with extensive defects of the tibial shaft. Effective methods for filling such defects are the methods of G.A. Ilizarov: bifocal or trifocal osteosynthesis with subsequent transport of fragments and (or) bone segments relative to each other (referred to as "bone transport method" in foreign literature), as well as acute, gradual, or combined shortening and subsequent lengthening.

Aim of the study: To compare the efficacy and safety of the bone transport (BT) method and the acute shortening with subsequent lengthening (ASL) method for filling (elimination) of gunshot defects of the tibial shaft.

Materials and methods The study included 60 male patients aged 18 to 59 years with gunshot defects of the tibial shaft ranging from 2 to 16 cm. They were divided into two groups comparable in main characteristics, depending on the treatment method applied. In the first group (30 subjects), the tibial defect was managed using the BT method, in the second group ($n = 30$) the ASL was applied.

Results In all patients of both groups, defects were eliminated, the length of the injured lower leg was restored, and the weight-bearing function of the limb was regained. According to the criteria of consolidation time at the docking site and maturation time of the regenerate, a statistically significant advantage of the ASL method was noted. The total treatment time and the external fixation index were greater in the BT group compared to ASL, but the differences were not statistically significant. The results on the ASAMI anatomical and functional scale were statistically significantly better in the ASL group. Substantial statistically significant differences between the groups were revealed in the number and types of minor and serious complications that developed during treatment. Non-union and invagination were observed only in the BT group. Differences regarding axis deviation of the segment and contracture of adjacent joints were not statistically significant.

Discussion The identified advantages of ASL are due to the absence of drawbacks that are characteristic of BT: prolonged absence of contact between bone fragments, technical difficulties and the long duration of moving a bone segment from one fragment to another and the necessity to achieve union simultaneously in two foci of bone damage (the defect zone and the regenerate zone).

Conclusion In the treatment of patients with gunshot defects of the tibial shaft, the use of BT and ASL methods ensured effectiveness with the possibility of achieving a positive result in up to 100 % of cases. The advantage of the ASL method in terms of safety indicators (type and number of complications) compared to BT was statistically significant.

Keywords: gunshot fracture, tibial diaphyseal defect, osteosynthesis, Ilizarov technique, bone transport, acute shortening

For citation: Davydov DV, Nelin MN, Artemiev AA, Kerimov AA, Maksimov AA, Nelin NI, Radaev PA. Comparison of bone transport and acute shortening methods in the treatment of gunshot defects of the tibial diaphysis. *Genij Ortopedii*. 2025;31(6):695-706. doi: 10.18019/1028-4427-2025-31-6-695-706.

INTRODUCTION

The widespread use of high-precision, high-power ammunition in current military conflicts has significantly increased the severity of limb injuries, complicated treatment, and worsened treatment outcomes [1, 2]. The anatomical features of the tibia pose additional challenges in the treatment of gunshot fractures of the segment. The problem is exacerbated by diaphyseal defects which form due to the impact of damaging factors on the segment, especially in the case of blast injuries [3]. The nature of tissue changes after a gunshot wound and the dynamics of the reparative processes in the wound, as well as the treatment aimed at necrotic tissue removal and at preventing infection progression, result in the formation of a bone defect [4]. Severe soft tissue damage complicates treatment, contributes to the development of complications, and affects the anatomical and functional outcomes [5].

The determining factor in choosing a treatment method for a gunshot fracture is the size of bone and surrounding tissue defects. Tetsworth et al. developed a classification and defined the size of a critical defect (⩾ 20 mm) [6]. Most researchers consider a defect to be critical if bone integrity cannot be restored without a specific surgical intervention.

To fill defects of the tibial shaft, free bone grafting with cancellous grafts [7], Ilizarov non-free bone grafting [8], the Masquelet induced membrane technique [9], free grafting with vascularized tissue complexes based on the fibula or other bones [10] are used, but the final treatment outcome of each of these techniques depends entirely on the condition of soft tissues. Microsurgical technologies assist a lot in repair of soft tissue defects. However, extensive cicatricial degeneration of the paravulnar tissues, typical of gunshot wounds, does not always allow for the creation of the necessary conditions for the application of a microvascular anastomosis and may result in flap necrosis, subsequent enlargement of the defect and pose an issue of amputation [11, 12].

Thus, for the successful treatment of patients with gunshot defects of the tibia, a method is required that is able to create conditions for the simultaneous elimination of bone and soft-tissue defects. The Ilizarov method, which provides dynamic control of the bone tissue regeneration process, offers wide possibilities for the treatment of patients with open and gunshot fractures, as well as their complications and consequences [13, 14]. The most common technique for gunshot fractures of the tibia with bone defects is the Ilizarov non-free bone grafting [15], known in the foreign literature as bone transport (BT). Its negative features include insufficient effectiveness of the impact on soft tissues for the purpose of wound closure and the development of cicatricial changes in the defect area, which hinder the achievement of contact between the transported fragments and slow down consolidation [16].

The Ilizarov techniques of acute, gradual or combined shortening followed by lengthening have not been so frequently used [17, 18], which, unlike BT, are characterized by shortening the limb segment in the area of the bone defect in order to achieve contact between the fragments as fast as possible [19]. The length of the shortened segment is restored by distraction after the signs of union in the area of contact of the fragments appear or after osteotomy of one or two fragments followed by distraction using bi- or polylocal osteosynthesis. A major advantage of acute shortening compared to BT is an early contact between the ends of the fragments with the possibility of simultaneous closure of the wound, which promotes rapid consolidation [20].

The available literature contains a few publications devoted to the use of acute shortening followed by lengthening (ASL) for gunshot fractures and gunshot defects [17]. The overwhelming majority of sources are studies of bone defect management for severe chronic infectious complications. In this regard, it is noted that the extent of possible correction is limited by the condition of the soft tissues and vascular bed. Most authors consider the presence of a defect of up to 5 cm to be an indication for the use of ASL, and those over 5 cm to be an indication for the use of BT.

A gunshot defect forms relatively fast before significant cicatricial changes in the soft tissues of the segment and vascular sclerosis develop. Given this, the possibility of safely repairing (eliminating) defects larger than 5 cm using ASL is promising.

Study hypothesis The ASL technique may be more effective and safer than the BT technique for eliminating gunshot defects of the tibia diaphysis longer than 4 cm (severe and massive defects according to the classification of Tetsworth et al. [6]) in the early stages after injury before the development of cicatricial changes in the soft tissues of the lower leg and fibrosis of the vascular bed.

Aim of the study: To compare the efficacy and safety of the bone transport (BT) method and the acute shortening with subsequent lengthening (ASL) method for filling (elimination) of gunshot defects of the tibial shaft.

MATERIAL AND METHODS

Study design: A single-center, open, prospective, comparative study approved by the institutional ethics committee of the Burdenko Main Military Clinical Hospital (Protocol No. 266 of May 24, 2023).

The study included 60 patients with gunshot defects to the tibia, divided into two groups of 30 patients (Table 1):

— Group 1: patients whose defects were treated using the BT technique;

— Group 2: patients whose defects were treated using the ASL technique.

Osteosynthesis in both groups was performed with the Ilizarov external fixator (EF), a wire-and-halfpin type.

Table 1

Basic characteristics of the groups

Parameters		Group 1 (BT), n = 30	Group 2 (ASL), n = 30	p
Age, years		33.0 ± 8.0	32.6 ± 9.2	0.835[1]
Bone defect size, mm		83.9 ± 30.3	82.7 ± 29.5	0.877[1]
Ratio of the defect size to tibia length, %		21.3 ± 7.6	21.1 ± 8.0	0.922[1]
Skin defect, cm^2 (interquartile range)		56.5 (80)	42.0 (103)	0.990[2]
Time to reconstructive surgery, days (interquartile range)		80.5 (46)	23.5 (26)	**< 0.001[2]**
Time of soft-tissue defect closure, days		73.2 ± 29.4	31.9 ± 20.1	**< 0.001[1]**
Bone defect size according to the classification of Tetsworth et al. [6], mm	21–40	3 (10.0 %)	3 (10.0 %)	0.876[3]
	41–80	13 (43.3 %)	12 (40.0 %)	
	> 80	14 (46.7 %)	15 (50.0 %)	

Notes: [1] — Student's t-test; [2] — Mann – Whitney U test; [3] — Pearson's χ^2 test

Inclusion criteria: male gender; age from 18 to 59 years; critical-size gunshot defect of the tibia diaphysis longer than 2 cm; patient consent to participate in the study; dynamic follow-up study for at least 3 years.

Exclusion criteria: female gender; age under 18 and over 59 years; intra-articular fractures of the tibia, bone fractures of adjacent segments of the injured limb, severe concomitant injuries to other areas (head, spine, pelvis) that hinder or exclude the possibility of patient activation, chronic diseases that affect bone tissue regeneration; patient refusal to participate in the study; unavailable dynamic follow-up study.

Statistical analysis The analysis was performed in SPSS. The Shapiro–Wilk test was used to check the normality of quantitative variables. Normally distributed quantitative variables were described using the mean and standard deviation $\bar{x}$ (±), while abnormally distributed variables were described using the median and interquartile range Me (IQR). Comparison of quantitative variables with a normal distribution was performed using the Student's t-test for independent samples, and with an abnormal distribution using the Mann – Whitney U-test. Qualitative variables are presented as absolute values and percentages. Group comparisons for qualitative variables were performed using the Pearson χ^2 test. Differences were considered statistically significant at $p < 0.05$.

In the overwhelming majority of cases in both groups, there were severe ($n = 13$ for BT, $n = 12$ for ASL) and massive defects ($n = 4$ and $n = 15$, respectively). However, no statistically significant differences in these parameters were found between the groups ($p = 0.876$).

Bone defect sizes were comparable in both groups, both an absolute size and as a percentage of tibial length ($p = 0.877$ and $p = 0.922$, respectively). Bone defects in both groups typically had a dual nature: a primary defect resulting from injury and a secondary defect resulting from a series of surgical debridements aimed at removing necrosis and preventing (controlling) infection. The final defect size was determined after additional resection during reconstructive surgery to ensure contact between fragments during BT or ASL procedures. No statistically significant differences were observed between the groups in terms of the area of soft-tissue defects.

Patients in Group 1 underwent surgical treatment aimed at wound closure prior to BT with specific techniques. The following procedures were used: local tissue grafting (nine patients); split-thickness skin graft (six); free full-thickness skin flap (one); vascularized flap (six); and a combination of techniques (eight).

In 19 patients in Group 2, wound closure was performed using local tissues simultaneously with acute shortening (AS), local grafting was additionally used in eight patients, and split-thickness skin grafting was used in three patients. The need for an additional preliminary surgery in the BT group resulted in significant differences in the timing of reconstructive surgery. In the BT group, reconstructive surgery (osteotomy) was performed on average on day 80.5 (46), while in the case of ASL (approximation of fragments) it was performed on day 23.5 (26) ($p < 0.001$).

Based on the comparison of baseline characteristics, it can be concluded that the groups were homogeneous in all clinically significant aspects. The study patients were followed for at least one year after removal of the external fixator.

The decision on treatment tactics was made by the surgeon based on the clinical presentation, characteristics of each individual case. Total bone loss was calculated as the sum of the bone defect length and the magnitude of any limb length discrepancy, if any.

The effectiveness of the methods used was assessed based on clinical and radiographic studies. Total healing time was defined as the time from injury to removal of the external fixator after convincing radiographic evidence of consolidation of the fragments at the docking site and maturation of the distraction regenerate, as well as restoration of limb weight-bearing function. The radiographic maturation time of the distraction regenerate was determined according to the criteria of Fischgrund et al. [21]. In addition, the time of external fixation and the external fixation index (EFI) were calculated separately, which was calculated by dividing the time of external fixation by the length of the regenerate (months/cm).

Clinical outcomes were assessed based on anatomical and functional parameters in accordance with the scoring system of Paley et al. [22].

The safety of the method was determined based on complications that developed during treatment, categorised as minor (managed with conservative measures), serious (surgical treatment was used), or sequelae (not resolved during treatment) [23].

BT technique has three stages.

The first stage begins after the injury and involves preparing for bone fragment(s) transport in the defect area. The lower leg is fixed with a halfpin-based external fixator (EF); surgical debridement is performed to remove necrotic tissue, foreign bodies, and small bone fragments, and conservative treatment is administered to control infection and minimize the defect. The resulting wound and exposed bone fragment parts are closed using a skin grafting technique.

The second stage begins after the wound has healed and continues while the fragment is being transported. For this purpose, an Ilizarov halfpin-based fixator is placed, and an osteotomy of one or both fragments is performed. After 7–10 days, fragment(s) transport is performed.

The third stage of treatment starts when contact is achieved between the fragment(s) and/or fragments. During this transport of bone fragment(s), osteochondral formations at their ends, and in some cases, invagination occur. To create conditions for consolidation, the pseudoarthrosis area is resected, and the ends of the fragment(s) and the fragment are brought together and compressed. In cases of hypotrophic pseudoarthrosis, bone grafting is performed with free autograft. The third stage ends with bone union at the docking site between the fragment(s) and the fragment and the maturation of the regenerate(s).

ASL technique also has three stages.

The first stage begins at the moment of injury and involves preparing the wound for reconstructive surgery. The leg is fixed with a halfpin-based external fixator. Surgical debridement is performed, followed by conservative treatment aimed at controlling infection and minimizing the defect.

The second stage begins with reconstructive surgery (shortening) and is completed when convincing signs of bone union appear.

The third stage starts with osteotomy of one or two fragments and distraction to form the regenerate(s) until the segment length is restored. It ends with consolidation and ossification of the regenerate(s).

ASL intervention

Necrotic tissue remnants are excised, and the ends of the tibial fragments are resected until a "blood dew" appears perpendicular to the tibial axis to increase the stability of the osteosynthesis. If necessary, the fibula is resected to the length of the tibial defect. An Ilizarov halfpin-based fixator is applied to approximate the bone fragments. Once contact is achieved, the pulsation of the arteries in the foot is assessed, and pulse oximetry is performed to determine the state of blood circulation. If signs of ischemia are detected, partial separation of the fragments is performed until the ischemia is eliminated, followed by a gradual (2–3 cm per day) approximation until complete contact is achieved. Shortening of the tibia results in approximation of the wound edges and closure of the defect by grafting with local tissues.

RESULTS

The analysis of treatment time revealed considerable differences between the BT and ASL techniques. The consolidation time at the docking site was statistically longer in the BT group as compared with the ASL group (459.2 ± 99.6) days versus (217.7 ± 67.7) day, $p < 0.001$. This difference can be explained by the features of the BT technique in which an additional time for contact between the transported fragment and the docking site fragment and by the need to overcome osseochondral formation and invagination (Table 2).

The time of regenerate formation and maturation was also significantly longer in BT (326.8 ± 95.7) days versus (228.6 ± 93.5) days in ASL, $p < 0.001$. This difference, in our opinion, may be due to the fact that at least three centers of regeneration are formed in BT, the end of the fragment, the opposing end of the transported fragment, and the regenerate itself. Osteogenesis in these zones in reduced regenerative potential may not meet the needs of the body.

The total treatment time and fixation time did not show statistically significant differences between the groups ($p = 0.09$ and $p = 0.695$, respectively). However, on average, the duration of treatment was

45 days shorter in ASL patients. One of the important factors may be the delay in wound closure associated with the need for additional surgery at the initial stage of treatment. Accordingly, the EFI was also lower in ASL (45.8 (29.8)) compared to BT (50.0 (13.6)), while the Mann – Whitney criterion was 0.506.

Table 2

Treatment results

Parameters	Group 1 (BT), $n = 30$	Group 2 (ASL), $n = 30$	p
Consolidation time at the docking site, days	459.2 ± 99.6	217.7 ± 67.7	**< 0.001[1]**
Time of formation and maturation of regenerate, days	326.8 ± 95.7	228.6 ± 93.5	**< 0.001[1]**
Total treatment time, days	474.3 ± 95.0	429.0 ± 108.2	0.09[1]
Fixation time, days	398.1 ± 108.9	388.5 ± 78.2	0.695[1]
External fixation index, days/cm (interquartile range)	50.0 (13.6)	45.8 (29.8)	0.506[2]
Anatomical results, ASAMI points (interquartile range)	4.5 (1.0)	5.0 (0.0)	**0.011[2]**
Functional results, ASAMI, points (interquartile range)	3.0 (1.0)	4.0 (2.0)	**0.003[2]**

Notes: [1] — Student's t-test; [2] — Mann – Whitney U test

In regard to the ASAMI score, the ASL group showed significantly better results. Thus, the median values of anatomical results in the ASL group were 5.0 (0.0) points versus 4.5 (1.0) points in the BT group ($p = 0.011$), and functional results were 4.0 (2.0) and 3.0 (1.0) points, respectively ($p = 0.003$).

The rate of complications differed significantly between the groups. Minor complications were more frequent in the BT group, (7.6 ± 2.7) cases per patient during treatment compared to (3.7 ± 2.4) in the ASL group ($p < 0.001$). Serious complications also prevailed in the BT group, 5.0 (3.0) cases versus 0 (1.0) in the ASL group (p < 0.001). Nonunion was observed only in the BT group, 23 (76.7 %) cases compared to their complete absence in the ASL group ($p < 0.001$). This critically important difference indicates a fundamental problem of the BT method, a high risk of pseudarthrosis at the docking site. Invagination was also characteristic only of the BT group, 19 (63.3 %) cases ($p < 0.001$), which is a specific complication of this method. This distribution of complications is explained by the long period of fragment transport after osteotomy until docking in the BT method and the need for additional surgical interventions to eliminate obstacles to union. Differences in the rate of other complications (axis malalignment and joint contractures) were not statistically significant. However, these complications affected the anatomical and functional results (Table 3).

To demonstrate the peculiarities of the Ilizarov techniques used for extensive defect management, we would like to show clinical reports.

Table 3

Complications

Complication type	Number		p
	Group 1 (BT), $n = 30$	Group 2 (ASL), $n = 30$	
Minor complications, number per patient	7.6 ± 2.7	3.7 ± 2.4	**< 0.001[1]**
Severe complications, number per patients (interquartile range)	5.0 (3.0)	0 (1.0)	**< 0.001[2]**
Nonunion, number (%)	23 (76.7)	0 (0)	**< 0.001[3]**
Invagination, number(%)	19 (63.3)	0 (0)	**< 0.001[3]**
Axial malalignment, number(%)	13 (43.3)	9 (30.0)	0.422[3]
Knee and (or) ankle joint contracture, number(%)	24 (80)	17 (56.7)	0.209[3]

Notes: [1] — Student's t-test; [2] — Mann – Whitney U test; [3] — Pearson's χ^2 test

Clinical reports

A 32-year-old patient (group 1) sustained injuries during combat operations: combined blast injury to the head and extremities; flame burns to the head, face, both hands, and both lower extremities, grades 2-3A-3B, S = 14 (6%); cerebral contusion; contusion of the left eyeball, penetrating corneal wound, scleral rupture, foreign body in the anterior chamber of the left eye; a through-and-through wound of the soft tissues of the left forearm; lacerated wound of the left hand, comminuted fracture of the middle phalanx of the 5th finger; **extensive lacerated wound of the left lower leg**, comminuted fracture of both bones in the upper and middle third with primary bone and soft tissue defect; traumatic shock, grade 3.

During the evacuation stages, treatment was aimed at stabilization of disorders and wound healing.

After stabilization of the condition and healing of the wounds on the left lower leg (Fig. 1), 72 days after the injury, an operation was performed: external transosseous compression-distraction osteosynthesis (Ilizarov method) of the left lower leg, osteotomy of the distal fragment of the left tibia. The tibial bone defect was 15 cm. On the 79th day after the injury, fragment transport was initiated to form a regenerate and fill the defect. On the 164th day after the injury (85 days after the osteotomy), in order to correct the position and direction of the fragment transport, the Ilizarov frame on the left lower leg was reassembled. The transport of the distal tibial fragment continued (Fig. 2).

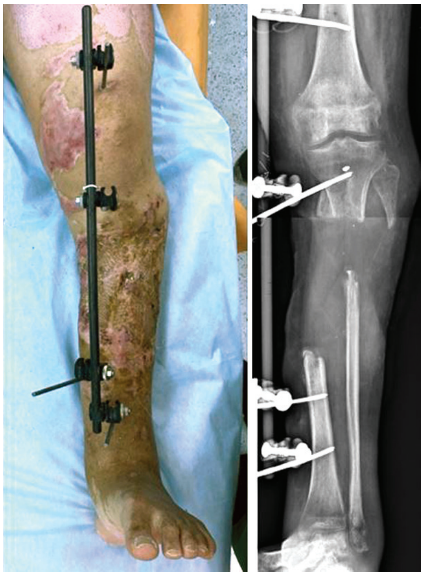

Fig. 1 Photo and radiograph of the left lower leg before the reconstructive operation

Fig. 2 Photo and radiograph of the left lower leg in the course of bone transport

On the 261st day after the injury (182nd day after osteotomy), contact was noted between the transported fragment and the proximal fragment through the invagination zone (Fig. 3). In order to ensure docking between the proximal fragment and the transported distal fragment, on the 262nd day after the injury (183rd day after osteotomy), resection of the invagination zone and the osteochondral area at the end of the proximal fragment and the transported fragment was performed, followed by open reduction of the fragments and reassembly of the Ilizarov fixator. Docking was achieved between the end parts of the proximal fragment and the transported fragment (Fig. 4). Subsequently, compression was produced between the proximal fragment and the fragment, and "regeneration training" was carried out using the "accordion" method.

Union between the proximal fragment and the transported fragment, as well as maturation of the regenerate, was noted on the 493rd day, and the Ilizarov fixator was removed (Fig. 5). Rehabilitation continued for 60 days (Fig. 6).

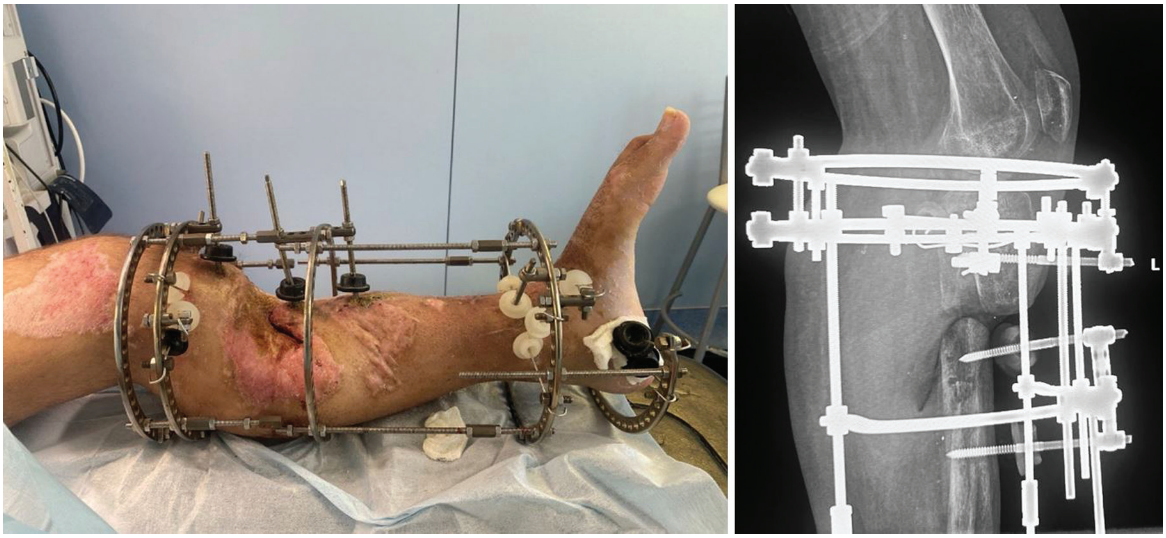

Fig. 3 Photo and radiograph of the left lower leg at the approximation of the proximal and transported fragments (invagination)

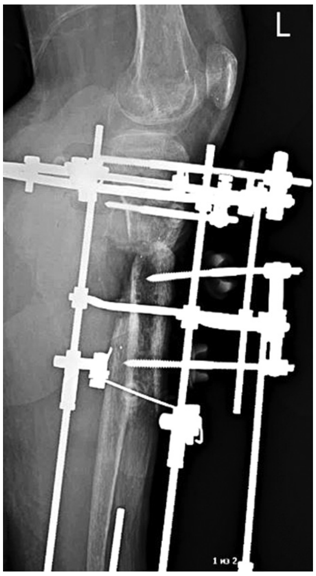

Fig. 4 Radiograph of the left lower leg following the surgery for invagination elimination, pseudarthrosis end resection and bone reduction, rearrangement of the Ilizarov fixator

Fig. 5 Full-length radiograph of the lower limbs upon treatment completion

Fig. 6 Patient weight-bearing on the left lower leg and its flexion in the left knee joint

The total treatment term was 553 days, external fixation duration was 43.7 days/cm, the ASAMI anatomical result was fair, and the ASAMI functional score was good.

A 44-year-old patient (group 2) sustained injuries while participating in combat operations: combined blast injury of the pelvis and both lower extremities; multiple shrapnel wounds of the perineum and lower extremities. **Extensive lacerated wound of the right lower leg, comminuted fracture of both bones in the upper and middle third with a primary bone and soft tissue defect** (Fig. 7). Extensive lacerated wound of the left foot associated with fractures of the 1st and 2nd metatarsal bones. Acute massive blood loss. Traumatic shock grade 2. Acute kidney injury.

During the evacuation stages, treatment was aimed at compensating for the disorders and wound healing.

After stabilization of the patient's condition and restoration of kidney function 34 days after the injury, a repeated surgical debridement of the wound was performed, including necrectomy of the tibia and fibula, external fixation of the right lower leg with the Ilizarov external fixator. The tibial bone defect was 11 cm (Fig. 8).

Signs of bone union were detected on day 126 after the injury (on the 92nd day after external fixator placement), and an osteotomy was performed in the lower third of the tibia (Figs. 9 and Fig. 10a).

The lengthening procedure continued 137 days after the shortening one (Fig. 10b) until the 263rd day after the injury (Fig. 10c). Bone union in the fracture contact zone was noted on the 192nd day after the initial surgery. Subsequently, "regenerate training" was performed using the "accordion" method. Maturation of the regenerate was noted 108 days after the cessation of lengthening. On the 371st day after the injury, the external fixator was removed. Rehabilitation continued for 60 days (Fig. 11).

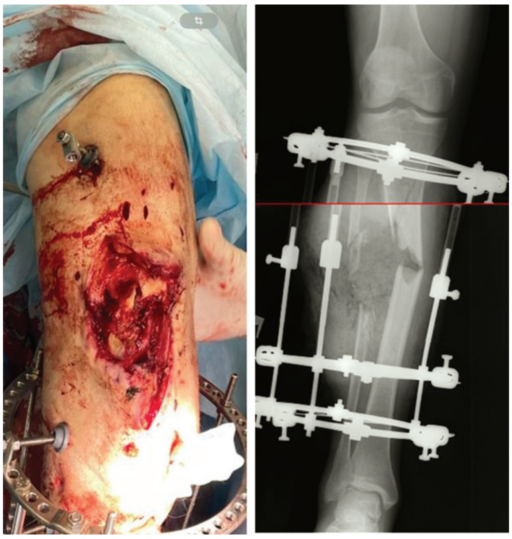

Fig. 7 Photo and radiograph of the right tibia upon admission

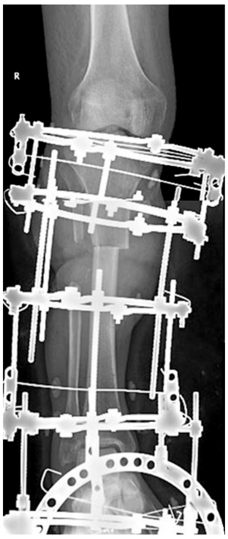

Fig. 8 Radiograph of the right tibia upon acute shortening phase

Fig. 9 Photo of the right tibia before performing osteotomy

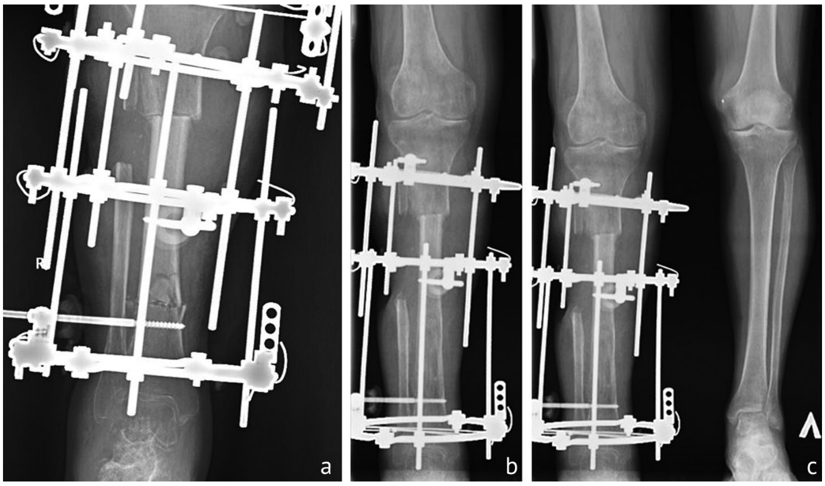

Fig. 10 Radiographs: (a) right tibia after osteotomy; (b) right tibia in the course of lengthening; (c) both tibias after lengthening of the right tibia

Fig. 11 Full-length radiograph and photo of the lower extremities upon treatment completion

Total treatment term was 431 days; EFI was 29.7 days/cm. Residual shortening made 2 cm. The anatomical ASAMI result was good and the functional ASAMI outcome was good.

DISCUSSION

In any pathology for which several treatment methods are available, the main issue is choosing the optimal method in each specific case. The size of the gunshot defect of the tibia serves as the main criterion for determining the indications for the choice of treatment tactics. In the available literature, we found recommendations according to which bone defects >10 cm should be corrected by BT [24], and bone defects < 8 cm by ASL [19]. These recommendations are based on a study of the experience of treating patients with the consequences and complications of open infected fractures. In such cases, reconstructive surgeries were performed a long time after the injury had been sustained and due to osteomyelitis, resulting in the formation of extensive cicatricial conglomerates in the bone defect area. Such changes cause technical difficulties during the surgery, increase the risk of intraoperative iatrogenic complications, ischemic disorders in the distal limb, and limit or make simultaneous approximation of fragments impossible. If ASL is used before fibrosis in the surrounding tissues has developed, safe fragment approximation is possible; it was confirmed by our observations and calculations. The maximum bone defect size in the BT group was 160 mm, while in the ASL group it was 140 mm, corresponding to 40% and 36.3% of the tibia length, respectively. Fragment approximation was achieved without distal ischemia. However, the elimination of the defect with BT technique during fragment transport occurs simultaneously with the formation of an interfragmentary scar, which may lead to nonunion at the docking site, invagination, and necessitates rearrangement of the external fixator and other surgeries aimed at combating complications.

Skin defects also have a significant impact on treatment decisions. Their size was comparable in both groups. BT requires preliminary preparation, including special wound closure procedures, which increases the work of the staff, the number of surgeries, and prolongs the overall treatment period. Our study revealed that the ASL technique is optimal, allowing for simultaneous bone deficiency elimination due to bone mass loss, coverage of the exposed bone, and wound closure.

When the fibula was intact and all other conditions were equal, we preferred BT, as this method preserves the true segment length, the relationships in the proximal and distal tibiofibular joints, and the relationship between the bone and tendon-muscle structures, which should positively impact the final functional outcome. Furthermore, fibula resection is an additional trauma and can lead to iatrogenic complications such as damage to arteries, veins, and nerve trunks. The presence of a fracture, and especially a fibula defect, predetermines greater freedom of choice and can serve as an additional justification for the ASL use. Attempts to manipulate fibula fragments during BT significantly complicate the procedure. However, in some cases, at certain BT stages, we also performed fibula osteotomy or resection to stimulate regeneration in the area of contact between fragments or regenerated bone.

Treatment strategy also determines timeframes. In our study, the total treatment duration in the BT group was longer than in the ASL group. This is due to a number of factors:

— Before starting BT, additional preliminary conservative and surgical treatment is necessary to close the wound; in ASL implementation, wound closure occurs immediately.

— The healing time at the contact zone of the fragments in ASL is slightly longer than that of a conventional fracture, 217.7 ± 67.7 days. In BT, the healing began upon reaching contact and was delayed due to the developed morphological changes similar to nonunion at the ends of the fragments, and took 459.2 ± 99.6 days. This, in turn, required 19 additional surgeries for invagination, 16 of which involved bone grafting.

— Fragment transport in BT is a more complex and time-consuming procedure, less comfortable for the patient than lengthening in ASL. The use of the BT method requires more care procedures by the medical staff and additional operations both during the actual transport to correct the fragment's position and direction of its movement (EFD rearrangement was performed in 24 patients) and during the docking of the fragments (bone grafting, elimination of invagination). In this regard, Tetsworth et al. introduced a planned bone grafting operation into the standard BT protocol when the contact is 1-cm distanced [25].

The specific features of the BT technique predetermine the development of specific complications common to all Ilizarov techniques.

The statistically significant advantage in the ASL technique in our study can be explained by the following factors:

— Early closure of a primarily infected gunshot wound prevents infection in the postoperative period and in the medium term.

— Early stable fixation of the external fixator (EF) system when contact between the fragments provides better conditions for bone and soft tissue healing.

— Transport of the bone fragment during BT further traumatizes the surrounding tissue, which also leads to complications, including those specific to BT (invagination, nonunion).

Managing complications make the treatment process more difficult and delays defect repair (removal and replacement of transosseous elements, rearrangement of external fixators, surgical debridement of suppurative foci, etc.).

Unlike other researchers, we found convincing, statistically significant differences in anatomical and functional outcomes between the groups. This is primarily explained by the differences between the observation groups in our study and those in the studies of other authors (groups of acute gunshot fractures with acute infection versus groups of sequelae and complications of open fractures with chronic infection and corresponding tissue degeneration of the segment). However, functional recovery largely depended on concomitant damage to functional tissues such as muscles, tendons, and nerves.

The results of our study demonstrate the fundamental advantages of the ASL technique over BT in the treatment of gunshot tibial defects:

— faster consolidation due to the immediate contact between the viable ends of the fragments;

— significantly lower complication rates;

— better functional outcomes with comparable overall treatment time.

CONCLUSION

The study results suggest that both methods of tibial shaft defect repair based on Ilizarov's discovery (bone transport or acute shortening and then lengthening) have the potential to achieve positive results, including in critical-size defects, when limb preservation is at stake after a gunshot fracture with an extensive defect of the bone and integumentary tissues.

However, in acute gunshot fractures of the tibia with primary and secondary soft-tissue defects and the tibia up to 40 % of its length, acute shortening followed by lengthening is preferable to the bone transport technique. The advantages of acute shortening include shorter treatment times, lower incidence of minor and major complications, a reduced number of planned and emergency surgeries and procedures during treatment, and simplified surgical techniques and treatment technologies.

Conflict of interests *The authors declare no obvious or potential conflicts of interest related to the publication of this study.*

Funding source *The study was not sponsored.*

Ethical statement *All studies on humans were conducted in accordance with the ethical standards of the World Medical Association Declaration of Helsinki "Ethical Principles for Medical Research Involving Human Subjects" and the "Rules of Clinical Practice in the Russian Federation", approved by Order of the Ministry of Health of the Russian Federation dated June 19, 2003, No. 266.*

REFERENCES

1. Kasimov RR, Prosvetov VA Samokhvalov IM, et al. The structure of combat surgical trauma and features of surgical care in advanced medical groups in the active phase of hostilities. *Military Medical Journal*. 2024;345(7):4-12. (In Russ.) doi: 10.52424/00269050_2024_345_7_4.
2. Trishkin DV, Kryukov EV, Chuprina AP, et al. The evolution of the concept of medical care for the wounded and injured with injuries of the musculoskeletal system. *Military Medical Journal*. 2020;341(2):4-11. (In Russ.) doi: 10.17816/RMMJ82214.

3. Brizhan' LK, Babich MI, Khominets VV, et al. The implementation of the general biological principles discovered by G.A. Ilizarov in treating the wounded and injured persons with defects of the lower limb long bone shafts. *Genij Ortopedii*. 2016;(2):21-26. (In Russ.) doi: 10.18019/1028-4427-2016-2-21-26.
4. Gololobov VG. *Regeneration of bone tissue during the healing of gunshot fractures*. St. Petersburg: Petersburg-the XXI century Publ.; 1997:21-38. (In Russ.)
5. Chililov AM, Akhmedov BA, Kozlov VK. Comparative efficiency of various techniques for complex treatment of patients with gunshot injuries to the extremities. *Polytrauma*. 2016;(4):52-62. (In Russ.)
6. Tetsworth KD, Burnand HG, Hohmann E, Glatt V. Classification of Bone Defects: An Extension of the Orthopaedic Trauma Association Open Fracture Classification. *J Orthop Trauma*. 2021;35(2):71-76. doi: 10.1097/BOT.0000000000001896.
7. Green SA. Skeletal defects. A comparison of bone grafting and bone transport for segmental skeletal defects. *Clin Orthop Relat Res*. 1994;(301):111-117.
8. Borzunov DY, Chevardin AV. Ilizarov non-free bone plasty for extensive tibial defects. *Int Orthop*. 2013;37(4):709-714. doi: 10.1007/s00264-013-1799-3.
9. Borzunov DYu, Mokhovikov DS, Kolchin SN, et al Problems and successes in the combined application of the Ilizarov and Masquelet technologies. *Genij Ortopedii*. 2022;28(5):652-658. doi: 10.18019/1028-4427-2022-28-5-652-658.
10. Sliesarenko SV, Badiul PA, Mankovsky B, Rudenko OI. One-stage reconstruction of bone defects with fibula perforator flap. *Issues of Reconstructive and Plastic Surgery*. 2021;24(2):28-40. (In Russ.) doi: 10.52581/1814-1471/77/03.
11. Lychagin AV, Gritsyuk AA, Korytin VS. Long-term complications of tibial injury. *Grekov's Bulletin of Surgery*. 2022;181(1):80-87. (In Russ.) doi: 10.24884/0042-4625-2022-181-1-80-87.
12. Bosse MJ, MacKenzie EJ, Kellam JF, et al. An analysis of outcomes of reconstruction or amputation after leg-threatening injuries. *N Engl J Med*. 2002;347(24):1924-1931. doi: 10.1056/NEJMoa012604.
13. Ilizarov GA. Clinical application of the tension-stress effect for limb lengthening. *Clin Orthop Relat Res*. 1990;(250):8-26.
14. Transosseous osteosynthesis for long bone defects. In: Solomin LN. (ed.) *Fundamentals of transosseous osteosynthesis*. Moscow: Binom; 2015;1:921-943. (In Russ.)
15. Paley D, Catagni MA, Argnani F, Villa A, Benedetti GB, Cattaneo R. Ilizarov treatment of tibial nonunions with bone loss. *Clin Orthop Relat Res*. 1989;(241):146-165.
16. Lychagin AV, Gritsyuk AA, Korytin VS. Treatment of tibial wound consequences: further development of the Ilizarov technology. *Genij Ortopedii*. 2022;28(1):69-75. doi: 10.18019/1028-4427-2022-28-1-69-75.
17. Lerner A, Reis ND, Soudry M. Primary limb shortening, angulation and rotation for closure of massive limb wounds without complex grafting procedures combined with secondary corticotomy for limb reconstruction. *Curr Orthop Pract*. 2009;20(2):191-194. doi: 10.1097/BCO.0b013e318193bfaa.
18. Plotnikovs K, Movcans J, Solomin L. Acute Shortening for Open Tibial Fractures with Bone and Soft Tissue Defects: Systematic Review of Literature. *Strategies Trauma Limb Reconstr*. 2022;17(1):44-54. doi: 10.5005/jp-journals-10080-1551..
19. Eralp L, Kocaoglu M, Celiktas M, Gülşen M. Is acute compression and distraction superior to segmental bone transport techniques in chronic tibial osteomyelitis? Comparison of Distraction Osteogenesis Techniques. *Acta Orthop Belg*. 2016;82(3):599-609.
20. Artemiev AA, Ivanov PA, Kashoob AM, et al. Shorting Resection and Correction of the Leg Length in the Treatment of Posttramatic Tibial Defects Complicated by Osteomyelitis. *Russian Sklifosovsky Journal "Emergency Medical Care"*.2021;10(2):309-317. doi: 10.23934/2223-9022-2021-10-2-309-317.
21. Fischgrund J, Paley D, Suter C. Variables affecting time to bone healing during limb lengthening. *Clin Orthop Relat Res*. 1994;(301):31-37.
22. Paley D, Maar DC. Ilizarov bone transport treatment for tibial defects. *J Orthop Trauma*. 2000;14(2):76-85. doi: 10.1097/00005131-200002000-00002.
23. Paley D. Problems, obstacles, and complications of limb lengthening by the Ilizarov technique. *Clin Orthop Relat Res*. 1990;(250):81-104.
24. Tetsworth KD, Dlaska CE. The art of tibial bone transport using the Ilizarov fixator. The suspension wire technique. *Tech Orthop*. 2015;30(3):142-155. doi: 10.1097/BTO.0000000000000136.
25. Tetsworth K, Paley D, Sen C, et al. Bone transport versus acute shortening for the management of infected tibial non-unions with bone defects. *Injury*. 2017;48(10):2276-2284. doi: 10.1016/j.injury.2017.07.018.

The article was submitted 03.09.2025; approved after reviewing 07.10.2025; accepted for publication 14.10.2025.

Information about the authors:

Denis V. Davydov — Doctor of Medical Sciences, Professor, Head of the Main Military Clinical Hospital named after N.N. Burdenko, dvdavydov@yandex.ru, https://orcid.org/0009-0005-2990-9511;

Maksim N. Nelin, MD — orthopaedic surgeon, nelinmaksimdoc@gmail.com, https://orcid.org/0009-0000-0198-7693;

Alexander A. Artemiev — Doctor of Medical Sciences, Associate Professor, orthopaedic surgeon, alex_artemiev@mail.ru, https://orcid.org/0000-0002-0977-805X;

Artur A. Kerimov — Candidate of Medical Sciences, Head of the Center for Traumatology and Orthopedics, kerartur@yandex.ru, https://orcid.org/0000-0001-5783-6958;

Andrey A. Maksimov — Candidate of Medical Sciences, Head of the Group, aam.moscow.hand.72@gmail.com;

Nikolay I. Nelin — Doctor of Medical Sciences, Head of the Research and Testing Center, nelinnik63@mail.ru, https://orcid.org/0009-0000-9777-742X;

Petr A. Radaev — pharmacist-technologist of the Analytical Group, teseychic@gmail.com, https://orcid.org/0009-0000-7313-3339.

Original article
https://doi.org/10.18019/1028-4427-2025-31-6-707-719

Assessment of using thread joysticks results for fragment reduction and bone allografting in the treatment of bone defects in patients with proximal humeral fractures

R.S. Titov[1]✉, A.M. Fain[1,2], A.Yu. Vaza[1], N.V. Borovkova[1], S.F. Gnetetskiy[1,2], I.I. Mazhorova[1], K.A. Rozhkov[1], K.I. Skuratovskaya[1]

[1] Sklifosovsky Research Institute for Emergency Medicine, Moscow, Russian Federation
[2] Russian University of Medicine, Moscow, Russian Federation

Corresponding author: Roman S. Titov, TitovRS@sklif.mos.ru

Abstract

Introduction Despite significant advances in the development of new fixation systems and improvements in surgical technologies, algorithms that guarantee anatomical reduction in proximal humerus fractures are lacking.

The **aim** of this study was to evaluate the clinical efficacy of using thread joysticks for fragment reduction and allogeneic bone grafting materials to repair bone defects in patients with proximal humerus fractures.

Material and methods A total of 219 patients with proximal humerus fractures were treated. The main group consisted of 123 patients and was treated according to the proposed by us osteosynthesis, while the comparison group included 96 patients was managed with traditional methods. Long-term outcomes were assessed at 1 to 4 years postoperatively using the Constant score, as well as two questionnaires: the Simple Shoulder Test (SST) and the Oxford Shoulder Score (OSS).

Results In the main group, the Constant score ranged from a maximum of 98 to a minimum of 6, with a mean of 69.8 and a median of 73. In the control group, the maximum score was 93, the minimum was 8, with a mean and median of 54. Poor results were observed in 9 patients (7.3 %) in the main group. Of these, 4 (3.3 %) were due to infection, 3 (2.4 %) to implant migration, and 2 (1.6 %) to poor compliance with rehabilitation, leading to shoulder joint contracture. In the comparison group, 32 patients (33.3 %) had poor outcomes. Among them, 15 (15.6 %) had persistent limitations in abduction and internal rotation, 10 (10.4 %) exhibited implant migration, 5 (5.2 %) developed infection requiring reoperation, and 2 (2.1 %) experienced severe post-traumatic arthritis and humeral head collapse.

Discussion The described technique has a number of advantages compared toexisting methods, which allows for stable fixation in cases of 3- and 4-part fractures and avoids the need for shoulder joint replacement. It features a clearly defined algorithm of procedures that simplifies the reduction and fixation of bone fragments, especially in defects of the proximal humerus.

Conclusion The application of this surgical technique reduced operative time and improved treatment outcomes in fractures of the proximal humerus.

Keywords: proximal humerus fracture, treatment of proximal humerus fractures, humeral osteosynthesis, bone grafting

For citation: Titov RS, Fain AM, Vaza AYu, Borovkova NV, Gnetetskiy SF, Mazhorova II, Rozhkov KA, Skuratovskaya KI. Assessment of using thread joysticks results for fragment reduction and bone allografting in the treatment of bone defects in patients with proximal humeral fractures. *Genij Ortopedii*. 2025;31(6):707-719. doi: 10.18019/1028-4427-2025-31-6-707-719.

INTRODUCTION

Proximal humerus fractures are a pressing issue in current traumatology, accounting for 5–7 % of all fractures in the adult population. Among elderly patients, this pathology ranks third in incidence, following femoral neck fractures and distal radius fractures. Particularly noteworthy is the fact that in individuals over 60 years of age, such injuries account for up to three-quarters of all humerus fractures, with the gender distribution showing a clear predominance of women with a ratios of 2:1–3:1 compared to men in the same age group [1, 2]. Epidemiological studies in recent years have recorded a steady trend toward an increase in their incidence, and the most growth have been observed among older patients [3, 4]. According to statistics, over the past decades, the incidence of such fractures has almost doubled in the population over 65 years of age.

Modern traumatology offers a significant arsenal of treatment methods, ranging from conservative management to a variety of surgical options [5–8]. However, the lack of uniform, standardized approaches to selecting optimal treatment tactics remains a serious problem, due to the wide range of possible treatment options and significant differences in the technical provision of medical institutions.

The timing of surgical treatment deserves special consideration. Numerous clinical observations indicate that a delay of more than five days in surgical intervention significantly increases the risk of serious complications such as avascular necrosis of the humeral head and secondary displacement of bone fragments. Split fractures of the humeral head and fracture-dislocations are particularly important. In these cases, anatomical reduction should be performed urgently, preferably within the first 48 hours after injury, to minimize the risk of ischemic complications [9].

The choice of the optimal fixation method remains controversial. Comparative studies of various osteosynthesis techniques, including osteosynthesis with locking plates and intramedullary osteosynthesis with locking nails, have not revealed significant differences in long-term treatment outcomes, even for comminuted fractures [10–12]. However, it should be noted that in patients with severe osteoporosis, even modern fixation devices may not provide sufficient stability.

The analysis of complications associated with plating indicates that up to 40 % of adverse outcomes, including impingement syndrome, migration of fixing elements, and so-called screw "cut-through", are associated with technical errors during surgical intervention [13]. It is important to note that increasing the number of fixing screws in the proximal fragment beyond four does not improve outcomes but may increase the risk of iatrogenic injury [14].

Blood supply to the humeral head is particularly important for prognosis. According to various authors, the incidence of avascular necrosis of the humeral head, as a complication of a proximal humeral fracture, varies widely, from 21 % to 75 % of cases [15]. Impaired vascularization can also lead to complications such as delayed consolidation or nonunion of the fracture and bone resorption of the humeral tuberosities.

In recent years, various bone defect augmentation techniques aimed at preserving the anatomical integrity of the joint have been actively discussed in the literature [16–21]. However, even with the use of modern technologies, osteosynthesis of some complex comminuted fractures of the proximal humerus remains technically unfeasible.

Researchers continue to refine the indications for primary shoulder arthroplasty due to proximal humerus fractures. It is now generally accepted that shoulder joint replacement may be the treatment of choice for complex three- and four-part fractures with significant damage to the articular surface, as well as in cases of previous osteosynthesis failures, when preservation of the natural humeral head is not possible. It should be noted that although current implant designs provide satisfactory pain relief, restoration of full limb function often remains challenging [20, 21, 22, 23].

Despite significant progress in the development of new fixation systems and the refinement of surgical technologies, there are still no clear algorithms to guarantee anatomical reduction for all types of proximal humeral fractures. Therefore, an analysis of the results of new surgical treatment techniques for this category of injuries is relevant [24, 25, 26].

Purpose To evaluate the clinical effectiveness of using thread joysticks for reduction of fragments and bone-grafting allogeneic materials for compensating bone tissue defects in patients with proximal humerus fractures.

MATERIALS AND METHODS

The study was conducted at the Sklifosovsky Research Institute of Emergency Care with the support of Grant No. 1603-22/23 dated April 21, 2023. The work used an original technique for osteosynthesis of the proximal humerus, protected by a Russian patent [27], the effectiveness of which was assessed during this prospective clinical study.

A total of 219 patients who completed the full course of treatment and follow-up were included in the study. The follow-up period ranged from one to four years. To compare treatment outcomes, two groups of patients were formed which clinical characteristics, gender, and age matched.

The study group included 123 patients who underwent osteosynthesis using the proposed technique. The gender distribution of the group was 27 men (22.0 %) and 96 women (78.0 %). Age ranged from 31 to 89 years (median 62 years). A distinctive feature of the surgical technique was the use of thread joysticks for fragment repositioning; in cases of severe bone mass deficiency, bone allografts were used.

The comparison group consisted of 96 patients, including 26 men (27.1 %) and 70 women (72.9 %), aged 18 to 84 years (median 62.5 years). In this group, reduction was performed using traditional methods such as wire joysticks, bone holders, and single-pronged hooks, without the use of allogeneic fibular head grafts. Screw fixation was performed according to standard recommendations to the subchondral zone of the humeral head.

Surgical interventions in both groups were performed four to five days after injury using a standard deltopectoral approach. Locking plates specifically designed for the proximal humerus were used for osteosynthesis. During surgery, the achieved neck-shaft angle, the condition of the medial calcarine edge, and the overall duration of the procedure were assessed. Postoperatively, the limb was immobilized with a sling for three to four weeks, while active therapeutic exercises were prescribed, the intensity of which was gradually increased as pain subsided.

To objectively evaluate long-term treatment outcomes, we used a comprehensive monitoring system, including the Constant systeme and two specialized questionnaires: the Simple Shoulder Test (SST) and the Oxford Shoulder Score (OSS). For SST results, a positive response was assigned 1 point and a negative one 0 points; the maximum possible total score was 12 points. The OSS assessed 12 parameters, ranging from 0 (worst outcome) to 4 points (optimal outcome), yielding a maximum score of 48 points. Patients' subjective satisfaction with the functional state of their operated limb was also considered.

To detect possible inflammatory reactions to the suture material, all patients underwent ultrasound examination of the shoulder joint at 1.5, three, and six months postoperatively. The ultrasound study criteria for inflammation included the presence of edema (thickening of the tendons), abnormal blood flow, fluid inclusions, and decreased tissue echogenicity.

Statistical analysis was performed using Statistica 13.3. Since most of the data had a non-normal distribution, nonparametric statistical methods were used. Continuous variables are presented as median (Me), interquartile range (Q1;Q3), minimum and maximum values, discrete data as absolute (*n*) and relative (%) values. The Mann–Whitney test was used to compare unrelated groups, and a probability calculator was used to analyze discrete data. Differences were considered statistically significant at $p < 0.05$, and values in the range of 0.05–0.1 were considered a trend.

Description of surgical intervention

The surgery was performed under local anesthesia with the patient in the supine position. For optimal approach, the injured humerus was shifted eccentrically toward the center of the operating table. The head was immobilized with additional supports, and the image intensifier was positioned on the side of the healthy shoulder. A standard deltopectoral approach allowed for sequential identification of key anatomical structures: the pectoralis major muscle, tendons of the long and short heads of the biceps, the intertubercular groove, and the greater and lesser tubercles of the humerus.

The first step of the technique involved isolating and suturing the subscapularis tendon with non-absorbable sutures (Terylene 5, FiberWire 2), which were then secured to a holder (Fig. 1). Next, the acromiocoracic ligament was identified, retracted superiorly, and the supraspinatus tendon was sutured. Selection of suture material is of particular importance; thinner and stronger sutures minimized knot size after fixation. Finally, the infraspinatus tendon was isolated and sutured, using traction on the previously sutured supraspinatus tendon to facilitate approach.

As a result, three suture joysticks (subscapular, supraspinatus, and infraspinatus) were created, providing complete control of the position of the bone fragments and the humeral head. A significant advantage of this technique was the absence of the risk of their cut-through, typical of traditional wire joysticks, especially in elderly patients with low bone mass. All suturing stages were performed using a single algorithm and the same type of suture material for all components of the rotator cuff (RC).

At the next surgical stage, threads from the RC tendons were sequentially passed through special holes in the plate designed for osteosynthesis of the proximal humerus (Fig. 2). Of particular importance is the fact that most fractures in this location develop in the conditions of severe osteoporosis and bone tissue deficiency. In such clinical situations, we actively used various types of allogeneic bone grafts: cancellous bone grafts and combined grafts made from the head of the fibula, the technology for the use of which is protected by a Russian patent [27]. Osteoplastic defect filling was required in 70 patients, which constituted 49.3 % of the total number of patients.

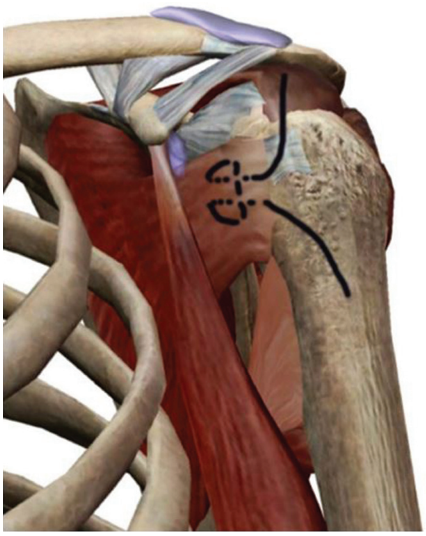

Fig. 1 Diagram of suturing the tendon with a stitch of the subscapularis muscle (other RC muscles are sutured in a similar way)

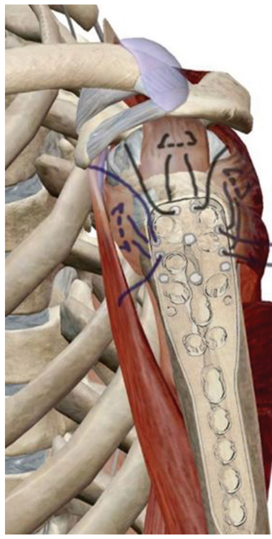

Fig. 2 Diagram of thread passing from RC tendons through the plate holes

The plate was then precisely positioned according to anatomical landmarks: behind the intertubercular groove, maintaining a distance of 5 mm from the superior edge of the greater tubercle. Primary fixation was performed using a central Kirschner wire, thereafter the plate position was monitored using an image intensifier tube (IIT), the position of the inserted wire was as a guide.

The next important manipulation was tensioning the sutures securing the RC elements while simultaneously applying finger pressure to the plate against the bony structures of the proximal humerus. This technique ensured precise and stable reduction of the bone fragments and a tight fit of the implant to the bone surface (Fig. 3).

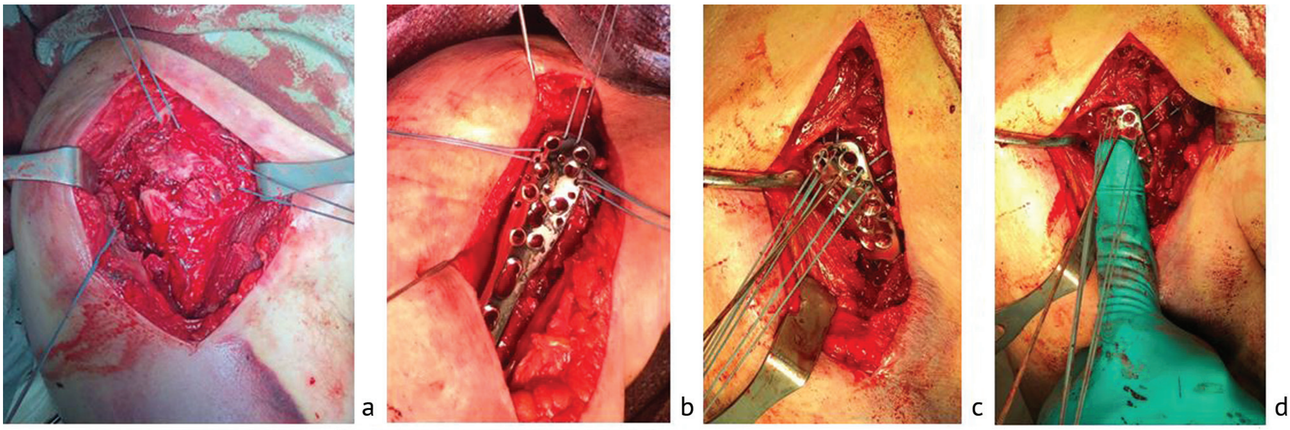
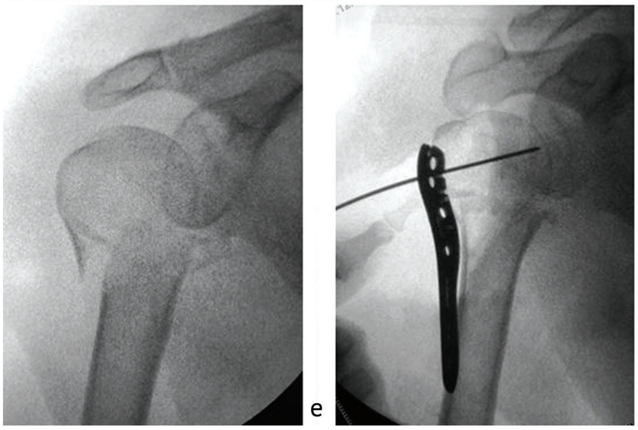

Fig. 3 Technique of fracture reduction: (a) view of the wound after suturing the RC tendons; (b) threading through the plate; (c) insertion of the central wires; (d) reduction on the plate; (e) image intensifier control before reduction; (f) reduction of the proximal humerus with the plate, image intensifier control

Upon reduction completion, plate fixation with locking screws was initiated. While holding the sutures taut and pressing the plate firmly against the bone, holes were sequentially drilled at the most convenient points on the plate, starting with the superoanterior quadrant. These holes were chosen for primary fixation due to their easy accessibility through the surgical approach and the ability to securely fix the proximal fragment. After inserting the proximal screws, the distal portion of the plate was fixed. A 3.5 mm cortical screw was inserted through the oval hole, carefully ensuring that the anterior edge of the plate was positioned behind the long head of the biceps brachii tendon. Throughout the fixation process, the position of the fragments and the implant was constantly monitored using the image intensifier; screw positioning was adjusted as necessary. Particular attention was paid to evenly distributing the force when tightening the screws to avoid plate distortion and ensure a tight fit across the entire bone surface. After completion of fixation, the stability of the structure and the quality of reduction were assessed (Fig. 4).

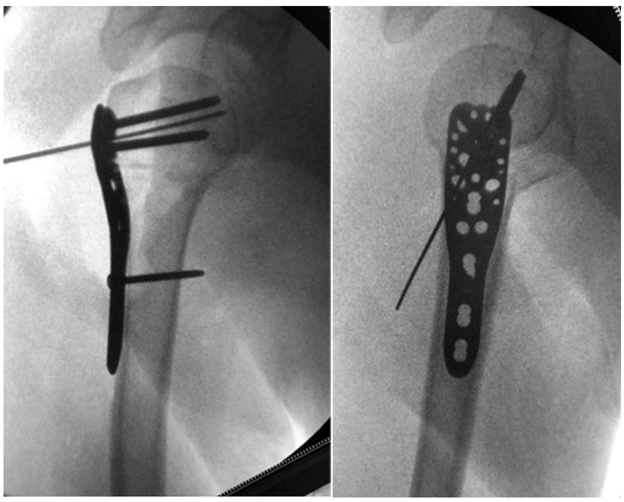

Fig. 4 Radiographic control of fracture reduction with the plate

The final stage of the surgery involved sequential tightening and fixation of the sutures to the plate, followed by removal of the temporary central Kirschner wire and insertion of additional locking screws. Particular attention was paid to the selection of proximal screw lengths. For AO-ASIF type C fractures, shortened screws were preferred due to the risk of developing partial avascular necrosis of the humeral head and the need to minimize the risk of bone cut through. Key aspects of successful reduction were: restoration of the anatomical volume of the humeral head through bone grafting and mandatory fixation of the rotator cuff tendons to the plate. A technical nuance associated with the initial fixation of the diaphysis deserves special mention: due to the excessive length of the reduction cortical screw, it was subsequently replaced with shorter screws (Fig. 5). This approach allowed us to optimize load distribution and reduce the risk of complications associated with excessive length of fixation elements.

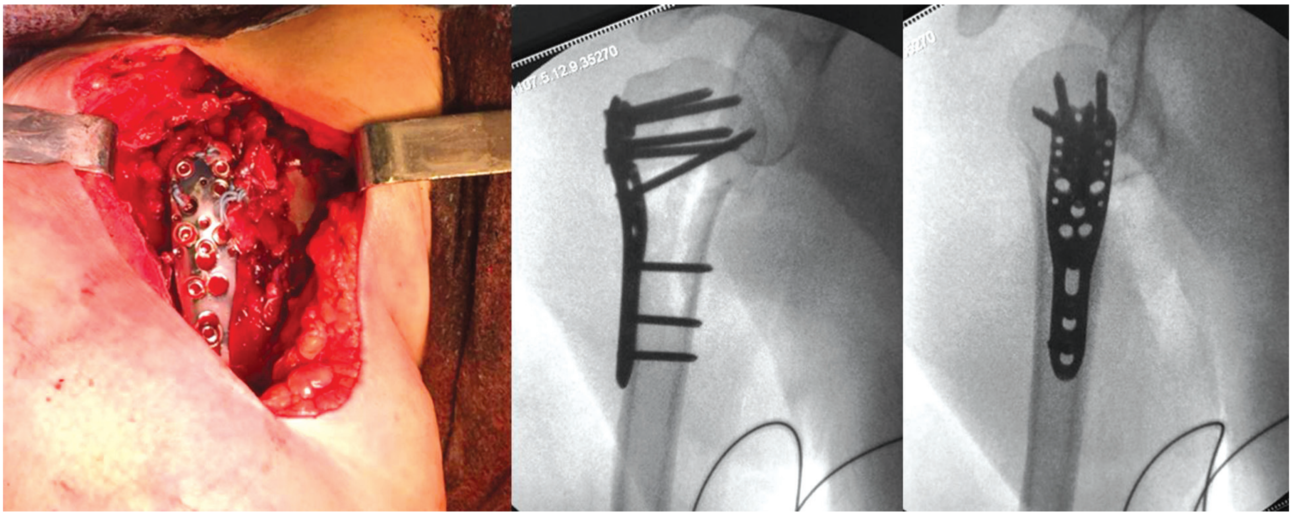

Fig. 5 Photo and radiographs of the final fixation of the fracture

In cases of severe bone defects, we systematically used various types of allogeneic grafts, which optimized conditions for fracture consolidation. Our arsenal included three main graft material types: compact cubes of cancellous bone, which provide good support; diaphyseal grafts from the fibula, which are characterized by high mechanical strength; and combined grafts from the head of the fibula, which combine the advantages of cancellous and compact bone (Fig. 6). The choice of a specific graft type was personalized in each case, and considered bone defect size and location, patient's age, and osteoporosis grade. Particular attention was paid to careful preparation of the graft bed and its close contact with the surrounding bone tissue, which was achieved by precisely adapting the graft shape to the characteristics of the defect. The use of allografts in combination with the proposed osteosynthesis technique allowed not only to restore bone integrity but also to create optimal biomechanical conditions for early functional rehabilitation of patients.

Cancellous bone grafts were used primarily to fill limited defects in the greater tuberosity region, where their porous structure optimally promoted revascularization and osteogenesis. In more complex cases (severe bone loss combined with damage to the cancellous and cortical components, as well as disruption of the medial calcarine edge), fibula allografts were used. These grafts provided the necessary mechanical support due to their anatomical shape and dense cortical structure. Precise graft modeling for tight contact with the fracture site was achieved through individual adjustment to a specific defect. The technical features of reduction with grafts, including the sequence of manipulations and fixation methods, are detailed in Fig. 7. This approach allowed for the restoration of not only the anatomical integrity but also the biomechanical function of the proximal humerus, even in the most complex clinical cases.

Fig. 6 Types of bone allografts: (a) cortical graft from the fibula; (b) cancellous bone graft; (c) combined bone graft from the head of the fibula

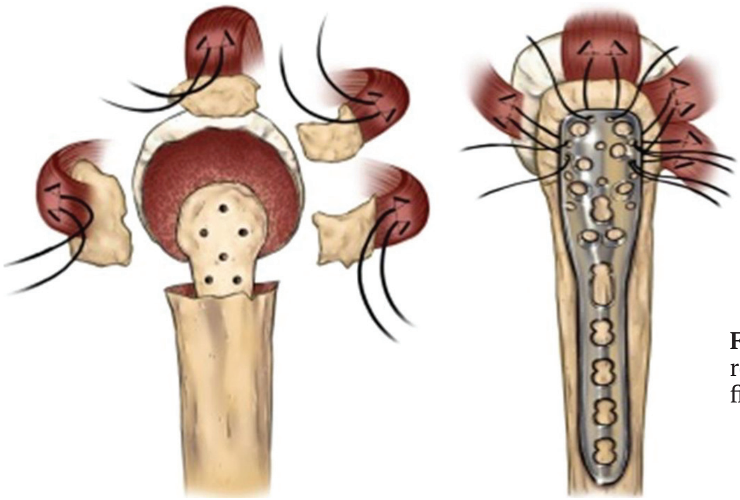

Fig. 7 Diagram of fracture reduction on an allogeneic fibula graft

RESULTS

According to SST score, good results were 9–12 points and poor ones were 1–8 points (Table 1). The patient groups matched by gender (study group — $p < 0.0001$, comparison group — $p < 0.0001$) and age; no statistically significant differences were found. The distribution of patients by fracture type is shown in Figure 8. In the study group, good results were achieved in 92.7 % which was significantly higher than in the comparison group (66.7 %, $p < 0.0001$, probability calculator).

Analysis of Constant – Murley data (Table 2, Fig. 9) showed that in the study group, the maximum score was 98 points and the minimum was 6 points, with an average of 69.8 points and a median of 73 points. In the comparison group, the maximum score was 93 points and the minimum was 8 points, with a lower average and median (both 54 points). These differences confirm the advantages of the proposed by us treatment method.

Table 1

Treatment results as a percentage according to questionnaire SST (n = 219)

SST points	Study group (n = 123)		Comparison group (n = 96)	
	n	%	n	%
1–8	9	7.3	32	33.3
9–12	114	92.7	64	66.7

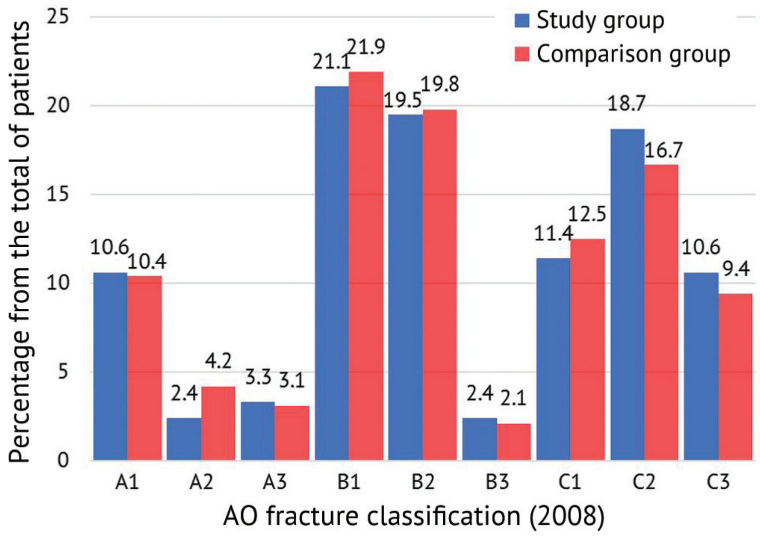

Fig. 8 Distribution of patients in two groups based on AO type of fracture (2008, AO)

Table 2

Descriptive statistics of the Constant – Murley questionnaire (1 to 100)

Variables	Value	
	Study group (*n* = 123)	Comparison group (*n* = 96)
Mean	69.8	54.0
Median	73.0	54.0
Minimum	6.0	8.0
Maximum	98.0	93.0
25th Percentile	58.0	42.0
75th Percentile	84.0	74.0
Geometric distribution	65.7	48.0
Standard deviation	19.2	22.0
Dispersion	371.0	493.0
Average deviation	15.3	22.0
Range	92.0	85.0
Interquartile range	26.0	32.0

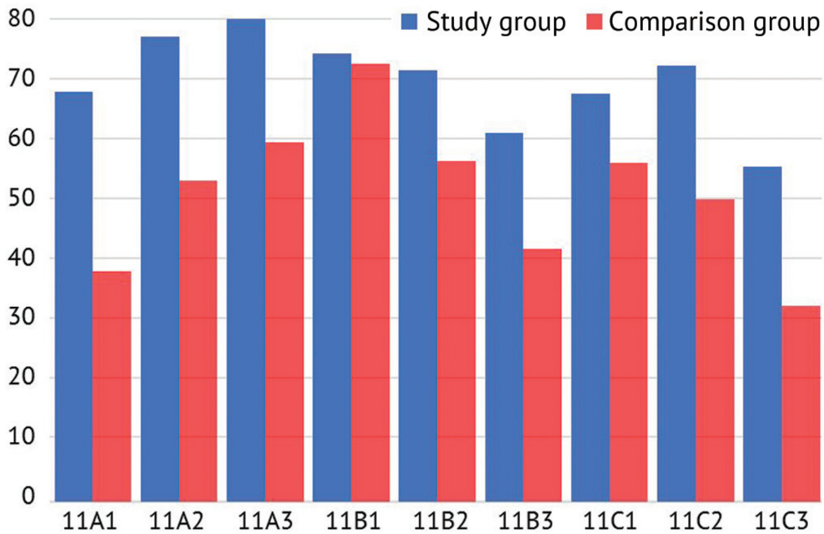

Fig. 9 Comparison of satisfaction with shoulder function according to the Constant – Murley system in the study group and the comparison group based on AO type of fracture

In the study group, nine (7.3 %) cases of poor treatment outcomes were recorded. The complication rate was as follows:

— infectious complications (suppuration) — 3.3 % (*n* = 4);

— migration of fixators — 2.4 % (*n* = 43);

—contractures due to non-compliance with the rehabilitation regimen— 1.6 % (*n* = 42).

In the comparison group, poor outcomes were recorded in 32 patients (33.3 %), including:

— persistent limitations of motion (abduction and placement behind the back) — 15.6 % (*n* = 415);

— migration of fixators — 10.4 % (*n* = 410);

— infectious complications — 5.2 % (*n* = 45);

— severe arthrosis with collapse of the humeral head — 2.1 % (*n* = 42).

The analysis of patient satisfaction using the SST score revealed a clear correlation between two key factors: patient age and the intraoperatively achieved neck-shaft angle (Fig. 10). The graphical dependence demonstrates a direct correlation between the neck-shaft angle value and functional outcome, which is particularly observed in young patients (blue curve). In older age patients, a decrease in satisfaction with the result was noted, even with anatomically correct angle restoration, which is explained by a combination of factors: an increased incidence of age-associated complications, decreased physical activity, and insufficient adherence to rehabilitation measures. The developed technique achieved a neck-shaft angle value of > 125° in all cases of the study group, creating optimal conditions for functional restoration. A group of patients (marked with a black circle) expressed low satisfaction despite adequate anatomical parameters. This fact is primarily associated with purulent complications, which significantly impair functional outcomes.

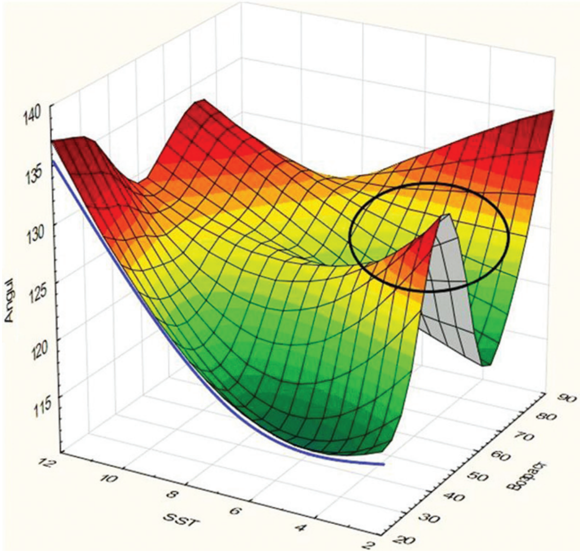

Fig. 10 Dependence of functional satisfaction on age and neck-shaft angle. 3D graphics

A comparative analysis showed that the average duration of surgery in the study group (96 min) was significantly shorter than in the comparison group (141 min) (Fig. 11). A clear relationship was observed between the duration of the procedure and functional outcomes: with an operation time of less than 110 min, patients demonstrated better SST scores (10–12 points). A particularly pronounced relationship was noted in young and middle-aged patients, where a reduction in the surgical time with the proposed technique led to a significant increase in satisfaction with the functional results. In the older age group, despite the relatively short average duration of surgery (80–90 min), such a pronounced relationship was not observed, which may be due to a combination of age-related factors, including comorbidities and specific rehabilitation potential. The obtained data

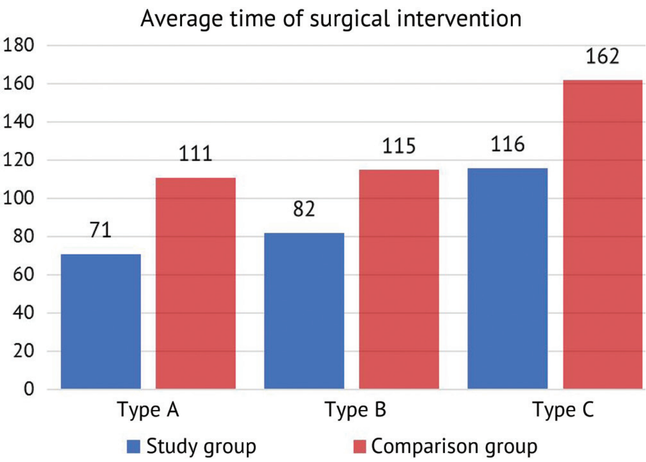

Fig. 11 Distribution of patients by the time of surgical intervention based on the AO type of fracture

convincingly demonstrate that the developed technique is not only technically effective but also allows for a significant reduction in surgical time, which has a positive effect on functional outcomes, especially in young and middle-aged patients (Fig. 12).

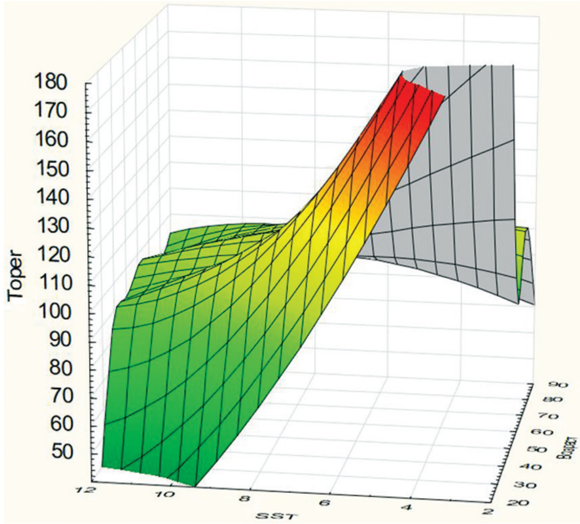

Fig. 12 Comparison of surgical intervention duration (Z-axis) in relation to functional satisfaction and patient age. 3D graphic presnetation

Postoperative ultrasound revealed that restricted range of motion and pain in the first 1.5 to 3 months after surgery were associated with persistent swelling of the rotator cuff tendons, most pronounced in the supraspinatus tendon. A comparative analysis of ultrasound data revealed no statistically significant differences in the intensity or duration of inflammatory changes between the study and comparison groups. The results confirm that the swelling was a natural reaction to surgery and not a consequence of the sutures used. The absence of differences between the groups indicates good biocompatibility of the materials used and the safety of the technique. It is particularly important that ultrasound signs of inflammatory changes were most often observed in the supraspinatus tendon, emphasizing the need for special attention to this area during rehabilitation. The obtained data substantiate the importance of ultrasound monitoring for timely adjustments in rehabiltation and confirm that the developed technique does not increase the risk of inflammatory complications compared to traditional approaches.

DISCUSSION

In three- and four-part humeral head fractures, the complex surgical challenge is precise alignment of the fragments, optimal plate positioning, and tight contact with the bone [28, 29, 30].

The most common method for reducing humeral head fragments is the use of joystick wires. However, this approach has a significant drawback, namely, the difficulty in accurately positioning the wires due to the displacement of the humeral head fragments under the acromion of the scapula. The acromial process significantly limits the manipulation of the joystick wires, often requiring repeated insertion, resulting in trauma to the bone tissue and surrounding soft tissues. Active manipulation of the fragments with wires often leads to their cutting, especially in elderly patients with osteoporosis. Each instance of wire extraction is accompanied by the loss of the achieved reduction and the need for reinsertion of the joystick. Formation of bone defects at the sites of poor wire placement worsens the conditions for definitive fracture fixation with a plate, as it reduces the supporting function of the screws. The thread joysticks, as described in this article, do not have these drawbacks.

Some authors additionally suggest using compression screws to ensure optimal plate contact with the bone surface, which is difficult to achieve in the conditions of low bone mass. There are recommendations for using holes in the plate to insert wire loops to achieve more secure fixation of small bone fragments. The combination of thread joysticks and a central pin allows for secure plate fixation to the bone in the conditions of osteopenia.

Techniques described in the literature often require preliminary fixation of the fragments with wires (two or three, and sometimes more) [6, 29]. The use of provision wires creates significant technical difficulties during subsequent placement and precise positioning of the plate. This is due to the fact that temporary fixators are often located in areas with the greatest bone mass of the fragments, forcing the surgeon to place the plate avoiding the wires. As a result, the locking screws passing through the plate holes and fixing the bone fragments are inserted in the areas of lower bone density. Repeated insertion of the wires leads to disruption of the achieved reduction and secondary displacement of the fragments. The proposed by us technique is based on a different algorithm that speeds up and simplifies the procedure.

Currently, surgical practice utilizes a technique that involves suturing the tendons of the supraspinatus and subsequent fixation to the plate to enhance structural stability. This technique involves suturing only the tendons that attach to the damaged bone fragments: for greater tubercle fractures, the supraspinatus and infraspinatus tendons are sutured, while for lesser tubercle fractures, the subscapularis tendon is fixed [9, 29]. However, in this approach, the supraspinatus tendons are sutured only at the fracture site, which leads to asymmetry in the tension vectors of the sutures during reduction and significantly complicates the process of precise plate positioning. Similar difficulties arise in the absence of a central pin, which performs the important function of centering the plate and ensuring its tight fit to the bone. The main surgical challenge lies in the difficulty of achieving anatomically precise and minimally invasive reduction of fragments while simultaneously eliminating obstacles to optimal plate placement.

Reduction of fragments requires the use of a significant number of auxiliary instruments, including multiple bone clamps. However, this technical approach is associated with a number of significant drawbacks. Firstly, manipulation of the clamps leads to additional trauma to the surrounding soft tissues. Secondly, there is a real risk of damaging vascular structures, particularly the posterior circumflex humeral artery and the axillary nerve, what can results in serious clinical consequences.

The literature describes a technique for fixing three- and four-part fractures of the posterior humeral circumflex humeral artery based on suturing the posterior humeral tendons followed by the use of an intramedullary nail [8, 10, 31]. This approach requires a transdeltoid surgical approach and is associated with a number of anatomical limitations and technical difficulties. To ensure full access to all necessary tendon structures, it is necessary to create a sufficiently large surgical field, which leads to increased trauma to the deltoid muscle, the risk of neuropathy of the axillary nerve and atrophy of the anterior portion of the deltoid muscle.

The bone fragment reduction method under consideration carries a significant risk of secondary displacement during implant placement: after traction on the fixation threads is released, the fragments return to their original position under muscular traction, and insertion of the intramedullary wire does not provide the centralized application of forces necessary to maintain reposition.

Additional technical difficulties arise from the specifics of proximal locking screw fixation. The bulky guides used for this purpose significantly interfere with maintaining traction via the joysticks, forcing the surgeon to perform the procedure in stages. This approach not only increases the duration of the surgery but also increases the likelihood of losing the achieved reduction, especially when working with osteoporotic bone tissue. This osteosynthesis method also has significant time limitations, demonstrating maximum effectiveness only when performed within the first five to seven days after the injury. After this term, the interfragmentary connective tissue scars create significant technical difficulties or completely exclude the possibility of precise reduction without performing additional surgical approaches for their excision.

The use of this technique in patients with osteoporotic bone changes, which is typical for the majority of patients with proximal humerus fractures, presents a particular challenge. Bone grafting is significantly complicated if an intramedullary nail is used. Accurate nail positioning, especially at the insertion site, is crucial. The slightest deviation from the optimal position leads to fixation failure, and subsequent removal of the nail creates insurmountable obstacles to alternative plate osteosynthesis due to secondary damage to bone structures and loss of anatomical landmarks.

This new technique for plate osteosynthesis of proximal humerus fractures minimizes soft tissue trauma through the use of thread joysticks, bone grafting materials, and a strict intraoperative procedure algorithm. It improves fixation quality and reduces complications.

The technique incorporates several fundamental components: allografts to restore humeral head anatomy in cases of bone mass deficiency, mandatory rotator cuff tendon suturing for additional stabilization in older patients, and a standardized fixation technique adapted for osteoporotic bone. These elements, taken together, ensure reliable fixation even in the most complex cases. The proposed technique demonstrates consistently good results regardless of patient age, although the best functional outcomes are observed in younger patients.

The data obtained convincingly demonstrate that the proposed comprehensive approach significantly improves treatment outcomes for patients with proximal humeral fractures. The technique combines technical simplicity with highly reproducible results, and makes its use a promising approach in modern traumatology. The advantages of the technique are evident not only in immediate postoperative results but also in the long-term follow-up, providing patients with rapid restoration of limb function and a high level of treatment satisfaction.

CONCLUSION

The surgical technique developed for patients with complex fractures of the surgical neck of the humerus represents an effective solution and demonstrates significant advantages over traditional approaches. A clearly structured algorithm facilitates the surgeon's surgical procedure, ensuring precise fragment reduction in patients of various age groups. A key achievement of the technique is a reduction in the average surgical time by 45 minutes (from 141 to 96 minutes) and improvement of functional outcomes, as demonstrated by an increase in the Constant – Murley score from 54 to 73 points.

Conflict of interests *None.*

Source of funding *The study was conducted with the support of Grant No. 1603-22/23 dated April 21, 2023.*

REFERENCES

1. Palvanen M, Kannus P, Niemi S, Parkkari J. Update in the epidemiology of proximal humeral fractures. *Clin Orthop Relat Res*. 2006;442:87-92. doi: 10.1097/01.blo.0000194672.79634.78.
2. Song JQ, Deng XF, Wang YM, et al. Operative vs. nonoperative treatment for comminuted proximal humeral fractures in elderly patients: a current meta-analysis. *Acta Orthop Traumatol Turc*. 2015;49(4):345-353. doi: 10.3944/AOTT.2015.14.0451.
3. Handoll HH, Elliott J, Thillemann TM, et al. Interventions for treating proximal humeral fractures in adults. *Cochrane Database Syst Rev*. 2022;6(6):CD000434. doi: 10.1002/14651858.CD000434.pub5.
4. Burkhart KJ, Dietz SO, Bastian L, et al. The treatment of proximal humeral fracture in adults. *Dtsch Arztebl Int*. 2013;110(35-36):591-597. doi: 10.3238/arztebl.2013.0591.
5. Tamimi I, Montesa G, Collado F, et al. Displaced proximal humeral fractures: when is surgery necessary? *Injury*. 2015;46(10):1921-1929. doi: 10.1016/j.injury.2015.05.049.
6. Magovern B, Ramsey ML. Percutaneous fixation of proximal humerus fractures. *Orthop Clin North Am*. 2008;39(4):405-416. doi: 10.1016/j.ocl.2008.05.005.
7. Siebenbürger G, Van Delden D, Helfen T, et al. Timing of surgery for open reduction and internal fixation of displaced proximal humeral fractures. *Injury*. 2015;46 Suppl 4:S58-62. doi: 10.1016/S0020-1383(15)30019-X.
8. Boudard G, Pomares G, Milin L, et al. Locking plate fixation versus antegrade nailing of 3- and 4-part proximal humerus fractures in patients without osteoporosis. Comparative retrospective study of 63 cases. *Orthop Traumatol Surg Res*. 2014;100(8):917-924. doi: 10.1016/j.otsr.2014.09.021.
9. Südkamp N, Bayer J, Hepp P, et al. Open reduction and internal fixation of proximal humeral fractures with use of the locking proximal humerus plate. Results of a prospective, multicenter, observational study. *J Bone Joint Surg Am*. 2009;91(6):1320-1328. doi: 10.2106/JBJS.H.00006.
10. Lekic N, Montero NM, Takemoto RC, et al. Treatment of two-part proximal humerus fractures: intramedullary nail compared to locked plating. *HSS J*. 2012;8(2):86-91. doi: 10.1007/s11420-012-9274-z.
11. Schulte LM, Matteini LE, Neviaser RJ. Proximal periarticular locking plates in proximal humeral fractures: functional outcomes. *J Shoulder Elbow Surg*. 2011;20(8):1234-1240. doi: 10.1016/j.jse.2010.12.015.
12. Agudelo J1, Schürmann M, Stahel P, et al. Analysis of efficacy and failure in proximal humerus fractures treated with locking plates. *J Orthop Trauma*. 2007;21(10):676-681. doi: 10.1097/BOT.0b013e31815bb09d.
13. Hertel R, Hempfing A, Stiehler M, Leunig M. Predictors of humeral head ischemia after intracapsular fracture of the proximal humerus. *J Shoulder Elbow Surg*. 2004;13(4):427-433. doi: 10.1016/j.jse.2004.01.034.

14. Vaza AYu, Fayn AM, Ivanov PA, et al. Analysis of the application of different bone grafting procedures in patients with intra-articular fractures. *The Russian Journal of Transplantation*. 2015;(4):6-12.
15. Chen H, Yin P, Wang S, et al. The Augment of the Stability in Locking Compression Plate with Intramedullary Fibular Allograft for Proximal Humerus Fractures in Elderly People. *Biomed Res Int*. 2018;2018:3130625. doi: 10.1155/2018/3130625.
16. Davids S, Allen D, Desarno M, et al. Comparison of Locked Plating of Varus Displaced Proximal Humeral Fractures With and Without Fibula Allograft Augmentation. *J Orthop Trauma*. 2020;34(4):186-192. doi: 10.1097/BOT.0000000000001679.
17. Biermann N, Prall WC, Böcker W, et al. Augmentation of plate osteosynthesis for proximal humeral fractures: a systematic review of current biomechanical and clinical studies. *Arch Orthop Trauma Surg*. 2019;139(8):1075-1099. doi: 10.1007/s00402-019-03162-2.
18. Panchal K, Jeong JJ, Park SE, et al. Clinical and radiological outcomes of unstable proximal humeral fractures treated with a locking plate and fibular strut allograft. *Int Orthop*. 2016;40(3):569-577. doi: 10.1007/s00264-015-2950-0.
19. Screw augmentation reduces motion at the bone-implant interface: a biomechanical study of locking plate fixation of proximal humeral fractures. *J Shoulder Elbow Surg*. 2015;24(12):1968-1973. doi: 10.1016/j.jse.2015.06.028.
20. Burkhart KJ, Dietz SO, Bastian L, et al. The treatment of proximal humeral fracture in adults. *Dtsch Arztebl Int*. 2013 ;110(35-36):591-597. doi: 10.3238/arztebl.2013.0591.
21. Besch L, Daniels-Wredenhagen M, Mueller M, et al. Hemiarthroplasty of the shoulder after four-part fracture of the humeral head: a long-term analysis of 34 cases. *J Trauma*. 2009;66(1):211-214. doi: 10.1097/TA.0b013e31815d9649.
22. Lanzetti RM, Gaj E, Berlinberg EJ, et al. Reverse Total Shoulder Arthroplasty Demonstrates Better Outcomes Than Angular Stable Plate in the Treatment of Three-part and Four-part Proximal Humerus Fractures in Patients Older Than 70 Years. *Clin Orthop Relat Res*. 2023;481(4):735-747. doi: 10.1097/CORR.0000000000002480.
23. Suroto H, De Vega B, Deapsari F, et al. Reverse total shoulder arthroplasty (RTSA) versus open reduction and internal fixation (ORIF) for displaced three-part or four-part proximal humeral fractures: a systematic review and meta-analysis. *EFORT Open Rev*. 2021;6(10):941-955. doi: 10.1302/2058-5241.6.210049.
24. Foruria AM. Plate Fixation of Proximal Humerus Fractures: How to Get It Right and Future Directions for Improvement. *Curr Rev Musculoskelet Med*. 2023;16(10):457-469. doi: 10.1007/s12178-023-09853-z.
25. Patel AH, Wilder JH, Ofa SA, et al. Trending a decade of proximal humerus fracture management in older adults. *JSES Int*. 2021;6(1):137-143. doi: 10.1016/j.jseint.2021.08.006.
26. Baker HP, Gutbrod J, Strelzow JA, et al. Management of Proximal Humerus Fractures in Adults-A Scoping Review. *J Clin Med*. 2022;11(20):6140. doi: 10.3390/jcm11206140.
27. Titov RS, Fain AM, Vaza AYu, et al. *Method for plastic surgery of bone defects of the humeral head in posterior blocked dislocations of the humerus*. Patent RF, no. 2831905. 2024. Available at: https://www.fips.ru/registers-doc-view/fips_servlet?DB=RUPAT&DocNumber=2831905&TypeFile=html. Accessed Jul 24, 2025. (In Russ.)
28. Nho SJ, Brophy RH, Barker JU, et al. Innovations in the management of displaced proximal humerus fractures. *J Am Acad Orthop Surg*. 2007;15(1):12-26. doi: 10.5435/00124635-200701000-00003.
29. Crosby LA, Neviaser RJ. *Proximal humerus fractures: Evaluation and management*. Springer; 2015:99-105. doi: 10.1007/978-3-319-08951-5.
30. Thelen S, Grassmann JP, Schneider M, et al. The influence of fracture severity on postoperative outcome and quality of life after locking plate fixation of proximal humeral fractures. *GMS Interdiscip Plast Reconstr Surg DGPW*. 2022;11:Doc03. doi: 10.3205/iprs000164.
31. Fu H, Wu J, Wu X. Intramedullary Nail for Treatment of Proximal Humeral Fracture: A Credible Fixation in Comminuted Calcar. *Orthop Surg*. 2023;15(8):2007-2015. doi: 10.1111/os.13616.

The article was submitted 25.03.2025; approved after reviewing 20.06.2025; accepted for publication 14.10.2025.

Information about the authors:

Roman S. Titov — Candidate of Medical Sciences, Senior Researcher,
TitovRS@sklif.mos.ru, https://orcid.org/0000-0002-2960-8736;

Alexey M. Fain — Doctor of Medical Sciences, Head of Research Department, Professor of the Department,
FainAM@sklif.mos.ru, https://orcid.org/0000-0001-8616-920X;

Alexander Yu. Vaza — Candidate of Medical Sciences, Head of Research Department,
VazaAU@sklif.mos.ru, https://orcid.org/0000-0003-4581-449X;

Natalia V. Borovkova — Doctor of Medical Sciences, Head of the Research Department,
BorovkovaNV@sklif.mos.ru, https://orcid.org/0000-0002-8897-7523;

Sergey F. Gnetetskiy — Doctor of Medical Sciences, Leading Researcher, Professor of the Department,
sgnetetskii@mail.ru, https://orcid.org/0000-0001-9932-1653;

Irina I. Mazhorova — Candidate of Medical Sciences, Senior Researcher,
shinycoin@yandex.ru, https://orcid.org/0000-0001-9109-0790;

Konstantin A. Rozhkov — rozhkov.co@gmail.com, https://orcid.org/0009-0005-9805-8693;

Kristina I. Skuratovskaya — research fellow, SkuratovskayaKI@sklif.mos.ru, https://orcid.org/0000-0003-3074-453X.

Original article
https://doi.org/10.18019/1028-4427-2025-31-6-720-728

An observational study on radiological and functional outcome of cross-pinning versus parallel pinning in supracondylar humerus fracture

K. Kumar, J. Khan, M. Jindal

Kalpana Chawla Government Medical College and Hospital, Karnal, Haryana, India

Corresponding author: Mohit Jindal, drmohitjindalortho@gmail.com

Abstract

Introduction Supracondylar humerus fractures are the most common elbow fractures in children, often resulting from falls on an outstretched hand. The standard treatment for displaced fractures involves closed reduction and percutaneous pinning. However, the optimal pin configuration — cross-pinning (medial-lateral) versus parallel pinning (lateral-lateral) — remains a topic of debate due to concerns regarding stability and risk of iatrogenic ulnar nerve injury.

Aims This study aims to compare the clinical and radiological outcomes of cross-pinning versus parallel pinning in the management of displaced supracondylar humerus fractures in children.

Methods A prospective observational study was conducted over 18 months at Kalpana Chawla Govt. Medical College, Karnal, Haryana. A total of 54 children aged 3–12 years with Gartland type III supracondylar humerus fractures were enrolled. Patients were divided into two groups based on the surgical technique: cross-pinning ($n = 27$) and parallel pinning ($n = 27$). Both groups were comparable in terms of demographics, mechanism of injury, and pre-operative neurovascular status. Functional and radiographic outcomes were evaluated using Flynn's criteria, Baumann's angle, carrying angle, and range of motion at follow-up intervals (3, 6, 10, 14, and 24 weeks).

Results Mean Baumann's angle, Carrying angle and range of motion showed no statistically significant differences between the two groups. At the final follow-up, 92.6 % of patients in the parallel pinning group had excellent outcomes per Flynn's criteria, compared to 51.9 % in the cross-pinning group ($p < 0.01$). One patient in the cross-pinning group developed ulnar nerve neuropraxia, whereas no cases of nerve injury were reported in the parallel pinning group.

Conclusion Parallel pinning demonstrated superior radiological and functional outcomes, with a lower risk of ulnar nerve injury compared to cross pinning. These findings suggest that parallel pinning should be the preferred method for stabilizing displaced supracondylar humerus fractures in children.

Keywords: supracondylar humerus fracture, cross-pinning, parallel pinning, Baumann's

For citation: Kumar K, Khan J, Jindal M. An observational study on radiological and functional outcome of cross-pinning versus parallel pinning in supracondylar humerus fracture. *Genij Ortopedii*. 2025;31(6):720-728. doi: 10.18019/1028-4427-2025-31-6-720-728.

INTRODUCTION

Supracondylar fractures of the humerus accounts for 18 % of paediatric fractures and 60 % of elbow fractures [1]. In 1959 Dr. J.J. Gartland [2] described that even expert trauma surgeons are anxious and apprehensive while managing supracondylar humerus fractures. Despite evolutions in the evaluation and treatment over the years, these fractures still pose considerable challenges to orthopaedic surgeons. They most frequently occur in children aged 5 to 7 years. The median age is approximately six years, and the incidence gradually decreases with age [3]. Extension-type fractures are much more common than flexion-type fractures and occur as a result of a fall on an outstretched hand [4]. Flexion-type fractures are more prevalent in older children [4].

Lateral pins and crossed-pins bicortical constructs can be used to treat supracondylar humerus fractures. Lateral pin configurations are frequently used and they reduce the risk of iatrogenic ulnar nerve injury.

The use of crossed-pins increases the risk of iatrogenic ulnar nerve injury; however, they improve the torsional rigidity of the construct as compared to the use of two lateral pins. A medial incision should be made of an adequate size that will allow the protection of the ulnar nerve before inserting a medial pin. A further way to reduce the risk of iatrogenic ulnar nerve injury is to extend the elbow while inserting the medial pin [5].

There is a debate about the best management approach to treat supracondylar fractures of humerus in children. Therefore, the present study was done to compare the outcome of the cross-pinning vs parallel pinning in displaced supracondylar humerus fracture in children.

The **aim** of this study is to compare the outcome of the cross-pinning versus parallel pinning for displaced supracondylar humeral fracture in children.

MATERIAL AND METHODS

This prospective observational clinical study was conducted at the Department of Orthopedics of Kalpana Chawla Government Medical College, Karnal, India from June 2023 to April 2025 after approval of institutional ethical committee. Informed written consent was taken from all the parents of children.

Sample size was calculated by taking values from previous studies at 80 % confidence interval and 70 % power using Kelsey Formula:

$n = 2\ (Z\alpha/2 + Z\beta)^2\ P(1–P)\ /\ 1\ (P_1 – P_2)^2$;

$P = P_1 + P_2\ /\ 2 = 2 + 33.3\ /\ 2 = 17.65\ \%$,

P_2 = prevalence in cross-pinning, P_2 = prevalence in parallel pinning.

In the study by R.K. Rupesh et al. [6], prevalence in cross-pinning = 2 % and prevalence in parallel pinning = 33.3 %. $Z\alpha/2$ = standard normal variate at 95 % confidence interval and 5 % level of significance = 1.96. $Z\beta$ = standard normal variate at 80 % power = 0.84. So, $n = 2\ [(1.96 + 0.84)^2\ (0.18)\ (0.82)]/(0.31)^2 = 24$ in each group. Taking drop-out rate of 10 % sample size in each group will be = 27. Group A (cross-pinning) had 27 patients. Group B (parallel pinning) had 27 patients. The decision to undergo cross or parallel pinning was made by the operating surgeon.

Children aged between 3–12 years with Gartland type III supracondylar humeral fracture were included in the study. While children with open fractures, fractures that require open reduction, fractures with vascular injuries, previous ipsilateral elbow fracture and those presenting after three days of injury were excluded from the study. The patients underwent anteroposterior and lateral radiographs. All displaced humerus supracondylar fractures were admitted and immobilized with an above-elbow splint and limb elevation. Surgical technique was standardized in terms of pin location, pin size (for weight 20 kg size 1.5-mm K-wire and for weight > 20 kg 2-mm K-wire was used), stability on the operation table, and elbow placement position.

A senior orthopedic surgeon performed the operation. In a supine position with the injured upper limb resting on the table edge, an anesthesia was administered to all patients. A closed reduction was performed. First, traction was applied longitudinally with the elbow in hyperextension and the forearm in supination. While maintaining traction, the medial or lateral displacement was corrected at the fracture site by administering a valgus or varus force. The posterior displacement of the distal fragment was then corrected by applying force to the posterior aspect of the fragment while the elbow was gently flexed and secured in hyperflexion and the reduction was confirmed by the image intensifier. For parallel pin fixation technique, two or three pins were inserted from the lateral aspect of the elbow across the lateral cortex in order to engage the medial cortex while maintaining hyperflexion of the elbow. At the fracture site, pins were positioned either in parallel or divergent configurations with adequate separation. For cross-pinning (medial-lateral) fixation technique, the lateral pin was inserted from the lateral cortex into the medial cortex while maintaining hyperflexion of the forearm. The medial pin was inserted with the elbow in extension. Under image intensification, the reduction was evaluated for sufficiency and fracture stability. The pins were bent to prevent migration and cut outside of the epidermis to facilitate removal in an outpatient clinic. A single parenteral dose of antibiotic was administered preoperatively 30 minutes before induction and postoperatively, according to child's weight. The extremity was immobilized postoperatively in a well-cushioned posterior splint with the elbow flexed to 90 degrees. Postoperative radiographs were taken to ascertain the stability of the reduction. All the children with supracondylar fractures of the humerus were assessed for vascular and neurological status at every follow-up visit. At the end of third postoperative week, K-wires were removed. Functional and radiographic outcomes were evaluated using Flynn's criteria, Baumann's angle, carrying angle, and range of motion at follow-up intervals (3, 6, 10, 14, and 24 weeks). Using the Flynn's criteria, the results were graded as excellent, good, fair, or poor based on the loss of range of motion and loss of carrying angle [7] (Table 1).

Table 1

Flynn's criteria for grading of functional and cosmetic results

Rating		Cosmetic factor: Carrying angle loss (°)	Functional factor: Movement loss (°)
Satisfactory	Excellent	0–5	0–5
	Good	5–10	5–10
	Fair	10–15	10–15
Unsatisfactory	Poor	> 15	> 15

Statistical Analysis

The analysis included profiling of patients on different demographic, radiological and clinical parameters. Descriptive analysis of quantitative parameters was expressed as means and standard deviation. Ordinal data were expressed as absolute number and percentage. Chi-square test was applied to compare carrying angle and range of motion between patients undergoing cross-pinning and parallel pinning. The normality of variables was checked by Kolmogorov – Smirnov test. Baumann's angle was compared between cross-pinning and parallel pinning using unpaired Student t-test. A p-value < 0.05 was considered statistically significant. All analysis was done using SPSS software, version 24.0.

RESULTS

In the present study, mean age of patients in cross-pinning group and parallel pinning group was 6.8 years and 7.3 years respectively, with no significant difference between them (p value = 0.82). It was observed that supracondylar fractures were most common between 6 to 10 years (Table 2)

In terms of gender distribution, 68.5 % of the children were males (n = 37) and rest were females (31.5 %, n = 17). The two study groups were similar with respect to gender distribution of patients (p-value = 0.76) (Table 3).

The mechanism of injury was fall from height in 13 % of children, 20.4 % had road traffic accident and 66.7 % had sports related injuries. Both study groups were similar with respect to mechanism of injury (p-value = 0.89) (Table 4).

It was observed that one child in the parallel pinning group had associated distal radial fracture. No other children had any other associated injury (Table 5).

Table 2

Comparison of age groups distribution between cross-pinning and parallel pinning group

Age groups (years)		Group Cross-pinning	Group Parallel pinning	Total patients
Less than 5	*n*	5	3	8
	%	18.50	11.10	14.80
6 to 10	*n*	20	22	42
	%	74.10	81.50	77.80
11 to 12	*n*	2	2	4
	%	7.40	7.40	7.40
Total	*n*	27	27	54
	%	100.00	100.00	100.00
p-value		0.88		
Mean age (years)		6.8 ± 1.7	7.3 ± 1.7	
p-value		0.82		

p-value analyzed using independent t-test.

Table 3

Comparison of gender distribution between cross-pinning and parallel pinning group

Gender		Group Cross-pinning	Group Parallel pinning	Total patients
Female	*n*	8	9	17
	%	29.60	33.30	31.50
Male	*n*	19	18	37
	%	70.40	66.70	68.50
Total	*n*	27	27	54
	%	100.00	100.00	100.00
p-value		0.88		

p-value analyzed using independent t-test.

Table 4

Comparison of mechanism of injury between cross-pinning and parallel pinning group

Mechanism of injury		Group Cross-pinning	Group Parallel pinning	Total patients
Fall from height	*n*	4	3	7
	%	14.80	11.10	13.00
Road traffic accident	*n*	5	6	11
	%	18.50	22.20	20.40
Sports	*n*	18	18	36
	%	66.70	66.70	66.70
Total	*n*	27	27	54
	%	100.00	100.00	100.00
p-value		0.88		

p-value analyzed using Fisher's exact test.

Table 5

Comparison of associated injury between cross-pinning and parallel pinning group

Associated injury		Group Cross-pinning	Group Parallel pinning	Total patients
Distal radial fracture	*n*	0	1	1
	%	0.00	3.70	1.90
None	*n*	27	26	53
	%	100.00	96.30	98.10
Total	*n*	27	27	54
	%	100.00	100.00	100.00
p-value		0.5		

p-value analyzed using Fisher's exact test.

Pre-operatively, in the cross-pinning group, 11.1 % had cubital region paresthesia and 18.5 % had ulnar nerve neuropraxia, while in the parallel pinning group 18.5 % had cubital paresthesia and 11.1 % had ulnar nerve neuropraxia. Both the groups were similar with respect to pre-operative neurovascular status (*p*-value = 0.64) (Table 6).

Mean operative time was 34.2 ± 3.05 min in the cross-pinning group, while it was 34.8 ± 0.5 min in the parallel pinning group, with no significant difference between them (*p*-value = 0.51) (Table 7).

Table 6

Comparison of pre-operative neurovascular status between cross-pinning and parallel pinning group

Mechanism of injury		Group Cross-pinning	Group Parallel pinning	Total patients
Fall from height	*n*	4	3	7
	%	14.80	11.10	13.00
Road traffic accident	*n*	5	6	11
	%	18.50	22.20	20.40
Sports	*n*	18	18	36
	%	66.70	66.70	66.70
Total	*n*	27	27	54
	%	100.00	100.00	100.00
p-value		0.88		

p-value analyzed using Fisher's exact test.

Table 7

Comparison of mean operative time between cross-pinning and parallel pinning group

Operative time (mins)				
Group Cross pinning		Group Parallel pinning		*p*-value
Mean	SD	Mean	SD	
34.26	3.058	34.85	3.416	0.51

p-value analyzed using independent t-test.

At 3-weeks post-operatively, mean carrying angle was found to be 9 ± 0.8 and 9 ± 0.9 degrees (*p*-value = 0.9) in the cross-pinning and parallel pinning group, respectively. Further on, the mean carrying angle was 9.6 and 9.5 degrees at post-operative week 6, 10.4 and 10.6 degrees at week 10, 11.6 and 11.4 degrees at week 14 and 10.1 and 10.3 degrees at post-operative week 24 in cross-pinning and parallel pinning group, respectively. The mean carrying angle was found to be statistically insignificant at different follow-up examination (Table 8).

The mean Baumann's angle was found to be statistically insignificant at different follow-up examinations (Table 9).

Table 8

Comparison of mean carrying angle between cross-pinning and parallel pinning group at different follow up

Postoperative carrying angle	Group Cross-pinning		Group Parallel pinning		*p*-value
	Mean	SD	Mean	SD	
3rd week	9.0	0.8	9.0	0.9	0.9
6th week	9.6	1.2	9.5	1.1	0.8
10th week	10.4	1.1	10.6	1.1	0.4
14th week	11.6	1.1	11.4	1.1	0.4
24th week	10.1	0.9	10.3	1.1	0.4

p-value analyzed using independent t-test.

Table 9

Comparison of mean Baumann's angle between cross-pinning and parallel pinning group at different follow up

Baumann's angle	Group Cross-pinning		Group Parallel pinning		*p*-value
	Mean	SD	Mean	SD	
3rd week	66.3	2.2	68.8	2.2	0.407
6th week	68.3	1.8	67.4	1.9	0.693
10th week	70.4	1.8	71.5	1.8	0.312
14th week	71.3	1.9	73.8	2.2	0.158
24th week	72.0	1.5	74.9	2.5	0.377

p-value analyzed using independent t-test.

It was observed that range of motion (ROM) was reduced in 18.5 % of cross-pinning patients and in 7.4 % of parallel pinning group at week 3. At 6th week, ROM was reduced in 11.1 % of cross-pinning and in 3.7 % of parallel pinning group patients. At subsequent follow ups, ROM was normal in all patients in both study groups (Table 10).

Table 10

Comparison of range of motion between cross-pinning and parallel pinning group at different follow-ups

Range of motion			Group Cross pinning	Group Parallel pinning	Total patients	*p*-value
3rd week	Normal	*n*	22	25	47	0.42
		%	81.50	92.60	87.00	
	Reduced	*n*	5	2	7	
		%	18.50	7.40	13.00	
6th week	Normal	*n*	24	26	50	0.61
		%	88.90	96.30	92.60	
	Reduced	*n*	3	1	4	
		%	11.10	3.70	7.40	
10th week	Normal	*n*	27	27	54	NA
		%	100.00	100.00	100.00	
14th week	Normal	*n*	27	27	54	NA
		%	100.00	100.00	100.00	
24th week	Normal	*n*	27	27	54	NA
		%	100.00	100.00	100.00	
Total		*n*	27	27	54	
		%	100.00	100.00	100.00	

p-value analyzed using Fisher's exact test.

Post-operatively, there was one patient in the cross-pinning group who had ulnar nerve injury. Other than that, none of the patients had pin loosening, superficial infection or any other complications (Table 11).

Post-operative neurovascular examination revealed ulnar nerve neuropraxia in only one patient from cross-pinning group which was not statically significant (Table 12).

Table 11

Comparison of post-operative complications between cross-pinning and parallel pinning group

Post-op complications		Group Cross pinning	Group Parallel pinning	Total patients	*p*-value
Ulnar nerve injury	*n*	1	0	1	0.31
	%	3.70	0.00	1.80	
Pin loosening	*n*	0	0	0	NA
	%	0.00	0.00	0.00	
Superficial infection	*n*	0	0	0	NA
	%	0.00	0.00	0.00	
None	*n*	26	27	53	0.31
	%	96.30	100.00	98.20	
Total	*n*	27	27	54	
	%	100.00	100.00	100.00	

p-value analyzed using Fisher's exact test.

Table 12

Comparison of post-operative neurovascular status between cross-pinning and parallel pinning groups

Post-op complications		Group Cross pinning	Group Parallel pinning	Total patients	*p*-value
Ulnar nerve neuropraxia	*n*	1	0	1	0.75
	%	3.70	0	1.8	
Normal	*n*	26	27	53	
	%	96.30	100	98.2	
Total	*n*	27	27	54	
	%	100.00	100.00	100.00	

p-value analyzed using Fisher's exact test.

Based on Flynn's criteria, at last follow-up, significantly higher proportion of patients in the parallel pinning group had an excellent outcome as compared to cross-pinning group (92.6 % vs 51.9 %, *p*-value < 0.01) which was statically significant. In the cross-pinning group, the outcome was good in 37 % and fair in 11.1 %, while in the parallel pinning group, the outcome was good in 3.7 % and fair in 3.7 % (Table 13).

Table 13

Comparison of post-operative outcomes based on Flynn`s criteria between cross-pinning and parallel pinning groups at final follow-up

Flynn criteria		Group Cross pinning	Group Parallel pinning	Total patients	*p*-value
Excellent	*n*	14	25	39	< 0.01
	%	51.90	92.60	72.20	
Good	*n*	10	1	11	
	%	37.00	3.70	20.40	
Fair	*n*	3	1	4	
	%	11.10	3.70	7.40	
Total	*n*	27	27	54	
	%	100.00	100.00	100.00	

p-value analyzed using Fisher's exact test.

DISCUSSION

The goal of surgery in any fracture should be secure fixation, early rehabilitation, early functional recovery and minimal/no complications. This prospective observational study was done to compare the outcome of the cross-pinning versus parallel pinning in displaced supracondylar humeral fracture in children. In the present study, mean age of children in cross-pinning group and parallel pinning group was 6.8 years and 7.3 years respectively, with no significant difference between them (*p*-value = 0.82). 68.5 % of the patients were males (*n* = 37) and rest were females (31.5 %, *n* = 17) which was similar to the study done by Afaque et al. [8]; in that study the mean age of the patient at the time of presentation was 6.8 ± 0.9 years in the lateral pinning group and 7.2 ± 0.8 years in the cross-pinning group. In study by Mandal et al. [9], males constituted 68.34 % of the study population while females constituted 31.66 % of the study population which showed similar gender distribution as in the present study. Whereas in a study by Rupesh et al. [6], the mean age of patients in cross-pinning and parallel pinning groups was 7.5 years and 7.7 years, respectively.

Out of 64 subjects, 34 subjects were males (53 %) and 30 were females (46 %). In another study done by Singh et al. [10], the mean age in the lateral pinning group was 8.26 years, whereas it was 8.54 years in the cross-pinning group. In the study done by Khan et al. [11], there were 50 (59.5 %) males and 34 (40.5 %) were females. Mean age of the patients in the cross-pinning group was 5.14 ± 9.88 years and in the parallel pinning group it was 6.14 ± 8.35 years.

In the present study, 13 % had a fall from height, 20.4 % had road traffic accidents and 66.7 % had sports related injuries. Study done by Khan et al. [11] showed similar findings in terms of mechanism of injuries which showed sports was the most common cause of fracture in 71.43 % of children followed by road traffic accident in 20.24 % and the rest were 8.3 % due to fall from the height. Whereas in the study done by Rupesh et al. [6], mechanism of injuries in majority of children (53 %) was slip and fall, 45.3 % had fall from height and 1.6 % had fall from height while playing. In the study by Singh et al. [10], the most common cause of injury was fall from height in 63.9 % of children followed by fall during playing in 29.5 % of children and by road traffic accidents in 6.5 % children. Afaque et al. [8] reported fall from height was the commonest mode of injury. In the present study, the mean operative time was 34.2 ± 3.05 minutes in the cross-pinning group, while it was 34.8 ± 0.5 min in the parallel pinning group, with no significant difference between them (p-value = 0.51) whereas the study done by Khan et al. [11] showed the mean surgical time in cross-pinning group was 30.42 ± 6.09 minutes while in the lateral pinning group it was 34.24 ± 2.16 minutes. In the present study, at 3-weeks post-operatively, the mean carrying angle was 9 ± 0.8 and 9 ± 0.9 degrees (p-value = 0.9) in the cross-pinning and parallel pinning groups, respectively. Furthermore, the mean carrying angle was 9.6 and 9.5 degrees at post-op 6th week, 10.4 and 10.6 degrees at post-op 10th week, 11.6 and 11.4 degrees at post-op 14th week and 10.1 and 10.3 degrees at post-op 24th week in cross-pinning and parallel pinning groups, respectively. The mean carrying angles were similar between cross-pinning and parallel pinning groups at all post-operative follow-ups. The mean Baumann’s angle was found to be statistically insignificant at different follow-up examination. Also, the range of motion was reduced in 18.5 % of cross-pinning children and in 7.4 % of parallel pinning group at 3rd week post-operative. At 6th week, ROM was reduced in 11.1 % of cross-pinning and in 3.7 % of parallel pinning group patients. At subsequent follow-ups, ROM was normal in all patients in both study groups. Study done by Rupesh et al. [6] showed similar results. It showed that the carrying angle in the cross pinning group vs parallel pinning group was 11.18 ± 1.99 vs 11.96 ± 1.92 degrees. The Baumann’s angle in the cross pinning group vs parallel pinning group was 71.59 ± 3.10 vs 71.65 ± 2.23 degrees. Also, in the study done by Singh et al. [10], there was no significant difference (p > 0.05) regarding the change in Baumann`s angle, carrying angle and elbow range of motion. Similar findings were observed in the study done by Eguia et al. [12] which showed that there was no significant difference in Baumann`s angle with p-value > 0.05 between groups.

Similar to our findings, Afaque et al. [8] also reported that the change in Baumann angle, change in carrying angle, range of motion in flexion and extension of the elbow were not significantly different at any point of time between two groups. In the study Younus et al. [13], the final clinical outcome at 6 months follow-up was assessed by examining range of motion at the affected elbow. 99 children achieved full range of motion at 6 months. The remaining 11 patients (5 of them had lateral pinning and 6 had crossed wiring) were advised to continue physiotherapy. The difference in this parameter was statistically insignificant among the two groups (p-value = 0.12). In a similar study, Sapkota et al. [14] observed that there was no statistical significance in comparing Baumann’s angle after the intervention and at the last follow-up examination. By comparing the mean, there was no significant change in Baumann’s angle.

In the present study, post-operatively there was one child in the cross-pinning group who had ulnar nerve neurapraxia. Other than that, none of the patients had pin loosening, superficial infection or any other complications. In a systematic review study, Brauer et al. [15] reported that the rate of iatrogenic injury of the ulnar nerve from cross-entry pin fixation was 3.3 % and cross-entry pin fixation method has 4.86 times higher risk for developing iatrogenic nerve injury than the lateral pinning fixation method. In the study done by Shim et al. [16], it was observed that the risk of iatrogenic nerve injury can be minimized with small incision over the medial aspect of the elbow and putting the elbow in extension at the time of medial pin. The majority of iatrogenic injury of the ulnar nerve due to placement of medial pin resolves spontaneously [17]. In the study done by Singh et al. [10], postoperative complication such as superficial pin-tract infection was present in 2 cases (6.67 %) of the lateral pinning group and one case (3.22 %) in the cross-pinning group.

All the infections subsided during follow-up. Iatrogenic ulnar nerve neuropraxia was present in 6.4 % of cases of the cross-pinning group, and it recovered fully within 3 weeks. Khan et al. [11] observed that the most common complication in the cross-pinning group was superficial infection in 5 cases (11.9 %) followed by pin loosening in 3 cases (7.14 %) and ulnar nerve neuropraxia in one case (2.4 %) but in the lateral pinning group the most common complication found in 4 cases (9.5 %) was superficial infection followed by pin loosening in 2 cases (4.8 %). In the study by Eguia et al. [12], 5 participants (3.5 %) experienced superficial pin-site infection (4 in the crossed pinning group and one in the lateral pinning group) (p-value = 0.05). Two participants in the lateral pinning group had postoperative neurological complications compared with none in the crossed pinning group (p-value = 1.0). Neurological complications were seen in one case due to radial nerve palsy. In the study by SAfaque et al. [8], two patients in the cross-pinning group developed tingling sensation and numbness in ulnar nerve distribution with intact motor function which was seen after two days of surgery. On subsequent follow-up, all three patients recovered. In the study done Younus et al. [13], three patients (2.7 %) had ulnar nerve injury which all eventually recovered. The difference in this important complication was statistically insignificant ($p = 0.082$). Four patients had superficial pin-site infection during the follow-up which was treated with oral antibiotics. Sapkota et al. [14] observed that there were 4 cases (11.76 %) with nerve palsy associated with supracondylar fractures. Three patients had radial nerve palsy and one had median nerve palsy. One patient had iatrogenic ulnar nerve injury following fixation with cross K-wires. All of them recovered completely by 3 months. Superficial pin-tract infection was detected in five cases at the time of pin removal.

In the present study, based on Flynn’s criteria, at the final follow-up, a significantly higher proportion of patients in the parallel pinning group had an excellent outcome as compared to the cross-pinning group, 25 patients (92.6 %) versus 15 patients (51.9 %), with p-value < 0.01. In the studies done by Rupesh et al. [6] and Flynn et al. [18], 100 % of the patients in the parallel group had excellent scores whereas in the cross-pinning group, 94 % had excellent results. Singh et al. [10] also observed that the final result was excellent in 49 cases (80.32 %) and was good in 12 cases (19.67 %). Excellent outcome was found in 23 cases (76.67 %) of the lateral pinning group and 26 cases (83.87 %) of the cross pinning group. The outcome of 7 cases (23.33 %) in the lateral pinning group and 5 cases (16.12 %) in the cross-pinning group was found good. Khan et al. [11] observed that according to Flynn’s criteria, excellent results in the cross-pinning group were found in 25 cases (59.5 %), good results in 12 cases (28.6 %) and fair results found in 5 cases (11.9 %) while in the lateral pinning group excellent results were found in 23 cases (54.8 %), good results in 15 cases (35.7 %) and fair results in 4 cases (9.5 %). Eguia et al. [12] found no significant differences between crossed versus lateral pinning groups in any patient reported outcomes (PROs). Mean QuickDASH scores were 1.6 in the crossed pinning group and 3.0 in the lateral pinning group (p-value = 0.14). Mean PROMIS (Patient-Reported Outcomes Measurement Information system) scores in the crossed pinning versus lateral pinning groups were 57 versus 56 for the upper extremity domain; 54 versus 53 for strength impact; and 12 in both groups for pain interference (all, p-value > 0.05). Afaque et al. [8] observed that according to Flynn's grading, 26 patients in the lateral pinning group and 24 patients in the cross-pinning group had excellent results, 7 patients in the lateral pinning group and 15 in the cross-pinning group had good result, 4 patients in the lateral pinning group and one in the cross-pinning group had fair results, respectively. None of the patients in either group had poor results on the basis of Flynn's criteria. Sapkota et al. [14] observed that according to Flynn’s criteria in both groups more than 95 percent of cases had good to excellent results.

Limitation A large sample size is needed to determine which approach is better (cross-pinning vs lateral pinning) to treat displaced supracondylar fracture of humerus.

CONCLUSION

Parallel pinning demonstrated superior radiological and functional outcomes with a lower risk of ulnar nerve injury compared to cross pinning. These findings suggest that parallel pinning should be the preferred method for stabilizing displaced supracondylar humerus fractures in children.

Future multicentric studies with larger sample size are required to support our finding.

Conflicts of interest *None.*

Funding *None.*

REFERENCES

1. Shenoy PM, Islam A, Puri R. Current Management of Paediatric Supracondylar Fractures of the Humerus. *Cureus*. 2020;12(5):e8137. doi: 10.7759/cureus.8137.
2. Gartland JJ. Management of supracondylar fractures of the humerus in children. *Surg Gynecol Obstet*. 1959;109(2):145-154.
3. Mostafa E, Imonugo O, Varacallo MA. Anatomy, Shoulder and Upper Limb, Humerus. 2023 Aug 7. In: *StatPearls* [Internet]. Treasure Island (FL): StatPearls Publishing; 2025.
4. Landin LA, Danielsson LG. Elbow fractures in children. An epidemiological analysis of 589 cases. *Acta Orthop Scand*. 1986;57(4):309-312. doi: 10.3109/17453678608994398.
5. Ersan O, Gonen E, İlhan RD, et al. Comparison of anterior and lateral approaches in the treatment of extension-type supracondylar humerus fractures in children. *J Pediatr Orthop B*. 2012;21(2):121-126. doi: 10.1097/BPB.0b013e32834dd1b2.
6. Rupesh RK, Mahendhira JV, Gopinath G. A comparative study of functional outcome of criss-cross pinning Vs parallel pinning for Gartland type III supracondylar humeral fractures in children in tertiary care centre. *Int J Orthop Sci*. 2023;5(1):170-174. doi: 10.22271/ortho.2023.v9.i1c.3292.
7. Flynn JC, Matthews JG, Benoit RL. Blind pinning of displaced supracondylar fractures of the humerus in children. Sixteen years' experience with long-term follow-up. *J Bone Joint Surg Am*. 1974;56(2):263-272.
8. Afaque SF, Singh A, Maharjan R, et al. Comparison of clinic-radiological outcome of cross pinning versus lateral pinning for displaced supracondylar fracture of humerus in children: A randomized controlled trial. *J Clin Orthop Trauma*. 2020;11(2):259-263. doi: 10.1016/j.jcot.2019.01.013.
9. Mandal J, Sarkar P, Singh A, et al. Study of clinical and radiological outcomes in paediatric supracondylar humerus fractures treated with 3 lateral pins versus crossed pins. *Int J Orthop Sci*. 2018;4(2):745-749. doi: 10.22271/ortho.2018.v4.i2k.108.
10. Singh SK, Singh P, Gill SP, et al. A comparative study of cross pinning versus lateral pinning technique in the management of completely displaced type-III supra condylar humerus fracture in the rural India children: A prospective study. *J Orthop Traumatol Rehabil*. 2021;13:122-128. doi: 10.4103/jotr.jotr_13_21,
11. Khan AA, Younas MO, Mehmood AS, Laraib BI. Compare the functional outcomes of closed reduction and percutaneous cross pinning versus lateral pinning in supracondylar fracture of humerus in children. *Pak J Med Health Sci*. 2021;15(8):2154-2156. doi: 10.53350/pjmhs211582154.
12. Eguia F, Gottlich C, Lobaton G, et al. Mid-term Patient-reported Outcomes After Lateral Versus Crossed Pinning of Pediatric Supracondylar Humerus Fractures. *J Pediatr Orthop*. 2020;40(7):323-328. doi: 10.1097/BPO.0000000000001558.
13. Younus S, Peracha A, Shah SK, et al. Percutaneous Pinning for Displaced Supracondylar Humerus Fractures in Pediatric Age Group: Comparison between Lateral Pinning Versus Crossed Pinning Techniques. *OROAJ*. 2018;11(3): 555817. doi: 10.19080/OROAJ.2018.11.555817.
14. Sapkota K, Wahegaonkar K, Ranjeet N, et al. Comparison of cross pinning versus lateral three pins in type three supracondylar fracture of distal humerus in children. *Asian J Me Sci*. 2019;10(2):58-61. doi: 10.3126/ajms.v10i2.22034.
15. Brauer CA, Lee BM, Bae DS, et al. A systematic review of medial and lateral entry pinning versus lateral entry pinning for supracondylar fractures of the humerus. *J Pediatr Orthop*. 2007;27(2):181-186. doi: 10.1097/bpo.0b013e3180316cf1.
16. Shim JS, Lee YS. Treatment of completely displaced supracondylar fracture of the humerus in children by cross-fixation with three Kirschner wires. *J Pediatr Orthop*. 2002;22(1):12-16.
17. Green DW, Widmann RF, Frank JS, Gardner MJ. Low incidence of ulnar nerve injury with crossed pin placement for pediatric supracondylar humerus fractures using a mini-open technique. *J Orthop Trauma*. 2005;19(3):158-163. doi: 10.1097/00005131-200503000-00002.
18. Flynn JC, Matthews JG, Benoit RL. Blind pinning of displaced supracondylar fractures of the humerus in children. Sixteen years' experience with long-term follow-up. *J Bone Joint Surg Am*. 1974;56(2):263-272.

The article was submitted 28.04.2025; approved after reviewing 29.05.2025; accepted for publication 14.10.2025.

Information about the authors:

Kuljit Kumar — MBBS, MS, Professor, koolguy0062008@gmail.com, https://orcid.org/0009-0007-6462-4102;

Javed Khan — MBBS, Junior Resident, drkhanjaved8887@gmail.com;

Mohit Jindal — MBBS, MS, Associate Professor, drmohitjindalortho@gmail.com, https://orcid.org/0000-0002-1699-456X.

Original article
https://doi.org/10.18019/1028-4427-2025-31-6-729-736

Algorithm for postoperative management of patients after ankle replacement surgery

G.P. Kotelnikov[1], V.V. Ivanov[1], A.N. Nikolaenko[1], A.P. Borisov[1]✉, N.A. Shchekotikhin[2], K.V. Antonova[1], M.G. Gadzhiev[1]

[1] Samara State Medical University, Samara, Russian Federation

[2] Samara Medical Institute REAVIS, Samara, Russian Federation

Corresponding author: Alexander P. Borisov, dr_borisov71@mail.ru

Abstract

Introduction Total ankle arthroplasty (TAA) can be associated with postoperative difficulties during the rehabilitation phase. A unified, tailored approach to rehabilitation and postoperative care is essential for the patients.

The **objective** was to evaluate clinical effectiveness of the algorithm developed for postoperative management of TAA patients to improve functional recovery, reduce postoperative complications for greater patient satisfaction.

Material and methods The study included 28 patients with impaired distal tibia and the ankle. The surgical treatment performed after a comprehensive examination included segmental resection of the distal tibia and ankle replacement of the original design. The implant had an articulating ankle joint and the distal tibia replacement. The algorithm developed for postoperative rehabilitation relied on a six-level approach borrowed from rehabilitation guidelines for total ankle arthroplasty devised at the Massachusetts General Hospital.

Results Postoperative management included multimodal analgesia with a regional component, multi-level prophylaxis of infection, antithrombotic protection and staged immobilization with early controlled loading. Primary wound healing was observed in all patients. The mean postoperative swelling measured with the visual swelling scale decreased from (3.8 ± 0.6) to (0.9 ± 0.4) scores after six weeks. Dorsiflexion measured (20 ± 3)°, plantar flexion was (36 ± 4)°, and 100 % of patients could regain a stable biphasic gait pattern at 16 weeks.

Discussion There are few detailed protocols for postoperative care and rehabilitation of TAA patients. The algorithm offered showed the effectiveness with the gait being almost normal with the range of motion and strength restored at four months. Patients reported high satisfaction measured with functional scales and subjective quality of life assessment.

Conclusion The step-by-step six-phase algorithm developed for postoperative management and rehabilitation of patients treated with segmental tibia resection and TAA facilitated a lower risk of postoperative complications, reduced function recovery time and high satisfaction ratings.

Keywords: implant, total replacement, ankle joint, stage immobilization, multimodal analgesia

For citation: Kotelnikov GP, Ivanov VV, Nikolaenko AN, Borisov AP, Shchekotikhin NA, Antonova KV, Gadzhiev MG. Algorithm for postoperative management of patients after ankle replacement surgery. *Genij Ortopedii*. 2025;31(6):729-736. doi: 10.18019/1028-4427-2025-31-6-729-736.

INTRODUCTION

Degenerative and inflammatory processes, post-traumatic and neoplastic lesions are common among conditions of the ankle joint and distal tibial metaphysis [1, 2]. Arthritis, arthrosis and ankylosis of various etiologies account for 59 % of the cases [2, 3]. Severe post-traumatic deformities of the bone and joints are noted in 22 % of cases and can be treated with reconstructive and plastic interventions. Acute and chronic osteomyelitis of the tibia and foot bones is diagnosed in 7 % of cases. Osteoporosis and uncommon secondary hyperparathyroid osteodystrophy are observed in a combined 8 % of patients. Tuberculous spondylitis and osteitis of the distal tibia are recorded in 2 % of patients [4, 5].

Ankle arthritis and arthrosis are the most clinically significant conditions. Saltzman et al. reported over 600 patients with arthritic ankles, 70 % were post-traumatic, 12 % were rheumatoid arthritis and 7 % were idiopathic osteoarthritis [5].

Tumor lesions of the distal metaepiphysis and articular end of the tibia account for approximately 2 % of all cases of the pathology in this location). Chondrosarcoma, osteosarcoma and Ewing's sarcoma (1–2 %) are the most common lesions of the distal tibia among malignant neoplasms [6]. One of the most common locations for giant cell tumor includes the distal tibia with destruction of the articular surface of the tibia [7]. Aneurysmal bone cysts and fibrous dysplasia (6 %) are observed in smaller numbers, with metastatic bone lesions accounting for up to 90 % of all tumor foci in this anatomical region [8]. Neoplasms affecting the distal tibia can be associated with massive bone destruction, often with the soft tissue component of the tumor extending beyond the cortical layer, with a relative deficiency of surrounding integumentary soft tissues, which limits the possibilities of soft tissue grafting and perplexed the strategy of reconstructive orthopedic treatment [9]. The complexity of this clinical scenario lies, on the one hand, in the surgical procedure (selecting a compact, robust implant and adequate soft tissue coverage), and, on the other hand, in the complete dissection of the capsular-ligamentous apparatus with the removal of the soft tissue block. Therefore, the lack of ligamentous attachment points creates difficulties in the postoperative period.

The development of a unified, tailored approach to rehabilitation and postoperative care for patients who have undergone ankle arthroplasty is a challenge. Optimal surgical outcomes are associated with strict adherence to postoperative care, aimed at stabilizing the prosthetic components, preventing infectious and thrombotic complications, ensuring adequate pain control, and developing proper movement patterns.

The **objective** was to evaluate clinical effectiveness of the algorithm developed for postoperative management of TAA patients to improve functional recovery, reduce postoperative complications for greater patient satisfaction.

MATERIAL AND METHODS

The study included 28 patients with involved distal tibia and ankle joint including 20 (71 %) male and 8 (29 %) female patients. The nosologies of the ankle lesions included benign tumors and tumor-like diseases (*n* = 18, 64 %), severe post-traumatic deformities (*n* = 10, 36 %).

All patients underwent ankle arthroplasty with replacement of the distal tibia according to the method developed (Russian Federation patent for invention No. 2923860 dated 30.07.2024) with an implant of an original design (Russian Federation patent for utility model No. 214964 dated 06.08.2022) (Fig. 1).

Fig. 1 Photo of the ankle implant developed to replace the distal third of the tibia

The patients received adequate pain relief postoperatively in accordance with the principles of multimodal analgesia. Promedol was administered for the first two days at a dose of 20–40 mg intramuscularly twice daily, followed by tramadol at a dose of 50–100 mg twice daily at three to four days. Between opioid analgesic administrations, nonsteroidal anti-inflammatory drugs (NSAIDs) were administered, primarily ketorolac at a dose of 30 mg intramuscularly.

Antibacterial therapy consisted of amoxicillin/clavulanate (amoxiclav) at a dose of 1.2 g intravenously three times daily for five days. Local antiseptic treatment included daily dressing changes using an alcohol-based antiseptic solution.

A semi-rigid ankle brace was used to ensure stable immobilization and promote initial healing of the postoperative wound.

The rate of restoration of mobility was measured in the prosthetic joint to include the magnitude and strength (dynamometric) of dorsiflexion and plantar flexion. Foot function was assessed using the American Orthopaedic Foot and Ankle Society (AOFAS) scale, pain intensity was assessed using a visual analog scale (VAS), and outcomes were evaluated using the PROMIS PF (Patient-Reported Outcomes Measurement Information System) scale.

Statistical processing of the results was performed using Microsoft Excel and Statistica for Windows, v. 13.0 (Stat. Soft. Inc.) spreadsheets. Descriptive statistics included the arithmetic mean and standard deviation for quantitative data. The normality of the distribution of characteristics was determined using the Shapiro – Wilk test. Differences were considered statistically significant at a significance level of $p < 0.05$.

All patients provided written voluntary consent to participate in the study and to publish the findings. The study was approved by the Ethics Committee of the Samara State Medical University of the Russian Ministry of Health (Protocol No. 7 dated March 6, 2024).

RESULTS

The algorithm developed for postoperative rehabilitation relied on a six-level approach borrowed from rehabilitation guidelines for total ankle arthroplasty devised at the Massachusetts General Hospital [10].

The clinical guidelines were developed for patients who have undergone classic ankle arthroplasty and we adapted them for step-by-step rehabilitation with a gradual increase in static and dynamic loads (Table 1).

Table 1

Algorithm for postoperative management and rehabilitation

Follow-up period	Limitations	Objectives	Therapy/Exercises	Criteria for progression
0–2 weeks	No axial load on the lower limb Walking with bilateral support	Reduced swelling Reduced pain Independence in everyday life	Cryotherapy Elevation of the shin Monitoring the condition around the incision Maintaining strength and motion in adjacent joints Using a gait brace (cam boot)	Reduced swelling Reduced pain
2–4 weeks	Walking with bilateral support Weight bearing only while standing Using a walking orthosis Sleeping in a walking orthosis Movement limitations (eversion, inversion, pronation, supination in the hip joint)	Suture removal Swelling reduction Pain reduction Reduction of calf muscle wasting Increased calf muscle strength	Elevated shin Monitoring the condition around the incision Maintaining strength and motion in adjacent joints Passive mobilization: dorsiflexion, plantaflexion Fine motor exercises for the toes Stretching the anterior and posterior thighs Open chain exercises with gentle resistance for the thigh and gluteal muscles Learning to ascend and descend stairs with bilateral support Practicing weight transfer onto the operated leg with floor weights (week three — 30 % of body weight; week four —50 % of body weight) Using a cam boot	Decreased swelling Decreased pain Increased passive and active range of motion in the hip joint by the fourth week (dorsiflexion, plantarflexion)
4–6 weeks	Walking with unilateral support (elbow crutch) Movement limitations (eversion, inversion, pronation, supination in the hip joint)	Full range of motion in the hip joint (dorsiflexion, plantaflexion) Full weight transfer in the orthosis during walking by the fifth week Transition to full walking without the orthosis by the sixth week	Active hip joint movement (dorsiflexion, plantaflexion) Practicing weight transfer onto the operated leg with floor weights (week five – 75 % of body weight; week six – 100 % of body weight) Practicing balance before weaning off unilateral support (by week six) Practicing step pattern by week six	Pain control Satisfactory single-leg balance test by week six Full weight bearing on the operated limb
6–8 weeks	Limitation of passive mobilization and stretching (eversion, inversion)	Walking without limping Satisfactory calf muscle strength Satisfactory single-leg balance test Unassisted stair ascent and descent	Calf Strength Exercises Incorporating Isometric Eversion and Inversion Exercises Starting in Week 8 Stair Climbing and Descent Exercises Without Support Balance Exercises Soft, Unstable Supports	Satisfactory gait pattern Full range of active motion in the hip joint (dorsiflexion, plantaflexion) Bilateral symmetrical calf muscle strength
8–12 weeks	Limitation of running and jumping	Ankle joint stability Full range of motion in the ankle joint Absence of pain when walking quickly	Exercises for calf strength Balance exercises Fast walking exercises	Fast walking test

Stage I (the first 14 postoperative days)

The main objectives were to control swelling, teach independent ambulation skills using crutches including walking up and down stairs and ramps, and initially increase range of motion and muscle strength in the hip, tibia and trunk muscles. Immobilization was achieved using an ankle brace, completely eliminating axial load on the operated limb to ensure proper healing of the postoperative wound by primary intention (Fig. 2). Prevention and treatment of edema included elevating the limb and, in some cases, applying dimethyl sulfoxide (DMSO) solution. Training in walking without support on crutches, isometric exercises for the lower limb muscles, and active therapeutic exercise (PT) for the hip and knee joints were also included.

Fig. 2 General view of ankle joint immobilization with an orthosis

Stage II (2–4 postoperative weeks)

The main goals of this stage were to reduce swelling, increase range of motion in the ankle joint, prevent muscle wasting, independently perform a home exercise program, and perform exercises to develop full axial load-bearing capacity. Rehabilitation measures included passive joint mobilization (dorsiflexion and plantar flexion), active exercises to strengthen the thigh and calf muscles, and continued isometric exercises and mobilization in adjacent joints (Fig. 3).

Fig. 3 Passive movements in the ankle joint performed by a physical therapy instructor

Stage III (4–6 postoperative weeks)

The main objectives were to increase range of motion in the ankle joint and restore the physiological walking pattern on various surfaces with a single point of support (crutch or cane). The program included both active and passive exercises for the lower limb joints and gentle use of a stationary bike (Fig. 4).

Fig. 4 Performing active movements in the ankle joint

Stage IV (6–8 postoperative weeks)

Objectives were continue increasing ankle mobility and transit to independent walking without additional support. If signs of complete wound healing were present, full range of motion was allowed by primary intention (Fig. 5). Exercises to develop proprioceptive sensitivity and muscle balance were recommended including moderate resistance exercises (e.g., with elastic bands) aimed at strengthening the foot and ankle muscles.

Fig. 5 Walking with a cane

Stage V (8–12 postoperative weeks)

The primary goal was to achieve optimal range of motion. Limiting long walks and avoiding high-intensity dynamic loads (particularly jumping) were recommended. Priority was given to functional exercises to improve control of the operated limb during daily activities. Target range of motion in the ankle joint: dorsiflexion — 10°, plantar flexion — 35°.

Stage VI (from 12 weeks after surgery onwards)

The goal was full restoration of functional activity and return to work and daily activities without pain or discomfort. Unrestricted walking was permitted, provided there were no signs of implant overload. The exercise program was continued, avoiding high-energy axial loads. Return to healthy lifestyle-level physical activity was permitted in the absence of contraindications, primarily low-impact activities (swimming, cycling, walking). Optimal range of motion: dorsiflexion up to 20°, plantar flexion up to 35°.

The rate of mobility restored in the prosthetic joint was comparable with the best data from foreign registries [11, 12]: dorsiflexion reached (20 ± 3)° after 16 weeks and was maintained without loss until the end of the observation period; plantar flexion was (36 ± 4)°, being close to the physiological norm. There were no complications associated with the implant design used, the surgical intervention performed, and the rehabilitation program implemented according to the developed algorithm.

Functional scores of the treatment assessment indicated clinical improvement after the rehabilitation. The AOFAS score increased from (58 ± 6) in the early postoperative period to (82 ± 7) after 12 weeks and to (90 ± 5) after six month, reflecting high subjective satisfaction with walking and absence of pain according to the VAS (0–1). The PROMIS PF score increased from (36 ± 4) to (53 ± 4) t-score, thus, the increase was 17 points, which exceeded the threshold of clinically significant change. Dorsiflexion strength (measured dynamometrically) increased from (78 ± 12) N to (145 ± 14) N, confirming full restorative adaptation of the anterior tibia muscles.

DISCUSSION

There is no consensus on the most appropriate postoperative care for patients who have undergone total ankle arthroplasty. Antithromboembolic agents, antibiotics, and analgesics are the main medications prescribed postoperatively [11].

Antithrombotic therapy is administered during the patient's immobilization period [12, 13]. According to European studies, postoperative antibiotic prophylaxis is rarely used. Usuell et al. suggested 1 g of intravenous cefazolin every eight hours to be administered to patients postoperatively for 24 hours with a high risk of infection (BMI 30 or higher, steroid use, smoking, diabetes, immunosuppression, malignant neoplasms, surgery time longer than three hours) [14]. Postoperative pain control is mandatory, with combinations of NSAIDs and narcotic analgesics most commonly used [15].

Tibia can be immobilized with a cast [16], a splint [17], or an orthopedic boot [18]. A splint and an orthopedic boot are usually better tolerated by patients, and in traumatic settings, they reduce postural sway and improve proprioceptive function providing better functional outcomes at a short term [19]. Regarding the duration of immobilization, patients are normally allowed to walk in regular shoes six weeks after surgery regardless of the type of immobilization used [11].

The postoperative rehabilitation program typically consists of gait training, proprioceptive exercises, lymphatic drainage, active and passive therapy for ankle mobility, stretching and strengthening of the triceps surae and Achilles tendon. Most patients initiated gait training, muscle stretching, and exercising at six postoperative weeks [20, 21]. Some authors would recommend rehabilitation programs to be initiated at 8–10 weeks postoperatively [22, 23].

There is a paucity of detailed physical therapy protocols for patients undergoing total ankle arthroplasty in the available literature. Only Kotela et al. reported a detailed regimen for individuals with inherited bleeding disorders. The protocol consisted of several phases. The preoperative phase (two to four weeks before surgery) included teaching patients how to perform proper postoperative exercises, walking with crutches on the floor and up stairs at 50 % weight-bearing, strengthening proprioception in the upper limb and trunk muscles, and balance training.

The second phase (up to two weeks after surgery) included breathing exercises, active ankle extension and flexion of the opposite leg, active flexion and extension of the toes of the operated limb, and magnetic therapy for 20 minutes per day. Subsequently (two to six weeks after surgery), active knee flexion and extension against gravity, ankle inversion/eversion with an elastic stretch band, ball rebounds, calf raises, and swimming for 10–30 minutes per day were recommended [24].

Our data provide reliable evidence that the multi-stage rehabilitation algorithm developed for patients undergoing total ankle arthroplasty with distal tibial replacement, combined with early functional activation, provides reliable protection against infectious and thrombotic complications. Key factors for success include early, gradual introduction of controlled axial loading, multimodal analgesia integrated with regional block, and a criterion-based transition between rehabilitation phases.

The algorithm offered enables almost complete normalization of gait, range of motion, and strength by the fourth month, which is twice as fast as traditional delayed loading regimens. High patient satisfaction is confirmed by functional scales (AOFAS ≥ 85 at six months) and subjective assessments of quality of life. The low rate of early complications and almost complete absence of serious infectious events indicate the advisability of short-term (up to 24 hours) systemic antibiotic prophylaxis with strict aseptic technique and local antiseptic measures to be observed.

CONCLUSION

A phased, protocol-based approach to postoperative care offered for patients undergoing total ankle arthroplasty with distal tibial replacement significantly improves the effectiveness of early rehabilitation, minimizing the risk of complications and improving functional outcomes. Reliance on modern principles of multimodal analgesia, rational antibacterial prophylaxis, and a strictly regulated transition between rehabilitation phases ensures rapid restoration of motion and stable weight-bearing capacity of the operated limb.

The obtained results confirm the clinical validity of the complex protocol as a safe and effective tool for managing the cohort of patients and suggest its potential for the use in specialized onco-orthopedic practice.

Conflict of interest *None of the authors has any potential conflict of interest.*

Funding *The study was conducted in accordance with the scientific research plan of Samara State Medical University. The authors received no financial support from drug manufacturers.*

REFERENCES

1. Herrera-Pérez M, Valderrabano V, Godoy-Santos AL, et al. Ankle osteoarthritis: comprehensive review and treatment algorithm proposal. *EFORT Open Rev*. 2022;7(7):448-459. https://doi.org/10.1530/EOR-21-0117.
2. Lee MS, Mathson L, Andrews C, et al. Long-term outcomes after total ankle arthroplasty: a systematic review. *Foot Ankle Orthop*. 2024;9(4):24730114241294073. https://doi.org/10.1177/24730114241294073.
3. Herrera-Pérez M, González-Martín D, Vallejo-Márquez M, et al. Ankle osteoarthritis aetiology. *J. Clin. Med*. 2021;10(19):4489. doi: 10.3390/jcm10194489.
4. Kotelnikov GP, Kolsanov AV, Nikolaenko AN, et al. Ankle replacement for severe post-traumatic deformation of the distal tibia: a case report. *Pirogov Russian Journal of Surgery*. 2024;(1):110-118. (In Russ.) doi: 10.17116/ hirurgia2024011110.

5. Saltzman CL, Salamon ML, Blanchard GM, et al. Epidemiology of ankle arthritis: report of a consecutive series of 639 patients from a tertiary orthopaedic center. *Iowa Orthop J*. 2005;25:44-46.
6. Greenwood AC, Arora RD, Shaikh H. Osteosarcoma (Osteogenic Sarcoma). 2024 Dec 11. In: *StatPearls* [Internet]. Treasure Island (FL): StatPearls Publishing; 2025.
7. Barashev AA, Mozulyaka VV, Ausheva TV, et al. The first results of combined treatment of giant cell tumor of bone. *South Russian Journal of Cancer*. 2020;1(4):6-14. (In Russ.) doi: 10.37748/2687-0533-2020-1-4-1.
8. Sonone A, Hande A, Gawande MN, et al. Aneurysmal bone cyst plus lesions: a case report and a literature review. *Cureus*. 2022;14(8):e27912. doi: 10.7759/cureus.27912.
9. Ahmed S, Deshpande SV, Chhatbar K. Osteosarcoma of the Distal Femur Presenting as Giant Cell Tumor: A Case Report. *Cureus*. 2022;14(12):e33173. doi: 10.7759/cureus.33173.
10. *Postoperative Protocols for Total Ankle Arthroplasty*. Clinical Guidelines. Boston: MGH Orthopedics; 2022. URL: https://www.massgeneral.org/assets/mgh/pdf/orthopaedics/sports-medicine/physical-therapy/rehabilitation-protocol-for-total-ankle-arthroplasty.pdf.
11. Mazzotti A, Viglione V, Gerardi S, et al. Post-operative management after total ankle arthroplasty: A systematic review of the literature. *Foot Ankle Surg*. 2022;28(5):535-542. doi: 10.1016/j.fas.2021.05.013.
12. Hofmann KJ, Shabin ZM, Ferkel E, et al. Salto Talaris Total Ankle Arthroplasty: Clinical Results at a Mean of 5.2 Years in 78 Patients Treated by a Single Surgeon. *J Bone Joint Surg Am*. 2016;98(24):2036-2046. doi: 10.2106/JBJS.16.00090.
13. Clough TM, Alvi F, Majeed H. Total ankle arthroplasty: what are the risks?: a guide to surgical consent and a review of the literature. *Bone Joint J*. 2018;100-B(10):1352-1358. doi: 10.1302/0301-620X.100B10.BJJ-2018-0180.R1.
14. Usuelli FG, Indino C, Maccario C, et al. Infections in primary total ankle replacement: Anterior approach versus lateral transfibular approach. *Foot Ankle Surg*. 2019;25(1):19-23. doi: 10.1016/j.fas.2017.07.643.
15. Borenstein TR, Anand K, Li Q, et al. A Review of Perioperative Complications of Outpatient Total Ankle Arthroplasty. *Foot Ankle Int*. 2018;39(2):143-148. doi: 10.1177/1071100717738748.
16. Tiusanen H, Kormi S, Kohonen I, Saltychev M. Results of Trabecular-Metal Total Ankle Arthroplasties With Transfibular Approach. *Foot Ankle Int*. 2020;41(4):411-418. doi: 10.1177/1071100719894929.
17. Berlet GC, Brandão RA, Consul D, et al. Short- to Midterm Follow-up of Cemented Total Ankle Replacement Using the INBONE II: A Retrospective Chart Review. *Foot Ankle Spec*. 2021;14(4):302-311. doi: 10.1177/1938640020913126.
18. Wainwright TW, Immins T, Antonis JHA, et al. Can the introduction of Enhanced Recovery After Surgery (ERAS) reduce the variation in length of stay after total ankle replacement surgery? *Foot Ankle Surg*. 2019;25(3):294-297. doi: 10.1016/j.fas.2017.12.005.
19. Lehtonen H, Järvinen TL, Honkonen S, et al. Use of a cast compared with a functional ankle brace after operative treatment of an ankle fracture. A prospective, randomized study. *J Bone Joint Surg Am*. 2003;85(2):205-211. doi: 10.2106/00004623-200302000-00004.
20. Boylan MR, Riesgo AM, Paulino CB, Sheskier SC. Does Total Ankle Arthroplasty Belong in the Comprehensive Care for Joint Replacement? *J Foot Ankle Surg*. 2018;57(1):69-73. doi: 10.1053/j.jfas.2017.08.008.
21. McDonald EL, Pedowitz DI, Shakked RJ, et al. When is it Safe to Drive After Total Ankle Arthroplasty? *Clin Orthop Relat Res*. 2020;478(1):8-15. doi: 10.1097/CORR.0000000000000881.
22. Lee GW, Santoso A, Lee KB. Comparison of Intermediate-term Outcomes of Total Ankle Arthroplasty in Primary and Ligamentous Post-traumatic Osteoarthritis. *Foot Ankle Int*. 2019;40(11):1273-1281. doi: 10.1177/1071100719866472.
23. Gaugler M, Krähenbühl N, Barg A, et al. Effect of age on outcome and revision in total ankle arthroplasty. *Bone Joint J*. 2020;102-B(7):925-932. doi: 10.1302/0301-620X.102B7.BJJ-2019-1263.R2.
24. Kotela A, Wilk-Frańczuk M, Jaczewska J, et al. Perioperative Physiotherapy for Total Ankle Replacement in Patients with Inherited Bleeding Disorders: Outline of an Algorithm. *Med Sci Monit*. 2017;23:498-504. doi: 10.12659/msm.898075.

The article was submitted 04.07.2025; approved after reviewing 17.07.2025; accepted for publication 14.10.2025.

Information about the authors:

Gennady P. Kotelnikov — Academician of the Russian Academy of Sciences, Doctor of Medical Sciences, Professor, Head of the Department, kaf_travma@samsmu.ru, https://orcid.org/0000-0001-7456-6160;

Viktor V. Ivanov — Candidate of Medical Sciences, Associate Professor, Associate Professor of the Department, viktor_travm@bk.ru, https://orcid.org/0000-0002-2813-5826;

Andrey N. Nikolaenko — Doctor of Medical Sciences, Associate Professor, Director of the Research Institute of Bionics and Personalised Medicine, nikolaenko.83@inbox.ru, https://orcid.org/0000-0003-3411-4172;

Alexander P. Borisov — Candidate of Medical Sciences, Associate Professor, Chief Specialist, dr_borisov71@mail.ru, https://orcid.org/0009-0008-9562-6394;

Nikita A. Shchekotikhin — 5th year student, side1994@inbox.ru, https://orcid.org/0009-0009-2934-8637;

Kristina V. Antonova — 6th year student, tina_antonova_2001@mail.ru, https://orcid.org/0009-0000-9958-1594;

Magomed G. Gadzhiev — resident, Gadzhiyev-98@mail.ru, https://orcid.org/0009-0000-8428-1003.

Original article
https://doi.org/10.18019/1028-4427-2025-31-6-737-743

Effectiveness of Bridle procedure for correction of foot drop syndrome due to peroneal nerve neuropathy

A.A. Grigoryan[1], L.G. Makinyan[1,2], A.M. Mannanov[2], Ch. Moldamyrzayev[1], M.A. Imankulov[1], W.M. Abu Zaalan[1,2]✉

Corresponding author: Wessam Moussa Abu Zaalan, wsameeexx@gmail.com

[1] Patrice Lumumba Peoples' Friendship University of Russia, Moscow, Russian Federation
[2] VDemikhov City Clinical Hospital, Moscow, Russian Federation

Abstract

Introduction Foot drop syndrome due to peroneal nerve neuropathy significantly impairs limb support and patient quality of life. The aim of this study was to evaluate the clinical effectiveness of the Bridle procedure compared to ankle arthrodesis and isolated tendon transfer.

Materials and methods A retrospective analysis of 27 patients was performed, divided into a main group ($n = 14$, Bridle technique) and a control group ($n = 13$, arthrodesis or tendon transfer). Functional outcomes were assessed using the AOFAS and VAS scales, along with rehabilitation duration, orthotic use, and complication rates. The mean follow-up period was 2.3 years.

Results The main group showed significantly better outcomes: AOFAS score improved from 38 to 82, VAS score decreased from 6.8 to 2.1, and the need for orthotic devices was reduced. In the control group, improvements were less pronounced (AOFAS: 37→65; VAS: 6.7→3.9). The complication rate was 14.3 % in the Bridle group versus 38.5 % in the control group.

Discussion The Bridle technique restores active dorsiflexion while preserving ankle mobility. Its functional and rehabilitation advantages make it preferable in cases of isolated peroneal nerve injury without severe deformities.

Conclusion The Bridle procedure is an effective joint-preserving surgical method for treating foot drop, providing superior clinical outcomes compared to alternative interventions.

Keywords: foot drop syndrome, peroneal nerve neuropathy, Bridle technique, arthrodesis, tendon transfer, dorsiflexion, rehabilitation.

For citation: Grigoryan AA, Makinyan LG, Mannanov AM, Moldamyrzayev Ch, Imankulov MA, Abu Zaalan WM. Effectiveness of Bridle procedure for correction of foot drop syndrome due to peroneal nerve neuropathy. *Genij Ortopedii*. 2025;31(6):737-743. doi: 10.18019/1028-4427-2025-31-6-737-743.

INTRODUCTION

Foot drop syndrome is a common disorder most often associated with peroneal nerve neuropathy, one of the most common mononeuropathies of the lower extremity. According to the literature, the incidence of mononeuropathies is up to 15 % of all peripheral neuropathies. Due to the growing number of road traffic injuries, orthopedic surgeries, and the incidence of diabetes, this pathology is becoming increasingly common. It results in unablity to lift the forefoot while walking, leading to a compensatory gait (steppage), poor posture, and decreased stability during movement [1]. Therefore, foot drop syndrome is acquiring high clinical significance and requires the search for functionally effective and joint-preserving surgical correction methods [2, 3, 4]. Foot drop syndrome significantly reduces quality of life, causing limping, difficulty finding footwear, the need for orthoses, an increased risk of falls, decreased physical activity, and social isolation [5, 6, 7]. The rates of using assistive means reflect the severity of the condition; without treatment, patients are often forced to use orthoses or canes [8]. The high incidence of trauma and the prevalence of diabetic and compression neuropathies necessitate the search for effective correction methods, including surgical ones [9, 10].

Peroneal nerve neuropathy is caused by anatomical vulnerability of the nerve in the region of the head of the fibula. The causes of the disease are varied and include trauma, metabolic and compressive effects, iatrogenic factors [11, 13, 14]. The most common antecedents are fractures of the proximal fibula, surgeries on the lower leg and knee joint, and prolonged compression of the nerve. Systemic diseases, including diabetes mellitus and vascular pathologies, play a significant role [6, 15]. In acute injury, surgical treatment is indicated and provides satisfactory results [16, 17]. The pathogenesis of the syndrome is associated with impaired conduction along the motor and sensory fibers innervating the anterior group of leg muscles, which causes loss of dorsiflexion of the foot and toes, as well as decreased sensitivity on its dorsum and the lateral surface of the lower leg. A compensatory steppage-type gait occurs. Without treatment, patients develop muscle atrophy, contractures, and equinus deformity, which significantly impair the weight-bearing function of the limb and require surgical correction [1, 18, 19, 20].

Surgical treatment of patients with foot drop syndrome is aimed at restoring dorsiflexion and improving weight-bearing ability of the limb. Current approaches include arthrodesis, isolated tenodesis, and Bridle reconstruction, each with its own indications and limitations [9, 21]. Arthrodesis provides stability and pain relief by immobilizing the ankle joint, but it impairs mobility and requires long-term rehabilitation; it is used for deformities, arthrosis, and the inability to restore function using soft tissue methods [22, 23, 24]. Tenodesis is a less invasive technique that involves fixation of the anterior tibialis muscle; however, the effectiveness of tenodesis is lower by severe atrophy or the presence of contractures [25].

The Bridle technique is considered the most physiological and functionally sound. It involves reconstruction with transposition of the anterior and posterior tibialis muscles and the peroneus longus muscle, which allows for the redistribution of forces and restoration of dorsiflexion of the foot [26, 27, 28]. Unlike arthrodesis, the Bridle technique helps maintain ankle mobility and, compared to tenodesis, provides more stable and symmetrical movement control [29]. Due to its high efficiency and low complication rate, the Bridle technique is recommended for patients with isolated peroneal nerve neuropathy and preserved foot anatomy.

The **aim** of this study was to evaluate the clinical effectiveness of the Bridle procedure compared to ankle arthrodesis and isolated tendon transfer in surgical treatment of foot drop syndrome.

MATERIALS AND METHODS

The study included 27 patients with foot drop syndrome caused by peroneal nerve neuropathy.

Inclusion criteria: post-traumatic or compression nerve injury with failure to respond to conservative therapy, severe impairment of dorsiflexion of the foot, and intact anatomical structure of the ankle joint.

Exclusion criteria: patients with systemic neurological diseases, diabetic polyneuropathy, severe foot deformities, and severe osteoarthritis.

Patients were divided into two groups: a study group (*n* = 14), in which the Bridle tendon reconstruction technique was utilized, and a control group (*n* = 13), which underwent an alternative surgical procedure (ankle arthrodesis or isolated tibialis anterior tenodesis). All surgeries were performed in a specialized orthopedic department, following a standardized protocol for anesthesia and postoperative care. The age and gender distribution of the patients is presented in Table 1.

Table 1

Characteristics of patients

Parameters		Study group (*n* = 14)	Control group (*n* = 13)
Males	*n*	8	7
	%	57	54
Females	*n*	6	6
	%	43	46
Age, years		39.28 ± 9.20 (25.9–59.7)	45.49 ± 8.38 (33.0–58.6)

The preoperative examination protocol included a patient medical history, physical examination, plantar ligation, ankle radiography in two projections, electroneuromyography (ENMG), and a consultation of a neurologist.

Foot function was assessed using the American Orthopaedic Foot and Ankle Society (AOFAS) score, and pain intensity was assessed using the visual analog scale (VAS). The average follow-up period was 2.3 years (range, 1.1 to 4.6 years). Outcome assessments were conducted at six weeks, six months, and one year postoperatively, and evaluated functional recovery, pain relief, the need for orthotics, and complications.

The Bridle procedure is an anatomical and functional reconstruction that redirects the strength of the remaining muscles to compensate for the loss of dorsiflexion of the foot due to peroneal nerve injury. The technique utilizes the tendons of the functioning calf muscles (posterior tibial, peroneus longus, and anterior tibial) to create a balanced tri-tendon complex that provides active dorsiflexion and stabilization of the foot in the sagittal and frontal planes.

The surgical approach starts with isolating the posterior tibial tendon, which is transected and brought to the anteromedial aspect of the leg. The peroneus longus tendon is then exposed, mobilized, and also brought to the anterior aspect. Next, the anterior tibial tendon is exposed, and the two structures are sutured into a single bundle. A strong triple suture is created, ensuring balanced tension. Restoration of dorsiflexion of the foot is achieved by redistributing the motor function of the muscles innervated by the intact branches of the tibial nerve. The surgery is performed with careful monitoring of the length and vector of traction, which is crutial for achieving a stable and functionally advantageous foot position.

A distinctive feature of this method is its joint-preserving nature, as ankle mobility is preserved and the anatomical structures are not subject to severe destruction. The postoperative period includes limb immobilization for four to six weeks, followed by a stage of active rehabilitation aimed at restoring muscle control and gait.

Data analysis was performed using Statistica 10.0 (StatSoft Inc., USA). Comparisons between the groups were made based on clinical and functional parameters, such as pain intensity and the need for orthotics.

All patients signed informed consent to participate in the study and to undergo surgical treatment. The study complies with the requirements of the World Medical Association Declaration of Helsinki (2013 edition) and was approved by the institutional ethics committee.

RESULTS

In the study group, where the Bridle method was used, restoration of the support function of the foot and the start of active rehabilitation was as early as six weeks after the intervention. By the eighth month after surgery, the majority of patients (85.7 %) showed significant improvement in function, including restoration of dorsiflexion, gait stabilization, and the elimination of the constant use of orthoses. The average AOFAS score in this group increased from 38.0 ± 6.2 to 82.0 ± 5.7 points, and the pain level on the VAS scale decreased from 6.8 ± 1.1 to 2.1 ± 0.9 points (Table 2).

Table 2

Results of comparison

Parameter		Study group (*n* = 14)	Control group (*n* = 13)
AOFAS	Before surgery	38.0 ± 6.2	37,0 ± 5,9
	After surgery	82.0 ± 5.7	65,0 ± 6,4
VAS	Before surgery	6.8 ± 1.1	6,7 ± 1,0
	After surgery	2.1 ± 0.9	3,9 ± 1,2
No orthotics	*n*	12	5
	%	85.7	38,5
Complications	*n*	2	5
	%	14.3	38,5
Сроки полной реабилитации, мес.		~8	~10

In the control group, which underwent arthrodesis or isolated tenodesis, improvements were also observed, but to a lesser extent. The average AOFAS score increased from 37.0 ± 5.9 to 65.0 ± 6.4 points, while the VAS decreased to 3.9 ± 1.2 points. Eight patients (61.5 %) still required orthotics during prolonged walking or physical activity. The duration of full rehabilitation was, on average, two months longer than in the study group.

Complications in the study group included two cases of minor tendon suture failure without significant clinical symptoms. In the control group, complications were observed in five patients, including limited range of motion, pain in the arthrodesis area, and a poor functional outcome.

The results demonstrate a clear advantage of the Bridle technique over arthrodesis and isolated tenodesis in the treatment of patients with foot drop syndrome. Patients treated with the Bridle technique showed higher functional outcomes (AOFAS), lower pain (VAS), faster recovery, and a lower need for orthoses. They also had a lower complication rate.

Case report

A 50-year-old patient presented with complaints of inability to dorsiflex his right foot, severe lameness, and difficulty in fiiting footware. He had a history of severe traumatic brain injury and orthopedic trauma resulting from a motor vehicle accident. He had previously undergone more than 13 surgeries for multiple femur and tibia fractures, including osteosynthesis, revisions, and reconstructions.

Clinical examination (Fig. 1a) revealed a complete lack of active ankle extension, severe atrophy of the anterior calf muscles, and a compensatory steppage gait. Electromyography (EMG) confirmed irreversible neuropathy of the common peroneal nerve. Conservative treatment proved ineffective. The patient underwent reconstructive surgery using the Bridle technique with the formation of a tri-tendon complex (Fig. 1b). The postoperative period was uneventful. After six weeks, the patient began staged active rehabilitation. By the fourth month, we observed restoration of weight-bearing ability in the limb, and by the eighth month, almost complete restoration of foot function and the elimination of orthoses (Fig. 1c). The functional outcome was 86 AOFAS points and 1 VAS point.

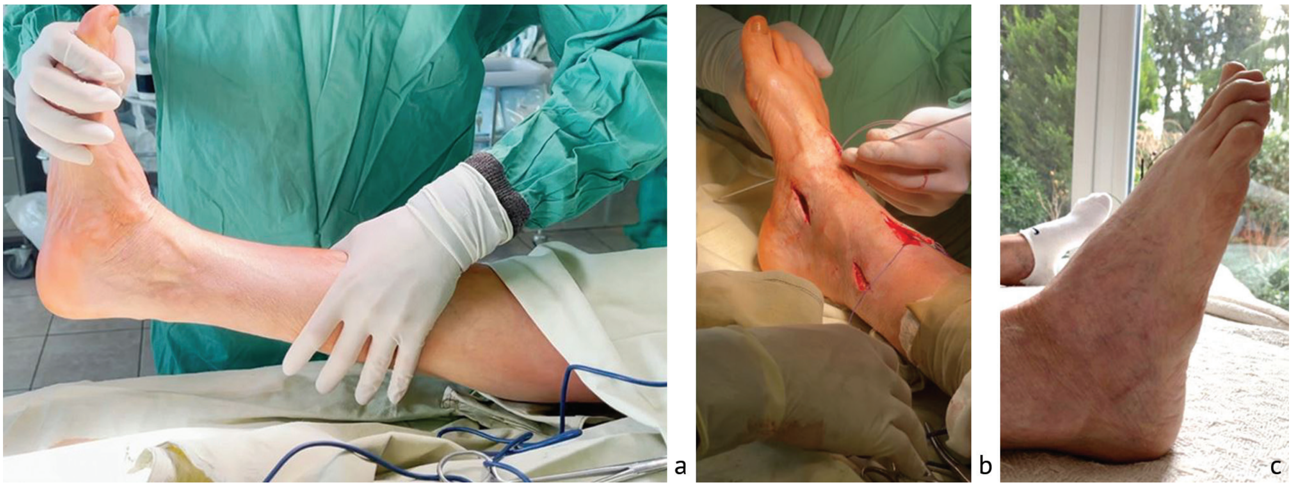

Fig. 1 Photo of the foot in a 50-yo patient with foot drop syndrome: (a) initial view; (b) intraoperative image; (c) at follow-up after 8 months.

Clinical improvement was restoration of symmetrical gait, elimination of compensatory movements, and a significant improvement in the patient's quality of life. Thus, this case confirms the high effectiveness of the Bridle method for isolated peroneal nerve neuropathy with severe functional impairment.

DISCUSSION

The obtained by us results convincingly demonstrate the clinical efficacy of the Bridle procedure in patients with foot drop syndrome caused by peroneal nerve neuropathy. A comparative analysis with traditional surgical approaches (arthrodesis and isolated tenodesis) demonstrated the superiority of the Bridle method across key criteria: restoration of active dorsiflexion, pain relief, shorter rehabilitation time, and no need in orthotic support.

Of particular importance in the Bridle technique is the ability to preserve physiological ankle mobility. While arthrodesis provides mechanical stability, it limits functionality and can lead to overloading of adjacent joints. Isolated tenodesis frequently achieves unstable results, especially in cases of severe muscle atrophy. The joint-preserving nature of the Bridle procedure is particularly relevant for restoring quality of life and reducing disability in working age patients. An additional benefit is the formalization of the pre- and postoperative management protocol, which improves the reproducibility of the approach.

Our data are consistent with the results of international studies confirming the high functional effectiveness of Bridle plasty. In particular, Carolus et al. note that the Bridle technique is effective in cases of isolated peroneal nerve injury and allows for the preservation of ankle joint mobility [10]. Poage et al. point to the preference of reconstructive techniques, especially in patients without rigid contractures [19]. In the domestic literature, the advantages of the Bridle method have not yet been sufficiently covered; however, the high clinical significance of the restoration of active dorsiflexion and a reduction in dependence on orthoses is noted [3].

Our results differ from some studies due to stricter inclusion criteria: patients with severe deformities, rigid contractures, and systemic polyneuropathy were excluded. This ensured a cleaner sample and increased the predictability of the results.

The main limitations remain the retrospective nature, small sample size, and lack of randomization. Nevertheless, the high reliability of the results is achieved through the use of validated scales (AOFAS, VAS), long-term follow-up (average 2.3 years), and uniform surgical standards.

A protocol for pre- and postoperative patient management has been proposed and tested, which can be used in clinical practice to optimize treatment outcomes. The Bridle technique can be recommended for surgical correction of foot drop in patients with isolated peroneal nerve neuropathy without deformities and with functioning donor muscles. This technique avoids the rigid fixation of the foot typical of arthrodesis and the instability inherent in isolated tenodesis. This method requires further evaluation in multicenter randomized trials with long-term follow-up and analysis of biomechanical parameters.

CONCLUSION

Compared to arthrodesis and isolated tenodesis, the Bridle technique provides better functional results with fewer complications and a shorter rehabilitation period. Based on these results, the indications for this type of intervention have been refined, including preserved foot mobility, absence of rigid deformities, and functioning donor muscles.

Conflict of interest *Not declared.*

Funding *Not declared.*

REFERENCES

1. Ewerbeck V, Wentzensen V, Holz F, et al. *Standard procedures in operative orthopedics and trauma surgery*. 3rd ed. Stuttgart: Thieme; 2006:928. (in German)
2. Bowley MP, Doughty CT. Entrapment Neuropathies of the Lower Extremity. *Med Clin North Am*. 2019;103(2):371-382. doi: 10.1016/j.mcna.2018.10.013.
3. Golubeva YuB, Andrievskaya AO, Gorelova IK, et al. Orthopedic services as a tool of medical rehabilitation of patients with foot drop syndrome. *S.S. Korsakov Journal of Neurology and Psychiatry*. 2020;120(10):91-99. (In Russ.) doi: 10.17116/jnevro202012010191.
4. Khizhnikova AE, Klochkov AS, Belova NV, et al. Foot drop: causes, clinical and instrumental diagnostics, and biomechanics. *Nervous Diseases*. 2024;(1):22-30. (In Russ.) doi: 10.24412/2226-0757-2024-13057.
5. Nori SL, Stretanski MF. Foot Drop [Internet]. In: *StatPearls*. Treasure Island (FL): StatPearls Publishing; 2025. Available from: https://www.ncbi.nlm.nih.gov/books/NBK554393/.
6. Novikov AV, Antonova VA. Neuropathy of the peroneal nerve as a complication after total knee arthroplasty: characteristics of rehabilitation. *N.N. Priorov Journal of Traumatology and Orthopedics*. 2020;27(4):41-45. (In Russ.) doi: 10.17816/vto57137.
7. Matsumoto J, Isu T, Kim K, et al. Impact of additional treatment of paralumbar spine and peripheral nerve diseases after lumbar spine surgery. *World Neurosurg*. 2018;112:e778-e782. doi: 10.1016/j.wneu.2018.01.154.
8. Yarikov AV, Makeeva OA, Baytinger AV, et al. Fibular tunnel syndrome: modern principles of diagnosis and treatment. *The Doctor*. 2023;34(11):5-9. (In Russ.) doi:10.29296/25877305-2023-11-01.
9. García-Martínez MÁ, Montejo González JC, García-de-Lorenzo Y Mateos A, Teijeira S. Muscle weakness: Understanding the principles of myopathy and neuropathy in the critically ill patient and the management options. *Clin Nutr*. 2020;39(5):1331-1344. doi: 10.1016/j.clnu.2019.05.027.
10. Carolus AE, Becker M, Cuny J, et al. The Interdisciplinary Management of Foot Drop. *Dtsch Arztebl Int*. 2019;116(20):347-354. doi: 10.3238/arztebl.2019.0347.
11. Desy NM, Wang H, Elshiekh MAI, et al. Intraneural ganglion cysts: a systematic review and reinterpretation of the world's literature. *J Neurosurg*. 2016;125(3):615-630. doi: 10.3171/2015.9.JNS141368.
12. Kretschmer T, Antoniadis G, Braun V, et al. Evaluation of iatrogenic lesions in 722 surgically treated cases of peripheral nerve trauma. *J Neurosurg*. 2001;94(6):905-912. doi: 10.3171/jns.2001.94.6.0905.
13. Huckhagel T, Nüchtern J, Regelsberger J, et al. Nerve trauma of the lower extremity: evaluation of 60,422 leg injured patients from the TraumaRegister DGU® between 2002 and 2015. *Scand J Trauma Resusc Emerg Med*. 2018;26(1):40. doi: 10.1186/s13049-018-0502-5.

14. Westhout FD, Paré LS, Linskey ME. Central causes of foot drop: rare and underappreciated differential diagnoses. *J Spinal Cord Med*. 2007;30(1):62-66. doi: 10.1080/10790268.2007.11753915.
15. Nedosekina MP. Acute neuropathy of the left common peroneal nerve in neurological practice: a clinical case. *Brain Universe*. 2021;3(1[8]):45-46. (In Russ.)
16. Matejcik V, Penzesova G. Surgery of the peripheral nerves. *Bratisl Lek Listy*. 2006;107(3):89-92.
17. Giuffre JL, Bishop AT, Spinner RJ, et al. Partial tibial nerve transfer to the tibialis anterior motor branch to treat peroneal nerve injury after knee trauma. *Clin Orthop Relat Res*. 2012;470(3):779-790. doi: 10.1007/s11999-011-1924-9.
18. Poage C, Roth C, Scott B. Peroneal nerve palsy: evaluation and management. *J Am Acad Orthop Surg*. 2016 Jan;24(1):1-10. doi: 10.5435/JAAOS-D-14-00420.
19. Bao B, Wei H, Zhu H, Zheng X. Transfer of Soleus Muscular Branch of Tibial Nerve to Deep Fibular Nerve to Repair Foot Drop After Common Peroneal Nerve Injury: A Retrospective Study. *Front Neurol*. 2022;13:745746. doi: 10.3389/fneur.2022.745746.
20. Merkulov VN, Imyarov ShD, Dorokhin AI. Tendomuscular transposition in old peroneal nerve injuries in children. *Pediatric Surgery*. 2014;(3):20-22. (In Russ.)
21. Takaishi Y, Okada M, Fujiwara D, et al. Surgical Results of Lumbar Degenerative Disease with Foot Drop. *No Shinkei Geka*. 2019;47(8):851-857. (In Jap) doi: 10.11477/mf.1436204036.
22. Vang Zh, Akhtyamov IF, Ziatdinov BG, Faizrakhmanova GM. Ankle arthrodesis: realities and prospects against the background of new technologies. Literature Review. *Bulletin of Rehabilitation Medicine*. 2022; 21(2): 115-126. (In Russ.) doi: 10.38025/2078-1962-2022-21-2-115-126.
23. Karapinar H, Sener M, Kazimoglu C, Akgun U. Arthrodesis of neuropathic ankle joint by Ilizarov fixator in diabetic patients. *J Am Podiatr Med Assoc*. 2009;99(1):42-48. doi: 10.7547/0980042.
24. Bek D, Demiralp B, Kürklü M, et al. Ankle arthrodesis using an Ilizarov external fixator in patients wounded by landmines and gunshots. *Foot Ankle Int*. 2008;29(2):178-184. doi: 10.3113/FAI.2008.0178.
25. Matsakyan AM, Shirmazanyan AG, Gorochovodatsky AV. Operations on the tendon of the posterior tibial muscle in the treatment of a static flat-valgus deformation. *Vestnik of the Smolensk State Medical Academy*. 2017;16(4):168-177. (In Russ.)
26. Johnson JE, Paxton ES, Lippe J, et al. Outcomes of the Bridle Procedure for the Treatment of Foot Drop. *Foot Ankle Int*. 2015;36(11):1287-1296. doi: 10.1177/1071100715593146.
27. McCall RE, Frederick HA, McCluskey GM, Riordan DC. The Bridle procedure: a new treatment for equinus and equinovarus deformities in children. *J Pediatr Orthop*. 1991;11(1):83-89.
28. Hastings MK, Sinacore DR, Woodburn J, et al. Kinetics and kinematics after the Bridle procedure for treatment of traumatic foot drop. *Clin Biomech (Bristol)*. 2013;28(5):555-561. doi: 10.1016/j.clinbiomech.2013.04.008.
29. Rodriguez RP. The Bridle procedure in the treatment of paralysis of the foot. *Foot Ankle*. 1992;13(2):63-69. doi: 10.1177/107110079201300203.

The article was submitted 05.06.2025; approved after reviewing 17.07.2025; accepted for publication 14.10.2025.

Information about the authors:

Artsrun A. Grigoryan — post-graduate student, Artsrun3204@mail.ru, https://orcid.org/0000-0003-0677-2960;

Levon G. Makinyan — Candidate of Medical Sciences, Associate professor of the Department, Head of Department, dr.makinyan@gmail.com, https://orcid.org/0000-0002-8813-143X;

Albert M. Mannanov — Candidate of Medical Sciences, orthopaedic surgeon, albertmannanov@gmail.com, https://orcid.org/0000-0002-4456-8218;

Chyngis Moldamyrzayev — post-graduate student, moldamirzayev@mail.ru, https://orcid.org/0009-0002-8501-0680;

Mikhail A. Imankulov — post-graduate student, Mikhail.imankulov@mail.ru, https://orcid.org/0000-0002-4398-1801;

Wessam Mussa Abu Zaalan — post-graduate student, orthopaedic surgeon, wsameeexx@gmail.com, https://orcid.org/0000-0003-3922-3052.

Original article
https://doi.org/10.18019/1028-4427-2025-31-6-744-755

Personalized approach to the treatment of patients with flat foot deformity: method for determining the level of osteotomy of anterior process of the the calcaneus

S.M. Gudi[1]✉, D.A. Semenova[2], V.V. Krikunova[1], K.O. Vasiliev[1], L.K. Skuratova[1], M.D. Luchshev[1], V.M. Prokhorenko[1], V.I. Shevtsov[3], I.A. Pakhomov[1]

[1] Novosibirsk Scientific Research Institute of Traumatology and Orthopedics named after Ya.L. Tsivyan, Novosibirsk, Russian Federation

[2] Novosibirsk National Research State University, Novosibirsk, Russian Federation

[3] Ilizarov National Medical Research Centre for Traumatology and Orthopedics, Kurgan, Russian Federation

Corresponding author: Sergey M. Gudi, smgudinsk@gmail.com

Abstract

Introduction Evans osteotomy remains one of the most common methods of surgical correction for mobile flat foot deformity by lengthening the lateral column. However, this technique is associated with damage to the articular facets (56–63 %), support of the talus (5–15 %), as well as the tendon of the flexor of the toes and the ibial nerve (11 %). The main causes of complications are insufficient visualization from the surgical approach and difficulties in accurately of the osteotomy level of the anterior process of the calcaneus. In this regard, despite the proven effectiveness of the Evans technique, further improvement of surgical techniques and the development of more accurate intraoperative control methods are required to minimize the risks.

The **aim** of the work is to analyze the results of surgical treatment of patients with flexible flatfoot by introducing an original method based on 3D modeling of the calcaneus and preoperative planning of the osteotomy level.

Materials and methods The study included 40 patients with mobile flat foot deformity, who were treated at the Novosibirsk Research Institute named after Y.L. Tsivyan. All participants underwent a comprehensive examination, which included a clinical examination, radiography of the feet with load (in direct and lateral projections), MSCT of the ankle joint and an assessment on the AOFAS scale. The patients were divided into two groups: the control group (n = 20), where standard Evans osteotomy was used, and the main group (n = 20) using the developed method. Postoperative follow-up was carried out for 12 months.

Results The study was dominated by patients with combined anterior and middle articular facets: 12 (60 %) cases in the main group and 13 (65 %) in the comparison group. It has been established that this type of structure of the subcutaneous joint is more often damaged by Evans osteotomy. In the comparison group, damage to the articular surfaces occurred in 9 (45 %) patients, while in the main group — only in 1 (5 %); $p \leqslant 0.05$. Damage to the talus support was noted only in the comparison group — in 3 (15 %) cases out of 20. In both groups, there was a significant improvement in subjective assessment on the AOFAS scale and radiographic parameters one year after surgery.

Discussion The application of the developed method made it possible to significantly reduce the frequency of intraoperative injuries to the articular facets of the talus joint and the support of the talus bone. Stable radiological indicators of deformity correction were observed without cases of recurrence or loss of achieved correction during the 12-month follow-up period.

Conclusion The personalized surgical approach demonstrates significant benefits, including a reduction in the incidence of complications and recurrence of deformity, which contributes to improved clinical outcomes and improved quality of life for patients with squamous foot deformity.

Keywords: lateral elongating osteotomy, articular facets of the subtalar joint, flat foot deformity, Evans operation, Hintermann operation, personalized surgery

For citation: Gudi SM, Semenova DA, Krikunova VV, Vasiliev KO, Skuratova LK, Luchshev MD, Prokhorenko VM, Shevtsov VI, Pakhomov IA. Personalized approach to the treatment of patients with flat foot deformity: method for determining the level of osteotomy of anterior process of the the calcaneus. *Genij Ortopedii*. 2025;31(6):744-755. doi: 10.18019/1028-4427-2025-31-6-744-755.

INTRODUCTION

Acquired flatfoot is characterized by a partial or complete decrease in the height of the foot arch. The main causes of this pathology are considered to be dysfunction of the posterior tibial tendon, resulting from tendinitis, microtrauma, neuroarthropathy, inflammatory arthritis, and ruptures of the plantar calcaneonavicular and deltoid ligaments [1]. The incidence of flatfoot, according to various authors [2, 3], varies from 26.6 % to 60.0 %. The most effective method of its correction is surgical treatment. A common joint-sparing surgical method is lengthening osteotomy of the anterior process of the calcaneus [4-6]. The most frequently used operations are the Evans and Hintermann operations, both methods have good clinical and radiographic results. The involved subtalar joint, according to the literature, has a variable structure in different nationalities. It is known that in most countries, including Russia, the most common type of the structure of the articular facets of the subtalar joint is united anterior and middle facets (56–64 %) [7–10].

In the Evans procedure, the osteotomy line runs parallel to the calcaneocuboid joint at a distance of 1.5 cm from it, between the anterior and middle articular facets. Accordingly, the fused facet will be damaged in 100 % of cases if this operation is used and it can lead to persistent pain after surgical treatment, the development of arthrosis of the subtalar joint, and patient dissatisfaction with the treatment results [11]. According to Jara ME, complications occur in 8–12 % of cases with the Evans osteotomy, such as pain in the area of the surgical intervention, nonunion, instability of bone fragments, hypercorrection, damage to the tendons of the peroneal muscles and the sural nerve [12].

One of the important anatomical structures involved in the formation of the subtalar joint is the talar support (sustentaculum tali). Accordingly, its injury can lead to a subsequent fracture, damage to the flexor digitorum longus tendon, and tarsal tunnel syndrome. As shown in their study by Bussewitz et al. [13], if the osteotomy initiates at a distance of 1.3 cm from the calcaneocuboid joint, the sustentaculum tali is injured in four out of 10 cases. The authors recommend intraoperative visualization of the articular facets or preoperative determination of their location and shape with subsequent planning of the osteotomy level and direction so that the sustentaculum tali and the fused articular facet are not at risk of damage. However, there is a problem with intraoperative visualization of the articular facets of the subtalar joint in order to determine the level and direction of the osteotomy line, which would allow avoiding their damage. It is necessary to develop and introduce into practice a method for intraoperative determination and control of the level and direction of the osteotomy of the calcaneus.

The **aim** of the work is to compare the results of surgical treatment of patients with flexible flatfoot by an original method based on 3D modeling of the calcaneus and preoperative planning of the osteotomy level with the classical Evans osteotomy method.

MATERIAL AND METHODS

An analysis of the surgical treatment outcomes of 40 patients was conducted who were treated for flat-valgus foot deformity at the Tsivyan Novosibirsk Research Institute of Traumatology and Orthopedics between February 2023 and January 2024. The study included 24 (60 %) women and 16 (40 %) men; the average age was 41.5 ± 10.3 years. Patients were randomly divided into two groups.

The inclusion criterion and indication for surgical treatment was the failure of conservative therapy administered to patients for at least six months prior to hospitalization. Conservative treatment included correction with orthotic insoles, a series of therapeutic exercises aimed at strengthening the calf muscles and arch of the foot, and courses of nonsteroidal anti-inflammatory drugs (NSAIDs) for pain relief. A detailed analysis of conservative treatment protocols (including the use of local injection therapy) was not conducted in this study, as this treatment was administered by various medical institutions prior to patient enrollment into the present study.

The comparison group included 20 patients (11 (55 %) women and 9 (45 %) men; average age was (40.0 ± 11.5) years), who underwent correction of foot deformities using the classical Evans osteotomy method. The study group included 20 patients (13 (65 %) women and 7 (35 %) men; their average age was (45.0 ± 14.0) years); they were treated with the proposed by us method.

Clinical examination

Patients' complaints, medical history, visual examination, and palpation were studied. The medial longitudinal arch height, the degree of heel valgus, range of motion in the ankle and subtalar joints, and the functional status of the posterior tibial tendon were evaluated. Patients passed a subjective assessment of their condition severity using the AOFAS (American Orthopaedic Foot and Ankle Society) evaluation system. This assessment was repeated one year after surgery at a follow-up visit.

Radiographic study

Each patient participating in the study underwent a weight-bearing foot radiographic study in two projections (AP and lateral) upon hospitalization and one year after surgery. Lateral X-rays were used to evaluate the calcaneal-plantar angle between the calcaneal tuberosity (Fig. 1a) and the transverse plane, as well as the talometatarsal angle between the axis of the talus and the axis of the first metatarsal (Fig. 1b). The AP angle between the axis of the talus and the first metatarsal was measured (Fig. 1c). Based on the preoperative measurements, longitudinal arch reduction, forefoot abduction, and foot valgus were assessed, as well as the corrective capacity of the proposed method. On the day after surgery, a non-weight-bearing radiography was performed to evaluate the osteotomy level, graft position, and the metal fixator. One year after surgical treatment, the degree of correction of the deformity and its retention over the year were measured on control radiographs with a load on the foot, the consolidation of the osteotomy area, the position of the graft and metal fixator, and deforming osteoarthrosis severity in the adjacent joints were analyzed.

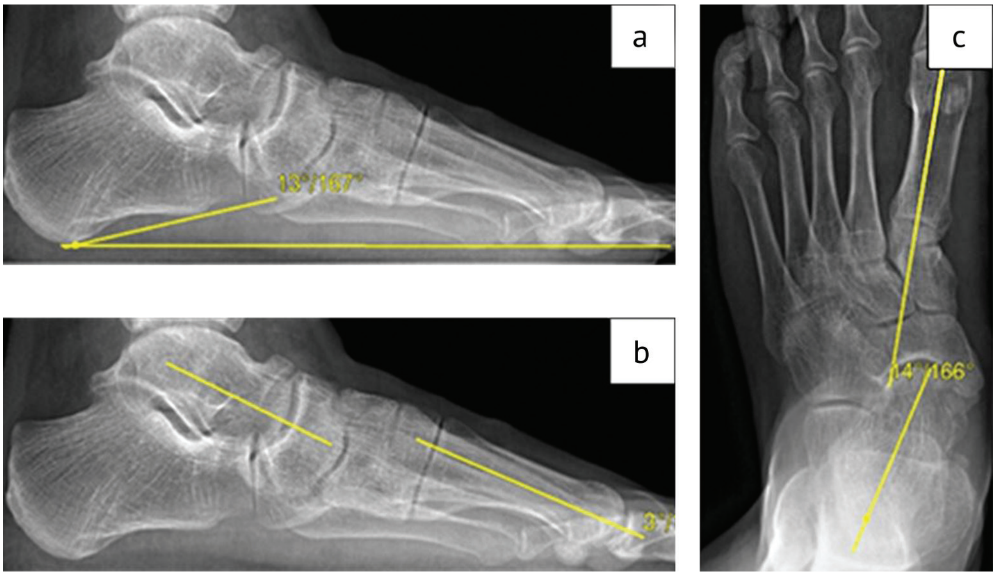

Fig. 1 Radiographs of the foot under loading: (a) lateral view, the angle between the calcaneus and the transverse surface; (b) lateral view, the angle between the axis of the talus and the first metatarsal; (c) direct view, the angle between the axis of the talus and the first metatarsal

Tomography

All patients underwent multislice computed tomography (MSCT) of the foot. The resulting images were sequentially processed, resulting in a 3D model of the calcaneus with visualized articular facets. Their shape and location were assessed.

The articular facets of the subtalar joint were systematized according to the classification of P. Bunning and C. Barnett [14]:

— Type A: The calcaneus has three separately located articular facets;

— Type B: The calcaneus has a fused anterior and middle facet and a separated posterior facet;

— Type C: The calcaneus has a single articular facet that combines the anterior, middle, and posterior facets.

On the first day after surgery, a repeated MSCT scanning of the foot was performed in both groups. In the study group, the integrity of the subtalar joint facets was assessed, and whether the level and direction of the osteotomy line corresponded to those calculated preoperatively. In the comparison group, the damage to the facets was assessed.

Surgical methods

According to the method of surgical treatment, all patients ($n = 40$) were divided into two equal groups: a comparison group ($n = 20$), in which patients underwent correction of flat-valgus foot deformity using the classical Evans osteotomy method, and a study group ($n = 20$), in which patients were treated using the developed by us method.

Surgical treatment in the comparison group

The surgery was performed using the standard Evans technique. An incision was made 1 cm distal to the lateral malleolus, directly above the anterior process of the calcaneus. The underlying tissues were mobilized using blunt dissection, the anterior process of the calcaneus was skeletonized, and two retractors were placed. The calcaneocuboid joint was exposed, and an osteotomy line was created 1.5 cm away from it and parallel to it. A distractor was then placed to shift the calcaneus fragments. The resulting space was filled with an allograft or autograft, resulting in the correction of the deformity, followed by plate fixation. The wound was closed layer by layer.

Surgical treatment in the study group

To treat patients using the developed by us method, a preoperative MSCT scan of the patient's foot was performed. 3D models of the calcaneus were created to visualize the articular facets on the surface. Their locations and shapes were determined using the classification of P. Bunning and C. Burnett. A series of measurements were then taken. A supposed osteotomy line was drawn between the articular facets (between the anterior and middle if the osteotomy was performed according to the Evans method; between the middle and posterior ones if the osteotomy was performed according to the Hintermann method). A perpendicular to the osteotomy line was drawn from the calcaneocuboid joint, and its angle relative to the lateral wall of the calcaneus was determined (Fig. 2).

During surgery, a guide wire was shaped based on the measurements taken. The AB distance of the guide wire was up to 1 cm, the BC distance corresponded to the perpendicular drawn from the calcaneocuboid joint to the osteotomy line, the CD distance was up to 5 cm, which corresponded to the surgical approach, and the BCD angle corresponded to the inclination of the osteotomy line relative to the lateral wall of the calcaneus (Fig. 3a).

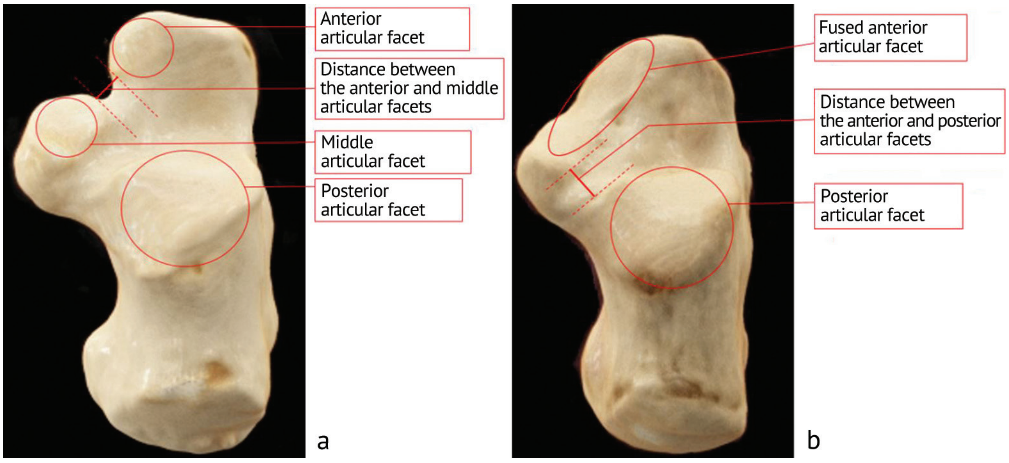

Fig. 2 Location of the articular facets of the subtalar joint on a 3D model of the calcaneus (a) and the method for determining the angle of inclination of the osteotomy relative to the lateral wall of the calcaneus (b)

With the patient in the supine position, a surgical approach was performed directly above the anterior process of the calcaneus. Using a blunt dissection, the anterior process of the calcaneus was skeletonized layer by layer, two retractors were placed, and the calcaneocuboid joint was visualized. A guide wire was inserted into the cavity of the joint so that segment BC corresponded to the perpendicular drawn to the osteotomy line, and angle BCD corresponded to the angle of inclination of the osteotomy line (Fig. 3b). Osteotomy was performed with a saw from the apex C of angle BCD in the direction of segment CD (Fig. 3c). A distractor was placed, the calcaneus fragments were shifted, and the space thus formed was filled with allo- or autograft, resulting in correction of the deformity and subsequent fixation with a metal construct. The wound was sutured layer by layer.

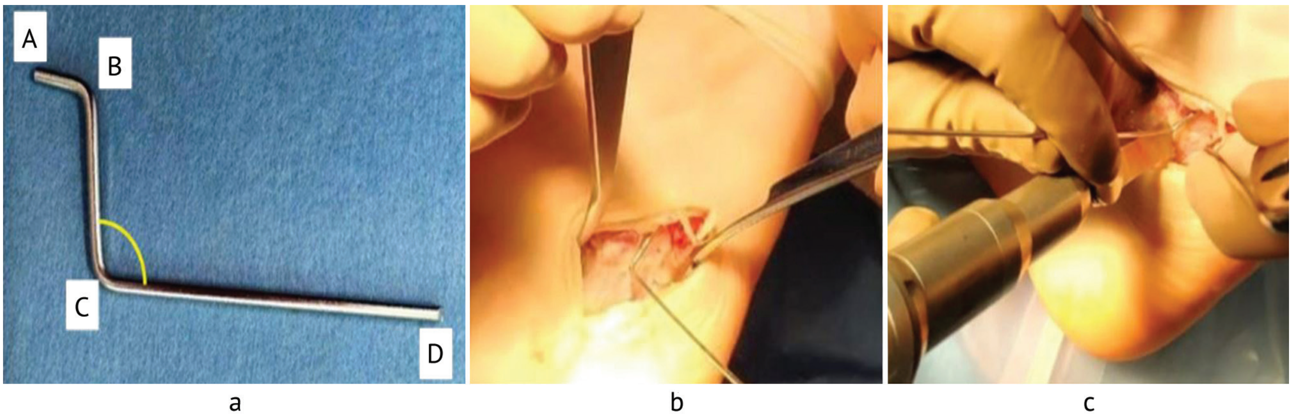

Fig. 3 Photos of the surgical stages in the study group: (a) guide wire prepared for surgery; (b) surgical approach, the guide wire is inserted into the calcaneocuboid joint, its long end corresponds to the direction of the osteotomy; (c) technique for performing osteotomy using a guide wire

Statistical method

The sample size was calculated based on the subtalar joint facet injury criterion, with injury occurring in 60 % of cases in the comparison group and 5 % in the study group. The required sample size was 32 patients, 16 in each group. This value was rounded to 20 patients in each group. The power of the study is 90 %.

Surgical treatment outcomes data for both groups were summarized in two tables which reflect patient age, facet type, and the presence or absence of facet injury after surgery. In the study group, a separate table reflects preoperative planning data (angle of the osteotomy relative to the lateral wall of the facet bone and the distance from the calcaneocuboid joint) and postoperative data (angle at which the osteotomy was performed and the distance from the calcaneocuboid joint). The resulting data were compared, and the error between the planned direction and the level at which the osteotomy was performed was calculated. In each patient group, radiographic deformity scores were assessed preoperatively and one year after surgery, and the data were compiled into a separate table. AOFAS questionnaire results were compared preoperatively and one year after surgery.

Statistical processing and data visualization were performed using Microsoft Office Excel (2016) and OriginPro (2021). The Mann–Whitney test was used to compare values between two samples with non-normal data distributions, and the Student's t-test was used for normal data distributions. Differences in the distribution of features were assessed using the chi-square test. Results with a p-value $\leqslant 0.05$ were considered statistically significant.

РЕЗУЛЬТАТЫ

All patients underwent a standard preoperative examination (clinical examination, radiography, and MSCT) on the day of admission to the hospital. The total duration of hospitalization was 4.1 ± 0.6 days, including 1.2 ± 0.4 preoperative days and 2.9 ± 0.8 postoperative observation days. After stabilization of their condition and control radiographs and MSCT, patients were discharged for further outpatient examination at their place of residence or referred to a rehabilitation center. There were no statistically significant differences in the duration of hospitalization between the groups ($p > 0.05$).

Results in the comparison group

According to the classification of P. Bunning and C. Barnett, seven patients (35 %) were classified as type A (mean age of 39.9 ± 10.6 years) while 13 patients (65 %) were classified as type B (mean age of 44.7 ± 13.6 years). Type C articular facets were not detected in this group.

According to the assessment of the subtalar joint facet condition after surgery, damage was observed in nine cases (45 %). The fused articular facet was most frequently damaged, in eight (61.5 %) of 13 cases; the posterior articular facet was not damaged in any of the patients. Damage to the talus support was detected in three cases (15 %).

Radiographic studies showed that on the follwoing day after surgery, the fixation screws were positioned in the calcaneus without affecting the surrounding joints. Fixation was stable, and no graft migration was detected. One year after surgery, weight-bearing radiographic study revealed a significant improvement in the studied parameters ($p \leqslant 0.05$; Table 1). One patient (5 %) experienced nonunion at the osteotomy site one year after surgery.

Table 1

Changes in radiographic angles before surgery and one year after surgery in the comparison group

Parameter	Time of study		p-value
	before surgery	one year after surgery	
Angle between the calcaneus and transverse plane, °	12.20 ± 2.42	19.05 ± 1.36	< 0.00001
The angle between the axis of the talus and the first metatarsal in the lateral view, °	10.65 ± 1.89	3.95 ± 1.27	< 0.00001
The angle between the axis of the talus and the first metatarsal in the frontal view, °	10.75 ± 1.73	4.00 ± 1.20	< 0.00001

Based on the AOFAS questionnaire, a patient survey conducted at a one-year follow-up revealed a significant improvement in subjective assessments: the mean score before surgery was 56.6 ± 10.8 points while after surgery it was 84.4 ± 5.6 points. Patients also reported an improved quality of life after surgery ($p \leqslant 0.05$). Reoperation was required in five (25 %) cases: one (5 %) due to pseudoarthrosis formation, and four (20 %) due to plate-peroneal tendons conflict, which resulted in persistent pain one year after surgery.

A case from the comparison group

A patient born in 1989 was admitted to the Tsivyan Novosibirsk Research Institute of Traumatology and Orthopedics with complaints of left foot deformity, pain in the midfoot by weight bearing, and pain when wearing shoes. According to the patient's medical history, the deformity of both feet had been present for a long time. The patient was followed by a traumatologist at a local outpatient clinic, but conservative therapy failed to produce significant improvement, and the deformity progressed. Based on a clinical examination, medical history, and radiographic data, a diagnosis of grade 2 flat-valgus foot deformity on the left and grade 1-2 bilateral hallux valgus was established. The patient underwent preoperative planning and surgical correction of the deformity using the classic Evans osteotomy. Preoperative ankle X-rays revealed the following parameters: calcaneal-plantar angle of 13°, talometatarsal angle of 14° in the AP projection, and 3° in the lateral view (Fig. 1). No MSCT was performed prior to surgery. The day after surgery, MSCT of the foot was performed, revealing the presence of a fused anterior and medial facets of the subtalar joint, damaged during surgery (Fig. 4).

Fig. 4 3D model of the calcaneus after surgery: damaged fused articular facet

One year after surgery, a follow-up X-ray of the ankle joint was performed with a weight-bearing test in two projections. The following parameters were obtained: calcaneal-plantar angle of 21°, talometatarsal angle of 3° in the AP view, and 4° in the lateral view. The AOFAS score showed an improvement from 53 points preoperatively to 87 points postoperatively.

Results in the study group

In the study group, eight patients (40 %) were classified as type A of P. Bunning and C. Barnett classification, average age of (33.8 ± 8.2) years, and 12 patients (60 %) were classified as type B, average age of (46.1 ± 8.8) years. According to the results of the articular facet assessment after surgery, performed in this group using the original method, damage was dtected in only one patient (5 %). No cases of damage to the sustentaculum tali were noted in the study group.

According to the evaluation of 3D models of the feet after surgery, the average error of the osteotomy angle determined preoperatively relative to the actual angle of the osteotomy was 1°, which is not statistically significant (p = 0.21). The distance from the calcaneocuboid joint to the intended osteotomy line, planned preoperatively, was (1.59 ± 0.28) mm, while after surgery it was (1.76 ± 0.24) mm. The error was 0.17 mm, which is not statistically significant (p = 0.13).

Based on radiographic results, the day after surgery, the fixation screws were positioned in the calcaneus and did not affect the joints. Fixation was stable, and no graft migration was observed. A follow-up with weight-bearing ankles one year later revealed a significant change in the angles ($p \leqslant 0.05$; Table 2). Reoperation was performed in two patients (10 %) due to plate-peroneal tendons conflict, which resulted in persistent local pain one year after surgery.

Table 2

Changes in radiographic angles before surgery and one year after surgery in the study group

Parameter	Time of study		p-value
	before surgery	one year after surgery	
Angle between the calcaneus and transverse plane, °	13.30 ± 2.00	19.70 ± 1.25	< 0.00001
The angle between the axis of the talus and the first metatarsal in the lateral view, °	9.45 ± 2.15	3.85 ± 1.67	< 0.00001
The angle between the axis of the talus and the first metatarsal in the frontal view, °	10.15 ± 1.98	4.15 ± 0.98	< 0.00001

A case from the study group

A patient born in 1996 was admitted to Tsivyan Novosibirsk Research Institute of Traumatology and Orthopedics (NNRITO) with complaints of deformities in both feet and foot pain that intensified after physical activity, more severe on the right side. A medical history stated that the deformity of both feet had been a problem for the patient since childhood. He was followed by a traumatologist-orthopedist at a local clinic; conservative therapy proved ineffective. Over the last few years, the patient felt increasing pain and discomfort in his feet, more severe on the right side, and difficulty wearing shoes and decided to consult at the NNRITO. Based on the patient's complaints, medical history, and clinical and radiographic data, the following diagnosis was established: acquired flat-valgus deformity of both feet, grades 2-3 on the right side, grade 2 on the left side; hallux valgus bilateralis, grades 1-2; bilateral tarsalgia syndrome, more severe on the right side.

Based on pre-surgical ankle X-ray results, the calcaneal-plantar angle was 17º, the talometatarsal angle in the AP view was 9º, and in the lateral view it was 6º.

Preoperative planning and surgical treatment were performed using the developed method. The patient's articular facets were type A, the distance from the calcaneocuboid joint was 1.5 cm, and the osteotomy line angle relative to the lateral wall of the calcaneus was 100º (Fig. 5). According to MSCT data, the day after surgery, none of the articular facets were damaged, and the osteotomy angle deviated from the planned angle by 1°. The distance from the calcaneocuboid joint deviated by 1 mm (Fig. 6).

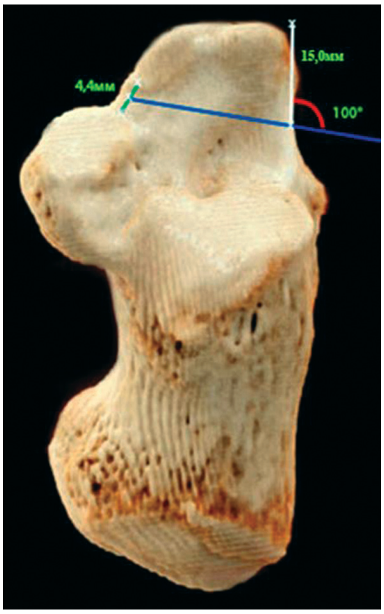

Fig. 5 Preoperative planning based on a 3D model of the calcaneus

Fig. 6 Results of surgical treatment according to MSCT data: visualization of intact facets and sustentaculum tali

One year after surgery, a radiographic study was performed in two weight-bearing views and the calcaneal-plantar angle (20°) and the talometatarsal angle in the frontal (3°) and lateral (3°) views were remeasured. At the one-year follow-up appointment, the AOFAS score showed a change from 42 points preoperatively to 89 points postoperatively.

Comparison of the results in the groups

Patients in both groups were compared based on several parameters: the proportion of patients with different types of articular facets, their condition (damaged/intact), changes in foot angles, and changes in AOFAS questionnaire results after surgery.

Reoperation was required in both groups due to interference between the metal fixator and the peroneal tendons (four cases in the comparison group, two in the study group).

Patients with type B prevailed in both groups. Significant differences were observed in assessing the condition of the articular facets of the subtalar joint. In the comparison group, damage was noted in almost half of the cases (45 %), while in the study group, only one case (5 %) of facet damage was detected. This difference was considered statistically significant ($p = 0.0035$).

To assess the corrective efficacy of the method developed, radiographic parameters obtained preoperatively and one year postoperatively were compared in the comparison and study groups. The data did not show statistically significant differences, which confirms the good corrective ability of the proposed method.

AOFAS score after the interventions did not have significant differences in the groups.

In the comparison group, which included 20 patients, surgical treatment for planovalgus deformity was performed using the classic Evans osteotomy. Postoperative MSCT imaging revealed damage to at least one subtalar joint facet in nine cases (45 %). Damage to the fused facet was most common (eight of nine cases, 89 %), which was considered statistically significant ($p = 0.043$). Damage to the talus support was observed in three (15 %) of the 20 cases.

In the study group, which also included 20 patients, surgical treatment was performed using the developed original method. According to postoperative MSCT of the ankle joint, damage to the articular facet was observed in one case (5 %) of a patient with type A. The assumed cause of the damage lies in an individual characteristic, due to which the distance between the posterior edge of the anterior and anterior edge of the middle facets is extremely small (0.14 cm). The error in the osteotomy direction calculated based on a 3D model of the calcaneus during preoperative planning was 1°, and the error in the distance from the calcaneocuboid joint to the supposed osteotomy line was 0.17 mm. Both indicators are not statistically significant.

DISCUSSION

In 1995, Mosca VS [15] modified the Evans osteotomy method by proposing the insertion of a bone raspatory into the subtalar joint between the anterior and middle articular facets for their protection. However, his method has drawbacks, such as the need to open the joint capsule and the difficulty in determining the required interval for insertion of the raspatory due to limited intraoperative visibility. This method is traumatic for the subtalar joint and does not exclude damage to the fused anterior and middle articular facets.

According to the method for determining the osteotomy level developed by Kenis et al., during radiographic control of the foot in the anteroposterior view where the talus support is visualized, the osteotomy line should be located directly in front of it [16]. The use of this method allows one to avoid damage to the talus support but does not exclude damage to the articular facets of the subtalar joint due to the impossibility of their visualization on X-ray images.

The osteotomy method proposed by Hintermann et al. successfully protects the anterior and middle articular facets of the subtalar joint [17]. However, preoperative MSCT of the ankle joint is necessary to determine the shape and location of the articular surfaces in order to plan treatment using the Hintermann method for a specific patient. The distance from the calcaneocuboid joint to the supposed osteotomy line should also be measured to determine its precise direction during surgery, thus protecting the articular facets of the subtalar joint and talus support from damage.

According to researchers who retrospectively evaluated the results of surgical treatment of 53 patients, 36 of whom underwent Hintermann osteotomy, radiological methods showed that in that group of patients, the anterior and middle articular facets of the subtalar joint remain intact in 100.0 % and 85.7 % of cases, respectively. The second group included 17 people who underwent the Evans operation; the articular facets in that group remained intact in only 42.9 % of cases for the anterior facet and in 71.4 % of cases for the middle facet. The posterior facet was uninjured in all described cases [18, 19].

Other researchers studied intraoperative deviations in the osteotomy line direction during the Hintermann procedure from the initially determined one during preoperative planning. The study was conducted on 60 foot models. Based on the anatomical features of the subtalar joint, the ideal distance for the osteotomy was considered to be 11.5 mm from the calcaneocuboid joint. According to the results, deviations from this direction were (2.5 ± 1.5) mm. Tangential damage to the middle articular facet was most frequently observed, but damage to the posterior facet was considered more significant, as it is the largest, primary weight-bearing area and plays a significant role in the biomechanics of the subtalar joint. Complete damage was observed in 10 cases out of 60, tangential damage in 11 cases out of 60. In total, the posterior facet was damaged in 21 models out of 60. However, the described study has some limitations associated with the variability in the structure of the articular facets of the subtalar joint, which were not reflected in the manufacture of foot models [20].

Pseudoarthrosis developed when the osteotomy line passed through the middle facet of the subtalar joint one year after surgery in one patient (5 %) in the comparison group. The patient required a re-operation. According to the literature, synovial fluid leakage may be a cause of nonunion in patients with intra-articular fractures and articular surface defects [21]. However, no such complications were observed in the study group. Thus, one of the causes of pseudoarthrosis formation during calcaneal osteotomy may be its passage through the articular surfaces with possible penetration of the synovial which prevents callus formation.

Re-operations were also required in both groups due to conflict between the plate and the peroneal tendons, leading to persistent pain one year after surgery and decreased patient satisfaction. We believe that this condition requires the development and implementation of an internal implant that eliminates these drawbacks.

To assess the effectiveness of plano-valgus foot deformity correction, we analyzed weight-bearing foot radiographs, focusing on parameters such as the angle between the calcaneal tuberosity and the transverse plane, and the talometatarsal angle between the axis of the talus and the axis of the first metatarsal. On frontal views with weight-bearing, the angle between the axis of the talus and the first metatarsal changed. Improvement in these parameters postoperatively indicates restoration of arch height and joint relationships. Our findings of radiographic improvement in the study group are consistent with published data and correspond to the expected effectiveness of the method.

Radiographically, the angle between the axes of the talus and first metatarsal decreased on average from 15° to 3° due to the elimination of forefoot abduction, which is a normal value for this parameter [22]. In our study, we obtained similar data. The angle between the talus and the horizontal surface increased by 5–10° after surgery and indicates restoration of the longitudinal arch height.

A limitation of the present study is a relatively short follow-up period (one year) without assessing long-term outcomes. It is also important to note that radiographic findings do not always correlate with clinical symptoms. Thus, some patients with ideal angular measurements experienced persistent pain at the surgical site, which may be due to the characteristics of the graft and the presence of metal hardware.

The variability of the anatomical structure of the subtalar joint requires a personalized approach to the choice of the anterior calcaneal osteotomy level in patients with flatfoot deformity.

CONCLUSION

The original method developed is based on 3D modeling of the calcaneus with preoperative planning and minimizes the risk of damage to the subtalar joint facets and other anatomical structures. This personalized treatment approach reduces the incidence of complications and deformity recurrence and improves clinical outcomes and patient quality of life.

__Conflict of interests__ None.

__Funding source__ There was no external financial support.

__Ethical approval__ The study was approved by the institutional ethics committee of the Tsivyan Novosibirsk Research Institute of Traumatology and Orthopedics of the Russian Ministry of Health (protocol dated July 11, 2024, No. 01-18/4853) and was conducted in accordance with the ethical standards of the Declaration of Helsinki of the World Medical Association.

__Informed consent__ Patients provided voluntary written informed consent for inclusion in the study.

REFERENCES

1. Flores DV, Mejía Gómez C, Fernández Hernando M, et al. Adult Acquired Flatfoot Deformity: Anatomy, Biomechanics, Staging, and Imaging Findings. *Radiographics*. 2019;39(5):1437-1460. doi: 10.1148/rg.2019190046.
2. Samarakoon JN, de Silva NL, Fernando D. Prevalence and associated factors of flat feet among patients with hypertension; findings from a cross sectional study carried out at a tertiary care hospital in Sri Lanka. *Archives of Physiotherapy and Rehabilitation*. 2020;3(4):076-083. doi: 10.26502/fapr0016.
3. Davydova NI. Flat feet and measures to combat them. In: Priorov NN. (ed). *Foot and issues of constructing rational footwear*. Moscow: TsITO; 1960:157. (In Russ.)
4. Tao X, Chen W, Tang K. Surgical procedures for treatment of adult acquired flatfoot deformity: a network meta-analysis. *J Orthop Surg Res*. 2019;14(1):62. doi: 10.1186/s13018-019-1094-0.
5. Protsko VG. *Surgical treatment of flat-valgus deformity of the feet in adults: Dokt. dis*. Moscow; 2018:204. Available at: http://dissovet.rudn.ru/web-local/prep/rj/index.php?id=38&mod=dis&dis_id=2314. Accessed Sept 12, 2025. (In Russ.)
6. Kenis VM, Lapkin YA, Husainov RK, Sapogovskiy AV. Flexible flatfoot in children (review). *Pediatric Traumatology, Orthopaedics and Reconstructive Surgery*. 2014;2(2):44-54. (In Russ.) doi: 10.17816/PTORS2244-54.
7. Hyer CF, Lee T, Block AJ, VanCourt R. Evaluation of the anterior and middle talocalcaneal articular facets and the Evans osteotomy. *J Foot Ankle Surg*. 2002;41(6):389-393. doi: 10.1016/s1067-2516(02)80085-0.
8. Wu J, Liu H, Xu C. The optimal procedure for lateral column lengthening calcaneal osteotomy according to anatomical patterns of the subtalar joint: an anatomical study in the Chinese population. *BMC Musculoskelet Disord*. 2022;23(1):751. doi: 10.1186/s12891-022-05715-w.
9. Byroshevskaya MV, Safiullina AF, Khayrullin RM. The frequency of types of calcaneus according by the modified classification of talar articular fasets. *Morphological statements*. 2014;22(1):26-32. (In Russ.) doi: 10.20340/mv-mn.2014.0(1):26-32.
10. Gudi SM, Semenova DA, Vasiliev KO, et al. The optimal method of lateral lengthening osteotomy of the calcaneus: CT study in the Russian population. *Genij Ortopedii*. 2024;30(6):855-862. doi: 10.18019/1028-4427-2024-30-6-855-862.
11. Raines RA Jr, Brage ME. Evans osteotomy in the adult foot: an anatomic study of structures at risk. *Foot Ankle Int*. 1998;19(11):743-747. doi: 10.1177/107110079801901106.

12. Jara ME. Evans osteotomy complications. *Foot Ankle Clin*. 2017;22(3):573-585. doi: 10.1016/j.fcl.2017.04.006.
13. Bussewitz BW, DeVries JG, Hyer CF. Evans osteotomy and risk to subtalar joint articular facets and sustentaculum tali: a cadaver study. *J Foot Ankle Surg*. 2013;52(5):594-597. doi: 10.1053/j.jfas.2013.03.006.
14. Bunning PS, Barnett CH. A comparison of adult and foetal talocalcaneal articulations. *J Anat*. 1965;99(Pt 1):71-76.
15. Mosca VS. Calcaneal lengthening for valgus deformity of the hindfoot. Results in children who had severe, symptomatic flatfoot and skewfoot. *J Bone Joint Surg Am*. 1995;77(4):500-512. doi: 10.2106/00004623-199504000-00002.
16. Kenis VM, Sapogovskiy AV. *Method for determining the level of osteotomy of the calcaneus during the Evans operation*. Patent RF, no. 2676665. 2019. Available at: https://patents.s3.yandex.net/RU2676665C2_20190109.pdf. Accessed Sept 12, 2025. (In Russ.)
17. Hintermann B, Valderrabano V, Kundert HP. Lengthening of the lateral column and reconstruction of the medial soft tissue for treatment of acquired flatfoot deformity associated with insufficiency of the posterior tibial tendon. *Foot Ankle Int*. 1999;20(10):622-629. doi: 10.1177/107110079902001002.
18. Ettinger S, Mattinger T, Stukenborg-Colsman C, et al. Outcomes of Evans Versus Hintermann Calcaneal Lengthening Osteotomy for Flexible Flatfoot. *Foot Ankle Int*. 2019;40(6):661-671. doi: 10.1177/1071100719835464.
19. Ettinger S, Sibai K, Stukenborg-Colsman C, et al. Comparison of Anatomic Structures at Risk With 2 Lateral Lengthening Calcaneal Osteotomies. *Foot Ankle Int*. 2018;39(12):1481-1486. doi: 10.1177/1071100718789435.
20. Polt M, Viehöfer AF, Casari FA, et al. Conventional vs Augmented Reality-Guided Lateral Calcaneal Lengthening Simulated in a Foot Bone Model. *Foot Ankle Int*. 2024;45(7):773-783. doi: 10.1177/10711007241237532.
21. Fayaz HC, Giannoudis PV, Vrahas MS, et al. The role of stem cells in fracture healing and nonunion. *Int Orthop*. 2011;35(11):1587-1597. doi: 10.1007/s00264-011-1338-z.
22. Schleunes SD, Campbell SN, Jones JM, et al. Radiographic Analysis of the Lateral Column Lengthening Procedure in Stage II Adult Acquired Flatfoot Deformity. *J Foot Ankle Surg*. 2022;61(6):1293-1298. doi: 10.1053/j.jfas.2022.04.005.

The article was submitted 24.07.2025; approved after reviewing 11.09.2025; accepted for publication 14.10.2025.

Information about the authors:

Sergey M. Gudi — Candidate of Medical Sciences, Researcher, Head of the Department, orthopaedic surgeon, smgudinsk@gmail.com, https://orcid.org/0000-0003-1851-5566;

Daria A. Semenova — student, semenovadasha544@mail.ru, https://orcid.org/0009-0005-6108-9365;

Valentina V. Krikunova — resident, krikunova-v12@yandex.ru, https://orcid.org/ 0009-0000-4418-3695;

Konstantin O. Vasiliev — radiologist, vasiliev_ko@maiol.ru, https://orcid.org/0009-0006-2726-1392;

Lilia K. Skuratova — junior research assistant, orthopaedic surgeon, lilipetrov@bk.ru, https://orcid.org/0000-0003-3736-3270;

Matvey D. Luchshev — post-graduate student, junior research assistant, orthopaedic surgeon, mat.luchshev@gmail.com, https://orcid.org/0000-0002-4975-9494;

Valery M. Prokhorenko — Doctor of Medical Sciences, Professor, Chief Researcher, vprohorenko@niito.ru, https://orcid.org/0000-0002-0655-9644;

Vladimir I. Shevtsov — Doctor of Medical Sciences, Professor, Corresponding Member of the Russian Academy of Sciences, shevtcov3838@mail.ru, https://orcid.org/0000-0001-7051-8065;

Igor A. Pakhomov — Doctor of Medical Science, Chief Researcher, orthopaedic surgeon, pahomovigor@inbox.ru, https://orcid.org/0000-0003-1501-0677.

Original article
https://doi.org/10.18019/1028-4427-2025-31-6-756-763

Stress radiography in the assessment of residual deformity of idiopathic clubfoot following serial casting (Ponseti method) in Thi-Qar province

Z.A. Abbas✉**, F.A. AlBaghdadi, W.G. Shaty**

College of Medicine, University of Thi-Qar, Iraq

Corresponding author: Zain Ali Abbas, ahmeds201258@yahoo.com

Abstract

Background Clubfoot, or congenital talipes equinovarus, is a congenital foot malformation and condition. Its early detection and identification can ensure the best possible long-term outcomes for the infant. Stress radiographs provide objective evidence of residual deformity, guiding further treatment.

Aim of the study was to compare radiographic findings of residual idiopathic clubfoot deformity in non-stress and stress positions to know the relationship of the angles difference and the type of treatment.

Material and Methods This study is a cross-sectional comparative study conducted at Al-Nasiriyah Teaching Hospital. Data was collected for the period from the 1st of March 2024 to the 1st of March 2025. The study includes 73.3 % males in a mean age of 1.7 years. Unilateral deformities among them were 80 %, equinus 85.2 % and adduction 66.7 %. 112 children with clubfoot deformities and 45 with idiopathic clubfoot cases (54 feet) which had residual deformity were included.

Results Stress radiographs revealed significant angular reductions in various deformities. Cutoffs of > 18° for the talo-first metatarsal angle in lateral view)adduction) and > 20° for the tibio-calcaneal angle (equinus), both with high sensitivity and specificity.

Discussion Clubfoot is more prevalent in male patients and often presents as a unilateral deformity. The most common residual deformities observed are equinus and adduction.

Conclusion Stress radiographs play a crucial role and show significant angular changes that help evaluate deformity flexibility and severity. Larger angle differences correlated with successful casting, while smaller differences predicted surgery.

Keywords: stress radiography, assessment, residual deformity, clubfoot, serial casting

For citation: Abbas ZA, AlBaghdadi FA, Shaty WG. Stress radiography in the assessment of residual deformity of idiopathic clubfoot following serial casting (Ponseti method) in Thi-Qar province. *Genij Ortopedii*. 2025;31(6):756-763. doi: 10.18019/1028-4427-2025-31-6-756-763.

INTRODUCTION

Clubfoot, or congenital talipes equinovarus, is a congenital foot malformation and condition. It is one of the most common musculoskeletal birth defects, presenting with four primary malformations that range in severity and degree of predicted contractures: Midfoot cavus, Forefoot adductus, Heel/hindfoot varus, and Hindfoot equinus [1].

Clubfoot, when identified early and treated effectively, has good success rates in correction and overall patient outcomes. Therefore, its early detection and identification can ensure the best possible long-term outcomes for the infant [2].

The incidence of clubfoot is reported to be between 0.5 and 2 cases per 1,000 newborns [3]. Males are twice as common as girls to be born with clubfoot [4].

Although the exact aetiology remains debated, the consensus favours multiple genetic and environmental risk factors that play varying levels of contributing roles in its clinical manifestations [5].

Approximately 7 % of clubfoot patients may present with an additional congenital defect at birth, and 7.6 % will exhibit a neurodevelopmental disorder of varying severity [6].

The foot in clubfoot is held in an abnormal position, with the toes pointing downward and inward (equinovarus). This leads to abnormal gait patterns and difficulty with normal weight-bearing. The rigidity of the deformity varies, with some cases being more flexible and others more resistant to correction [7].

Characteristic foot abnormalities include midfoot cavus, forefoot adductus, hindfoot varus and equinus, varying in severity and rigidity. The Pirani scoring system is the most commonly used method to assess severity due to its reliability [1].

The Pirani system entails evaluating six distinct factors in the foot. Each parameter is assigned a score of 0, 0.5, or 1 based on its severity. This rating establishes a minimum score of 0 per foot and a maximum value of 6. Three factors pertain to the hindfoot, whereas three relate to the midfoot [8].

Stress radiography plays an important role in evaluating residual deformities after the treatment of clubfoot using the Ponseti method. Although clinical examination is the primary tool for assessing the correction, stress radiographs provide detailed imaging that helps in visualizing subtle deformities that may not be evident during physical examination. These radiographs are taken under specific forces to highlight joint and bone alignment and stability in the foot [9, 10].

Stress radiographs provide objective evidence of residual deformity, guiding further treatment. If residual deformities are detected, additional interventions such as repeat casting, Achilles tenotomy, or even surgical procedures (e.g., tibialis anterior tendon transfer) may be necessary to prevent the recurrence of the deformity [11].

Aim To study the difference between degrees of angles of stress view and nonstress view of the residual deformity in idiopathic clubfoot and its relationship with type of treatment casting or surgical imtervention.

MATERIALS AND METHOD

This study is a cross-sectional comparative study conducted at Al-Nasiriyah Teaching Hospital to compare radiographic findings of clubfoot deformity in non-stress and stress positions and to assess the extent of residual deformities following Ponseti treatment of idiopathic club foot. Data was collected for the period from the 1st of March 2024 to the 1st of March 2025.

During the study period, 112 children with clubfoot deformities consulted the clubfoot clinic at Al-Nasiriyah teaching Hospital, and 45 with idiopathic clubfoot cases (54 feet) which had residual deformity were included in the study. The remaining patients were excluded because they had other types of clubfoot deformity.

The study included 45 patients who were diagnosed with clubfoot; their mean age was 1.7 years and ranged between 3 months and 5 years. 73.3 % of them were male and 26.7 % of them were female. A positive family history of clubfoot was present in 24.4 % of patients. The consanguinity was present in 46.7 %. All these data are presented in Table 1.

Table 2 shows clinical features related to the clubfoot, regarding the site of the problem; it was unilateral in 80 % of patients and 20 % of them had bilateral involvement. Regarding the residual deformities, 85.2 % had equinus deformity, 66.7 % had adduction and only 14.8 % of them had cavus.

Table 1

Patients' sociodemographic characteristics

Variables		%	No.
Age	3 months — 5 years		
	Mean ± SD	1.7 ± 0.9	
Gender	Male	33	73.3
	Female	12	26.7
Residency	City center	29	64.4
	Rural	16	35.6
Family history	Yes	11	24.4
	No	34	75.6
Cosenguanity	Yes	21	46.7
	No	24	53.3

Table 2

Clubfoot-related characteristics

Variables			No. of feet	%
Site of deformity	Unilateral (N = 36)	Right	26	72.2
		Left	10	27.8
	Bilateral (N = 9)		18	33.3
Residual deformity	Varus		16	29.6
	Adduction		36	66.7
	Equinus		46	85.2
	Cavus		8	14.8

The Patients with incomplete treatment using the Ponseti method, patients unable to tolerate or cooperate during stress radiography, and other types of clubfoot such as postural, syndromic and neurological types were excluded from the study.

A prepared data collection sheet was used to gather the data for the following variables: demographic data (including age, gender, residency and socioeconomic status); family history (consanguinity of parents, age of father and mother and number of siblings); clinical presentation (including the site of the problem, unilateral or bilateral, and pre-and post-treatment severity) and were evaluated using the Pirani score as determined by an orthopaedic specialist. The patient was referred for radiographic imaging taken in two views: anteroposterior and lateral with and without stress. Each patient underwent radiographic imaging of the affected foot using X-RAY 500 MA (manufactured by GU/USA). Non-Stress Position: The foot is positioned in a neutral alignment with no external manipulation. Stress Position: Manual pressure is applied by the examiner to attempt correction of the deformity during radiography used to differentiate between rigid and flexible deformities. Two types of stress were applied. Abduction stress was used to check the forefoot and midfoot flexibility. Dorsiflexion stress was used to evaluate the hindfoot flexibility and ankle joint range of motion.

To obtain radiographs that ensure consistent pressure, one of the patient's relatives was informed how to apply the stress to capture corrected angles.

The following angles were measured.

Talocalcaneal Angle measures hindfoot alignment since decreased angles indicate residual varus. This angle was measured by obtaining an anteroposterior (AP) radiograph of the foot. Identify the central axis of the talus (line drawn along the talar body and neck) and the central axis of the calcaneus. Measure the angle formed by the intersection of these two lines. The normal value range between 25° and 40°. Below this value indicates residual varus deformity (Fig. 1).

Tibiocalcaneal Angle evaluates ankle position and Achilles tendon flexibility. This angle is measured by obtaining a lateral radiograph of the ankle. Identify the longitudinal axis of the tibia and the axis of the calcaneus. Measure the angle formed at the intersection of these two lines. Between 60° to 90° is the normal value and any increase in this value is considered as equinus deformity (Fig. 2).

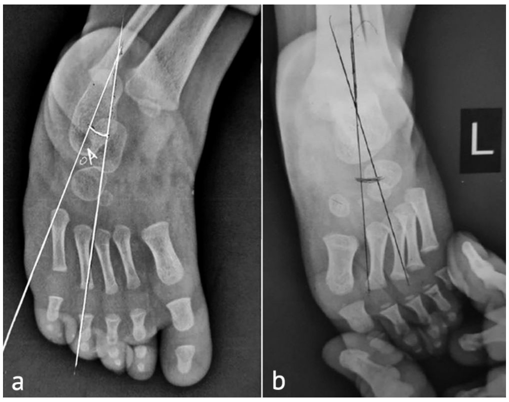

Fig. 1 Talo-calcaneal angle: (a) classic view; (b) stress view

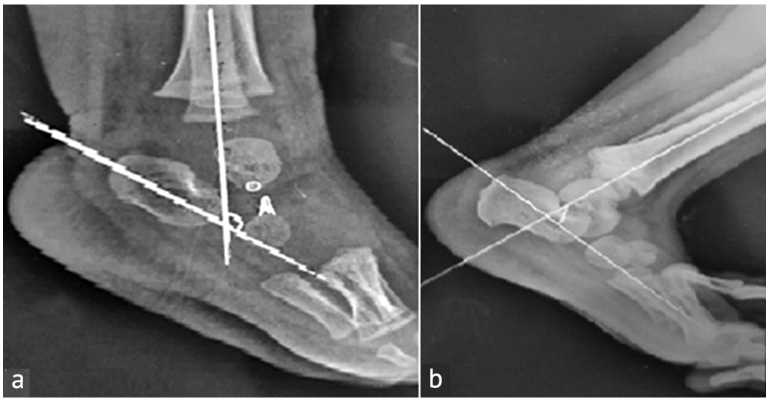

Fig. 2 Tibiocalcaneal angle: (a) classic view; (b) stress view

Talus-first metatarsal Angle (AP view) evaluates the alignment and structure of the midfoot and forefoot. It assesses medial-lateral alignment. The angle is formed between the long axis of the talus and the long axis of the first metatarsal. It is 0 to 20° in normal foot; any angle more than this range will consider forefoot adduction (Fig. 3).

Talo-first metatarsal angle (lateral view) assesses the longitudinal arch of the foot and the vertical alignment of the talus with the first metatarsal. It evaluates the degree of arch collapse or elevation. The normal value is 0 to 4° (Fig. 4).

Fig. 3 Talo-first metatarsal angle (AP view): (a) classic view; (b) stress view

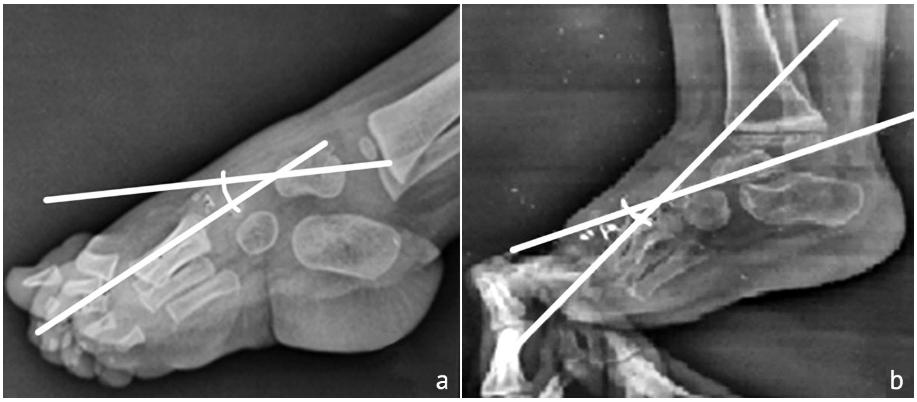

Fig. 4. Talo-first metatarsal angle (lateral view): (a) classic view; (b) stress view

Each measurement was performed by one radiology specialist and one orthopaedic specialist to ensure reliability and reduce observer bias. The College of Medicine, the University of ThiQar Ethical Committee, and the Thi-Qar Health Directorate's ethical committee all awarded their ethical approval. Participants' anonymity and confidentiality were preserved for the whole investigation. Additionally, informed consent was obtained from patients' parents or legal guardians.

A computerized statistical program called the Statistical Package for Social Sciences (SPSS) version 26 was used to enter and analyze the data. The proper statistical tests were conducted: two samples independent t-tests were used for the continuous variable, and a Chi-square test was used for categorical variables. The significance threshold (p-value) is set at $\leqslant 0.05$ for all statistical analyses.

RESULTS

A significant decrease in the talocalcaneal angle was observed as the angle changed from 25.25° to 17.25° after the application of stress and the p-value = 0.001. Table 3 shows the difference in angles before and after the application of stress among different residual deformities.

Table 3

Difference in angles before and after the application of stress in different residual deformities

Variables		With stress	Without stress	*P*-value
		(Mean ± SD)		
Varus	Talo-calcaneal angle	25.25 ± 2.29	17.25 ± 1.43	0.001
Adduction	Talo-first metatarsal angle (ap)	40.11 ± 4.8	19.22 ± 8.03	0.001
Cavus	Talo-first metatarsal angle (lateral)	20.0 ± 2.3	8.0 ± 0.0	0.002
Equinus	Tibio-calceneal angle	115.42 ± 7.01	97.1 ± 7.45	0.001

Regarding the adduction deformity, the stress showed a significant reduction in the talo-first metatarsal angle (AP view) as the $p = 0.001$.

While the talo-first metatarsal angle (lateral view) also showed a significant reduction of angle with stress application from 20.0° to 8.0° and the $p = 0.002$.

Similarly, the talo-calcaneal angle and the tibio-calcaneal angle reduced with stress application ($p = 0.001$).

The surgery was required in 26 patients (48.1 % of feet), and 28 patients (51.9 %) with residual deformity were treated with plaster casting.

Table 4 shows the association between the angle differences after the application of stress and the decision of casting or surgery. Regarding the varus deformity, the mean difference in the talo-calcaneal angle after stress was 7 among those who needed surgery and it was 9 among those who needed casting and the mean difference shows a statistically significant association with the fate of patients since p-value=0.002.

Talo-first metatarsal angle (AP view) for the adduction deformity, showed a significantly lower angle mean difference in the surgery group in comparison to the casting group (16.0 vs 24.0 among both groups respectively) and the $p = 0.001$.

Talo-first metatarsal angle (lateral view) for the cavus deformity, the mean difference in the angle after stress was 14.0 among the casting group and a lower mean 10.0 among the surgery group andthe $p = 0.005$.

Finally, eqiunus deformity, tibio-calcaneal angle shows a mean difference of 23.7 in the casting group and a lower mean difference of 13.45 in the surgery group. The larger mean difference indicates the need for casting in all residual deformity of idiopathic clubfoot, for varus, adduction, equinus and the cavus.

As $p = 0.05$ there is a significant role for the angle difference after stress application in determining the proper treatment method.

Table 4

Association between mean difference in angles with and without stress and the fate of patients

Variables		Surgery Mean difference	Casting Mean difference	*P*-value
Varus	Talo-calcaneal angle	7.00 ±1.01	9.00 ± 1.06	0.002
Adduction	Talo-first metatarsal angle (ap)	16.0 ±5.65	24.0 ± 4.62	0.001
Cavus	Talo-first metatarsal angle (lateral)	14.00 ± 0.00	10.00 ± 0.00	0.005
Equinus	Tibio-calceneal angle	13.45 ± 4.9	23.7 ± 1.59	0.001

The ROC curve for the angle difference to choose casting and sensitivity, specificity and area under the curve were presented in Table 6, Figures 1 and 2. For adduction, when the talo-first metatarsal angle (AP view) showed a difference of more than 18 degrees the need for casting with 100 % sensitivity and only 57.1 % specificity. Regarding the equinus deformity, the tibio-calcaneal angle difference of > 20 degrees indicates the need for casting with a sensitivity and specificity of 100 % (Fig. 5 and 6).

Table 6

ROC curve for the angle difference to choose casting and sensitivity, specificity and area under the curve

Variables		Cut off point	Sensitivity	Specificity	*AUC*
Adduction	Talo-calcaneal angle	> 18	100.0	57.1	86.4
Equinus	Talo-first metatarsal angle (ap)	> 20	100.0	100.0	100.0

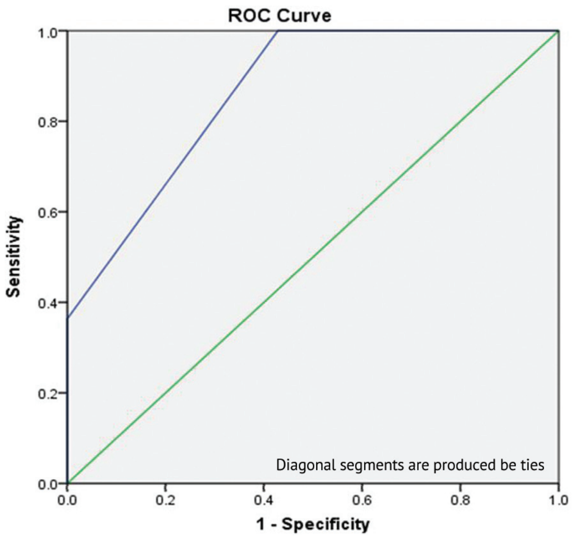

Fig. 5 ROC curve results for talo-first metatarsal angle (AP)

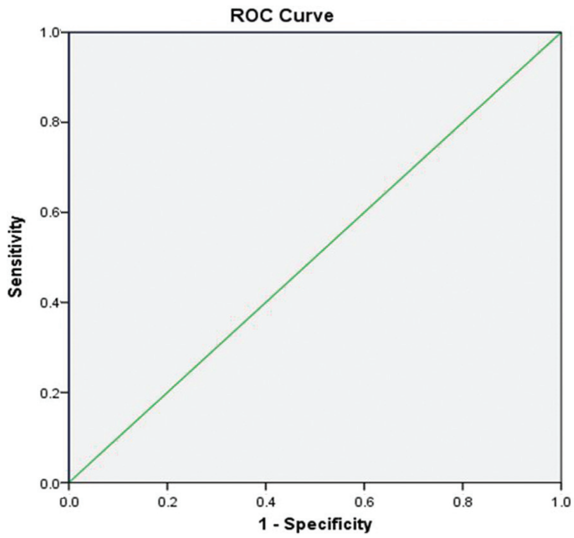

Fig. 6 ROC curve results for the tibio-calcaneal angle

DISCUSSION

Congenital talipes equinovarus (CTEV), commonly known as clubfoot, is a complex pediatric orthopaedic condition characterized by musculoskeletal deformities, primarily involving the ankle and foot [1]. This study aimed to evaluate the utility of stress radiographs in assessing residual deformities in clubfoot patients and to determine their role in guiding treatment decisions between surgical and non-surgical interventions.

The study population included 45 patients with a mean age of 1.7 years, predominantly male (73.3 %), with nearly half having a history of consanguinity (46.7 %) and a quarter reporting a positive family history of clubfoot (24.4 %) (Table 1). These findings align with previous literature indicating a male predominance and a higher prevalence in populations with consanguineous marriages, suggesting a genetic predisposition [12]. Genetics likely has a role to play, although a specific gene alteration remains unclear. Research shows that 24.4 % of cases have an associated family history, though it has not identified a definite mode of inheritance [1].

Unilateral involvement was significantly more common (80 %) than bilateral cases (20 %) (Table 2), which is slightly different from the existing epidemiological data by 1) who found that clubfoot is usually bilateral in more than 50 % of the cases. Among residual deformities, equinus was the most frequent (85.2 %), followed by adduction (66.7 %) and cavus (14.8 %). This pattern reflects the classic presentation of clubfoot, where equinus and adduction are typically the most persistent deformities [13].

Table 3 demonstrates a statistically significant improvement in key radiographic angles following the application of stress. Notably, the talo-calcaneal angle (associated with varus deformity) significantly decreased from 25.25° to 17.25° ($p = 0.001$), indicating improved alignment. Similarly, significant reductions were noted in the talo-first metatarsal angles (AP and lateral views) for adduction and cavus deformities ($p = 0.001$ and $p = 0.002$, respectively), and in the tibio-calcaneal angle for equinus ($p = 0.001$). These findings suggest that stress radiographs offer an objective and quantifiable method for assessing the flexibility and severity of residual deformities, as supported by Sambandam et al. (2016) and J. Li et al. (2024) who emphasized the value of dynamic radiography in treatment planning [9, 14].

Interestingly, nearly half of the patients (48.1 %) required surgical intervention, while 51.9 % were managed with casting (Table 4) and this is in line with the findings from Recordon et al. (2021) [15].

A significant association was found between the magnitude of angular change under stress and treatment modality. In particular, greater angle differences were consistently associated with conservative management (e.g., adduction deformity angle difference: 24.0° in the casting group vs. 16.0° in the surgical group, $p = 0.001$). This pattern suggests that greater flexibility under stress may predict successful casting outcomes, a concept supported by Sambandam et al. (2016), and Gunalan et al. (2016) who advocated for stress testing to differentiate flexible from rigid deformities [9, 16] .

The ROC analysis (Table 6, Fig. 1 and 2) confirmed the diagnostic utility of angle differences in guiding treatment. The talo-first metatarsal angle (AP view) had an AUC of 86.4 %, with a cutoff of > 18° indicating surgery with 100 % sensitivity. Similarly, the tibio-calcaneal angle in equinus deformity had perfect sensitivity and specificity at a > 20° difference (AUC = 100 %). These findings highlight the excellent predictive power of stress radiography for surgical decision-making, echoing similar conclusions by Kappel et al. (2020) and Radler et al. (2007) who demonstrated that rigid deformities with minimal radiographic response to stress necessitated operative correction [17, 18].

Overall, this study provides robust evidence supporting the int Stress radiographsegration of stress radiographs into routine evaluation of residual clubfoot deformities. By quantifying angular changes, clinicians can make more informed decisions regarding the need for surgery, potentially avoiding unnecessary operative interventions in cases amenable to casting. This approach may also standardize treatment across different settings and improve outcomes through earlier identification of rigid deformities.

Despite its strengths, this study has several limitations. The relatively small sample size may limit the generalizability of findings. Additionally, interobserver variability in radiographic interpretation was not assessed, which could influence angle measurements. Lastly, long-term functional outcomes were not evaluated, which are critical to understanding the ultimate efficacy of surgical versus conservative approaches.

CONCLUSIONS

The study highlights that clubfoot is more prevalent in male patients and often presents as a unilateral deformity. The most common residual deformities observed are equinus and adduction. Stress radiographs play a crucial role by showing significant angular changes that help evaluate deformity flexibility and severity. Larger angular differences indicate better flexibility and successful outcomes with casting, while smaller differences suggest the need for surgical intervention. Specific angle thresholds, like a talo-first metatarsal angle difference < 18° and a tibio-calcaneal angle difference > 20°, reliably predict the necessity for surgery with high sensitivity and specificity. Overall, stress radiographs are validated as an objective tool for assessing and guiding treatment decisions for residual clubfoot deformities.

Conflicts of interest *The authors declare no conflict of interest regarding this article.*

Funding *None.*

Ethical approval *The Medical Ethical Committee of The College of Medicine, University of Thi-Qar approved this study (no. 7/54/142 on 27/2/2024).*

REFERENCES

1. Barrie A, Varacallo MA. Clubfoot. In: *StatPearls* [Internet]. Treasure Island (FL): StatPearls Publ.; 2023. Available at: https://www.ncbi.nlm.nih.gov/books/NBK551574. Accessed Jun 19, 2025.
2. Karol LA, Jeans KA. This is a narrative review of the functional evaluation of clubfoot treatment with gait analysis. *Ann Transl Med*. 2021;9(13):1105. doi: 10.21037/atm-20-6922.
3. Smythe T, Kuper H, Macleod D, et al. Birth prevalence of congenital talipes equinovarus in low- and middle-income countries: a systematic review and meta-analysis. *Trop Med Int Health*. 2017;22(3):269-285. doi: 10.1111/tmi.12833.
4. Wallander H, Hovelius L, Michaelsson K. Incidence of congenital clubfoot in Sweden. *Acta Orthop*. 2006;77(6):847-852. doi: 10.1080/17453670610013123.
5. Kruse LM, Buchan JG, Gurnett CA, Dobbs MB. Polygenic threshold model with sex dimorphism in adolescent idiopathic scoliosis: the Carter effect. *J Bone Joint Surg Am*. 2012;94(16):1485-1491. doi: 10.2106/JBJS.K.01450.
6. Di Mascio D, Buca D, Khalil A, et al. Outcome of isolated fetal talipes: A systematic review and meta-analysis. *Acta Obstet Gynecol Scand*. 2019;98(11):1367-1377. doi: 10.1111/aogs.13637.
7. Merrill LJ, Gurnett CA, Siegel M, et al. Vascular abnormalities correlate with decreased soft tissue volumes in idiopathic clubfoot. *Clin Orthop Relat Res*. 2011;469(5):1442-1449. doi: 10.1007/s11999-010-1657-1.
8. Dyer PJ, Davis N. The role of the Pirani scoring system in the management of club foot by the Ponseti method. *J Bone Joint Surg Br*. 2006;88(8):1082-1084. doi: 10.1302/0301-620X.88B8.17482.
9. Sambandam SN, Gul A. Stress radiography in the assessment of residual deformity in clubfoot following postero-medial soft tissue release. *Int Orthop*. 2006;30(3):210-214. doi: 10.1007/s00264-005-0057-8.
10. Saleim AR, AlBaghdadi FA, Hasni I. The Accuracy of Radiographers Preliminary Image Evaluations of Axial Radiographs: a Prospective Longitudinal Study at Al-Hussein Hospital, Iraq. *SEEJPH*. 2024:695-702. doi: 10.70135/seejph.vi.1360.
11. Noh H, Park SS. Predictive factors for residual equinovarus deformity following Ponseti treatment and percutaneous Achilles tenotomy for idiopathic clubfoot: a retrospective review of 50 cases followed for median 2 years. *Acta Orthop*. 2013;84(2):213-217. doi: 10.3109/17453674.2013.784659.
12. Tayebi N, Yazdani K, Naghshin N. The prevalence of congenital malformations and its correlation with consanguineous marriages. *Oman Med J*. 2010;25(1):37-40. doi: 10.5001/omj.2010.9.
13. Parsa A, Moghadam MH, Jamshidi MH. Relapsing and residual clubfoot deformities after the application of the ponseti method: a contemporary review. *Arch Bone Jt Surg*. 2014;2(1):7-10.
14. Li J, Xun F, Xu C, et al. Early Radiographic Characteristics of the Lateral Talocalcaneal Angle and its Predictive Significance for Relapse in Patients With Idiopathic Clubfoot Treated With the Ponseti Method. *J Foot Ankle Surg*. 2024;63(6):646-652. doi: 10.1053/j.jfas.2024.05.009.
15. Recordon JAF, Halanski MA, Boocock MG, et al. A Prospective, Median 15-Year Comparison of Ponseti Casting and Surgical Treatment of Clubfoot. *J Bone Joint Surg Am*. 2021;103(21):1986-1995. doi: 10.2106/JBJS.20.02014.
16. Gunalan R, Mazelan A, Lee Y, Saw A. Pattern of Presentation and Outcome of Short-term Treatment for Idiopathic Clubfoot / CTEV with Ponseti Method. *Malays Orthop J*. 2016;10(3):21-25. doi: 10.5704/MOJ.1611.009.
17. Kappel A, Mortensen JF, Nielsen PT, et al. Reliability of stress radiography in the assessment of coronal laxity following total knee arthroplasty. *Knee*. 2020;27(1):221-228. doi: 10.1016/j.knee.2019.09.013.
18. Radler C, Manner HM, Suda R, et al. Radiographic evaluation of idiopathic clubfeet undergoing Ponseti treatment. *J Bone Joint Surg Am*. 2007;89(6):1177-11183. doi: 10.2106/JBJS.F.00438.

The article was submitted 05.05.2025; approved after reviewing 16.06.2025; accepted for publication 14.10.2025.

Information about the authors:

Zain Ali Abbas — ?????

Firas Abdulla AlBaghdadi — ?????

Wahby Ghalib Shaty — Assistant Professor (Orthopaedics), https://orcid.org/0000-0002-1267-3881.

Contribution of the authors:

Abbas Z.A. — Conceptualization; Data Curation; Investigation; Methodology; Project administration; Resources; Software; Writing – original draft and Writing – review & editing.

AlBaghdadi F.A. — Conceptualization; Data Curation; Investigation; Methodology; Project administration; Writing — original draft and Writing — review & editing.

Shaty W.G. — Conceptualization; Data Curation; Investigation; Methodology; Project administration; Resources; Writing — original draft and Writing — review & editing.

Original article
https://doi.org/10.18019/1028-4427-2025-31-6-764-772

Effect of the Panton – Valentine leukocidin gene *Staphylococcus aureus* on the course of the infectious process in orthopedic patients

A.D. Shakhmatova[1]✉, O.S. Tufanova[1], E.M. Gordina[1], A.R. Kasimova[1,2], V.V. Shabanova[1], S.A. Bozhkova[1]

[1] Vreden National Medical Research Center of Traumatology and Orthopedics, St. Petersburg, Russian Federation

[2] Academician I.P. Pavlov First St. Petersburg State Medical University, St. Petersburg, Russian Federation

Corresponding author: Alexandra D. Shakhmatova, tridakhna@list.ru

Abstract

Introduction *Staphylococcus aureus* is a leading pathogen causing osteoarticular infections. Panton – Valentine leukocidin (*PVL*) is considered one of the key of virulence factors with its role being poorly explored in orthopedic infections.

The **objective** was to evaluate the occurrence of the *PVL* gene in *S. aureus* strains, the effect on laboratory markers of inflammation and on the course of the infectious process in orthopedic patients.

Material and methods A retrospective analysis of 130 *S. aureus* strains isolated from 100 patients was performed. The presence of the *lukS-PV* and *lukF-PV* genes was determined using PCR. Laboratory parameters (CRP, ESR, leukocytes, neutrophils, and procalcitonin) and long-term treatment outcomes were assessed.

Results *PVL* was detected in 15 % of strains *S. aureus*. No statistically significant effect of *PVL* on the levels of routine inflammatory markers was found. A key finding was that the presence of the *PVL* gene was associated with an increased risk of adverse outcome.

Discussion The findings can be associated with debates on the clinical significance of *PVL*. Despite a significant impact on outcome The absence of significant differences in systemic inflammatory markers suggests that the negative effect of *PVL* is rather mediated by other mechanisms than by global inflammation activation measured by routine tests. These include direct cytotoxic tissue damage, impaired immune cell function, and the emergence of specific immunological processes. The association identified between *PVL* and the MRSA phenotype is consistent with the global epidemiological picture, where this toxin is a marker of hypervirulent community-acquired strains.

Conclusion The presence of *PVL* is a significant risk factor for a poor outcome of orthopedic infection suggesting the need for its detection for risk stratification and optimization of patient management strategy. Conclusion The presence of *PVL* is a significant risk factor for an unfavorable outcome of orthopedic infection, which indicates the need for its detection for risk stratification and optimization of patient management tactics.

Keywords: *Staphylococcus aureus*, Panton – Valentine leukocidin, orthopedic infection, virulence factors, treatment outcome

For citation: Shakhmatova AD, Tufanova OS, Gordina EM, Kasimova AR, Shabanova VV, Bozhkova SA. Effect of the Panton – Valentine leukocidin gene *Staphylococcus aureus* on the course of the infectious process in orthopedic patients. *Genij Ortopedii*. 2025;31(6):764-772. doi: 10.18019/1028-4427-2025-31-6-764-772.

INTRODUCTION

Staphylococcus aureus remains one of the most significant pathogens causing musculoskeletal infections. According to our data, *S. aureus* remained high-frequency isolation (31.3 %) over a 12-year observation period between 2011 and 2022 [1]. Similar data were presented by Tsiskarashvili et al. who reported *S. aureus* as the leading causative agents of periprosthetic joint infection over a six-year period amounting to more than 30 % [2]. *S. aureus* is characterized by the ability to form biofilms and by different mechanisms of resistance to antibacterial drugs complicating the fight against infection and requiring long-term administration of drugs or their combinations [3]. A number of studies have demonstrated the tropism of staphylococci for bone tissue cells [4, 5]. This affinity is ensured by the presence of various virulence factors that allow *S. aureus* to adsorb on the surface of the bone matrix and penetrate into bone tissue cells.

The cytotoxin Panton-Valentine leukocidin (*PVL*) is one of the significant virulence factors that realizes the pathogenic potential of *S. aureus*. This two-component protein causes lysis of blood cells, including neutrophils, monocytes, and macrophages leading to tissue necrosis and enhancing the systemic inflammatory response of the body [6]. *PVL* components encode the *lukS-PV* and *lukF-PV* genes, located on mobile genetic elements, facilitating the spread of this gene among bacterial strains [7].

With the data available, the role of *PVL* in the pathogenesis of orthopedic infections remains poorly understood. Infections of other localizations caused by *S. aureus* containing *PVL* usually proceed in a more severe form, are prone to more frequent relapses, accompanied by a risk of reinfection and characterized by formation of larger abscesses [8, 9]. Considering that the *PVL* toxin mediates its action through direct cytotoxicity and modulation of inflammation, it can be assumed that its production by staphylococci will be associated with changes in the profile of laboratory markers of systemic inflammation (such as C-reactive protein, leukocytes, neutrophils and procalcitonin), but with more frequent adverse clinical outcomes [10].

The **objective** was to evaluate the occurrence of the *PVL* gene in *S. aureus* strains, the effect on laboratory markers of inflammation and on the course of the infectious process in orthopedic patients.

MATERIAL AND METHODS

Between January 1, 2023 and December 31, 2023, 104 *S. aureus* strains were isolated from 75 patients with bone infections of the limbs and major joints who underwent surgery in the Center's departments. The study included 26 *S. aureus* strains isolated from the blood of 25 patients in the Purulent Osteology Department between January 1, 2012 and December 31, 2024.

Patients were selected for the study using the Mikrob-2 microbiological monitoring program and the Across-Engineering information system based on microbiological examination of biomaterial obtained from patients.

All patients had orthopedic infection caused by *S. aureus*. Based on the medical records after discharge, a database created included:

— anthropometric data (age, gender);
— localization of the infectious process;
— laboratory blood tests at the time of admission (leukocytes, neutrophils count, ESR (erythrocyte sedimentation rate), CRP (C-reactive protein) level, PCT (procalcitonin) in patients with bacteremia).

Patients were divided into two groups depending on the presence or absence of the *PVL* gene in the causative agent of the infection: group 1 (*n* = 19), *PVL*-positive *S. aureus*, group 2 (*n* = 81), *PVL*-negative *S. aureus*.

A separate comparison of laboratory markers of the inflammatory process was conducted in patients with bacteremia caused by *S. aureus* and with a wound infection without bacteremia. For this purpose, patients with bacteremia were divided into two subgroups based on the presence of the *PVL* gene in *S. aureus*: subgroup 1 (*n* = 7), the *PVL* gene was present, subgroup 2 (*n* = 18), the *PVL* gene was absent.

The outcome was then assessed for 47 patients (47 %). A telephone survey was conducted, asking standard questions about whether they had any clinical or laboratory signs of recurrent infection within two years of the index surgery, and whether they had undergone repeat debridement procedures. In cases of fatal outcome, interviews were conducted with the patient's relatives. A favorable outcome (according to the Delphi criteria) was defined as the absence of clinical and laboratory signs of recurrent infection and the absence of debridement procedures within two years of the index surgery [11]. As a result, patients were divided into two subgroups: group A (*n* = 29) with a favorable outcome, and group B (n = 18) with a poor outcome.

Gender- and age-related parameters and laboratory test results (leukocyte and neutrophil counts, ESR, CRP, the proportion of MR strains among *S. aureus*, and the proportion of patients with *PVL* strains of *S. aureus*) at admission were compared. The proportion of patients with *S. aureus* bacteremia was assessed in patients of the comparison groups.

Laboratory methods

Microbiological testing of patient biomaterial was performed in accordance with international standards. Until 2021, bacterial identification was performed biochemically on Microlatest panels (Erba Lachema) using an iEMS Reader MF (Labsistems, Finland). Since 2021, bacterial identification was performed using MALDI-TOF-MS, the FlexControl system and MBT Compass 4.1 software (Bruker Daltonics, Germany), with a score of ⩾ 2.0. The sensitivity of bacterial cultures to antibacterial drugs was assessed in accordance with EUCAST requirements (v.2-13).

Nucleic acids (NA) were isolated as follows: the *S. aureus* concentration required for NA isolation was diluted with distilled water to a turbidity of 1 μF (BioSan, Latvia). Then, 200 μl of the suspension were collected and additional lysis of the bacterial culture was performed in the presence of 20 mg/ml lysostaphin (Sigma Aldrich, USA) and 50 mg/ml lysozyme (Amresco, USA) in Tris-EDTA buffer for 60 minutes at 37°C. In accordance with the manufacturer's protocol, Magno-Sorb (Amplisens, Russia) was used to isolate nucleic acids using the Auto-Pure S32 system for automated nucleic acid isolation and purification (Allsheng, China). RNA was removed from DNA samples using the RNase A enzyme (Biolabmix, Russia) in accordance with the manufacturer's protocol. The concentration of isolated DNA and RNA was measured using an Implen NP80-Touch spectrophotometer (Implen, Germany). A sample was considered pure at a 260/280 ratio of 1.8–2.0 and a 260/230 ratio of ~2.0.

Real-time PCR was performed according to the manufacturer’s protocol BioMaster HS-qPCR SYBR Blue (2X) (Biolabmix, Russia) using a CFX-96 amplifier (BioRad, USA). Primers for *PVL* detection were *luk-PV-f* (ATCATTAGGTAAAATGTCTGGACATGATCCA) and *luk-PV-r* (GCATCAAGTGTATTGGATAGCAAAAGC), which amplify a 433-bp fragment specific for the *lukS/F-PV* genes encoding the two-component *PVL S/F* protein, as described by McClure et al. [12]. Oligonucleotide synthesis was produced by Evrogen (Russia). PCR temperature conditions: initial denaturation at 94 °C for 4 min; 30 amplification cycles (denaturation at 94 °C for 45 s, annealing at 56 °C for 45 s, and elongation at 72 °C for 30 s); and a final elongation at 72 °C for 2 min. For visualization, 5 µl of the PCR amplicon were loaded with dye into a 1.2 % agarose gel containing ethidium bromide, followed by electrophoresis at 100 V for 1 h and visualization using the ChemiDoc MP Imaging System (BioRad, USA).

Statistical analysis

The data were recorded in the form of spreadsheets in MS Office Excel, 2007 (Microsoft, USA), visualization of the data structure and the analysis were performed using GraphPad Prism 9.0 (USA) and IBM SPSS STATISTICS (version 27). Quantitative indicators were assessed for compliance with normal distribution using the Kolmogorov – Smirnov test. With the absence of normal distribution, quantitative data were described using the median (Me) and the lower and upper quartiles (Q1-Q3). Categorical data were described using absolute values and percentages. Comparison of two groups for a quantitative indicator, the distribution of which differed from normal, was performed using the Mann – Whitney U test. To assess the risk in the comparison groups, the odds ratio (OR, 95 % CI) was calculated. Comparisons of percentages in the analysis of four-field contingency tables were performed using the Pearson chi-square (χ^2) test (for expected value greater than 10) or Fisher's exact test (for expected value less than 10). Associations were assessed using Cramer's test. Differences in the parameters between groups were considered statistically significant at $p < 0.05$.

Ethical Standards

Upon admission to the hospital, all patients signed informed voluntary consent to the processing of personal data for scientific and educational purposes, the possible presence of students during medical interventions, and the use of patient information constituting a medical secret for educational and scientific purposes.

RESULTS

Frequency of PVL-positive S. aureus isolated from biomaterial of patients with orthopedic infection

B In the studied cohort, the *PVL* gene was detected in 15 % (*n* = 19) of *S. aureus* strains. The majority of *PVL*-positive isolates were characterized by resistance to cefoxitin (58 %, *n* = 11). There were 12 % of *PVL*-positive cultures Among MSSA strains and 17 % among MRSA.

Analysis of the relationship between the presence of the PVL gene and the sex of patients

The *PVL* gene was detected among *S. aureus* strains without statistically significant differences between the male and female groups (χ^2 = 0.455; *p* = 0.500). *PVL*-positive *S. aureus* were isolated from 11 of 51 male patients (21.6 %) and from eight (16.3 %) of the 49 female patients (Table 1).

Table 1

Distribution of the *PVL* gene depending on the sex of patients

Group	Males (*n* = 51)		Females (*n* = 49)		*p*
	abs.	%	abs.	%	
Group 1	11	21.6	8	16.3	0.500
Group 2	40	78.4	41	83.7	

Analysis of the relationship between the presence of the PVL gene and the age of patients

The analysis was performed for 99 patients, one patient with missing age data was excluded. There was no statistically significant difference in the mean age between groups 1 and 2 (t = 1.03; *p* = 0.306). The mean age was (58.2 ± 12.7) years (Me = 58) in the PVL^+ group and (54.6 ± 15.3) years (Me = 54) in the PVL^- group (Table 2).

Table 2

Comparison of the age of patients in groups with and without the *PVL* gene

Group	*n*	Mean age ± SD	The median [Q1–Q3]	*p*
Group 1	18	58.2 ± 12.7	58 [49–66]	0.306
Group 2	80	54.6 ± 15.3	54 [41–64]	

Analysis of infection localization depending on the presence of the Panton-Valentine gene

Patients with infection caused by PVL^+ strains had knee joint involvement in half of the cases ($n = 9$), with hip involvement being less common. In contrast, hip involvement was predominant in the PVL^- group, accounting for 45 % of cases ($n = 35$) (Fig. 1). The distribution by localization showed similar trends in both groups, with, ajor joint involvement being predominant.

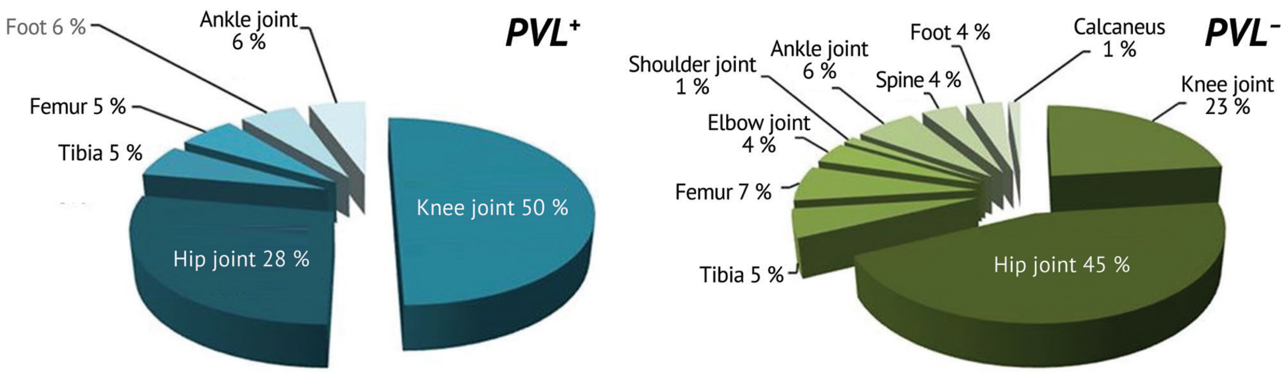

Fig. 1 Localization of the infectious process depending on the presence of the *PVL* gene

Comparison of laboratory test results in patients with PVL-positive and PVL-negative S. aureus

A comparative analysis of inflammatory markers revealed no statistically significant differences between the study groups despite the expected significant reduction in leukocyte and neutrophil levels due to the potential cytotoxic effect of *PVL*. There was a trend toward a higher median CRP level in patients of Group 1 compared to Group 2 (by 60 %) was detected which was not statistically significant (Table 3).

Table 3

Comparison of laboratory parameters of the inflammatory process in patients with *PVL*-positive (group 1) and *PVL*-negative *S. aureus* (group 2)

Description	Group 1 ($n = 19$)	Group 2 ($n = 83$)	*p*
Leukocytes, 10^9/L, Me [Q1–Q3]	9.7 [6.9–13.6]	8.6 [6.9–11]	0.587
Neutrophils (% from the level of leukocytes), Me [Q1–Q3]	5.7 [4.5–8.7]	5.5 [3.8–8.9]	0.713
CRP, mg/L, Me [Q1–Q3]	67 [12.0–215.0]	42 [12.0–117.0]	0.358
ESR, mm/h, Me [Q1–Q3]	46.0 [40.0–70.0]	48.0 [27.0–74.5]	0.649

Severity of systemic inflammation assessed by laboratory parameters in groups with different PVL status in patients with bacteremia

To evaluate the effect of the Pantone leukocidin gene on the severity of systemic inflammation, patients with bacteremia caused by *S. aureus* were divided into two subgroups: subgroup 1 ($n = 7$) *PVL*-positive strains and subgroup 2 ($n = 18$) *PVL*-negative strains (Table 4). A steady trend towards higher median values of procalcitonin (by 28 %), CRP (by 7.5 %), and ESR (by 8 %) was observed in subgroup 1, compared to subgroup 2 despite the lack of statistical significance. The median level of leukocytes was almost identical, and the level of neutrophils was higher in patients of subgroup 2. The lack of statistical differences in the comparison groups could be explained, among other things, by their small number.

Table 4

Comparison of laboratory parameters of systemic inflammation in patients with *PVL*-positive and *PVL*-negative *S. aureus* bacteremia

Description	Subgroup 1 (n = 7)	Subgroup 2 (n = 18)	p
PCT, ng/mL, Me [Q1–Q3]	0.9 [0.3–1.9]	0.7 [0.2–1.6]	0.622
Leukocytes, 10^9/L, Me [Q1–Q3]	14.0 [9.9–17.0]	14.4 [8.9–17.6]	0.949
Neutrophils (% from the level of leukocytes), Me [Q1–Q3]	8.7 [3.1–12.8]	10.3 [5.5–14.4]	0.467
CRP, mg/L, Me [Q1–Q3]	215.0 [179.5–290.0]	200.0 [145.5–310.0]	0.727
ESR, mm/h,Me [Q1–Q3]	85.0 [43.0–85.0]	78.5 [29.5–84]	0.260

Severity of systemic inflammation assessed by laboratory parameters in groups with different PVL status in patients with wound infection without bacteremia

A comparative analysis of laboratory parameters of systemic inflammation revealed no statistically significant differences between the groups (p > 0.05 in all cases). The leukocyte count was 7.7×10^9/L [6.7–9.8] in group 1, 8.2×10^9/L [6.6–9.7] in group 2 (p = 0.964). The absolute number of neutrophils was comparable: 5.4×10^9/L (group 1: 4.5–7.1; group 2: 3.7–7.1; p = 0.587). The level of CRP reached 25 mg/L [5.5–66.3] in group 1, 25 mg/l [6.3–54.5] in group 2 (p = 0.940). The ESR index showed no significant differences: 45.5 mm/hour [39.3–56.5] in group 1 and 45 mm/hour [24-71] in group 2 (p = 0.958).

Assessment of the impact on the outcome of complex treatment of orthopedic infection PVL

The influence of various factors was assessed in patients with the known outcome (n = 47) (Table 5). The patients were divided into two groups: group A having a favorable outcome (n = 62 %), group B featuring an unfavorable outcome (n = 38 %). No statistically significant differences in various parameters of laboratory test results on admission were observed. The presence of the Panton-Valentine leukocidin gene in *S. aureus* strains increased the risk of unfavorable outcome by 4 times (p = 0.029, 95 % CI: 1.114–13.851, Cramer's V 0.318, moderate association). The proportion of patients with bacteremia was statistically significantly lower among patients in group 1 than among patients in group 2: 10.7 % versus 38.9 % (p = 0.02).

Table 5

Comparison of laboratory parameters in study group A and group B

Description	Group A (n = 29)	Group B (n = 18)	p
Leukocytes, 10^9/L, Me [IQR]	8.5 [6.7–12.4]	9.7 [7.0–13.5]	0.450
Neutrophils (% from the level of leukocytes), Me [IQR]	5.6 [4.5–8.1]	5.7 [4.2–10.5]	0.609
ESR, mm/h, Me [IQR]	52 [39.3–70.0]	45 [27.0–76.0]	0.740
CRP, mg/L, Me [IQR]	42.0 [17.0–82.0]	55.0 [16.0–219.0]	0.279
The proportion of patients with *PVL* strains *S. aureus*, n (%)	7 (24.1)	10 (55.6)	**0.029***

DISCUSSION

The role of the *PVL* gene as a virulence factor remains controversial. A number of studies associate its presence with severe necrotizing infections of the skin and soft tissues, and necrotizing pneumonia [13, 14, 15]. Other studies did not reveal a significant association between the carriage of the *PVL* gene and the severity of the systemic inflammatory response or mortality [16]. Our findings showed that the presence of the *PVL* gene in *S. aureus* was a significant risk factor for the development of an adverse clinical outcome, increasing its odds by almost fourfold (OR = 3.93, 95 % CI: 1.11–13.85, p = 0.029). The conclusion is the central finding of our study and is consistent with the fundamental concept of *PVL* as a potent cytotoxin that damages the membranes of neutrophils and other immunocompetent cells, which can potentially lead to a more severe course of infection and disturbed innate immune system [17, 18, 19].

Our findings indicated 57.9 % (n = 11) of all *PVL*-positive strains being methicillin-resistant isolates (MRSA) and were fully consistent with the global epidemiological picture and could be explained by modern evolutionary concepts [20]. Despite the fact that the proportion of MRSA isolates was expectedly lower than the proportion of MSSA, the *PVL* gene was associated predominantly with the MRSA phenotype. This observation was not random and reflected the process of clonal selection and successful dissemination of specific strains [21].

A key explanation is that the *PVL* gene is a marker for so-called "community-acquired" MRSA (CA-MRSA) strains [22, 23]. These clones, the so-called biovariants, unlike "hospital-acquired" (HA-MRSA), have acquired evolutionary advantages for spreading in community settings in the absence of significant antibiotic pressure. This advantage is virulence, provided, in part, by Panton-Valentine leukocidin.

The lack of a statistically significant effect of the *PVL* gene on individual laboratory markers of systemic inflammation (CRP, ESR, leukocytes, neutrophils, procalcitonin) was an interesting and somewhat controversial finding when considered in isolation. With the trends toward increased median values in the PVL^+ group for all parameters, the differences did not reach significance, which was likely due to the limited sample size and high variability of the parameters. However, this result does not refute the main conclusion, but rather indicates that the negative impact of *PVL* gene on outcome is likely mediated not so much by global activation of systemic inflammation measured by routine methods, but by other mechanisms, which may include:

— direct cytotoxic damage to target tissues and organs [10, 24],

— disturbed neutrophil functions (chemotaxis, phagocytosis, NET formation) even without their quantitative change [25, 26];

— induction of specific anti-inflammatory cascades that are not routinely measured [27, 28].

This assumption is consistent with the publication of Motomura et al. [29], who reported that *PVL*-associated necrotizing pneumonia was characterized by a severe course with pronounced lung damage with only a moderate increase in systemic markers of inflammation.

Our data contribute to resolving the existing debate about the clinical significance of *PVL*. On the one hand, our finding of a significant association with outcome is consistent with a number of studies linking PVL with severe necrotizing skin and soft tissue infections and pneumonia [13, 14]. On the other hand, our data on the variability of the inflammatory response echo studies that did not find a direct correlation between *PVL* and laboratory markers or mortality [15]. This discrepancy can be explained by the heterogeneity of the studied populations (type of infection, comorbid background), differences in study design and the predominant influence of other virulence factors (e.g., α-toxin), which can mask or modulate the effect of *PVL* [30].

The main limitation of our study is the small sample size, which may have resulted in a failure to achieve statistical significance in the analysis of individual laboratory parameters (type II error) and wide confidence intervals in the risk assessment. The retrospective design of the study does not allow for the complete elimination of unaccounted confounding factors. Prospective studies in larger cohorts are needed to confirm the obtained results.

CONCLUSION

The presence of the *PVL* gene in *Staphylococcus aureus* strains is an aggravating risk factor for adverse clinical outcomes in orthopedic infections. This fact confirms the role of *PVL* as an important virulence factor contributing to a more severe course of the disease and a worse prognosis in patients.

With the important role of *PVL* in determining risk, its impact on infection outcome is not always accompanied by statistically significant changes in the levels of routine laboratory markers of systemic inflammation, such as CRP, ESR, leukocytes, or procalcitonin. This suggests that the pathogenic mechanisms underlying the impact of *PVL* on clinical outcome may be mediated by global activation of inflammatory processes measured by standard markers and by other pathways. Determining the presence of *PVL* in clinical isolates of *S. aureus* represents a promising tool for risk stratification and optimization of clinical management. This approach may facilitate more accurate prognosis of the disease course and informed treatment decisions. Further investigation of the impact of *PVL* on specific patient immunological profiles and its interaction with other bacterial virulence factors is essential. Studying these aspects will allow for a better understanding of the pathogenetic mechanisms underlying severe infectious outcomes and the development of new prevention and treatment strategies.

Conflict of interest *None of the authors has any potential conflict of interest.*

Funding *The authors received no financial support for the research and/or authorship of this article.*

Informed consent *Upon admission to the hospital, all patients signed informed voluntary consent for the processing of personal data and the use of anonymized patient information for educational and scientific purposes.*

REFERENCES

1. Kasimova AR, Tufanova OS, Gordina EM, et al. Twelve-Year Dynamics of Leading Pathogens Spectrum Causing Orthopedic Infection: A Retrospective Study. *Traumatology and Orthopedics of Russia*. 2024;30(1):66-75. (In Russ.) https://doi.org/10.17816/2311-2905-16720.
2. Tsiskarashvili AV, Melikova RE, Novozhilova EA. Analysis of six-year monitoring of common pathogens causing periprosthetic joint infection of major joints and the tendency to resistance. *Genij Ortopedii*. 2022;28(2):179-188. doi: 10.18019/1028-4427-2022-28-2-179-188.
3. Bozhkova SA, Gordina EM, Markov MA, et al. The Effect of Vancomycin and Silver Combination on the Duration of Antibacterial Activity of Bone Cement and Methicillin-Resistant Staphylococcus aureusBiofilm Formation. *Traumatology and Orthopedics of Russia*. 2021;27(2):54-64. (In Russ.) doi: 10.21823/2311-2905-2021-27-2-54-64.
4. Senneville E, Brière M, Neut C, et al. First report of the predominance of clonal complex 398 Staphylococcus aureus strains in osteomyelitis complicating diabetic foot ulcers: a national French study. *Clin Microbiol Infect*. 2014;20(4):O274-O277. doi: 10.1111/1469-0691.12375.
5. Dunyach-Remy C, Courtais-Coulon C, DeMattei C, et al. Link between nasal carriage of Staphylococcus aureus and infected diabetic foot ulcers. *Diabetes Metab*. 2017;43(2):167-171. doi: 10.1016/j.diabet.2016.09.003.
6. Chen H, Zhang J, He Y, et al. Exploring the Role of Staphylococcus aureus in Inflammatory Diseases. *Toxins (Basel)*. 2022;14(7):464. doi: 10.3390/toxins14070464.
7. Malachowa N, DeLeo FR. Mobile genetic elements of Staphylococcus aureus. *Cell Mol Life Sci*. 2010;67(18):3057-3071. doi: 10.1007/s00018-010-0389-4.
8. Linz MS, Mattappallil A, Finkel D, Parker D. Clinical Impact of Staphylococcus aureus Skin and Soft Tissue Infections. *Antibiotics (Basel)*. 2023;12(3):557. doi: 10.3390/antibiotics12030557.
9. Hofstee MI, Siverino C, Saito M, et al. Staphylococcus aureus Panton-Valentine Leukocidin worsens acute implant-associated osteomyelitis in humanized BRGSF mice. *JBMR Plus*. 2024 4;8(2):ziad005. doi: 10.1093/jbmrpl/ziad005.
10. Qu MD, Kausar H, Smith S, et al. Epidemiological and clinical features of Panton-Valentine Leukocidin positive Staphylococcus aureus bacteremia: A case-control study. *PLoS One*. 2022;17(3):e0265476. doi: 10.1371/journal.pone.0265476.
11. Diaz-Ledezma C, Higuera CA, Parvizi J. Success after treatment of periprosthetic joint infection: a Delphi-based international multidisciplinary consensus. *Clin Orthop Relat Res*. 2013;471(7):2374-2382. doi: 10.1007/s11999-013-2866-1.
12. McClure JA, Conly JM, Lau V, et al. Novel multiplex PCR assay for detection of the staphylococcal virulence marker Panton-Valentine leukocidin genes and simultaneous discrimination of methicillin-susceptible from -resistant staphylococci. *J Clin Microbiol*. 2006;44(3):1141-1144. doi: 10.1128/JCM.44.3.1141-1144.2006.
13. Vlaeminck J, Raafat D, Surmann K, et al. Exploring Virulence Factors and Alternative Therapies against Staphylococcus aureus Pneumonia. *Toxins (Basel)*. 2020;12(11):721. doi: 10.3390/toxins12110721.
14. Urish KL, Cassat JE. Staphylococcus aureus Osteomyelitis: Bone, Bugs, and Surgery. *Infect Immun*. 2020;88(7):e00932-19. doi: 10.1128/IAI.00932-19.
15. Costa CA, Inácio H, Trevas S, Simas Â. Panton-Valentine Leukocidin in Necrotizing Pneumonia: A Case Report. *Cureus*. 2025;17(2):e78774. doi: 10.7759/cureus.78774.
16. van Hal SJ, Jensen SO, Vaska VL, et al. Predictors of mortality in Staphylococcus aureus Bacteremia. *Clin Microbiol Rev*. 2012;25(2):362-386. doi: 10.1128/CMR.05022-11.
17. Kailasan S, Kant R, Noonan-Shueh M, et al. Antigenic landscapes on Staphylococcus aureus pore-forming toxins reveal insights into specificity and cross-neutralization. *MAbs*. 2022;14(1):2083467. doi: 10.1080/19420862.2022.2083467.

18. Touaitia R, Mairi A, Ibrahim NA, et al. Staphylococcus aureus: A Review of the Pathogenesis and Virulence Mechanisms. *Antibiotics*. 2025;14(5):470. doi: 10.3390/antibiotics14050470.
19. Harada S, Kawada H, Maehana S, et al. Panton-Valentine Leukocidin Induces Cytokine Release and Cytotoxicity Mediated by the C5a Receptor on Rabbit Alveolar Macrophages. *Jpn J Infect Dis*. 2021;74(4):352-358. doi: 10.7883/yoken.JJID.2020.657.
20. Jiang J-H, Cameron DR, Nethercott C, et al. Virulence attributes of successful methicillin-resistant Staphylococcus aureus lineages. *Clin Microbiol Rev*. 2023;36(4):e0014822. doi: 10.1128/cmr.00148-22.
21. Mohamadou M, Essama SR, Ngonde Essome MC, et al. High prevalence of Panton-Valentine leukocidin positive, multidrug resistant, Methicillin-resistant Staphylococcus aureus strains circulating among clinical setups in Adamawa and Far North regions of Cameroon. *PLoS One*. 2022;17(7):e0265118. doi: 10.1371/journal.pone.0265118.
22. Shohayeb M, El-Banna T, Elsawy LE, El-Bouseary MM. Panton-Valentine Leukocidin (PVL) genes may not be a reliable marker for community-acquired MRSA in the Dakahlia Governorate, Egypt. *BMC Microbiol*. 2023;23(1):315. doi: 10.1186/s12866-023-03065-8.
23. Kawakami T, Yokoyama K, Ikeda T, et al. Severity and intractableness of skin infections caused by Panton–Valentine leukocidin-positive methicillin-resistant Staphylococcus aureus. *J Cutan Immunol Allergy*. 2023;6(3):94-97. doi: 10.1002/cia2.12294.
24. Grebe T, Sarkari MT, Cherkaoui A, Schaumburg F. Exploration of compounds to inhibit the Panton-Valentine leukocidin of Staphylococcus aureus. *Med Microbiol Immunol*. 2024;213(1):19. doi: 10.1007/s00430-024-00803-1.
25. Monteith AJ, Miller JM, Maxwell CN, et al. Neutrophil extracellular traps enhance macrophage killing of bacterial pathogens. *Sci Adv*. 2021;7(37):eabj2101. doi: 10.1126/sciadv.abj2101.
26. Jhelum H, Čerina D, Harbort CJ, et al. Panton-Valentine leukocidin-induced neutrophil extracellular traps lack antimicrobial activity and are readily induced in patients with recurrent PVL + -Staphylococcus aureus infections. *J Leukoc Biol*. 2024;115(2):222-234. doi: 10.1093/jleuko/qiad137.
27. Chung EJ, Luo CH, Thio CL, Chang YJ. Immunomodulatory Role of Staphylococcus aureus in Atopic Dermatitis. *Pathogens*. 2022;11(4):422. doi: 10.3390/pathogens11040422.
28. Rasquel-Oliveira FS, Ribeiro JM, Martelossi-Cebinelli G, et al. Staphylococcus aureus in Inflammation and Pain: Update on Pathologic Mechanisms. *Pathogens*. 2025;14(2):185. https://doi.org/10.3390/pathogens14020185.
29. Motomura Y, Miyazaki M, Kamada M, et al. Genotypic Shift and Diversification of MRSA Blood Stream Isolates in a University Hospital Setting: Evidence from a 12-Year Observational Study. *Antibiotics (Basel)*. 2024;13(7):670. doi: 10.3390/antibiotics13070670.
30. Olaniyi RO, Pancotto L, Grimaldi L, Bagnoli F. Deciphering the Pathological Role of Staphylococcal α-Toxin and Panton-Valentine Leukocidin Using a Novel Ex Vivo Human Skin Model. *Front Immunol*. 2018;9:951. doi: 10.3389/fimmu.2018.00951.
31. Bennett MR, Thomsen IP. Epidemiological and Clinical Evidence for the Role of Toxins in S. aureus Human Disease. *Toxins (Basel)*. 2020;12(6):408. doi: 10.3390/toxins12060408.

The article was submitted 10.09.2025; approved after reviewing 12.09.2025; accepted for publication 14.10.2025.

Information about the authors:

Aleksandra D. Shakhmatova — biologist, junior researcher, tridakhna@list.ru, https://orcid.org/0000-0003-4879-4359;

Olga S. Tufanova — clinical pharmacologist, junior researcher, katieva@mail.ru, https://orcid.org/0000-0003-4891-4963;

Ekaterina M. Gordina — Candidate of Medical Sciences, senior researcher, emgordina@win.rniito.ru, https://orcid.org/0000-0003-2326-7413;

Alina R. Kasimova — Candidate of Medical Sciences, clinical pharmacologist, Associate Professor, kasi-alina@yandex.ru, https://orcid.org/0000-0001-6284-7133;

Valentina V. Shabanova — bacteriologist, vvshabanova@win.rniito.ru, https://orcid.org/0000-0001-5009-3143;

Svetlana A. Bozhkova — Doctor of Medical Sciences, Professor, Head of the Department, clinpharm-rniito@yandex.ru, https://orcid.org/0000-0002-2083-2424.

Original article
https://doi.org/10.18019/1028-4427-2025-31-6-773-779

Exploring the link between bone biomarkers and proinflammatory cytokines in patients with osteoarthritis

R.A. Al-Mosawi[1], S.N. Abed Shubar[2], B.B. Aldin[2], A.A. Al-Fahham[3]✉

[1] Al-Furat Al-Awsat Technical University, Najaf, Iraq
[2] Al-Furat Al-Awsat Technical University, Mussaib, Iraq
[3] University of Kufa, Iraq

Corresponding author: Ali A. Al-Fahham, fahham925@gmail.com

Abstract

Background Osteoarthritis is multifactorial joint disorder marked by the progressive breakdown of articular cartilage, alterations in the underlying subchondral bone, and chronic inflammation of the synovial membrane.

Objective To measure serum levels of bone biomarkers (osteocalcin and sclerostin) in osteoarthritis patients as compared to healthy controls and also to find out the link of these biomarkers with proinflammatory cytokines including IL-6, IL-17, IL-1β and TNF-α.

Materials and methods A case-control study was implemented on 65 osteoarthritis patients and 35 healthy controls participants. Blood samples were taken from participants after obtaining written informed consent. Serum levels of cytokines and bone markers were measured using ELISA. Pain disability and intensity were measured using the "Chronic Pain Grade questionnaire".

Results Compared to controls, patients with osteoarthritis had significantly higher levels of IL-1β, TNF-α, IL-6, and IL-17 ($P < 0.0001$ for all). Osteocalcin levels were dramatically lower in the osteoarthritis group than the controls (mean ± SD: 23.50 ± 19.30 ng/mL vs. controls 48.90 ± 5.20 ng/mL), while sclerostin levels were much higher (11.70 ± 1.10 ng/mL in osteoarthritis vs. 3.80 ± 0.90 ng/mL in controls, $P < 0.0001$). Osteocalcin showed a moderate positive correlation with IL-17, IL-6, and TNF-α; sclerostin showed a negative correlation with these cytokines.

Discussion A strong positive correlation exists between osteocalcin and proinflammatory interleukins. The downregulation of sclerostin in OA also shares common pathways with proinflammatory cytokines that drive expression of osteocalcin. Inflammation results in osteocyte apoptosis or their dedifferentiation, and this further lowers the population of sclerostin-secreting cells in the subchondral bone. This is how the reverse correlation is explained between sclerostin and proinflammatory cytokines in OA.

Conclusions Results show a robust inflammatory-bone axis in the pathogenesis of osteoarthritis. High proinflammatory cytokines might bring about osteocalcin expression and also inhibit sclerostin, leading to pathological subchondral bone alteration. These biomarkers reflect disease activity and therefore could be used for early detection as well as monitoring and phenotypic stratification of osteoarthritis.

Keywords: Sclerostin, Osteocalcin, Osteoarthritis, IL-1β, TNF-α, IL-6, IL-17

For citation: Al-Mosawi RA, Abed Shubar SN, Aldin BB, Al-Fahham AA. Exploring the link between bone biomarkers and proinflammatory cytokines in patients with osteoarthritis. *Genij Ortopedii*. 2025;31(6):773-779. doi: 10.18019/1028-4427-2025-31-6-773-779.

INTRODUCTION

Osteoarthritis is a multifactorial disease of the joints involving progressive degradation of the cartilage surface and changes in the underlying bone as well as chronic inflammation of the synovial membrane. The interplay between proinflammatory cytokines and bone biomarkers exerts a critical role in the pathophysiology of OA, influencing progression of the disease and treatment outcomes. Sclerostin is a product of osteocytes and well comparably known to suppress the differentiation of osteoblasts and promote the differentiation of osteoclasts. This idea has been recently introduced and evolved [1]. In OA, the imbalance between bone formation and resorption leads to joint degeneration. The pathway of Wnt signaling performs major functions in the formation of bones [2]. Suppression of Wnt signaling by sclerostin may lead to decreased bone formation; this can be taken as an influence on OA. Results showed normal sclerostin levels in people with type 1 diabetes but elevated levels in type 2 patients; most of them have low bone turnover [3]. This dysregulation applies to OA since that means altered bone metabolism which then compromises the integrity of joints. It has been suggested that anti-sclerostin therapies serve as a therapeutic pathway for OA by restoring the balance of bone remodeling and, hence, reestablishing healthy joints [2]. Osteocalcin, like a marker mainly for bone formation, has received more attention for its systemic functions, including modulation of glucose metabolism and energy homeostasis. In other words, since its levels correlate with changes in cartilage structure over time, osteocalcin levels could be indicative of the quantity of cartilage volume loss in OA patients [4]. The interplay of sclerostin with osteocalcin is very important in the context of OA. Control of osteocalcin by other factors, for example leptin, may indirectly influence its levels and therefore bone formation and the health of cartilage [5]. Abnormal leptin production by osteoblasts in OA could also drive altered osteocalcin levels further complicating the metabolic aspects of this disease. Also, using sclerostin and osteocalcin levels as markers in osteoarthritis could give clues into how the disease works. Latest studies hint that although osteocalcin levels might not vary much between OA patients and controls, they are important for the picture of bone and cartilage metabolism [6]. Osteoarthritis has long been known as a non-inflammatory disorder of the joints, but recently it has been established that there is the involvement of low-grade inflammation which remains sustainable for the development and progression of the disease. The major pro-inflammatory cytokines participating in inducing that resultant inflammatory state are IL-6, TNF-α, IL-1β, and IL-17 in the OA disease state which are key mediators in the molecular cascade leading to cartilage degradation, synovial hyperplasia, osteophyte formation, and pain sensitization [7]. Though the existing literature is very insightful, there are gaps in knowledge regarding the exact roles of sclerostin and osteocalcin in OA and their link to cytokines. The aim of this work is to assess serum levels of bone biomarkers (osteocalcin and sclerostin) in OA patients as compared to healthy controls and also to find out the link of these biomarkers with proinflammatory cytokines including IL-6, IL-17, IL-1β and TNF-α.

Objective To measure serum levels of bone biomarkers (osteocalcin and sclerostin) in Osteoarthritis patients as compared to healthy controls and also to find out the link of these biomarkers with proinflammatory cytokines including IL-6, IL-17, IL-1β and TNF-α.

MATERIALS AND METHODS

Patients and data collection

This case-control cross-sectional study was carried out at the Medical City complex in Baghdad, Iraq. It extended from August 2024 to April 2025. A sample of 65 patients diagnosed with osteoarthritis was enrolled from the rheumatology and orthopedic outpatient clinics. Controls were a group of 35 age- and sex-matched apparently healthy individuals free of joint diseases or any systemic inflammatory condition, recruited during the same period. Demographic data (age and body mass index) were collected through direct interviews and physical measurements. The classification of BMI adopted WHO criteria. Levels of IL-6, IL-17, IL-1β, TNF-α, osteocalcin, and sclerostin in the serum were measured by performing commercially utilized sandwich ELISA kits (R&D Systems, USA) as per instructions provided by the manufacturer. For sclerostin, samples were added to Wells of a microplate already coated with capture antibody specific to sclerostin. Then detection was carried out using an enzyme-linked secondary antibody. After thoroughly washing away unbound reagents, substrate solution was added and allowed to incubate until color development occurred. Absorbance was read at 450 nm; use was made of a standard curve to determine concentration in each sample. Pain disability and intensity were measured using the "Chronic Pain Grade questionnaire", a validated 7-item self-report tool assessing pain intensity and pain-related disability. The scores are reported on a 0–100 scale, where greater severity and impact on function correspond to higher scores.

Statistical Analysis

Data were analyzed using IBM SPSS Statistics version 25.0 (SPSS Inc., Chicago, IL, USA). The test normality was assessed by the Kolmogorov–Smirnov test. Data that showed normal distribution were displayed in mean ± standard deviation (SD). The OA patients and controls were compared using an independent samples t-test. Pearson's correlation coefficient evaluated correlations between biomarkers and clinical parameters. The results of the ROC curve analysis for the discriminative ability of sclerostin and osteocalcin to distinguish OA patients from healthy individuals are provided below. A P-value < 0.05 was regarded as a significant difference.

RESULTS

Table 1 reveals the age data in the subgroups, BMI categories, and pain scores for healthy controls and osteoarthritis (OA) patients. Statistical comparisons of age $P = 0.22$ and BMI ($P = 0.17$) between the two groups were not significant, indicating good demographic matching. However, pain intensity and pain-related disability scores were greater in OA patients than in healthy participants; 58.33 ± 16.23 versus 9.67 ± 2.5 and 53.33 ± 16.23 versus 7.89 ± 4.2, respectively; $P < 0.001$ for both comparisons clinically burdensome results regarding pain and disability in the OA group.

Table 1

Comparison of age, BMI and pain scores between OA patients and control

Items	OA Patients $N = 65$		Control $N = 35$		T-Test (P-value)
	Mean	SD	Mean	SD	
Age	56.87	13.93	52.67	20.5	2.79 (0.22)
BMI	29.56	9.72	23.98	10.3	3.79 (0.17)
Pain Intensity	58.33	16.23	9.67	2.5	6.54 (0.000)
Pain Disability	53.33	16.23	7.89	4.2	5.36 (0.000)

The findings indicated that patients with osteoarthritis had significantly raised levels of serum sclerostin (11.70 ± 1.10 ng/mL) compared to healthy controls who had levels of 3.80 ± 0.90 ng/mL (Fig. 1). In turn, the levels of osteocalcin were dramatically lower in patients (23.50 ± 19.30 ng/mL) vs controls (48.90 ± 5.20 ng/mL), and both variations were significant at $P < 0.0001$ (Fig. 2). This indicates that bone metabolism is deranged in osteoarthritis with increased inhibition of bone formation via sclerostin and decreased osteoblastic activity shown by the lower osteocalcin level.

The comparison of serum proinflammatory cytokine levels between the osteoarthritis patients and healthy controls showed that the concentrations of all the cytokines measured were statistically increased in the osteoarthritis group. IL-1β, TNF, IL-6, and IL-17 were statistically greater in osteoarthritis patients (means: 11.5, 15.34, 36.8, and 45.8 pg/mL, respectively) compared to controls (means: 8.4, 11.39, 8.4 and 13 .8 pg/mL respectively). The variations were all extremely significant at a probability level of ($P < 0.0001$). These findings further emphasize the central role of systemic inflammatory response in the pathophysiology of osteoarthritis and confirm these cytokines' modes of action regarding disease progression and symptom severity (Table 2).

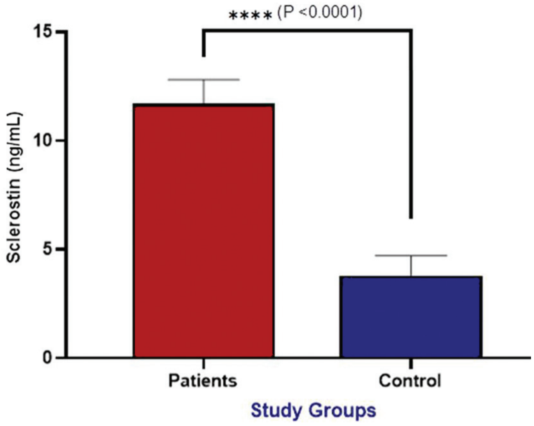

Fig. 1 Assessment of serum sclerostin (ng/mL) between patient and control groups

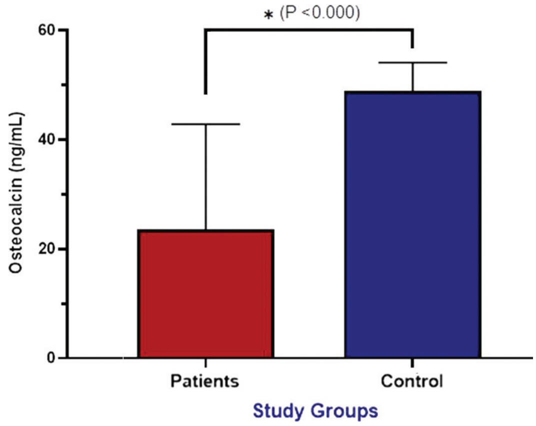

Fig. 2 Assessment of serum osteocalcin (ng/mL) between patients and control groups

Table 2

Comparison of proinflammatory cytokines between patients and control

Proinflammatory Cytokines	OA Patients $N = 65$		Control $N = 35$		T-Test (*P*-value)
	Mean	SD	Mean	SD	
IL-1β (pg/mL)	11.5	2.01	8.4	2.5	4.61 (0.000)
TNF (pg/mL)	15.34	5.71	11.39	4.3	3.57 (0.000)
IL-6 (pg/mL)	36.8	7.60	8.4	1.9	6.2 (0.000)
IL-17 (pg/mL)	45.8	9.47	13.8	1.5	7.5 (0.000)

The analysis of diagnostic performance has revealed sclerostin to have a strong potential as a biomarker for osteoarthritis with an area under the curve of 0.82 which is fairly good. At a cut-off value of 5.8 sclerostin reported a sensitivity of 78 % and specificity of 82 % which means it can fairly well identify those individuals who have osteoarthritis from those who do not. The *p*-value obtained 0.029 also adds to the evidence in favor of the reliability of sclerostin in this case. These findings strengthen the potential clinical application of sclerostin as a non-invasive biomarker in the future for detecting and assessing the risk of osteoarthritis at an early stage (Table 3, Fig. 2). The correlation matrix exhibited that sclerostin showed highly significant positive correlations with TNF ($r = 0.423$, $p = 0.000$), IL-6 ($r = 0.342$, $p = 0.003$), and IL-17 ($r = 0.298$, $p = 0.005$). Thus, a direct involvement of inflammatory activity in increased expression of sclerostin is suggested. The other way round, osteocalcin revealed the most significant negative correlations with the above-mentioned cytokines: TNF ($r = -0.385$, $p = 0.001$), IL-6 ($r = -0.345$, $p = 0.003$), and IL-17 ($r = -0.312$, $p = 0.004$), hence an inverse relationship with inflammation status on bone formation activity. The above proinflammatory cytokine did not correlate with IL-1β expression. The different degrees of expression of the two major genes associated with bone remodeling confirm the report by the authors that inflammatory mediators have a differential regulatory effect on the expression of these genes (Fig. 3).

Table 3

Pearson correlation coefficient between bone biomarkers and interleukins

Proinflammatory Cytokines	Sclerostin	Osteocalcin
IL-1β	$r = 0.121$ (0.351)	$r = -0.106$ (0.420)
TNF	$r = 0.423$ (0.000)	$r = -385$ (0.001)
IL-6	$r = 0.342$ (0.003)	$r = -0.345$ (0.003)
IL-17	$r = 0.298$ (0.005)	$r = -0.312$ (0.004)

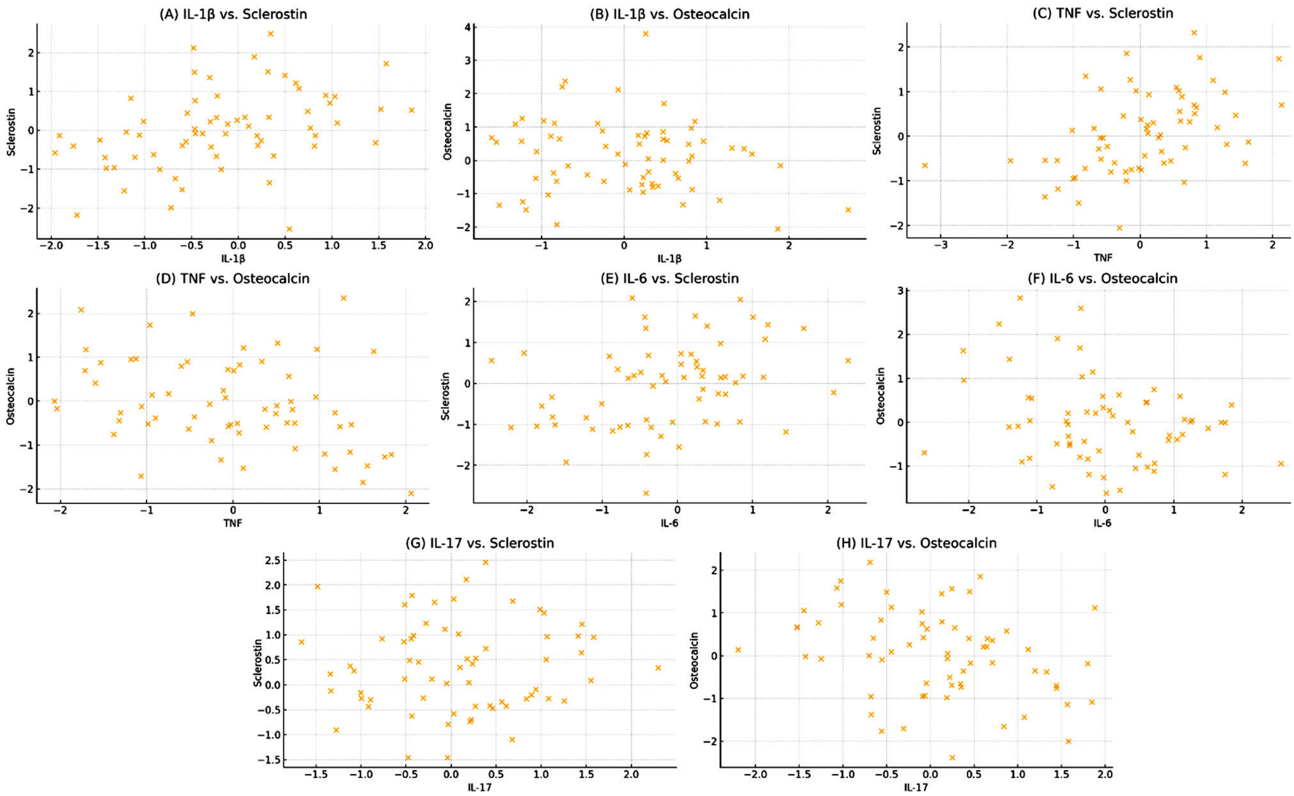

Fig. 3. Scatter plots showing the correlation and regression line between proinflammatory cytokines and bone markers in osteoarthritis patients (A) IL-1β and sclerostin. (B) IL-1β and osteocalcin. (C) TNF and sclerostin. (D) TNF and osteocalcin. (E) IL-6 and sclerostin. (F) IL-6 and osteocalcin (G) IL-17 sclerostin (H) IL-17 and osteocalcin

DISCUSSION

Osteoarthritis is the most prevalent degenerative joint disorder. In osteoarthritis (OA), the subchondral bone gets remodeled and the inflammatory microenvironment greatly affects both the expression and systemic levels of related proteins such as osteocalcin and sclerostin. Osteocalcin is a non-collagenous protein secreted by osteoblasts that has key importance in marking bone formation. It has been found elevated in patients with OA; thus, its synthesis reflects increased turnover of bone characteristic of the disease, along with the formation of osteophytes [8]. Sclerostin from osteocytes, a known inhibitor in the pathway of Wnt/β-catenin signaling, is mostly inhibited in OA particularly where there is active subchondral bone formation, i.e., in osteophyte regions [9]. On the other hand, recent data have shifted this view since chronic low-grade inflammation mainly mediated by proinflammatory cytokines appears to be central to the pathogenesis and evolution of OA. The proinflammatory cytokines included in the current study are strong mediators in the molecular cascade that leads to degradation of the cartilage; hyperplasia of synovium, osteophyte formation, and pain sensitization [10]. The concentration levels of IL-1β in OA synovial fluid are typically within 10–150 pg/mL. Healthy individuals normally have significantly lower concentrations; their levels are often undetectable or < 10 pg/mL [11]. Higher levels of IL-1β have been accompanied by a positive correlation with disease severity, joint space narrowing, and radiographic grading in OA patients [12]. It underscores the importance not just as a mechanistic contributor but a potential biomarker for disease activity and progression. Another essential inflammatory cytokine in OA is TNF-α. Its producing cells are macrophages, synovial fibroblasts, and chondrocytes; that is, practically any cell residing within the joint. Levels of TNF-α in serum and synovial fluid in OA patients (normally run between 15 and 100 pg/mL control values) are below 10–15 pg/mL [13]. Higher levels of TNF-α have also been correlated with pain, stiffness, and limitation of function in joints among OA population [12]. Similarly, in OA joints, IL-6 is secreted by chondrocytes, synoviocytes, and osteoblasts; it is more commonly in response to the stimulation by IL-1β and TNF-α [14]. Raised levels of IL-6 have been determined in the blood and joint fluid of OA patients, usually between 10–

300 pg/mL, much higher than in healthy people (< 10 pg/mL) [15]. Greater amounts of IL-6 are linked to more pain in the joints, severity seen on X-rays, and loss of cartilage measured by MRI images [16]. IL-6 helps in central pain sensitization and could explain why some OA patients have worse symptoms than would be expected from the amount of damage. It is mostly secreted by T helper cells 17 (Th17) and this proinflammatory cytokine is ever more identified in the pathology of OA. It has been found that IL-17 levels are greatly elevated in the serum and synovial fluid of OA patients as compared to the norm, and its concentrations most times range between 20–150 pg/mL [17]. These cytokines hardly ever act alone. They typify the pro-inflammatory milieu seen within the OA-affected joint. For instance, IL-17 can signal chondrocytes to secrete IL-1β and TNF-α which further improve IL-6 secretion, creating a positive feedback loop [18]. Such crosstalk perpetuates the high degree of local and systemic inflammation seen in concert with ongoing joint destruction. Raised levels of TNF-α, IL-1β, IL-17, and IL-6 together have been linked with poorer clinical outcomes; in other words, the higher pain scores and the greater functional limitations are the faster radiographic progression is [19]. In osteoarthritis, the cross-talk bone remodeling and inflammation hold a central position in the pathogenesis of the disease. Important molecular mediators of bone metabolism are osteocalcin and sclerostin. These two proteins quite opposed in function and regulation. In OA, osteocalcin is upregulated and sclerostin suppressed simultaneously, reflecting a shift toward a bone-anabolic phenotype from a chronic low-grade inflammatory state. A negative correlation was reported between sclerostin and studied interleukins [20]. The increase in osteocalcin seems to be very much related to proinflammatory cytokines. These cytokines, IL-6, IL-1β, and TNF-α have been proven to activate osteoblast progenitor cells through intracellular signaling cascades delivering messages that eventually result in gene expression of osteocalcin [21–22]. Moreover, under conditions of chronic inflammation these same cytokines can stimulate Wnt/β-catenin signaling that paradoxically increases osteoblast differentiation and matrix protein synthesis such as osteocalcin [23]. In OA, at the bone-cartilage interface, the inflammatory microenvironment together with mechanical stress allows for osteoblastic hyperactivity and angiogenesis to come about. This further raises osteocalcin levels and pathological bone formation [9]. Therefore, a strong positive correlation exists between osteocalcin and proinflammatory interleukins. The more these latter cytokines are involved in inflammation, the more they accelerate bone turnover in OA. The downregulation of sclerostin in OA also shares common pathways with proinflammatory cytokines that drive expression of osteocalcin. The inflammatory signaling pathways under which IL-1β, IL-17, and TNF-α suppress SOST gene expression involved that allowed for unrestrained osteogenesis. Inflammation results in osteocyte apoptosis or their dedifferentiation, and this further lowers the population of sclerostin-secreting cells in the subchondral bone. Thus, it furthers the abnormal bone formation environment to prevail [20]. This is how the reverse correlation is explained between sclerostin and proinflammatory cytokines in OA.

CONCLUSION

The studied proinflammatory cytokines (IL-17, IL-1β, TNF-α, IL-6) mediate osteoarthritis; they act by enhancing inflammation and damage to cartilage as well as changing the subchondral bone. In this regard, they increase osteocalcin levels by promoting the activity of osteoblasts and inhibit sclerostin allowing pathological bone formation. The positive correlation of osteocalcin with cytokines and inverse correlation with sclerostin reflects an inflammatory-driven imbalance in bone remodeling. Collectively, these molecules provide a clue to the pathophysiology of osteoarthritis and could perhaps be biomarkers indicative of disease activity and progression.

Conflict of interest *Not declared.*

Funding *The authors rely only on their own financial support.*

Ethics approval *The proposal in this research was recommended by the bioethical board of the College of in the University of Baghdad (No. 245 in 2025).*

Consent to participate *Before data collection and blood sampling, all patients included in the study were asked to provide written informed consent.*

REFERENCES

1. Han Y, You X, Xing W, et al. Paracrine and endocrine actions of bone-the functions of secretory proteins from osteoblasts, osteocytes, and osteoclasts. *Bone Res*. 2018;6:16. doi: 10.1038/s41413-018-0019-6.
2. Maeda K, Kobayashi Y, Koide M, et al. The Regulation of Bone Metabolism and Disorders by Wnt Signaling. *Int J Mol Sci*. 2019;20(22):5525. doi: 10.3390/ijms20225525.
3. Katrine H, Jakob S-L, Torben H, et al. Mechanisms in endocrinology: Diabetes mellitus, a state of low bone turnover – a systematic review and meta-analysis. *Eur J Endocrinol*. 2017; 176(3): R137–R157. doi:10.1530/EJE-16-0652.
4. McColm J, Hu L, Womack T, et al. Single- and multiple-dose randomized studies of blosozumab, a monoclonal antibody against sclerostin, in healthy postmenopausal women. *J Bone Miner Res*. 2014;29(4):935-943. doi: 10.1002/jbmr.2092.
5. Dirckx N, Moorer MC, Clemens TL, Riddle RC. The role of osteoblasts in energy homeostasis. *Nat Rev Endocrinol*. 2019;15(11):651-665. doi: 10.1038/s41574-019-0246-y.
6. Berry PA, Jones SW, Cicuttini FM, et al. Temporal relationship between serum adipokines, biomarkers of bone and cartilage turnover, and cartilage volume loss in a population with clinical knee osteoarthritis. *Arthritis Rheum*. 2011;63(3):700-707. doi: 10.1002/art.30182.
7. Kapoor M, Martel-Pelletier J, Lajeunesse D, et al. Role of proinflammatory cytokines in the pathophysiology of osteoarthritis. *Nat Rev Rheumatol*. 2011;7(1):33-42. doi: 10.1038/nrrheum.2010.196.
8. Li G, Yin J, Gao J, et al. Subchondral bone in osteoarthritis: insight into risk factors and microstructural changes. *Arthritis Res Ther*. 2013;15(6):223. doi: 10.1186/ar4405.
9. Chin KY, Ekeuku SO, Pang KL. Sclerostin in the development of osteoarthritis: A mini review. *Malays J Pathol*. 2022;44(1):1–18.
10. Terkawi MA, Ebata T, Yokota S, et al. Low-Grade Inflammation in the Pathogenesis of Osteoarthritis: Cellular and Molecular Mechanisms and Strategies for Future Therapeutic Intervention. *Biomedicines*. 2022;10(5):1109. doi: 10.3390/biomedicines10051109.
11. Glyn-Jones S, Palmer AJ, Agricola R, Price AJ, Vincent TL, Weinans H, Carr AJ. Osteoarthritis. *Lancet*. 2015;386(9991):376-87. doi: 10.1016/S0140-6736(14)60802-3.
12. Benito MJ, Veale DJ, FitzGerald O, et al. Synovial tissue inflammation in early and late osteoarthritis. *Ann Rheum Dis*. 2005;64(9):1263-1267. doi: 10.1136/ard.2004.025270.
13. Sokolove J, Lepus CM. Role of inflammation in the pathogenesis of osteoarthritis: latest findings and interpretations. *Ther Adv Musculoskelet Dis*. 2013;5(2):77-94. doi: 10.1177/1759720X12467868.
14. Fernandes JC, Martel-Pelletier J, Pelletier JP. The role of cytokines in osteoarthritis pathophysiology. *Biorheology*. 2002;39(1-2):237-246.
15. Kamel S, Khalaf R, Moness H, Ahmed S. Serum and Synovial Fluid Levels of Interleukin-17A in Primary Knee Osteoarthritis Patients: Correlations With Functional Status, Pain, and Disease Severity. *Arch Rheumatol*. 2022;37(2):187-194. doi: 10.46497/ArchRheumatol.2022.7931.
16. Wenham CY, Conaghan PG. The role of synovitis in osteoarthritis. *Ther Adv Musculoskelet Dis*. 2010;2(6):349-359. doi: 10.1177/1759720X10378373.
17. Liu Y, Peng H, Meng Z, Wei M. Correlation of IL-17 Level in Synovia and Severity of Knee Osteoarthritis. *Med Sci Monit*. 2015;21:1732-6. doi: 10.12659/msm.893771.
18. Beringer A, Thiam N, Molle J, et al. Synergistic effect of interleukin-17 and tumour necrosis factor-α on inflammatory response in hepatocytes through interleukin-6-dependent and independent pathways. *Clin Exp Immunol*. 2018;193(2):221-233. doi: 10.1111/cei.13140.
19. Lawrence A, Boesel J, Martinez Aguilar R, et al. A Review and Meta-Analysis of Biomarkers in Early-Stage Osteoarthritis. *Orthop Surg*. 2025;17(7):1913-1923. doi: 10.1111/os.70064.
20. Vasiliadis ES, Evangelopoulos DS, Kaspiris A, et al. The Role of Sclerostin in Bone Diseases. *J Clin Med*. 2022;11(3):806. doi: 10.3390/jcm11030806.
21. Liao Y, Ren Y, Luo X, et al. Interleukin-6 signaling mediates cartilage degradation and pain in posttraumatic osteoarthritis in a sex-specific manner. *Sci Signal*. 2022;15(744):eabn7082. doi: 10.1126/scisignal.abn7082.
22. Zheng L, Wang W, Ni J, et al. Role of autophagy in tumor necrosis factor-α-induced apoptosis of osteoblast cells. *J Investig Med*. 2017;65(6):1014-1020. doi: 10.1136/jim-2017-000426.
23. Steyn PJ, Dzobo K, Smith RI, Myburgh KH. Interleukin-6 Induces Myogenic Differentiation via JAK2-STAT3 Signaling in Mouse C2C12 Myoblast Cell Line and Primary Human Myoblasts. *Int J Mol Sci*. 2019;20(21):5273. doi: 10.3390/ijms20215273.

The article was submitted 05.05.2025; approved after reviewing 16.06.2025; accepted for publication 14.10.2025.

Information about the authors:

Rabab Ali Al-Mosawi — Ph.D., Lecturer, rababali.inj@atu.edu, https://orcid.org/0000-0002-8796-9011;

Safa Nihad Abed Shubar — Ph.D., Lecturer, safa.abd@atu.edu.iq, https://orcid.org/0009-0004-6319-8314;

Baraa Bahaa Aldin — Ph.D., Lecturer, barra.ahmed.ims@atu.edu.iq, https://orcid.org/0009-0002-4299-7577;

Ali A. Al-Fahham — Ph.D., Professor, fahham925@gmail.com, https://orcid.org/0009-0005-2108-1668.

Original article
https://doi.org/10.18019/1028-4427-2025-31-6-780-797

Stress and strain of the radial shaft with marginal notch and compensating elements explored with computer modelling

N.M. Aleksandrov[1]✉, V.D. Veshutkin[2], A.E. Zhukov[2], I.D. Veshaev[1]

[1] Privolzhsky Research Medical University, Nizhny Novgorod, Russian Federation
[2] Nizhny Novgorod State Technical University named after R.E. Alekseev, Nizhny Novgorod, Russian Federation

Corresponding author: Nikolay M. Aleksandrov, aleksandrov-chetai@rambler.ru

Abstract

Introduction The incidence of pathological fracture of the radius at the site of a marginal defect following graft harvesting reaches 31 %. A finite element computer simulation model allows for non-invasive determination and prediction of the stress and strain (SS) of the bone, the strength and susceptibility to fracture under various loads and strengthening methods.

The **objective** was to present the results of the finite element analysis on the influence of various marginal notch shapes, bone curvature and methods for increasing the strength on the SS of the radial shaft.

Material and methods Based on anatomical preparations of the human radius, solid-state linear-elastic modeling of the entire cortical diaphysis of the radius was performed including the shaft with rectangular and triangular marginal notches, curvature in two planes using different reinforcing plates and fixation methods under non-destructive tensile, compressive, torsional and bending loads. The longitudinal stability of the bone was determined. ANSYS and NX Siemens software packages were used in the study.

Results A triangular cutout reduced bone stress by 21.4 % in tension and by 51.5 % in torsion as compared to a rectangular cutout increasing the longitudinal stability margin by 1.18 times. Bi-planar bone curvature increased stress and reduced the tensile load-bearing capacity by 2.89 times. A 2 mm thick semi-tubular plate, compared to a flat narrow plate of similar thickness and 10 mm width reduced the level of maximum stresses in the bone model by 1.2–1.5 times in tension and by 3.5–3.9 times in torsion for different cutouts. Measurements of longitudinal stability for a semitubular plate increased critical stresses by 1.3–1.5 times for different osteotomies as compared to a bone without a cutout and plate.

Discussion With all the loads, the strength conditions of the bone model with a cutout were provided when fixed with a plate at least 2 mm thick on four 2.0 mm bicortical screws inserted two distally and two proximally to the cutout.

Conclusion The findings demonstrated practical use of bone plates reducing SS of the radius with any cutout.

Keywords: radial bone-cutaneous flap, marginal defect of the radius, stress and strain of the bone, notch compensation, strength of the radius, computer modelling

For citation: Aleksandrov NM, Veshutkin VD, Zhukov AE, Veshaev ID. Stress and strain of the radial shaft with marginal notch and compensating elements explored with computer modelling. *Genij Ortopedii*. 2025;31(6):780-797. doi: 10.18019/1028-4427-2025-31-6-780-797.

INTRODUCTION

A radial forearm free flap (RFFF) is used in reconstructive surgery to replace tissue defects [1, 2]. With its obvious advantages, this method is associated with the morbidity of the donor site and cannot be widely used. Harvesting the graft for transfer or relocation to the recipient site results in the formation of a marginal defect in the radial shaft. The incidence of pathological fracture of the radius at the marginal defect reaches 31 % [3, 4]. Treatment of the complication which causes functional and cosmetic impairment of the hand and forearm, presents a surgical challenge and requires lengthy treatment periods and significant financial costs. Experts' opinions on methods for preventing the complications remain controversial. There are conflicting opinions in the literature regarding the influence of the shape of the marginal notch on the strength of the radius: from complete denial to a significant weakening effect [5, 6]. Most authors recognize the role of prophylactic fixation of the donor radius [7, 8, 9]. Analysis of the works on the topic shows that many issues remain debatable, and the opinions of specialists are contradictory [10]. There are no publications reporting the effect of different osteotomies on bone strength; fixation methods, types of metal plates, the number, diameter of screws, their placement for fixing the plate to the bone have not been substantiated; mechanisms of loosening the screws have not been explored. Most authors evaluate residual bone strength and select a method for fracture prevention based on clinical and radiological data [11, 12]. An effect of the factors on bone strength is essential for development and substantiation of the methods for its strengthening and prevention of pathological fractures. Evolution of software and computer technology facilitated high reliability (95–99 %) and clarity in simulating the behavior of a product under the influence of various loads, including mechanical loads, and probabilistic assessment of the reliability of the constructs [13, 14]. The finite element method (FEM) is one of the most common methods for solving problems in mechanics including biomechanics [15]. The finite element model (FEM) is the bone model for the numerical solution of strength problems in biomechanics [15]. The level of internal mechanical stress is one of the key parameters that must be determined to assess a material's strength. A finite element computer simulation model allows for non-invasive determination and prediction of bone's mechanical response for various loads and predisposition (susceptibility) to destruction at the site of maximum mechanical stresses under loads, provides clarity, visualization, and accessibility of analysis of the parameters of the entire object [16, 17]. The advantages of FEM include the possibility to explore structures composed of several materials of any shape, and the feasibility of considering various boundary conditions [18, 19]. According to the literature, FEM allows us to determine the strength of the radius, examine the stability of orthopedic implants, which facilitates the implementation of measures to prevent fractures [20]. The available literature contains rather contradictory data obtained by computer modeling methods regarding the mechanical properties of the radial bones with various forms of marginal osteotomy, methods of compensating for the resulting defects, fixation of the plate and strengthening of the bone under tension, compression, bending and torsion [21, 22]. There are no publications reporting the influence of bone curvature on its strength. The choice of the type of plate, the number and size of screws, the nature of their implementation from the standpoint of bone stress and strain (SS), are not sufficiently substantiated, the longitudinal stability of the model with a cutout and a plate has not been studied [23, 24], and this is a limiting factor in the development of methods for preventing pathological fractures. Therefore, knowledge of the nature of stress distribution in intact bone and after the formation of a marginal notch, in the *bone-fixator* system, is necessary to adequately determine the method of preventive bone strengthening.

The **objective** was to present the results of the finite element analysis on the influence of various marginal notch shapes, bone curvature and methods for increasing the strength on the SS of the radial shaft.

MATERIAL AND METHODS

3D models of the radial shaft were created using a CAD computer-aided design system:

— without cutout and initial deflection;

— without a cutout with an initial bend in one (horizontal or vertical) or two planes;

— with a triangular cutout and an initial bend in one or two planes;

— with a rectangular cutout and an initial bend in one or two planes,

— with similar cutouts and bends with bone flat and semi-tubular plates fixed with two, four and six screws of different lengths and diameters;

— with a rectangular cutout and a compensating insert fixed with two screws.

Models of a *screw–bone* pair were created in a similar manner with a rectangular cutout replaced by a cortical insert of identical shape and size, fixed with screws and reinforced with a bone plate.

FEM calculations were performed using ANSYS and Siemens NX software packages to measure stresses. To simplify the calculations, the bone tissue of the radial shaft was assumed to be solid, homogeneous, linear, elastic (linear-elastic), continuous, and isotropic. It is accepted that compact bone is isotropic, since it has a common lamellar and relatively homogeneous structure, and the characteristics of strength and elasticity do not change in the radial shaft.

Measurements included the volumetric dynamic non-destructive loading SS on a linear-elastic isotropic hybrid model of the radial shaft, obeying the generalized Hooke's law, in compliance with the hypotheses of the technical theory of beam bending, since the graft is mostly harvested from this part of the bone in the clinic.

SS was assessed on the basis of the third and fourth theories of strength using the von Mises criterion providing an idea of the overall stress intensity and also combines the normal and shear stresses acting on the object. The choice of this criterion used to characterize the properties of a viscous material, is due to the use of metal compensating elements (plate, screws) in the model.

The parameters effecting the maximum bone stress were examined to include the shape and depth of the cut, the curvature of the bone in one or two different planes, the nature of the defect compensation, the type of plate, its dimensions (width, length, thickness), number of plates, the methods of insertion and the size of the screws fixing the plate to the bone with a rectangular and triangular cutout.

Critical stresses were tested for longitudinal stability of the bone. A spatial geometric model of the bone was constructed in the first stage of the study, then the model was broken down into finite elements (FEs) using a finite element mesh generator program. The complex three-dimensional geometry of the radial diaphysis and the analysis of the construction and behavior of various CEMs determined the choice of a three-dimensional CEM of the bone.

A 10-node second-order isoparametric tetrahedral element (CTetra 10) was used as the finite element type to form a volumetric solid mesh. The elements had three degrees of freedom at each node. Movement along the coordinate axes was optimal for displaying irregularly shaped objects with complex geometry in the software packages used.

Sections of anatomical specimens of the radius were used to construct a three-dimensional linear FEM model. The geometric calculation model consisted of a cylindrical structure with a cross-section composed of a semicircle and two lateral trapezoids symmetrical about a common axis. The geometry of the bone section and the initial curvature of the bone in two planes corresponded to the actual average dimensions obtained experimentally on cadaver (anatomical) material.

The physical characteristics of the model materials were specified in the second stage. The elastic moduli and Poisson's ratios of the various materials used in the calculations were taken from literature sources or obtained experimentally.

The mechanical properties adopted for bone material included Young's modulus of 0.2×10^5 MPa, Poisson's ratio (transverse deformation coefficient) of 0.3, tensile strength of 120 MPa, and density $\rho = 2400$ kg/m^3. For plates and screws made of VT6 titanium, Young's modulus measured 1.15×10^5 MPa, and Poisson's ratio was 0.32. The friction coefficient μ for the *metal-to-metal* contact pair was taken to be 0.15, and for the *bone-to-metal* pair, 0.3. The permissible normal tensile stresses of 60 MPa were taken from the condition of 0.5 of the ultimate strength (two times the safety factor). For torsion, the permissible shear stress was generally taken to be 0.5 times the normal stress (in accordance with the third strength hypothesis, i.e., 0.25 times the ultimate strength). In our cases, approximately 0.2 times the ultimate strength was adopted. The relative depth of the triangular and rectangular notches h_0/H was 0.16 and 0.33 (H being the height of the section of the intact bone, h_0 being the depth of the notch).

Bone deflection was modeled in two directions: x = 3.73 mm; y = 6.38 mm. A *screw-bone* pair was simulated. Simplified models of fixators of varying thickness (1 mm, 2 mm, 2.5 mm, 3 mm) were created for a flat reconstructive plate, a semitubular plate, and fixation screws; and screw models with diameters of 2 mm, 3.5 mm and 4.5 mm, lengths of 4 mm, 13 mm and 18 mm, were constructed according to their real dimensions. The number of elements in the model varied from 21,351 to 51,157, the number of nodes from 37,763 to 82,186, and the element sizes from 4.98 mm to 0.2 mm, depending on the size, nature, and characteristics of the simulated object and its objectives. The smallest finite element size and the largest number of nodes were used to model the screw and its connection to the bone. The mesh was thickened in areas where stress concentration was expected, in areas of thinning of the cortical plate and in areas with complex geometry.

Tension, compression (longitudinal stability, longitudinal bending, longitudinal deformation), torsion and complex loading (tension and bending) were examined. Bones subjected to compression can undergo longitudinal bending under load, and the bone model was tested for stability. The following boundary conditions were set. A rigid clamp was installed along the cross-sectional surface at one free end of the bone. Movement along all planes was ruled out, while uniform pressure or torque was applied to the other end along the cross-sectional plane.

A load was applied to the bone model in the third stage. Depending on the model type and the study objective, the static physiological load on the bone was 981 N, 800 N, or 400 N for tension and compression, and always 0.1 Nm for torsion. The load of 981 N applied corresponds to the weight of an average male. A load of 400 N was used to simplify calculations and determine changes in stress field boundaries and maximum stress values more accurately.

When the bone interacts with the metal plate, forces from the bone are transmitted to the plate by the screws. Since the plate prevents longitudinal deformation of the bone under load, the screw is primarily subject to shear forces. Furthermore, the bone's curvature causes bending stresses during tension and axial loads on the screw. For this reason, factors influencing the strength of screw fixation in bone were examined under axial and tangential loads on the screw head inserted outside the plate. When studying the stress in *screw-cortical bone* contact pairs (at the screw-bone interface), the bone was secured at both ends using rigid fixation. The magnitude of the tangential load was 100 N, and the axial load was 50 N, 100 N, 150 N. The stress values in the plate and screws were used as an additional criterion.

A qualitative and quantitative assessment of the stress fields of intact bone was performed after the formation of cutouts of various shapes and sizes with curvature in various planes without defect compensation and after prophylactic bone strengthening. The magnitude and zone of maximum stress concentration in various sections of the cutout of the shaft, plate and screws, the change in the area of the zone of maximum stress concentration under compression-tension and torsion were determined depending on the shape, depth of the cut, the curvature of the bone in two planes and the methods of its preventive strengthening with a metal plate on screws.

Bone stress values were chosen as the criterion for evaluating the effectiveness of the fixation plate. The use of FEM allowed us to identify and describe areas of local stress concentration, and explore their quantitative values and gradients within and across the bone surface.

RESULTS

The SDS of the bone model without cutouts or curvatures was characterized by a smooth distribution of the parameters across the model's surface, with no sharp changes. This bone model had no areas of stress concentration during tension and compression. Tensile stresses were uniformly distributed, and their values were the lowest of all the calculated cases considered. When stretching a bone model with vertical curvature, peak stresses were determined at the interosseous margin, and for a horizontal curvature, at the anterior margin. The presence of bone curvature in two planes under tensile conditions resulted in the occurrence of bending stresses also in two planes (Fig. 1). In these cases, peak stress areas were located in the interosseous and posterior margins of the radius. The area of increased stress during torsion of bone models with curvature was located along the anterior edge and the anterior surface of the bone.

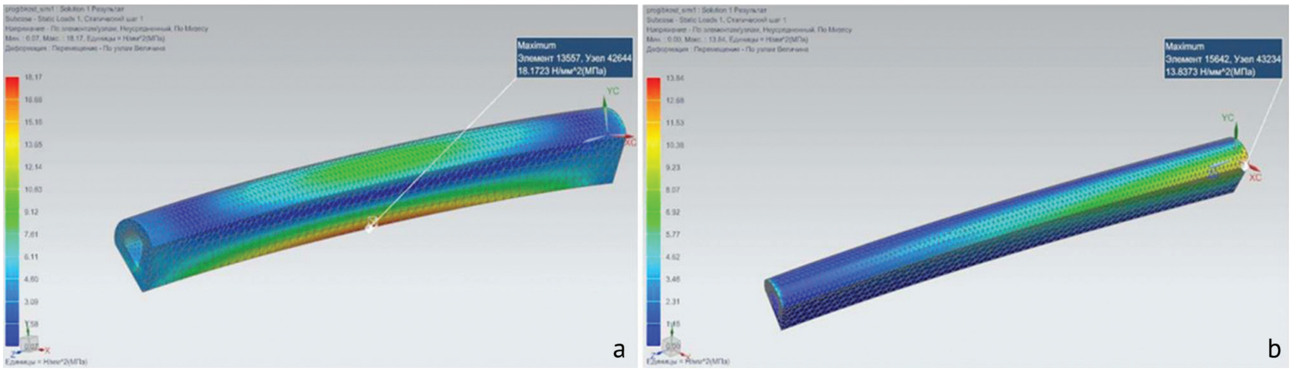

Fig. 1 Distribution of equivalent stresses according to von Mises in a bone without a notch with an initial deflection in two directions: (a) under tension; (b) under torsion

The bone model with curvature and a notch experienced the greatest stress in the notch area under all loading conditions. Areas of stress concentration were observed in areas with geometric changes. The formation of the notch caused stress concentrations in the corners of the triangular and rectangular notches and increased stress levels across the entire horizontal portion of the rectangular notch and the anterior surface of the bone under all types of loading. As the notch depth increased, peak stresses and their distribution area also increased under tension and torsion for all types of bone curvature. As expected, maximum tensile, compressive, and torsional stresses were observed at the location where the bone model's cross-section was minimal. In the presence of bone curvature and a notch, the stress distribution was non-uniform. When stretching and having a bend in the bone in the horizontal plane, the maximum stress was noted along the front edge of the notch of any shape.

When bending the bone in the vertical plane, maximum stress was observed in the interosseous margin area for any cutout shape. When bending the bone model in two planes, pronounced stress concentrations were observed in the following areas:

— interosseous margin of the bone in the zone of maximum deflection;

— in the corner of the triangular cutout along the back edge (under stretching-compression);

— across the entire plane or along the rear edge of the longitudinal part of the rectangular cutout, depending on its depth (Fig. 2, 3).

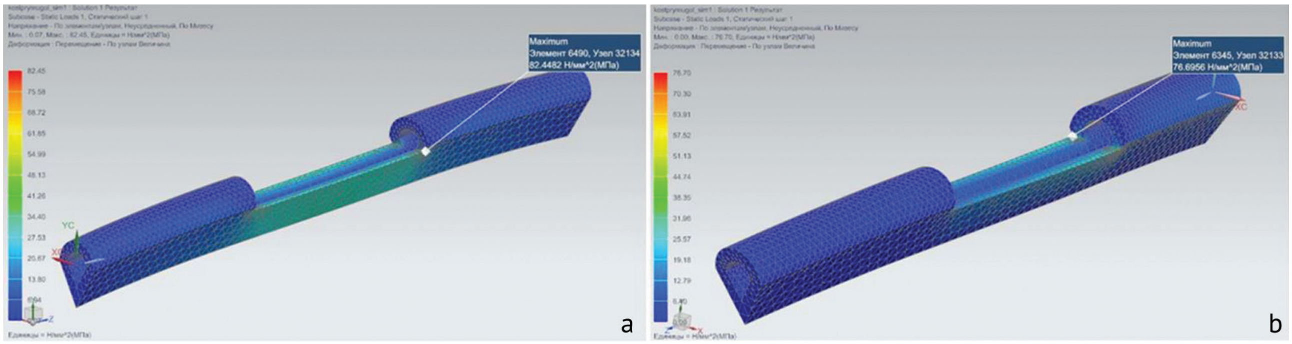

Fig. 2 Distribution of equivalent stresses according to von Mises in a bone with a rectangular notch and with an initial deflection in two directions: (a) under tension; (b) under torsion

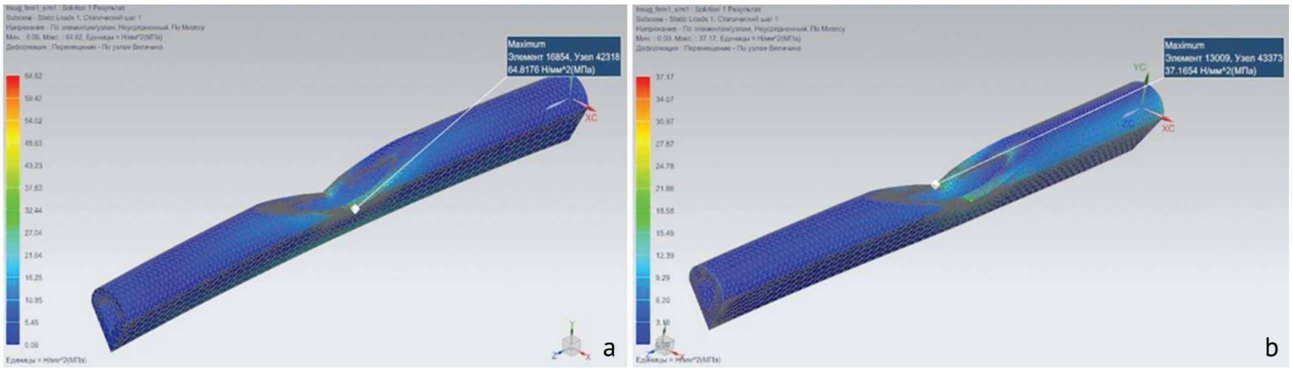

Fig. 3 Distribution of equivalent stresses according to von Mises in a bone with a triangular notch and with an initial deflection in two directions: (a) under tension; (b) under torsion

During torsion, stress concentrations were noted in the area of the notch: for a triangular notch, at the corner of the notch; for a rectangular notch, across the entire plane or along the edges of the longitudinal portion of the notch, depending on its depth. The zone of greatest stress along the length of the bone for a triangular notch was significantly smaller than for a rectangular notch, both under tension and torsion.

The calculations showed that the structural shape of the cutout, which ensures the greatest load perception during tension and torsion, has a triangular shape with a depth of $h_0/H = 0.16$ (where h_0 is the depth of the cutout, H is the height of the bone section without the cutout). As the depth of the bone cut with curvature increased to $h_0/H = 0.33$, the peak values of maximum stresses increased for all cut shapes.

Table 1

Equivalent von Mises stresses in bones of different shapes under tension and torsion

Types of loading	von Mises stresses depending on bone shape, MPa			
	without cutout and initial deflection	without cutout with initial dent	with a triangular cutout and an initial bend	with a rectangular cutout and an initial bend
Stretching, F = 400 N	6.28	18.17	64.82	82.45
Torsion, M = 0,1 N·m	12.93	13.84	37.17	76.70

As Table 1 shows, the bone without the notch and initial curvature experiences the lowest stress. The presence of initial curvature increases the stress by 2.89 times in tension and only 1.1 times in torsion compared to the bone model without the notch. Based on the results, it can be concluded that the highest stresses were observed with a rectangular notch and initial bone deflection in both directions under all types of loading. For the same notch depth, a triangular shape is preferable to a rectangular one, as it produces lower stress levels under the same loading. The stress of the triangular notch is 78.6 % of the stress of the rectangular notch in tension and 48.5 % in torsion, that is, the triangular notch reduces the stress level by 21.4 % in tension and 51.5 % in torsion.

The presence of bone curvature causes increased tensile stress in the model without damage by 2.89 times due to the appearance of stress from bending, in conditions of its combination with a triangular cutout — by 10.32 times, with a rectangular cutout — by 13.13 times compared to the model without curvature and cutout. Bone curvature increases the torsional stress level by 1.1 times in the absence of damage, 2.88 times with a triangular notch, and 5.93 times with a rectangular notch (Table 1). The stresses caused by the presence of the notch and bone curvature are summed up.

The results of the analysis of the bone model behavior under compressive load showed that the model under a load of 981 N cannot operate without loss of stability under any type of artificial cut, since the critical stresses for the first form of lost stability were an order of magnitude lower than the maximum stresses identified for a given load, in contrast to the model without a cutout. The model with a triangular cutout had a greater margin of safety for longitudinal stability (1.18 times) compared to the model with a rectangular cutout (Table 2).

Table 2

Stresses acting in samples with different cuts when solving the problem of longitudinal stability

Bone shape	Stress σ, MPa	
	σ_{max}	σ_{cr} for the first form of lost stability
No cutout	31.76	54.18
Rectangular cutout	47.60	39.96
Triangle cutout	59.23	46.99

A review of the literature shows that narrow plates are most often used for osteosynthesis in practice. Due to this and the fact that bone with a triangular notch and plate was found to be stronger in most respects than bone with a rectangular notch and plate, only the strengthening variant of bone with a triangular notch was further investigated. The bone model with a cutout and a plate and the plate in the defect projection showed greater stress in the defect area under all types of loading, cutout, and deflection. Stress concentrators arose at the points of geometric changes, as well as at the contact points between the parts (Fig. 4).

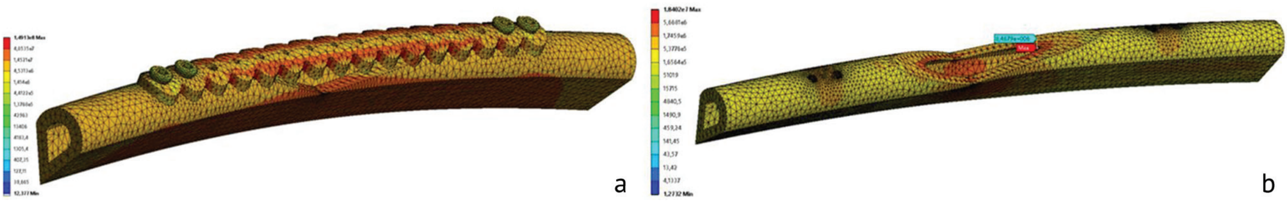

Fig. 4 Distribution of the von Mises equivalent stress in a bone with a triangular notch under compression (four screws, plate thickness 2 mm): (a) general distribution in the model, (b) distribution in the bone

The stresses along the plate's length between the screws in the notch area were distributed almost uniformly across the plate's width and concentrated between the screws. Beyond the screws, the stresses in the cantilevered areas were zero. The highest bone stresses were observed in the screws closest to the notch. With a through screw placement, zones of increased stress were identified in the area where the screws exited, which were more pronounced in the screws located next to the defect.

The criterion for assessing the effectiveness of the plate included the reduction in stress in the bone with the overlay in relation to the stress in the bone without the overlay. In models with a rectangular cutout replaced by a cortical insert of identical shape and size, fixed with screws and reinforced with a bone plate, the maximum stress during stretching was noted in the plate at the level of the corner of the cutout. The area of maximum bone stress was determined at the interosseous margin at the same level. When fixing the insert with screws alone, the areas of maximum bone stress were observed at the corners of the notch and at the interosseous margin at the same levels. In this model, the use of the plate reduced the maximum bone stress by 2.21 times.

When the model is stretched, the stress level in the bone would depend on the plate thickness and the number of screws (Fig. 5). The stress exceeded the permissible values under the conditions using a 1 mm thick plate. Compared to this calculated case, a decrease in stress was observed in the bone model with a 2 mm thick plate. A direct relationship between stress reduction and the number of screws was also noted. The acceptable stress level was achieved by modeling a 2 mm thick plate on four screws with monocortical insertion. The strength requirement was met when using a 2 mm thick plate. An inverse relationship was observed between the stress values and the plate thickness. The strength condition was also met when using a 3 mm thick plate. A decrease in stress was observed in the bone model with a 3 mm thick plate compared to the model with a 2 mm thick plate.

It can be concluded that a 3 mm thick plate was most effective in terms of maximum stress. To conserve material, a 2 mm thick plate can be employed, as the calculated equivalent stresses in the bone do not exceed the tensile strength and differ only slightly from those in the bone model with a 3-mm-thick plate. The stresses in a 2-mm-thick plate using four screws differ insignificantly from those using six screws. The stresses in a 2 mm thick plate using four screws differ insignificantly from those using six screws. Therefore, using a 2 mm thick plate with four screws can be sufficient, as using plates with more screws in a clinical setting is more traumatic. The lowest stress in the bone was observed with use of a 3 mm thick plate on six fixing screws, therefore this fixation system is desirable in the presence of a pronounced bend and an increase in the depth of the cut of more than half the bone with the stress increasing sharply in it.

As the graph shows, increasing the number of screws has no effect on bone stress during torsion (Fig. 5). Increasing the plate thickness reduces bone stress under all types of loads. Stress within the plate also decreases with increasing plate thickness, and at 3 mm, the number of fixation screws has little effect.

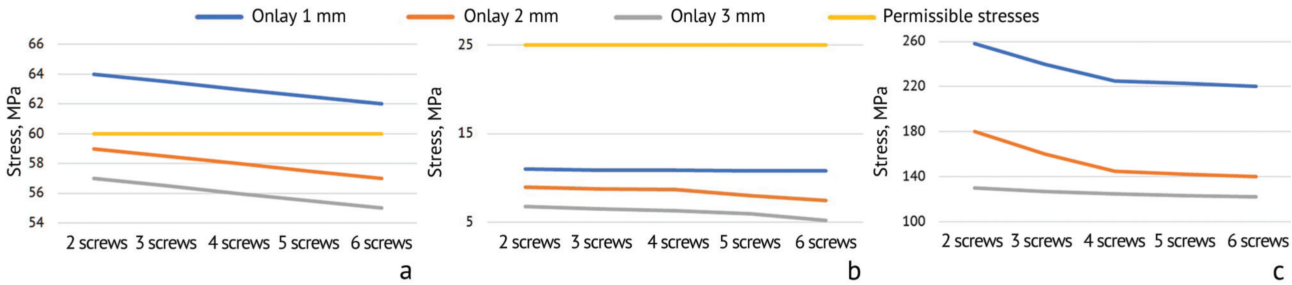

Fig. 5 Graphs of the dependence of equivalent stresses on the plate thickness and the number of fixing screws: (a) in the bone under tension; (b) in the bone under torsion; (c) in the plate under tension

The stress distribution in the plate-bone-screw system was examined on a bone model with a triangular cutout and a plate on two screws with different plate thicknesses under tension (Table 3) and torsion (Table 4). Based on the results of the calculations performed under tension and torsion, it can be concluded that the stress in the plate, bone, and screw is linearly related to plate thickness. As plate thickness increases, stress decreases in each element of our working plate-bone-screw model. The highest concentration was found in the plate, suggesting that it could absorb most of the loads arising from bone extension and torsion. The lowest stresses were found in the screw.

Table 3

Values of equivalent stresses according to von Mises depending on the plate thickness under tension with a load of F = 980 N

Plate thickness, mm	Stress σ, MPa		
	in the plate	in the bone	in the screw
2.0	154.69	121.48	46.00
2.5	126.16	111.34	30.20
3.0	124.93	110.49	23.89

Table 4

Values of equivalent stresses according to von Mises depending on the thickness of the plate under torsion with a load of M = 0.1 N·m

Plate thickness, mm	Stress σ, MPa		
	in the plate	in the bone	in the screw
2.0	58.32	19.43	13.07
2.5	55.62	16.80	12.70
3.0	52.88	14.77	10.31

The plate played a key role under all types of loads, relieving the bone tissue. The screws absorbed the stress in the bone and transferred it to the plate. Regardless of the plate thickness, the stress in the bone did not exceed the tensile strength, and it did not even exceed the permissible stress under torsional stress. This was due to the fact that the plate reduced the angle of torsion due to its rigidity, thereby reducing the level of stress in the bone to a greater extent than with stretching.

The calculation of bone models for longitudinal stability was produced for artificial injuries of rectangular and triangular shape with a relative cut depth $h_0/H = 0.33$, with a deflection f_x and f_z, with the immersion of six screws fixing a semi-tubular plate 2 mm thick to the bone, to a depth of 13 mm. The analysis of the results of the influence of bone strengthening with a plate on longitudinal stability is presented in Table 5.

Table 5

Destructive and critical loads acting on bones with notches

Strength indicators		Load values				
		no cutout	rectangular cutout	triangular cutout	rectangular cutout with plate	triangular cutout with plate
Stretching	σ_{str}, MPa	—	47.60	44.44	41.95	39.68
	P_{destr}, N	—	**2473**	**2649**	**2806**	**2967**
Compression	σ_{str}, MPa	31.76	47.60	44.44	30.61	30.51
	P_{destr}, N	3706	**2473**	**2649**	**3846**	**3858**
	$K = P_{cr}/P_{str}$	−1.219	−3.544	−4.057	−5.128	−5.425
	P_{cr}, N	**4238**	**3477**	**3980**	**5030**	**5322**

The design load P_{str} is assumed to be 981 N, and the failure load P_{destr} is calculated upon reaching the ultimate strength of $\sigma_g = 120$ MPa. The failure load of the bone without the notch exceeds the design load by 3.78 times, which is the load safety factor. Calculations showed that the critical load of a defective bone is 1.4–1.5 times higher than the failure load. Bone failure will occur due to compression, not buckling. The plate increases the critical load by 1.45 times for a rectangular notch and by 1.34 times for a triangular notch, and also increases the breaking load for a rectangular cutout by 1.56 times, and for a triangular cutout by 1.46 times. The critical and maximum stresses in the bone are presented in Table 6.

Table 6

Critical and maximum stresses acting in specimens with different notch shapes and semi-tubular plates under compression

Type of the bone cut with the plate	Stress, MPa	
	maximum σ_{max}	critical $\sigma_{cr\,1}$
rectangular cutout	30.61	58.08
triangular cutout	30.51	61.55

Data analysis shows that the bone model with a metal plate under a design load of 981 N can operate without loss of stability under any type of artificial cut, since the critical stresses for the first form of lost stability appeared to be twice as high as the identified maximum stresses under the design load.

A comparative analysis of the effectiveness of the influence on stress in a bone model with different cutouts with a relative depth of $h_0/H = 0.33$, with a deflection of f_x and f_z, a flat narrow and semi-tubular plate with a thickness of 2 mm and the immersion of six fixing screws to a depth of 13 mm was produced (Table 7).

A semi-tubular plate, compared to a flat narrow compensating plate with a width of 10 mm, reduced the stress under tension by 1.2 times for an artificial cutout of a rectangular cross-section, by 1.5 times for an artificial cutout of a triangular cross-section; under torsion, by 3.9 times for a rectangular cross-section of the cutout, 3.5 times for the triangular section of the artificial cutout.

Table 7

Comparison of maximum and critical stresses in bone with different cutout shapes and fixation methods

Type of cutout	σ_{max} when stretched, MPa		τ_{max} in torsion, MPa		Critical stress of the 1st form of lost stability $\sigma_{\chi\rho\ 1}$, MPa	
	flat plate	semi-tubular plate	flat plate	semi-tubular plate	no plate and cutout	semi-tubular plate
Rectangular cutout	36.47	30.59	5.914	1.505	39.96	58.08
Triangular cutout	47.03	30.53	5.51	1.55	46.99	61.55

Under tension, stress values corresponded to those of intact bone, amounting to 31.59 MPa, while under torsion, values were similar, amounting to 60–70 % of the work of intact bone, equal to 0.757 MPa. A 1.3–1.5-fold increase in critical stress was noted when using a semitubular plate compared to a bone model without curvature or notch. The proposed plate's stability criterion showed higher values than those for intact bone, equal to 54.18 MPa. The semitubular plate could offer better load capacity, both in torsion and tension, than a 10 mm wide flat plate. Load capacity increased with increasing plate thickness. In stretching, specimens with 4 mm of screw penetration performed best; in torsion, specimens with 4 mm and 13 mm of screw penetration performed nearly identically. The specimen with a through-thickness screw penetration resulted in increased stress in the bone at the screw insertion site.

Stress and strain of the *screw-bone* pair model was analyzed to identify mechanisms of screw instability leading to the development of osteosynthesis complications. A study of the stress fields during screw-bone interaction under tangential and axial loading showed that the highest stress concentration in the screw occurred near the head with the shear force from the plate applied (Fig. 6). In bone, the highest stress concentration occurred in the region of maximum stress in the screw, namely, at the screw's entry into the bone.

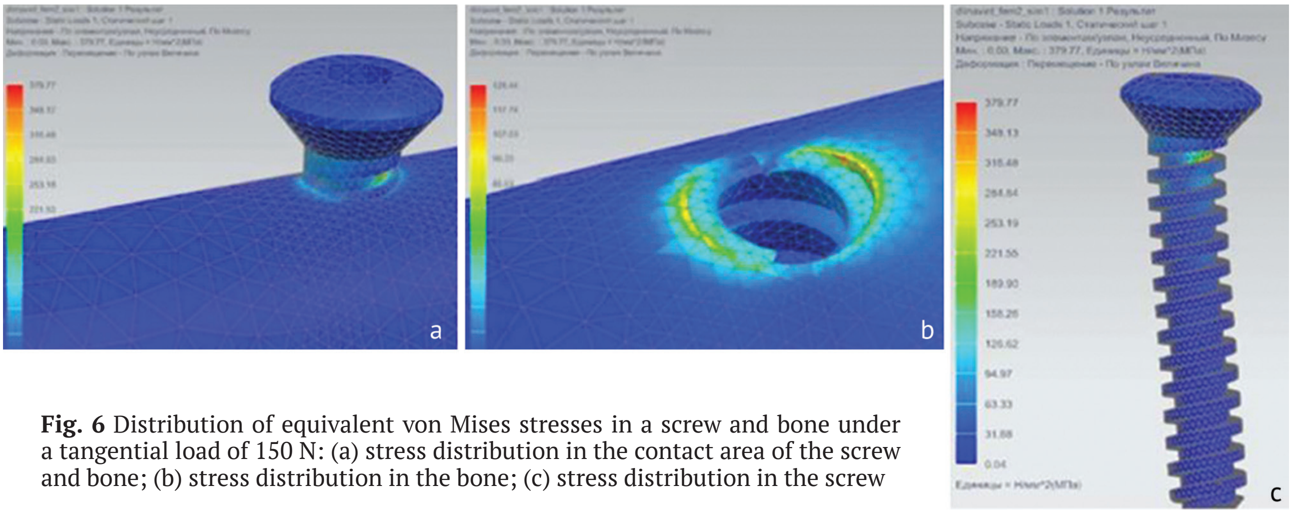

Fig. 6 Distribution of equivalent von Mises stresses in a screw and bone under a tangential load of 150 N: (a) stress distribution in the contact area of the screw and bone; (b) stress distribution in the bone; (c) stress distribution in the screw

The quantitative parameters of mechanical stresses under shear loads on the screw are presented in Tables 8, 9, and 10. The presented results showed the linear stress dependence on the applied load (Table 8). As the bone layer thickness decreases, the stresses increase. At a thickness of 2.8 mm and a load of 150 N, the bone stress exceeded even the tensile strength of 130 MPa.

A screw was considered short if it passed through one cortex, and long if it passed through both cortices. As the screw length increased, the bone stress increased, and at a load of 150 N, it exceeded the bone's tensile strength (Table 9). The thickness of the cortical bone was taken to be 3.14 mm.

Table 8

Values of equivalent stresses in bone and screw depending on the thickness of the cortical bone under tangential loads

Load F, H	Stress in the bone σ, MPa		Stress in the screw σ, MPa	
	t = 3,14 mm	t = 2,8 mm	t = 3,14 mm	t = 2,8 mm
50	31.13	46.52	52.41	109.92
100	72.26	93.04	104.82	219.84
150	108.39	139.1	157.23	330.49

Note: t, cortical thickness.

Table 9

Values of equivalent stresses in the bone and screw depending on the screw length under tangential loads

Load F, H	Stress in the bone σ, MPa		Stress in the screw σ, MPa	
	Short screw	Long screw	Short screw	Long screw
50	31.13	42.81	52.41	126.59
100	72.26	85.63	104.82	253.18
150	108.39	128.44	157.23	379.77

Table 10

Values of equivalent stresses in the bone and screw depending on the screw diameter under tangential loads

Load F, H	Stress in the bone σ, MPa		Stress in the screw σ, MPa	
	D = 3.5 mm	D = 4.5 mm	D = 3.5 mm	D = 4.5 mm
50	31.13	20.51	52.41	24.27
100	72.26	41.02	104.82	48.54
150	108.39	61.53	157.23	72.81

Measurements suggested linear relationship between stress and load applied for screws of different diameters. As the screw diameter increased, the stress in the bone decreased, but even with smaller screw diameters, the stress did not exceed the bone's tensile strength (Table 10). However, a shear load on a screw of 50 N, for most screw parameters and cortical thicknesses, led to increased shear stresses in the bone, exceeding the permissible values, with the exception of a 4.5 mm diameter screw. At higher loads, the permissible values were exceeded in all cases.

There was a linear stress dependence on the shear load applied for various screw parameters (diameter and length) and bone thickness (thickness) facilitating stress prediction under such a load. The stress distribution pattern was the same for all load values. The stress distribution pattern was the same for all load values. The stresses that generated in the bone did not exceed or reach the tensile strength for various screw parameters (length and diameter), but exceeded the tensile strength with a decrease in the thickness of the cortical bone and an increase in the length of the screw under a load of 150 N. The shear stresses increased in the screw and the bone with an increase in the length of the screw.

Under axial loading, the highest stress concentration in the screw was observed at the site of the first three threads, and in the bone, at the entry site of the screw. The maximum stress in the bone depended linearly on the applied axial load on the screw during its tightening. Under a load of 150 N, the maximum equivalent stress in the bone was 88.4 MPa, which exceeded the permissible stress values in the bone leading to a risk of bone destruction and resorption at the contacting plate-bone site with the connection elements and unstable osteosynthesis (Fig. 7). The graph showed that an axial load on the screw exceeding 100 N caused maximum normal stresses in the bone that exceeded their permissible values.

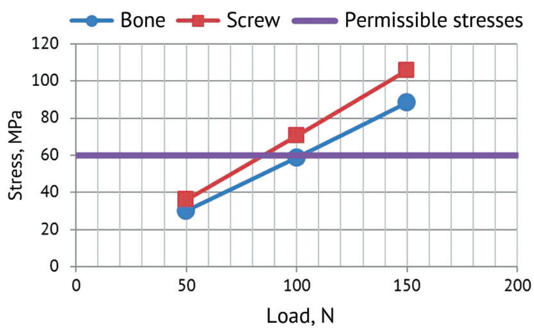

Fig. 7 Graph of the dependence of the equivalent stress in the bone and screw on the axial load applied

Maximum stresses in the bone depended linearly on the load applied. This allows the obtained results to be extended to other applied loads and predict the stress level under a known load in order to avoid unwanted destruction (local microdestruction) of the cortical bone around the holes and thread stripping due to excessive tightening of the screw. Therefore, the stress and strain of a bone model with a cutout depends on many factors including the type of the loads, methods of defect repair, which should be taken into account in clinical practice for the development of measures to increase the residual strength of the donor radius.

DISCUSSION

Practical questions reported in the study included how the formation of a notch and the presence of bone curvature in two planes affect the stress and strain of a bone model, what approaches and methods can ensure an increase in the residual strength of the bone and the permissible level of stress in it.

In recent years, the global literature has seen an increase in publications devoted to the application of the finite element method in traumatology and orthopedics, including simulated radial fractures. The method has proven to be very informative in exploring bone strength [16, 17, 25] and it can be used to predict the occurrence and prevention of fractures of the intact radius [16, 17]. It has been established that skeletal models constructed using finite elements provide a non-invasive assessment of the strength and stability of the implant [20]. The authors used computed tomography data from experimental animal bones and artificial bones to construct the FE model. A high degree of correlation between the parameters of the FE model and cadaveric bone was noted [16, 17, 19], which is confirmed by our studies conducted on human anatomical specimens and models based on them. Studies have been published on FE modeling of bone with a marginal defect with the integrity of one of the cortical bones preserved [22]. There are no studies on FE modeling of the radius with a similar defect and compensating elements based on anatomical preparations of human bone using the theory of beam and cross-section bending.

A notch formed in the radial diaphysis model caused a significant increase in the maximum normal stress values compared to the intact bone, which could be explained by a decreased cross-sectional area and the geometric moment of inertia at the notch site. Increased stress indicated a decrease in strength and a greater risk of fracture under real conditions.

Surgeons' opinions regarding the influence of the notch shape on residual bone strength remain controversial. Some authors suggest that a navicular (radial, scaphoid) or keeled (triangular) notch created during graft formation and harvesting can prevent radial fractures, without the use of prophylactic osteosynthesis [26]. Another group of specialists does not see this as necessary, suggesting that it only helps prevent the depth of the incision from being exceeded and improves access and visibility in the surgical area [8, 27, 28].

The extent of the increase in stress depending on the beveling of the osteotomy plane and the increase in the depth of the notch has not been sufficiently explored, and the data are contradictory [28, 29, 30]. The formation of such a notch can be accompanied by a minimal effect and lead to an increase in bone torsional strength of 5 % only [28, 29], while others report a significant positive effect of the osteotomy shape on bending and torsional strength [30]. Our data are consistent with the results of the TEM of other authors, with the peak stress values in four-point bending and torsion being 24–30 % higher with a rectangular osteotomy than with a beveled one [30]. This result can be explained by the fact that a rectangular cutout has two stress concentrators at the corners of the defect, while a triangular cutout has one, with a lower stress concentration coefficient. Theoretically, a radius (boat-shaped, shuttle-shaped) cutout would have an even lower stress concentration by rounding (smoothly changing the shape) the notch in the narrowest part of the remaining bone. However, the normal stress in the bone was still higher in the case than the permissible values, and therefore the formation of a triangular or radial notch must be combined with other strengthening methods [28]. Increased depth of the notch led to a disproportionate increase in stress in the bone, especially during torsion, regardless of the shape of the notch [30]. The role of bone bending in the genesis of the stress and strain has not been explored. Our findings showed that the presence of bone curvature led to an increase in normal tensile stresses by almost three times compared to a bone model without curvature. The increase in tensile-compressive stress in the presence of bone curvature can be explained by the occurrence of a longitudinal bending moment due to the occurrence of eccentric forces with the severity being dependent on the magnitude of the bending, which was proven by the method of mathematical modeling [31]. The presence of a notch combined with a bone curvature weakens the bone significantly according to the principle of superposition of forces,with normal tensile stresses and bending stresses caused bythe presence of a bend and a bone defect being summed up. This is confirmed by distribution of voltage fields.

The longitudinal stability of the notched bone remains unexplored. In real-world conditions, this type of impact can occur under axial loading (compression) on the forearm during a fall or impact. We believe that the loss of longitudinal stability of the notched bone occurs due to the reduction of the geometric moment of inertia of the section and the presence of the initial curvature of the bone, which leads to the eccentricity of the compressive and tensile forces, that is, to eccentric tension and compression. The presence of the notch can lead to eccentricity of the force and the occurrence of a bending moment. The greater margin of safety of a bone with a triangular notch in terms of longitudinal stability compared to a rectangular notch is explained by the weakening of its cross-section over a greater length with the moment of inertia of the section of the bone is less at the rectangular cut.

There are reports on the increased strength of the radius with a marginal defect fixed with a bone bridge plate under bending and torsion conditions [6, 18, 21, 28]. The influence of flat straight and T-shaped plates on the stress and strain of a finite element model of a bone with a marginal notch was explored [22]. However, the mechanisms by which maximum bone stress changes when using other types of plates, including semitubular ones, have not been studied. At the current stage of reconstructive surgery, the size, placement of the plate, the number and size of fixation screws, and the method of their placement have also not been definitively determined. There is no data on the comparative analysis of the effectiveness of options for prophylactic osteosynthesis of bone with a marginal defect using FEM under different types of loading [8, 21]. Quantitative analysis of the stress fields of the model with a plate showed that fixation with a 2 mm thick plate on four screws (two on each side of the defect) with a diameter of 2.0 mm, inserted bicortically, is sufficient to reduce the stress in the bone, since they do not exceed the permissible values in this case, although they are close to them. There is a slight decrease in the stress in the bone with a thicker plate and more screws. Increased number of screws and, consequently, the plate length in clinical settings leads to increased duration, increased invasiveness, and the risk of impaired bone circulation. The results can be explained by the fact that the cross-sectional area is the measure of plate stiffness under simple tension and compression. Increasing the plate thickness from 1 mm to 2 mm doubles the cross-sectional area, and the stiffness, while increasing it from 2 mm to 3 mm increases it by a third. For this reason, a 2 mm thick plate can be used, as the stress in the bone decreases only slightly compared to a 3 mm thick plate. The excess of permissible bone stress in the model with a 1 mm thick plate can be explained by insufficient rigidity of the plate and the high stress within it with resultant greater stress in the bone.

The number of fixing screws required can also be justified through a qualitative analysis of the model's stress fields. A study of the influence of the number of fixing screws, their location, and plate thickness on the nature of stress distribution in various elements of the model showed that the primary load during prophylactic bone strengthening with a plate is borne by the fixation plate and the remaining cortical layer of the radius in the notch area. These areas of bone have reduced load-bearing capacity, and the load from them is transferred to the reinforcing plate via screws outside the notch increasing the strength of the defect. With the screws adequately placed, the tensile-compressive load between them depends on their number: the more screws, the less stress being applied to the screws and bone material. If the screws are arranged in a longitudinal row and there is little friction between the plate and the bone material, the load on each screw will depend on the distance between the screws and their distance from the defect.

The presence of friction between the plate and bone will theoretically reduce the load on the screws, as some of it will be absorbed by the friction surfaces. However, with a smooth contact surface of the supporting plate, this reduction may be insignificant. The areas of the reinforcing plate in the cutout area and the screws closest to the defect were the most heavily loaded due to their location near the weakened portion of the bone. This can be explained by their location in a zone of high stress due to their location near the bone with a reduced cross-section and, consequently, lower rigidity, experiencing the greatest deformations (longitudinal and angular displacements) and stresses together with the plate in the cutout area compared to intact areas. The stresses will be lower in the pair of screws next to the defect and in the presence of a third pair of screws, even lower, which is consistent with the results of other studies conducted using FEM [22]. With three or more screws, the primary load is supported by the first two screws, while subsequent screws bear significantly lighter loads and are therefore ineffective. The greatest stress relaxation occurred in the area of the two end screws. This stress distribution in the screws during tension-compression in the calculation model can be explained not only by the presence of a weakened bone area, as well as misalignment of the bone and supporting plate axes and the occurrence of eccentric forces leading to bone bending and rotation. The findings are consistent with the results of other studies conducted with FEM to analyze the stress distribution between screws on a model of a diaphyseal fracture fixed with a dynamic compression plate (DCP) and a fixation compression plate with angular stability (LCP) as well as when exploring long-term results of extracorporeal osteosynthesis of long tubular bones with radiographs [18, 22].

Under torsional loads, the stress in the bone is lower than the permissible value, even for a 1 mm thick plate. This is because the plate significantly reduces the torsional angle due to its rigidity, so the number of screws and the plate thickness have little effect on the stress magnitude. However, in the case of using flat plates when fastened with one screw on each side, a single screw does not prevent rotation and possible shifting of the plate under loading, which is excluded when fixing with two screws on each side of the defect or using a semi-tubular plate.

The maximum shear stress occurring in the plate can be observed in the screws closest to the defect. With greater number of screws, the torsion angle decreases due to the increased stiffness of the connection. As the plate thickness increases, the stress within it decreases and is little affected by the number of screws, which can be explained by the increased cross-sectional area of the model and the strength (rigidity due to the high modulus of elasticity of the metal) of the connection. Fastening with fewer screws (one on each side) is ineffective for torsional load, even when installing such plates. When the bone is twisted, the load distribution between the screws is different, and it can be assumed that when fastening with two pairs of screws, the torsional rigidity of the resulting section can be sufficient, since the twisting angles are small and an increase in the number of screws has little effect on these parameters. Taking these facts into account, it can be assumed that fixation with a narrow plate 2 mm thick on four screws 4 mm in diameter provides sufficient strength even under tangential loads on the calculation model.

An analysis of the stress distribution in various elements of our *bone–screw–plate* model showed that the greatest stresses were obtained in the plate, and the least in the screws during tension–compression and torsion of the bone. This result can be explained by the fact that screws are subject to predominantly shear stresses, which are typically lower than normal stresses. The screw-contact zone in the plate is subject to predominantly normal bearing stresses, while normal and shear stresses are present in the bone. As plate thickness increases, stresses in the structural elements decrease linearly. Increasing plate thickness would lead to increased fixation rigidity in clinical settings causing a "stress-shielding" effect, weakening of the bone [6, 32, 33] and plate protrusion above soft tissue or prolapse [33]. This can be accompanied by greater trauma of the intervention, the risk of damage to muscles, nerves, blood vessels, impaired bone circulation and the development of infectious complications [34].

The plate's lower profile would occupy minimal tissue volume in real-world conditions, facilitating suturing of the tissues above the plate without tensioning the wound edges. The plates may offer a potential advantage over 3.5 mm thick plates in accelerating fracture healing due to reduced stress shielding, allowing forces to be distributed evenly along the length. Experimental studies on a composite anatomical model of the forearm bone demonstrated plastic deformation of the low-profile plate without fracture, thanks to its flexibility despite excessive loads which potentially prevents re-fracture observed with the use of thicker plates [33].

The advantages we have identified with a semi-tubular plate over a flat narrow plate can be explained by the fact that a bone model with a plate shaped to envelop the cylindrical surface of the bone bears a greater load due to the increased rigidity of the connection in two directions due to the shape of the metal construct. Increasing the plate thickness leads to a reduced stress in all elements of the *bone-screw-plate* system, since the area and moment of inertia of the cross-section of the joint increase. This plate, compared to a narrow straight plate, reduces the level of stress in the bone to a greater extent during tension and torsion (the main mechanism contributing to the fracture, in which the load on the radius cannot be absorbed by the ulna). According to the longitudinal stability criterion, the triangular-notched bone reinforced with the plate exhibits higher critical stress values than the intact bone. The triangular-notched bone model reinforced with the plate exhibits higher critical stress values than the rectangular-notched model and a similar plate in longitudinal bending and torsion suggesting the practical use of a triangular cutout in combination with prophylactic fixation with a bone plate. It can be assumed that similar patterns can occur with other types of loads. This is consistent with the surgeons' opinion on the need to bevel the corners of the cut and shape it triangular or scaphoid in combination with prophylactic bone plating [8, 22]. With the residual strength of the radius increased with plate fixation a larger cross-section of bone can be harvested allowing reconstruction of a larger defect without the risk of the radius fracture. A graft thickness not exceeding 1/2 the diameter or the bone circumference can be harvested without prophylactic bone fixation [6, 21].

There are isolated reports of successful fracture prevention by replacing the defect with an autogenous bone insert fixed with screws. According to our data, replacing a rectangular defect with a compensating insert without prophylactic plating does not provide adequate stress reduction in the bone, and high stress concentration values remain in the corners of the cutout for the period of insert consolidation.

The strength of the screw-bone connection is crucial for ensuring the stability of bone plating. The problem of screw instability during metal osteosynthesis remains a pressing issue. Screw loosening is the most common complication of plating. Screw loosening leads to serious complications, failed plating and bone fractures. are poorly understood. Microcracks, bone fractures at the screw site, bone resorption caused by excessive stress in the perifocal bone surrounding the screw are most common mechanisms underlying this phenomenon. This raises the question of the parameters and placement of plate-fixing screws to ensure the necessary bone strength. Some authors report the advantages of bicortical fixation [6, 8], while others report the advantages of monocortical screw placement [24, 35]. We analyzed the stresses and deformations of the bone and screw at the connection site depending on the diameter, length of the screw, and the thickness of the cortical layer. Mechanisms of screw instability, the strength of screw pull-out or screw-in under axial load was explored on experimental models made from different artificial (synthetic) materials, including bone plating [36, 37, 38, 39, 40] and using the FE method [41, 42, 43].

Our findings showed that pure tension-compression and torsion caused the main load on the screws fixing the plate as the shear load from the plate, causing shear stresses. The bone also experienced bending from the longitudinal load due to the existing curvature, so the normal load transmitted from the reinforcing rigid plate to the screw is added to the shear, tending to tear the screws out of the bone when there was a significant difference in the bending rigidity of the bone (especially the damaged area) and the plate. When the plate was placed on the convex side of a curved bone, such a pull-out load occurred under compression and under tension on a concave side. The load was greater with the screw being closer to the apex of the bone's curve. For this reason, the tangential loads on the screw and the axial loads in the screw-bone contact pair at the bone-screw interface were explored. We found that the tangential stresses, and consequently the bone deformation, increased with increasing screw length, decreasing screw diameter and decreasing cortical bone thickness. The findings can be interpreted as follows. Increasing the contact area of the screw-bone pair leads to a decrease in stress in all elements of the screw-bone-plate system. The lowest stress in the bone was observed in the model with monocortical insertion of a short screw (3.5–4.0 mm). The lower level of shear stresses with short screws fastened through one cortex may be due to the shorter length, due to which the screw practically does not bend and a lower bending moment is generated under tangential loading. The screw penetrated by 3.5–4.0 mm provides less secure plate attachment due a greater risk of screw to be torn out of the bone under tension, especially if the bone is curved. A larger contact screw and the bone area would provide greater strength and rigidity either by increased thickness of the cortical layer, the diameter of the screws, or by increasing their number, length and placing the screws through both cortices. The stresses in the screw during this procedure may be somewhat higher due to the increased arm of the tangential force applied from the plate, despite the increased area of the screw contraction with the bone. A long screw traverses two cortices and can bend under shear load on the head, increasing the stress due to the bending moment. In practice, this necessitates a tradeoff between the greater invasiveness of the surgery and the reduced risk of plate detachment due to screw pullout. An increased thickness of the cortex can lead to decreased stress in all elements of the screw-bone system with the contact area of the screw-bone pair increased.

With a thinner cortex, the contact area with the screw decreases leading to increased stress, which is more significant than with changes in screw parameters. Based on the facts, it can be concluded that a decreased thickness of the cortex, which is more common in osteoporosis in women is associated with increased number, diameter, length of screws and thickness of the plate increasing the screw-bone contact area, and ultimately, the strength and rigidity of fixation. Due to the fact that a normal axial load is transferred from the plate to the screw during stretching and compression of the bone, which tends to pull out the screw, its bicortical placement is practical especially in cases of large curvature of the bone and the close location of the screw or defect to the apex of the curvature. Tangential and normal stresses acting on a screw are essential for identifying instability mechanisms [44, 45]. Our results are consistent with the literature data, suggesting radial and axial stresses acting on the screw fixing the plate [18, 44, 45]. In this case, shear stresses play a leading role in screw loosening, since the volume of bone resorption in the perifocal area appear to be greater under radial loading than axial loading for all types of loading [18]. For this reason, the primary indicator of screw loosening risk may be its shear resistance rather than axial pullout strength. According to the researchers, radial screw resistance is more associated with physiological craniocaudal loads,and the strength of the screw under axial load mainly determines the ability of the bone to resist torsion [18, 44]. Higher values of tangential and normal stresses for the perifocal bone at the site of insertion of the central screws indicate the potential for primary resorption, bone damage and, ultimately, loosening or fracture of the screws. According to available literature, bone resorption is caused by mechanical stress exceeding the bone's tensile strength. According to other authors, the critical threshold for bone resorption is approximately 50 MPa, which is lower than the ultimate strength of the cortical layer of the normal radius bone under torsion [18]. The data were obtained using a FE model of the tibial diaphysis fixed with a plate and by analyzing radiographs of long bones after plating [18]. According to our data, placement of screws into the bone is associated with resorption or destruction of bone tissue in the perifocal area in case of exceeded longitudinal (axial) load, equal to 100 N with the permissible stress (60 MPa) almost reached and a decreased thickness of the cortical layer. Stable fixation of the two central screws experiencing the greatest shear stresses can be provided by increasing the diameter and length for bicortical placement, especially with large bone curvature and decreased thickness of the cortical layer. In practice, maximum caution is needed for screw placement without exceeding the permissible axial load, avoiding unwanted damage to the cortex.

Therefore, the SS model of the radial diaphysis allowed us to understand mechanisms of strength reduction, obtain an idea of the residual strength of the bone after the formation of rectangular and triangular marginal notches, and the use of various methods for compensating for the defect and preventing pathological fracture. The findings can be extrapolated to the clinic, with a certain degree of conventionality, for the development of methods for the prevention and treatment of patients with fractures of the osteotomized radius, since they provide an idea of the strength properties of the bone and the mechanisms for achieving screw stability when fixing it with a plate. We believe that internal fixation of the radius with a plate and screws can prevent fractures, resulting in reduced morbidity to acceptable levels, which will expand the indications for the use of RFFF in many areas of surgery.

CONCLUSION

The presence of a notch and bone curvature in two planes significantly increased the level of normal mechanical stress in the bone model. The bone model with a triangular notch exhibited lower stress levels than the model with a rectangular notch. The findings substantiated the need to strengthen the radius shaft with a marginal notch using a bone plate, regardless of a shape, which will reduce the mechanical stress on the bone below the permissible level. Bone models with a semitubular plate demonstrated an advantage over models with a flat narrow plate providing a greater reduction in stress levels. Bone stress decreased with increasing cortical and plate thickness, and with the number and diameter of screws.

Conflict of interest *None of the authors has any potential conflict of interest.*

Funding *The authors received no specific funding for this work.*

REFERENCES

1. Silverman DA, Przylecki WH, Shnayder Y, et al. Expanding the Utilization of the Osteocutaneous Radial Forearm Free Flap beyond Mandibular Reconstruction. *J Reconstr Microsurg*. 2016;32(5):361-365. doi: 10.1055/s-0035-1571251.
2. Chappell AG, Ramsey MD, Dabestani PJ, Ko JH. Vascularized Bone Graft Reconstruction for Upper Extremity Defects: A Review. *Arch Plast Surg*. 2023;50(1):82-95. doi: 10.1055/s-0042-1758639.
3. Kearns M, Ermogenous P, Myers S, Ghanem AM. Osteocutaneous flaps for head and neck reconstruction: A focused evaluation of donor site morbidity and patient reported outcome measures in different reconstruction options. *Arch Plast Surg*. 2018;45(6):495-503. doi: 10.5999/aps.2017.01592.
4. Archibald H, Stanek J, Hamlar D. Free Flap Donor-Site Complications and Management. *Semin Plast Surg*. 2022;37(1):26-30. doi: 10.1055/s-0042-1759795.
5. Clark S, Greenwood M, Banks RJ, Parker R. Fracture of the radial donor site after composite free flap harvest: a ten-year review. *Surgeon*. 2004;2(5):281-286. doi: 10.1016/s1479-666x(04)80098-2.
6. Avery CM, Parmar S, Martin T. The use of a T-shaped contoured unilocking titanium radial plate for prophylactic internal fixation of the radial osteocutaneous donor site. *Br J Oral Maxillofac Surg*. 2010;48(8):648-650. doi: 10.1016/j.bjoms.2010.01.013.
7. Werle AH, Tsue TT, Toby EB, Girod DA. Osteocutaneous radial forearm free flap: its use without significant donor site morbidity. *Otolaryngol Head Neck Surg*. 2000;123(6):711-717. doi: 10.1067/mhn.2000.110865.
8. Shnayder Y, Tsue TT, Toby EB, et al. Safe osteocutaneous radial forearm flap harvest with prophylactic internal fixation. *Craniomaxillofac Trauma Reconstr*. 2011;4(3):129-136. doi: 10.1055/s-0031-1279675.
9. Tankersley A, Velasco Martinez I, Medina A. Use of cervicothoracic rotation flap and osteocutaneous radial forearm free flap for a complex multilayered cheek defect reconstruction. *Case Reports Plast Surg Hand Surg*. 2020;7(1):98-104. doi: 10.1080/23320885.2020.1806070.
10. Loeffelbein DJ, Al-Benna S, Steinsträßer L, et al. Reduction of donor site morbidity of free radial forearm flaps: what level of evidence is available? *Eplasty*. 2012;12:e9.
11. Waits CA, Toby EB, Girod DA, Tsue TT. Osteocutaneous radial forearm free flap: long-term radiographic evaluation of donor site morbidity after prophylactic plating of radius. *J Reconstr Microsurg*. 2007;23(7):367-372. doi: 10.1055/s-2007-992342.
12. Silverman DA, Przylecki WH, Arganbright JM, et al. Evaluation of bone length and number of osteotomies utilizing the osteocutaneous radial forearm free flap for mandible reconstruction: An 8-year review of complications and flap survival. *Head Neck*. 2016;38(3):434-438. doi: 10.1002/hed.23919.
13. Pimenov SA. Application of NX nastran for reliability assessment of metal structures. *J Sc Intensive Technol*. 2012;(5):70-76. (In Russ.)
14. Omarov MD, Muslimova FN. Analytical review of the methodology of computer modeling. *Int J Applied Fundamental Research*. 2015;(3-1):11-14. (In Russ.) URL: https://applied-research.ru/ru/article/view?id=6466.
15. Edwards WB, Troy KL. Finite element prediction of surface strain and fracture strength at the distal radius. *Med Eng Phys*. 2012;34(3):290-298. doi: 10.1016/j.medengphy.2011.07.016.
16. Matsuura Y, Kuniyoshi K, Suzuki T, et al, Takahashi K. Accuracy of specimen-specific nonlinear finite element analysis for evaluation of distal radius strength in cadaver material. *J Orthop Sci*. 2014;19(6):1012-1018. doi: 10.1007/s00776-014-0616-1.
17. Jiang H, Robinson DL, McDonald M, et al. Predicting experimentally-derived failure load at the distal radius using finite element modelling based on peripheral quantitative computed tomography cross-sections (pQCT-FE): A validation study. *Bone*. 2019;129:115051. doi: 10.1016/j.bone.2019.115051.
18. Feng X, Lin G, Fang CX, et al. Bone resorption triggered by high radial stress: The mechanism of screw loosening in plate fixation of long bone fractures. *J Orthop Res*. 2019;37(7):1498-1507. doi: 10.1002/jor.24286.
19. Liu J, Mustafa AK, Lees VC, et al. Analysis and validation of a 3D finite element model for human forearm fracture. *Int J Numer Method Biomed Eng*. 2022;38(9):e3617. doi: 10.1002/cnm.3617.
20. Campbell GM, Glüer CC. Skeletal assessment with finite element analysis: relevance, pitfalls and interpretation. *Curr Opin Rheumatol*. 2017;29(4):402-409. doi: 10.1097/BOR.0000000000000405.
21. Bowers KW, Edmonds JL, Girod DA, et al. Osteocutaneous radial forearm free flaps. The necessity of internal fixation of the donor-site defect to prevent pathological fracture. *J Bone Joint Surg Am*. 2000;82(5):694-704.
22. Avery CM, Bujtár P, Simonovics J, et al. A finite element analysis of bone plates available for prophylactic internal fixation of the radial osteocutaneous donor site using the sheep tibia model. *Med Eng Phys*. 2013;35(10):1421-1430. doi: 10.1016/j.medengphy.2013.03.014.

23. Roberts JW, Grindel SI, Rebholz B, Wang M. Biomechanical evaluation of locking plate radial shaft fixation: unicortical locking fixation versus mixed bicortical and unicortical fixation in a sawbone model. *J Hand Surg Am*. 2007;32(7):971-975. doi: 10.1016/j.jhsa.2007.05.019.
24. Overturf SJ, Morris RP, Gugala Z, Lindsey RW. Biomechanical comparison of bicortical locking versus unicortical far-cortex-abutting locking screw-plate fixation for comminuted radial shaft fractures. *J Hand Surg Am*. 2014;39(10):1907-1913. doi: 10.1016/j.jhsa.2014.06.141.
25. Hosseini HS, Dünki A, Fabech J, et al. Fast estimation of Colles' fracture load of the distal section of the radius by homogenized finite element analysis based on HR-pQCT. *Bone*. 2017;97:65-75. doi: 10.1016/j.bone.2017.01.003.
26. Thoma A, Khadaroo R, Grigenas O, et al. Oromandibular reconstruction with the radial-forearm osteocutaneous flap: experience with 60 consecutive cases. *Plast Reconstr Surg*. 1999;104(2):368-378; discussion 379-80. doi: 10.1097/00006534-199908000-00007.
27. Swanson E, Boyd JB, Mulholland RS. The radial forearm flap: a biomechanical study of the osteotomized radius. *Plast Reconstr Surg*. 1990;85(2):267-272.
28. Avery CM, Best A, Patterson P, et al. Biomechanical study of prophylactic internal fixation of the radial osteocutaneous donor site using the sheep tibia model. *Br J Oral Maxillofac Surg*. 2007;45(6):441-446. doi: 10.1016/j.bjoms.2006.10.010.
29. Meland NB, Maki S, Chao EY, Rademaker B. The radial forearm flap: a biomechanical study of donor-site morbidity utilizing sheep tibia. *Plast Reconstr Surg*. 1992;90(5):763-773.
30. Bujtar P, Simonovics J, Váradi K, et al. Refinements in osteotomy design to improve structural integrity: a finite element analysis study. *Br J Oral Maxillofac Surg*. 2013;51(6):479-485. doi: 10.1016/j.bjoms.2012.09.015.
31. Aleksandrov NM, Veshutkin VD, Zhukov AE, et al. The application of mathematical simulation for studying the strength properties of a donor radius. *Russian Journal of Biomechanics*. 2017;21(2):147-165. (In Russ.) doi: 10.15593/RZhBiomeh/2017.2.03.
32. Hirashima T, Matsuura Y, Suzuki T, et al. Long-term Evaluation Using Finite Element Analysis of Bone Atrophy Changes after Locking Plate Fixation of Forearm Diaphyseal Fracture. *J Hand Surg Glob Online*. 2021;3(5):240-244. doi: 10.1016/j.jhsg.2021.05.013.
33. Wahbeh JM, Kelley BV, Shokoohi C, et al. Comparison of a 2.7-mm and 3.5-mm locking compression plate for ulnar fractures: a biomechanical evaluation. *OTA Int*. 2023;6(3):e278. doi: 10.1097/OI9.0000000000000278.
34. Zhao X, Jing W, Yun Z, et al. An experimental study on stress-shielding effects of locked compression plates in fixing intact dog femur. *J Orthop Surg Res*. 2021;16(1):97. doi: 10.1186/s13018-021-02238-3.
35. Shanmugam R, Jian CYCCS, Haseeb A, Aik S. Comparing biomechanical strength of unicortical locking plate versus bicortical compression plate for transverse midshaft metacarpal fracture. *J Orthop Surg (Hong Kong)*. 2018;26(3):2309499018802511. doi: 10.1177/2309499018802511.
36. Bronsnick D, Harold RE, Youderian A, et al. Can high-friction intraannular material increase screw pullout strength in osteoporotic bone? *Clin Orthop Relat Res*. 2015;473(3):1150-1154. doi: 10.1007/s11999-014-3975-1.
37. Wang T, Boone C, Behn AW, et al. Cancellous Screws Are Biomechanically Superior to Cortical Screws in Metaphyseal Bone. *Orthopedics*. 2016;39(5):e828-e832. doi: 10.3928/01477447-20160509-01.
38. Jazini E, Petraglia C, Moldavsky M, et al. Finding the right fit: studying the biomechanics of under-tapping with varying thread depths and pitches. *Spine J*. 2017;17(4):574-578. doi: 10.1016/j.spinee.2016.11.019.
39. Varghese V, Saravana Kumar G, Krishnan V. Effect of various factors on pull out strength of pedicle screw in normal and osteoporotic cancellous bone models. *Med Eng Phys*. 2017;40:28-38. doi: 10.1016/j.medengphy.2016.11.012.
40. Wu LC, Hsieh YY, Tsuang FY, et al. Pullout strength of different pedicle screws after primary and revision insertion: an in vitro study on polyurethane foam. *BMC Musculoskelet Disord*. 2023;24(1):863. doi: 10.1186/s12891-023-07015-3.
41. Geng JP, Ma QS, Xu W, et al. Finite element analysis of four thread-form configurations in a stepped screw implant. *J Oral Rehabil*. 2004;31(3):233-239. doi: 10.1046/j.0305-182X.2003.01213.x.
42. Eraslan O, Inan O. The effect of thread design on stress distribution in a solid screw implant: a 3D finite element analysis. *Clin Oral Investig*. 2010;14(4):411-416. doi: 10.1007/s00784-009-0305-1.
43. Oswal MM, Amasi UN, Oswal MS, Bhagat AS. Influence of three different implant thread designs on stress distribution: A three-dimensional finite element analysis. *J Indian Prosthodont Soc*. 2016;16(4):359-365. doi: 10.4103/0972-4052.191283.
44. Feng X, Qi W, Zhang T, et al. Lateral migration resistance of screw is essential in evaluating bone screw stability of plate fixation. *Sci Re*p. 2021;11(1):12510. doi: 10.1038/s41598-021-91952-3.
45. Feng X, Luo Z, Li Y, et al. Fixation stability comparison of bone screws based on thread design: buttress thread, triangle thread, and square thread. *BMC Musculoskelet Disord*. 2022;23(1):820. doi: 10.1186/s12891-022-05751-6.

The article was submitted 04.02.2025; approved after reviewing 21.04.2025; accepted for publication 14.10.2025.

Information about the authors:

Nikolay M. Aleksandrov — Doctor of Medical Sciences, Leading Researcher, aleksandrov-chetai@rambler.ru;

Vladimir D. Veshutkin — Candidate of Technical Sciences, Associate Professor of the Department;

Aleksandr E. Zhukov — Candidate of Technical Sciences, Associate Professor of the Department;

Ivan D. Veshaev — Postgraduate Student.

Original article
https://doi.org/10.18019/1028-4427-2025-31-6-798-804

Acromioclavicular joint dislocation: reconstruction of coracoclavicular ligament with fiber tape by using a new knot technique

M.B. Shinde✉, M.R. Patel, B. DasGupta, A. Sharma, K. Sarwey, S. Jethliya, R. Jain, D. Kedia, S. Chunawala, C. Kowe, S. Chiwadshetti, Y.N. Singh

H.B.T. Medical College and Dr. R.N. Cooper hospital, Mumbai, Maharashtra

Corresponding author: Mahesh B. Shinde, mahesh.shinde.1466@gmail.com

Abstract

Introduction Injuries to the acromioclavicular joint (ACJ) can range from modest, transient pain to significant displacement, chronic pain, and shoulder biomechanical changes that result in long-term disability.

We **aimed** to evaluate the functional outcome of anatomical reconstruction of the ACJ using fiber tape, as in type III–VI AC joint dislocations.

Materials and Methods In this study, 28 patients with AC joint dislocation (Rockwood type III–VI) were managed by surgical fixation using fiber tape from November 01, 2019, to October 31, 2024, at the tertiary care center. After providing written informed consent, the study enrolled patients who satisfied the inclusion criteria. The mean age of the participants was 36.50. Preoperative, three-month, and six-month UCLA shoulder scores were assessed.

Results The UCLA scores increased from 29.20 at three months to 35 at six months. Radiological evaluation at each visit suggested a 100.0 % success rate of this method. No participants had surgical site infection (SSI).

Discussion Several treatment options have been described for managing AC joint dislocations, including various implants and fixation methods, such as Bosworth screws, wires, locking plates, and hook plates. Unfortunately, these methods often lead to hardware-related complications, necessitating implant removal. The advantages of fiber-tape fixation technique include short surgery time, small incisions, fast recovery, cost-effectiveness, and ease of reproducibility.

Conclusions Open reduction internal fixation with a knot using fiber tape for type III–VI AC joint injuries is a viable surgical option. It has the advantages of being stable, single surgery, and excellent functional outcomes. However, extensive multicentric comparative studies are required to draw definitive conclusions.

Keywords: Fiber tape, Acromioclavicular joint, open reduction, loop end, Rockwood type

For citation: Shinde MB, Patel MR, DasGupta B, Sharma A, Sarwey K, Jethliya S, Jain R, Kedia D, Chunawala S, Kowe C, Chiwadshetti S, Singh YN. Acromioclavicular joint dislocation: reconstruction of coracoclavicular ligament with fiber tape by using a new knot technique. *Genij Ortopedii*. 2025;31(6):798-804. doi: 10.18019/1028-4427-2025-31-6-798-804.

INTRODUCTION

The acromioclavicular joint (ACJ) is one of the important components of the shoulder girdle and plays a significant role in normal shoulder movements and biomechanics [1]. Several mechanisms can lead to ACJ injuries, such as direct or indirect trauma. These injuries can be minor, with temporary joint pain, but can sometimes lead to substantial displacement, persistent pain, and alterations in shoulder biomechanics, resulting in long-term impairment [2, 3]. Young, active males are more prone to these injuries. Rockwood classified these injuries into six types based on the integrity of the acromioclavicular ligament (AC ligament) and coracoclavicular ligament (CC ligament) [4]. Type I (a mild sprain of the AC ligament with the CC ligament intact) and Type II (a ruptured AC ligament with a sprained CC ligament) injuries are best managed conservatively. However, Type III (a ruptured AC and CC ligaments), Type IV (posterior displacement of the clavicle into the trapezius), Type V (gross and severe displacement of the distal clavicle superiorly), and Type VI (a dislocated AC joint with the clavicle displaced inferiorly to the acromion or coracoid) require surgical intervention [5]. Additionally, fractures at the lateral end of the clavicle are associated with injuries to the CC ligaments [6, 7]. Injury to the CC ligament leads to superior migration of the clavicle lateral end, associated with pain, deformity, and skin tenting. The goal of surgery is to reduce the acromioclavicular and coracoclavicular intervals [8].

Several surgical techniques and implants have been described for the management of ACJ dislocation and lateral end clavicle fractures. Hook plate fixation is the most commonly performed procedure for these injuries. However, this surgery is associated with some complications, such as hardware prominence, irritation, and shoulder stiffness, which may require a second surgery to remove the implant [9]. Other fixation techniques include open reduction and internal fixation with cannulated cancellous screws, suture fixation, acromioclavicular pin fixation, and the use of a semitendinosus graft. The CC screw and suture fixation methods are associated with a risk of fracture of the clavicle or coracoid process [10]. Pin migration is a potential complication with AC pin fixation, and donor site morbidity is a concern with the semitendinosus graft [11, 12].

We describe a new technique that uses a fiber tape. This novel study employs a special fiber tape knot for fixation and prospectively analyzes the fixation of Type III–VI ACJ injuries and lateral end clavicle fractures. As far as we are aware, this surgery is not frequently performed.

The study **aims** to investigate the long-term outcomes and functional improvements achieved through the use of this special knot with a fiber tape for the fixation of Type III–VI ACJ injuries at three-month and six-month follow-ups, using the UCLA shoulder scoring system. Analyzing the efficacy of this technique prospectively offers important insights into its potential as a cutting-edge method in orthopedic surgery. Furthermore, by enhancing surgical methods and rehabilitation regimens for patients with lateral end clavicle fractures and ACJ injuries, this study may improve the patient's overall recovery and quality of life.

MATERIALS AND METHODS

This is a prospective outcome study carried out at the department of orthopaedics of a tertiary care center from January 2020 to December 2023, after the approval of the institutional ethics committee. All patients between 18 and 60 years of age, presenting with acute AC dislocation (Rockwood type III–VI, within two weeks of injury) and lateral end clavicle fractures, were included in the study. Patients with chronic AC dislocation (more than two weeks), polytrauma, open fractures, or fractures of the coracoid process, acromion, scapula, or proximal humerus, as well as those with type I, type II, or type III AC dislocations as per the Rockwood classification, critically ill patients, or patients unfit for anesthesia, and patients under 18 years or over 60 years of age, were excluded from the study. Based on the inclusion criteria patients were enrolled in this study and their informed consent was taken. All data were documented in the study proforma. The UCLA shoulder score is used to evaluate functional outcomes at three and six months [13, 14].

Our study group involved 28 patients who underwent anatomical reconstruction for AC joint injury. The mean (SD) of age (years) of our study group ranging from 20 to 50 years was 36.50 (9.86). The majority 26 (93 %) of the participants in the group were males. The two most typical injury mechanisms were road traffic accident 14 (50 %) and fall from stairs 9 (32 %, respectively). Twenty-one (75.0 %) participants in the group had Rockwood classification type III while seven patients (25.0 %) in the group had Rockwood classification type V.

Surgical Technique

All acute Rockwood III–VI ACJ separations and lateral end clavicle fractures were considered for reconstruction. The patients were given either regional or general anesthesia, depending on the ASA grade or the anesthetist's preference. Preoperative broad-spectrum antibiotics were administered. A beach chair position was given, and scrubbing, painting, draping, and marking done (Fig. 1). Approximately five centimeters in length, a vertical skin incision was made from the clavicle lateral end to the coracoid process tip and the coracoid process was identified (Fig. 2). From 4 cm of the lateral end of the clavicle, a 4-mm tunnel was drilled. The loop end of the fiber tape was passed from medial to lateral with a passer so the loop end is on the lateral side and the free end is on the medial side of the coracoid (Fig. 3). The looped end was passed through the drill hole at the lateral end of the clavicle and brought anteriorly (Fig. 4). The free ends of the fiber tape were then passed through the loop and tied under tension with a special knot. A diagrammatic representation of this technique is shown in Figures 1–9.

Fig. 1 Landmark and marking

Fig. 2 Identification of coracoid process (CP)

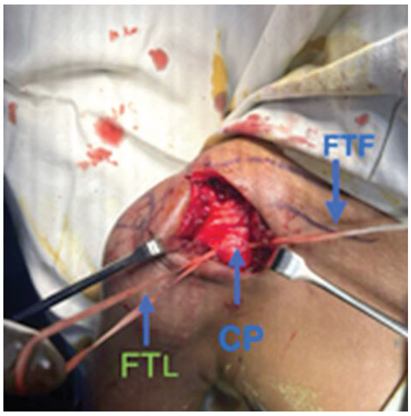

Fig. 3 Passing the fiber tape (FTL — a loop end and FTF — a free end)

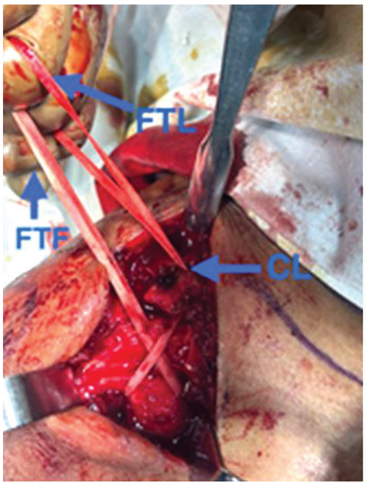

Fig. 4 Passing the loop end (FTL) from the clavicle (CL)

Fig. 5 Making a knot with the loop end

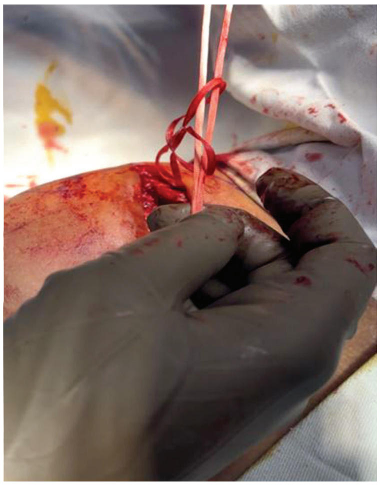

Fig. 6 Passing the free end through a knot in loop end

Fig. 7 Pulling the free end through a knot in loop end

Fig. 8 Pre-op X-ray

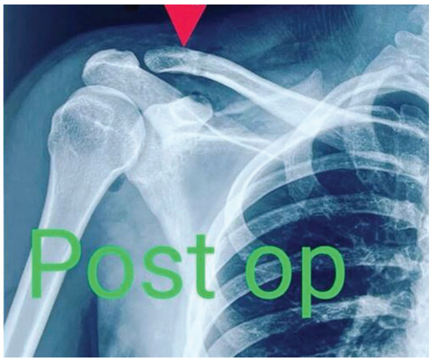

Fig. 9 Post-op X-ray

Postoperative rehabilitation began the following day. During follow-up visits, patients were evaluated for functional outcomes using the UCLA shoulder score at three and six months.

Statistical analysis of the data was performed using SPSS software, version 22. The Wilcoxon test was conducted to calculate the *p*-value, with a *p*-value of < 0.05 considered statistically significant.

RESULTS

The mean (SD) UCLA score increased from 29.20 (1.68) (range 30–35) at three months to a maximum of 35.00 at the six-month review. The improvement in the UCLA score at six months was statistically significant (Wilcoxon test: $V = 0.0$, $P = 0.001$). Radiological evaluation confirmed 100 % reduction and congruence among the participants.

Most of the group participants (96.5 %) had no complications. Only one patient (3.5 %) showed deep vein thrombosis (DVT). No participants in the group had surgical site infections.

DISCUSSION

Rockwood type III–VI AC joint dislocations require surgical intervention to restore shoulder girdle function. Clinically, these dislocations may present with bruising, swelling, and skin tenting. X-rays of the affected shoulder help in determining the type of AC joint dislocation. Several treatment options have been described for managing AC joint dislocations, including various implants and fixation methods, such as Bosworth screws, wires, locking plates, and hook plates. Unfortunately, these methods often lead to hardware-related complications, necessitating implant removal and procedure-specific issues.

Lin et al. [15] conducted a USG study showing that hook plates may cause subacromial shoulder impingement and rotator cuff lesions. Other issues include hardware prominence and the need for a second surgery to remove the implant. Kirchhoff et al. [16] found that the Weaver–Dunn procedure, along with its modifications, is associated with high rates of re-dislocation and coracoid fractures. This may be because the transferred ligaments are weaker than native coracoclavicular (CC) ligaments and cannot replicate their natural anatomy, as demonstrated by Galasso et al. [17]. AC joint pin fixation is also associated with complications such as pin breakage and migration, which can injure vital structures, including the brachial plexus, as reported by Ma et al. [18].

The use of a semitendinosus graft is associated with donor site morbidity, and no study has shown that biological fixation is superior to the use of fiber tapes. As a result, autogenic, allogenic, and synthetic grafts have been developed to anatomically restore the CC ligaments, leading to improved structural and functional outcomes and reduced complications. This study aims to reconstruct the CC ligaments in both AC joint dislocations and lateral end clavicle fractures using a fiber tape with a special knot in Rockwood type III–VI AC joint dislocations.

In our study, most patients were 20–50 years old. The highest incidence of injury was observed in the male population (93 %). High-grade injuries were primarily caused by road traffic accidents (50 %), followed by falls from stairs (32 %) and slip-and-fall incidents (18 %). Seventy-five percent of the cases reported were type III, while the remaining cases were type V dislocations. Similar demographic findings were reported by Chillemi et al. [19], who found that 50 % of dislocations occurred in the 20–40 year age group. The incidence was 1.8 per 10,000 people per year in their study, with a male-to-female ratio of 8.5:1 and sports injuries as the most prevalent mechanism. Sports injuries were the most common traumatic mechanism, and Rockwood type III dislocations were the most common. Our results are also consistent with those of Nordin et al. [20], who reported the incidence of ACJ dislocation to be two per 10,000 persons annually, with a male preponderance in the younger age group. They also found good clinical and radiological outcomes, along with a low failure rate at follow-ups.

We used a fiber tape for the reconstruction of the coracoclavicular ligament (CCL) in both AC joint dislocations and lateral end clavicle fractures. The loop end of the fiber tape is passed below the coracoid process from medial to lateral, and a 4 mm drill hole is created 4 cm medial to the AC joint. The loop end is then passed through this hole, and a knot is used to reconstruct the CCL ligament. We regularly followed up our patients, evaluating their UCLA scores and X-rays at three and six months. Guzman et al. [21] used fiber tape for AC joint repair with the suture cerclage tension system in 16 patients, considering it a viable and cost-effective technique for restoring vertical and horizontal stability. The effectiveness of fiber tape in AC joint dislocation was demonstrated by Vrgoč et al. [22], who showed that fiber tape offers a shorter recovery period and a significantly more cost-effective outcome in their study on 16 patients. Tully et al. [23] used fiber tape augmentation with semitendinous allograft in the management of AC joint dislocations. Solanki et al. [24] used fiber tape in 2020 for the treatment of lateral end clavicle fractures, showing a 100 % union rate and excellent clinical outcomes with minimal complications.

We used the UCLA scoring system to assess functional outcomes in operated patients at three and six months postoperatively. We observed an improvement in the UCLA average score from 33.10 at three months to 35 at six months, which is considered an excellent score. This improvement in the UCLA score was statistically significant (p-value = 0.001). Joukainen et al. [25] used the UCLA scoring system to evaluate functional outcomes in the treatment of AC joint dislocation. Similarly, Wang et al. [14] used the UCLA scoring system to assess functional outcomes, including clinical and radiological recovery, following coracoclavicular and acromioclavicular ligament reconstruction using an allogenic tendon graft. Their study reported excellent outcomes for acute AC dislocation.

In our study, the radiological evaluation during follow-up confirmed 100 % reduction and convergence at six months. No donor site morbidity was reported. However, DVT was observed in one patient that was managed conservatively.

The advantages of this technique include short surgery time, small incisions, fast recovery, cost-effectiveness, and ease of reproducibility. It is also easy to tie the knot without assistance, and the knot automatically tightens. Additionally, the deforming forces from the trapezius muscle contribute to further tightening of the knot, preventing upward displacement of the clavicle.

The limitations of this study include its non-comparative design and a small sample size. Therefore, more extensive, multicenter, and comparative studies are needed to draw definitive conclusions.

CONCLUSION

Surgical fixation of Rockwood type III–VI AC joint dislocations and lateral end clavicle fractures with using a special fiber tape knot is a viable option with excellent outcomes. Overall, this surgical technique is cost-effective for the treatment of both AC joint dislocation and lateral end clavicle fractures.

Conflicts interests *There are no conflicts of interest.*

Funding *None.*

Ethics approval and consent to participate *Ethics committee approval was taken from institutional ethics board.*

Consent for publication *Consent was taken from all the participants.*

Availability of data and materials *The datasets used in and/or analyzed in the current study are available from the corresponding author upon reasonable request.*

REFERENCES

1. Velasquez Garcia, A., Salamé Castillo, F., Ekdahl Giordani, M. et al. Anteroinferior bundle of the acromioclavicular ligament plays a substantial role in the joint function during shoulder elevation and horizontal adduction: a finite element model. *J Orthop Surg Res*. 2022;17(1):73. doi: 10.1186/s13018-022-02966-0.
2. Berthold DP, Muench LN, Dyrna F, et al. Current concepts in acromioclavicular joint (AC) instability - a proposed treatment algorithm for acute and chronic AC-joint surgery. *BMC Musculoskelet Disord*. 2022;23(1):1078. doi: 10.1186/s12891-022-05935-0.
3. de Groot C, Verstift DE, Heisen J, et al. Management of Acromioclavicular Injuries - Current Concepts. *Orthop Res Rev*. 2023;15:1-12. doi: 10.2147/ORR.S340531.
4. Gorbaty JD, Hsu JE, Gee AO. Classifications in Brief: Rockwood Classification of Acromioclavicular Joint Separations. *Clin Orthop Relat Res*. 2017;475(1):283-287. doi: 10.1007/s11999-016-5079-6.
5. Martetschläger F, Kraus N, Scheibel M, et al. The Diagnosis and Treatment of Acute Dislocation of the Acromioclavicular Joint. *Dtsch Arztebl Int*. 2019;116(6):89-95. doi: 10.3238/arztebl.2019.0089.
6. Karuppaiah K, Bilal A, Colegate-Stone T, et al. Outcome following management of unstable lateral end clavicle fractures with locking plate and coracoid anchor augmentation. *Shoulder Elbow*. 2022;14(2):181-188. doi: 10.1177/1758573220981708.
7. Sarda P. Lateral Clavicle Fractures with Coracoclavicular Ligament Disruption (Neer's Type IIB): Review of Literature and a New Technique for All-Suture Fixation. *Indian J Orthop*. 2019;53(3):465-471. doi: 10.4103/ortho.IJOrtho_485_18.
8. Lindborg CM, Smith RD, Reihl AM, et al. Current Concepts in Management of Acromioclavicular Joint Injury. *J Clin Med*. 2024;13(5):1413. doi: 10.3390/jcm13051413.
9. Shaty W. The Results of Hook Plate Fixation in Acute Acromioclavicular Joint Dislocation and Distal Clavicle Fractures. *Orthop Rev (Pavia)*. 2024;16:120306. doi: 10.52965/001c.120306.
10. Ahmed AF, Salameh M, Kayali H, et al. Open reduction and tunneled suspensory fixation for lateral end of clavicle fractures: surgical technique. *JSES Rev Rep Tech*. 2022;2(3):345-349. doi: 10.1016/j.xrrt.2022.02.010.
11. Ulusoy A, Turgut N, Cilli F, Unal AM. Reconstruction of Coracoclavicular Ligaments with Semitendinosus Autograft and Temporary Kirschner Wires is a good option for Chronic Acromioclavicular Joint Instability. *Malays Orthop J*. 2024;18(1):99-105. doi: 10.5704/MOJ.2403.013.
12. Tomlinson DP, Altchek DW, Davila J, Cordasco FA. A modified technique of arthroscopically assisted AC joint reconstruction and preliminary results. *Clin Orthop Relat Res*. 2008;466(3):639-645. doi: 10.1007/s11999-007-0085-3.
13. Nolte PC, Lacheta L, Dekker TJ, Elrick BP, Millett PJ. Optimal Management of Acromioclavicular Dislocation: Current Perspectives. *Orthop Res Rev*. 2020;12:27-44. doi: 10.2147/ORR.S218991.
14. Wang G, Xie R, Mao T, Xing S. Treatment of AC dislocation by reconstructing CC and AC ligaments with allogenic tendons compared with hook plates. *J Orthop Surg Res*. 2018;13(1):175. doi: 10.1186/s13018-018-0879-x.
15. Lin HY, Wong PK, Ho WP, et al. Clavicular hook plate may induce subacromial shoulder impingement and rotator cuff lesion--dynamic sonographic evaluation. *J Orthop Surg Res*. 2014;9:6. doi: 10.1186/1749-799X-9-6.
16. Kirchhoff C, Braunstein V, Buhmann S, et al. A salvage procedure for failed weaver-dunn reconstruction. *Oper Orthop Traumatol*. 2008;20(2):176-181. doi: 10.1007/s00064-008-1240-z.
17. Galasso O, Tarducci L, De Benedetto M, et al. Modified Weaver-Dunn Procedure for Type 3 Acromioclavicular Joint Dislocation: Functional and Radiological Outcomes. *Orthop J Sports Med*. 2020;8(3):2325967120905022. doi: 10.1177/2325967120905022.
18. Ma R, Smith PA, Smith MJ, et al. Managing and recognizing complications after treatment of acromioclavicular joint repair or reconstruction. *Curr Rev Musculoskelet Med*. 2015;8(1):75-82. doi: 10.1007/s12178-014-9255-6.
19. Chillemi C, Franceschini V, Dei Giudici L, et al. Epidemiology of isolated acromioclavicular joint dislocation. *Emerg Med Int*. 2013;2013:171609. doi: 10.1155/2013/171609.
20. Nordin JS, Olsson O, Lunsjö K. Acromioclavicular joint dislocations: incidence, injury profile, and patient characteristics from a prospective case series. *JSES Int*. 2020;4(2):246-250. doi: 10.1016/j.jseint.2020.01.009.
21. Guzman AJ, Rayos Del Sol S, Dela Rueda T, et al. Open Acromioclavicular Repair With a Suture Cerclage Tensioning System: A Case Series. *Cureus*. 2023;15(1):e34018. doi: 10.7759/cureus.34018.
22. Vrgoč G, Japjec M, Jurina P, et al. Operative treatment of acute acromioclavicular dislocations Rockwood III and V-Comparative study between K-wires combined with FiberTape(®) vs. TightRope System(®). *Injury*. 2015;46 Suppl 6:S107-12. doi: 10.1016/j.injury.2015.10.053.
23. Tully NW, Glover MA, van der List JP, et al. Open Acromioclavicular Joint Reconstruction via Cerclage With Semitendinosus Allograft. *Video J Sports Med*. 2024;4(4):26350254241235673. doi: 10.1177/26350254241235673.

24. Solanki KP, Soundarapandian RS, Manoharan S. A novel surgical technique for arthroscopic fixation of lateral end clavicle fracture using FiberWire and FiberTape. *J Arthrosc Surg Sports Med*. 2020;1(2):199-206. doi: 10.25259/JASSM_27_2020.
25. Joukainen A, Kröger H, Niemitukia L, et al. Results of Operative and Nonoperative Treatment of Rockwood Types III and V Acromioclavicular Joint Dislocation: A Prospective, Randomized Trial With an 18- to 20-Year Follow-up. *Orthop J Sports Med*. 2014;2(12):2325967114560130. doi: 10.1177/2325967114560130.

The article was submitted 13.05.2025; approved after reviewing 02.06.2025; accepted for publication 14.10.2025.

Information about the authors:

Mahesh B. Shinde — Dr., Senior resident, Department of Orthopaedics, mahesh.shinde.1466@gmail.com;

Mihir R. Patel — Dr., Assistant Professor, Department of Orthopaedics, mrpatel1981@gmail.com;

Bibhas DasGupta — Dr., Head and Professor, Department of Orthopaedics, Email- bibhasdasgupta@gmail.com;

Atharva Sharma — Dr., Senior Resident, Department of Orthopaedics, atharva.rs1996@gmail.com;

Kshitij Sarwey — Dr., Junior resident, Department of Orthopaedics, kshitijsarwey@gmail.com;

Sanket Jethliya — Dr., Junior resident, Department of Orthopaedics, sanketjethliya1@gmail.com;

Riddhi Jain — Medical student, Department of Orthopaedics, ridhij161@gmail.com;

Deep Kedia — Medical student, Department of Orthopaedics, deepkedia19@gmail.com;

Samreen Chunawala — Medical student, Department of Orthopaedics, samreenchunawala2003@gmail.com;

Chhavi Kowe — Medical student, Department of Orthopaedics, chhavikowe@gmail.com;

Shreyasi Chiwadshetti — Medical student, Department of Orthopaedics, chiwadshetti.s@gmail.com;

Yash Nav Singh — Medical student, Department of Orthopaedics, yash131200@gmail.com.

Contribution of the authors:

All authors have made substantial contributions to the conception, design of the work, the acquisition, analysis, and interpretation of data, the creation of new software used in the work, drafted the work, or substantively revised it.

All authors have approved the submitted version (and any substantially modified version that involves the author's contribution to the study) and agreed both to be personally accountable for the author's contributions and to ensure that questions related to the accuracy or integrity of any part of the work, even ones in which the author was not personally involved, are appropriately investigated, resolved, and the resolution documented in the literature.

Original article
https://doi.org/10.18019/1028-4427-2025-31-6-805-812

Automated 24-hour control of distraction forces: a new technology for limb lengthening

A.V. Popkov, N.A. Gorodtsov✉, P.P. Buravtsov

Ilizarov National Medical Research Centre for Traumatology and Orthopedics, Kurgan, Russian Federation

Corresponding author: Nikolai A. Gorodtsov, gorodcov17@gmail.com

Abstract

Introduction The classic Ilizarov technology of transosseous distraction osteosynthesis provides rigid fixation, accurate bone control in frontal and sagittal planes addressing all types of deformities and the limb length. Long-term Ilizarov fixation can be associated with adverse events and distraction forces are to be monitored. A new technology for limb lengthening using automated 24-hour control of distraction force facilitates optimal rate of deformity correction and can reduce Ilizarov fixation when combined with intramedullary titanium pins with a bioactive coating.

The **objective** was to demonstrate continuous distraction force control technology in the correction of varus deformity of the tibia and anatomical lengthening.

Material and methods Simultaneous tibial lengthening and correction of tibial deformity was produced with a new automated distractor (patent RU No. 2763644) measuring forces of the external fixation device every time with the gearbox switching on.

Results and discussion Continuous distraction force control was well illustrated in an Ilizarov patient treated with combined distraction osteosynthesis. The use of the device was associated with a shorter bone consolidation time (IO = 15 days/cm) after sequential distraction osteosynthesis with genu varum eliminated and the bone lengthened.

Conclusion Dynamic distraction force control with a new automated device allowed for monitoring the lengthening process, identifying potential complications, adjusting the distraction rate, reducing osteosynthesis time by two to four times.

Keywords: limb lengthening, tibial deformity, Ilizarov apparatus, transosseous automated distraction apparatus

For citation: Popkov AV, Gorodtsov NA, Buravtsov PP. Automated 24-hour control of distraction forces: a new technology for limb lengthening. *Genij Ortopedii*. 2025;31(6):805-812. doi: 10.18019/1028-4427-2025-31-6-805-812.

INTRODUCTION

It is generally recognized that a reliable solution to the problem of limb deformity correction and segment lengthening was found with the Ilizarov apparatus developed in the mid-20th century, which remains the primary tool in the hands of experienced orthopedic and trauma surgeons. Since first publication, significant changes have occurred in the external fixatrion device and in surgical techniques. The fixation unit (the shape and material of the supports with connecting elements, the protective coating with anti-inflammatory and bioactive elements), the transport and angular correction units (rods, hinges, long connection plates) have been improving with the invasiveness of surgical interventions decreasing [1–13]. By improving the limb lengthening process, orthopedic surgeons from different countries approached the need to automate the process, which resulted in automatic transport units developed for external fixation devices with a fixed [14–16] first, and then adjustable lengthening rate [17]. The innovation allowed for deformity correction and limb lengthening to be produced simultaneously [13, 18]. The intention to identify a reliable optimal operating rate for the units led to the creation of autodistractors capable of measuring distraction forces to control the process of reparative osteogenesis [19].

The **objective** was to demonstrate continuous distraction force control technology in the correction of genu varum and anatomical lengthening.

MATERIAL AND METHODS

The Ilizarov external fixation device with three automatic distractors has been used for distraction osteosynthesis and was patented as the transosseous automated distraction apparatus (RU patent no. 2763644 C1 “Transosseous automated distraction apparatus and automated transportation unit”, manufactured by the Kurganpribor plant, Fig. 1) [20]. The frame can provide gradual, round-the-clock operation of the transportation units.

The software controls the process of almost unlimited limb lengthening from 0.15 mm/day with 0.025 mm increments with each motor activation, and receives data on distraction times, lengthening rate, distraction forces applied to each rod of the external fixation device, and dynamics of the total distraction forces with the frame over the required period of time (forces are measured with each motor activation).

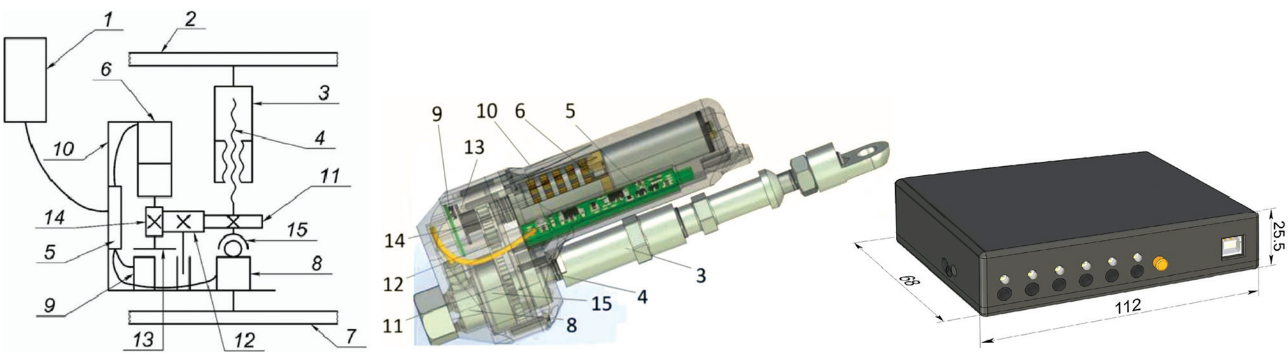

Fig. 1 Diagrams and photoes of the transosseous automated distraction device and automatic transportation unit [20]

The transosseous automated distraction device comprises supports connected by automated transportation units, each incorporating a housing, a geared motor electrically connected to a controller, and a lead screw with a nut. The automatic transport unit is configured with a gear transmission connecting the lead screw and the geared motor. The lead screw nut is made of a cold-flowing, antifriction fluoropolymer and installed with end-on tightening. Mounted within the housing is a sector disk secured to one of the gears of the gear transmission and the rotation sensor, electrically connected to the controller. The controller is located within the housing of the automatic transportation unit. A longitudinal force sensor is installed at the lead screw attachment point and electrically connected to the controller. Gradual transport of the rings of the external fixation device is achieved by reducing the apparatus's weight and dimensions providing feedback in the form of monitoring the forces at the lead screw attachment point [20].

Clinical observation methods are represented by radiological monitoring of reparative bone regeneration using the Shimadzu Sonialvision 4 system (Japan).

A titanium implant of two hydroxyapatite-coated wires, 15 cm long and 1.8 mm in diameter, was placed intramedullary into the tibia to stimulate bone formation. The implant was coated at the Tomsk Polytechnic University using the MAO (microarc oxidation) technology [21]. Hydroxyapatite (Fluidinova, Portugal) was used as a component for the production of composite materials.

A *clinical example* demonstrates correction of genu varum in a 65-year-old patient diagnosed with congenital varus deformity of the tibiae of 20°, stage 2 gonarthrosis. The procedure was performed using transosseous distraction osteosynthesis with the Ilizarov external fixator in automatic mode. The patient suggested that the deformities (Fig. 2a) had been present since birth and had dreamed of correcting them his entire adult life. The patient developed moderate pain in his knee joints in the last 2–3 years. His physically active lifestyle as a military service member allowed him to run, swim and hike regularly. The surgery performed 09.07.24 included subcondylar partial corticotomy of the left tibia, combined osteosynthesis of the tibia with the Ilizarov apparatus.

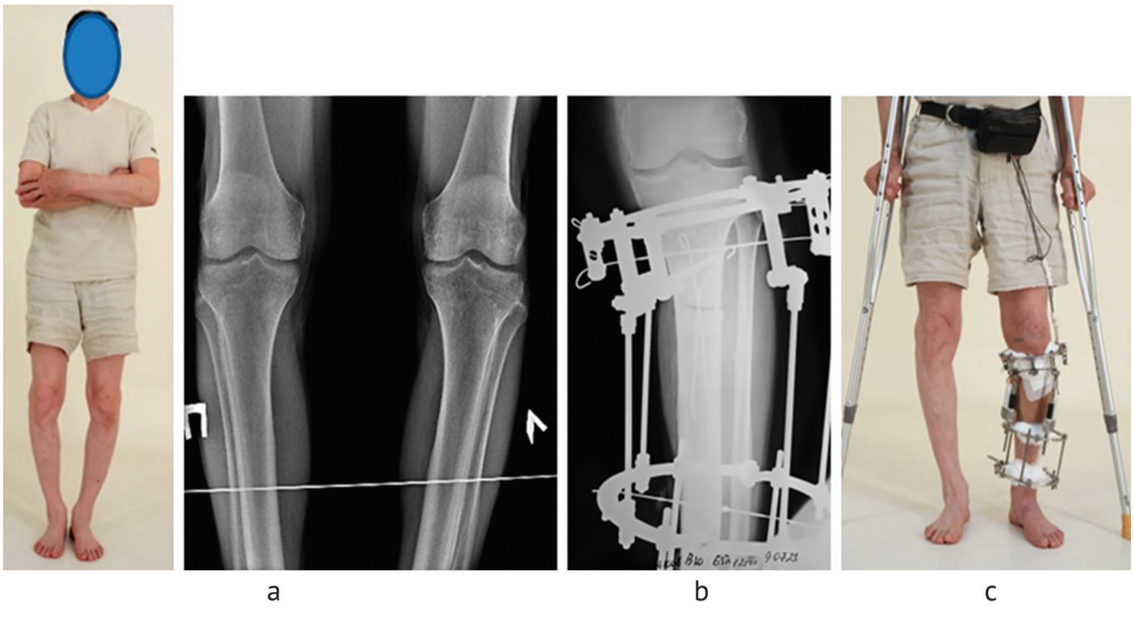

Fig. 2 Photograph and radiographs of the patient before treatment (a); postoperative radiograph of the left tibia (b); photo of the patient during automated lengthening of the tibial bones and simultaneous correction of the deformity (c)

The surgery started with the intramedullary insertion of a bioactive hydroxyapatite (HA)-coated implant. Using a 5-mm-diameter burr, oblique holes (one each on the lateral and medial aspects of the bone) communicating with the medullary canal were created in the cortex of the proximal metaphysis of the bone to be lengthened through pre-existing soft tissue punctures. Two bioactive HA-coated pins were inserted through the holes. With the pin entered the canal to the specified depth, the excessive length of the pin was cut off, the end bent and inserted under the fascia of the limb segment [22].

With implant inserted, the soft tissues were sutured tightly, and transosseous osteosynthesis of the tibia was performed using the Ilizarov external fixator and a standard technique that allowed for simultaneous tibia lengthening and deformity correction. At the final stage of the surgery, a narrow, 6 mm-wide chisel was used to perform a partial corticotomy at the apex of the tibial deformity, ensuring maximum bone preservation at the lateral aspect. The wounds were sutured tightly, aseptic dressings applied, a control radiograph produced and the frame systems stabilized (Fig. 2b). Fibula was osteotomized in the lower third.

RESULT

The deformity was gradually corrected postoperatively under the constant control of the distraction forces of the Ilizarov frame. Three automated distractors were placed postoperatively (the leading distractor locating along the medial aspect of the tibia, two supporting distractors being along the anterior-lateral and postero-lateral aspects of the tibia) in such a way that the hinges were projected at the level of the continuated bisector of the genu varum angle [23]. Distraction was performed at a rate of 1 mm/day along the leading rod (0.025 mm in 40 increments per day) following a seven-day latency. The patient was encouraged to walk with crutches bearing weight on the operated leg (Fig. 2c). Dynamic, rapid increase in the distraction forces to 200N allowed the doctor to increase the distraction rate to 3 mm/day after two days (Fig. 3); the level of distraction forces continued to gradually increase over the course of a week.

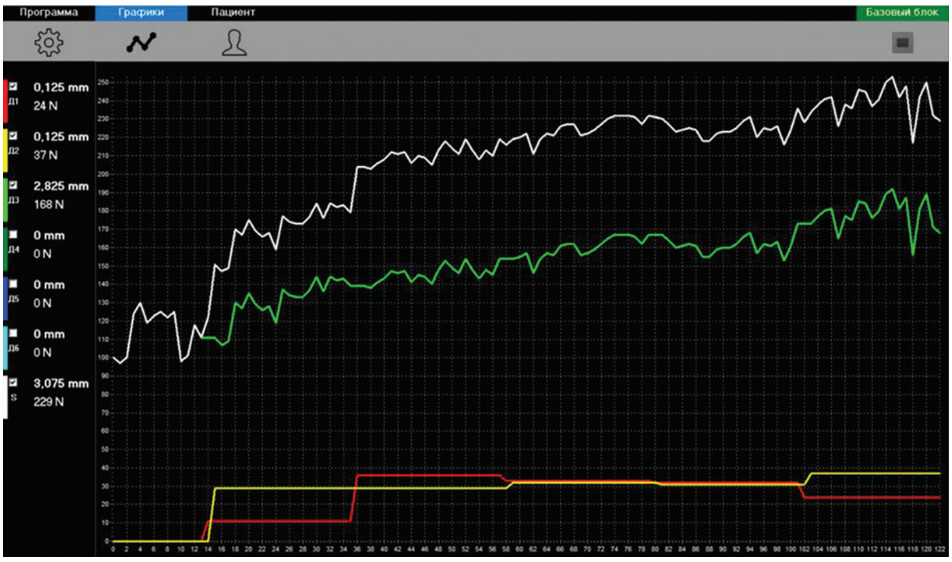

Fig. 3 Dynamics of distraction forces in the first six days of lengthening: the green graph showing dynamics in the forces with the leading autodistractor, the red and yellow colors demonstrating dynamics of the forces with the supporting rods of the frame, the white graph reflecting dynamics with the total force exerted by the Ilizarov external fixator

The continued dynamic increase in distraction forces indicated the preservation of the direct connection between the bone fragments due to the periosteum at the lateral aspect. A clicking sound the patient heard after 7-day distraction (July 22, 2024) with the functioning distractor was accompanied by moderate pain. The attending physician reported no Ilizarov maladjustments. Measured distraction forces suggested they dropped sharply to 20 N after reaching 290 N indicating disruption in the bone (Fig. 4).

Based on accurate clinical, radiographic and biomechanical data, distraction was discontinued for two days and restarted at a rate of 1 mm/day with daily monitoring of distraction forces. Subsequent dynamic monitoring revealed a gradual increase in distraction forces to 190 N. Concurrent clinical monitoring indicated gradually completed correction of genu varum and distraction was discontinued on July 31, 2024 with the intended objective achieved (Fig. 5).

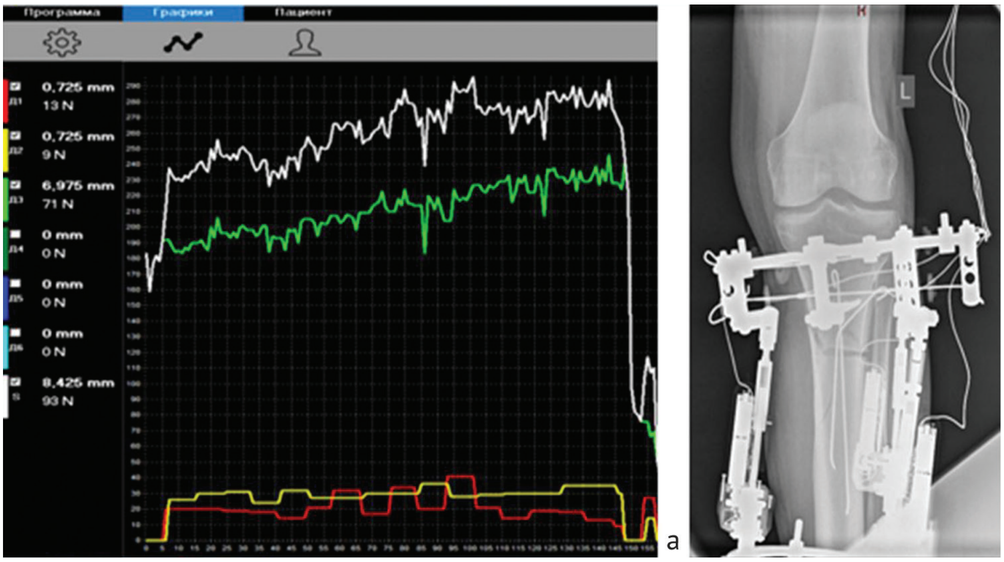

a b

Fig. 4 Dynamics of distraction forces with a sharp drop in the resistance level (a); control radiograph of the left tibia on the day of the disruptive event in the distraction forces (b)

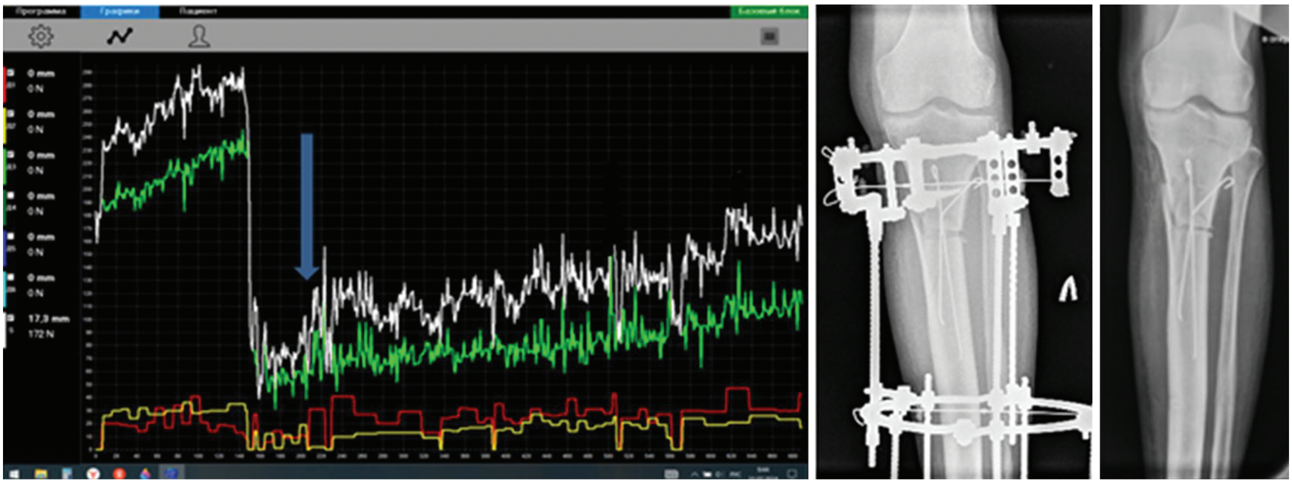

a b c

Fig. 5 Dynamics of distraction forces recorded on 31.07.24: the arrow indicates the re-start of lengthening along the leading rod (a); control radiograph of the left tibia on the day of accomplished distraction period (b) and on the day the external fixation device was removed (c)

Two weeks later, the Ilizarov apparatus was removed following a clinical consolidation test. The overall osteosynthesis index (OSI) was 15 days/cm (Fig. 5c). The functional length of the left limb exceeded that of the right limb by 4 cm after correction of the deformity; there was no swelling, and skin sensitivity was preserved. Range of motion in the ankle joint was unlimited, and measured within 120° in the knee joint. A clinical consolidation test revealed no mobility in the distraction regenerate site and the patient could gradually increase weight-bearing while walking and consider another surgery to correct genu varum on the right.

The surgical technique used on the right tibia was identical to that used on the left tibia (Fig. 6a). Distraction using the leading distraction rod was initiated at a seven-day latency. The dynamics of distraction forces reflected a gradual increase in the resistance of the elongated tissues from 10 to 200 N suggesting the bone integrity (Fig. 6a). A radiograph of the tibia bones demonstrated relatively rapid bone consolidation after deformity correction (Fig. 6b). The Ilizarov fixation of the right tibia lasted 21 days, which generally corresponded to the osteosynthesis index of 22 days/cm.

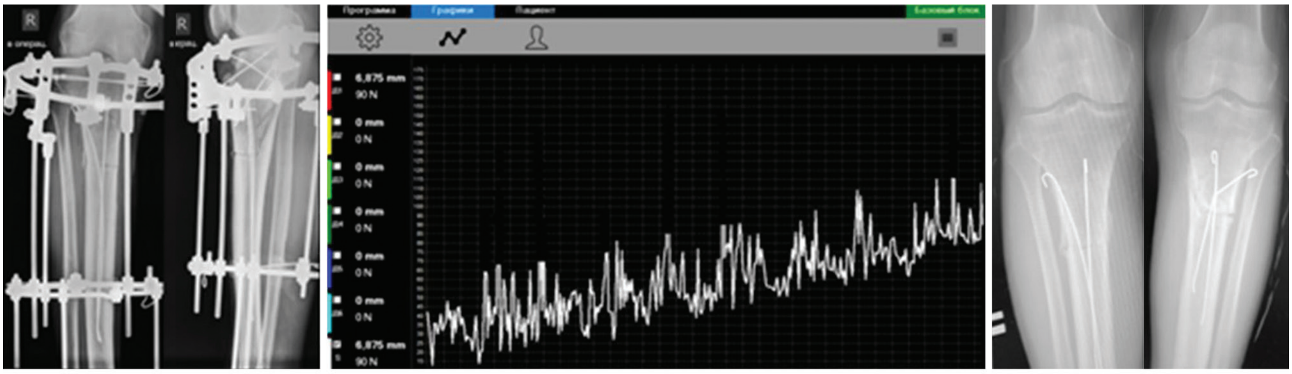

a b c

Fig. 6 Radiographs of the right tibia on the day of surgery (a), dynamics of distraction forces during correction of genu varum on the right side (b), radiographs of both tibiae after the treatment completed (c)

One month after removal of the external fixator, the patient could walk with full weight-bearing using no additional supporting devices with his limb length being equal. His range of motion in the knee joint measured 120° with the limb alignment being satisfactory for the patient.

Therefore, the autodistractor with force control used in combination with intramedullary implants coated with hydroxyapatite can provide optimal conditions for distraction regeneration, and increased bone formation activity is manifested in the formation of a distraction regenerate bone, accompanied by a pronounced periosteal reaction and increased cross-sectional area of the bone.

DISCUSSION

The new transosseous automated distraction device [20], unlike other autodistractors, is capable of controlling distraction forces. Data is collected on a control unit. The data are transmitted to a dedicated computer application [19], which analyzes the distraction force data and sets the distraction rate. The new technology allows for the correction of segmental deformities and restoration of the required limb length maximizing the potential for reparative osteogenesis. The new device provides monitoring of the dynamics of distraction forces to facilitate identification of incomplete bone osteotomy, premature bone consolidation, regenerate ossification and regenerate rupture. There is a considerable difference between the new distraction device assisting early detection of adverse events and the autodistractor developed by Shevtsov, Burlakov and Nemkov [24, 25] and have long been used in clinical practice.

We have previously shown that automatic high-fraction distraction can provide optimal conditions for reparative osteogenesis, and endosseous implants with a hydroxyapatite coating additionally stimulate the process and allow an increase in the distraction rate to 3 mm/day [26]. The overall duration of osteosynthesis is significantly reduced: IO = 2–3 days/cm during lengthening of the tibia in large experimental animals and IO = 15 days/cm in clinical settings.

CONCLUSION

Dynamic control of distraction forces with the new automated distractor allows for monitoring the lengthening process and promptly diagnosing potential complications, adjusting the distraction rate to the ptimal level and reducing osteosynthesis time by two to four times compared to international literature data. The use of the new automated distractor helps reduce the incidence of complications associated with prolonged limb fixation using the Ilizarov external fixation device.

Conflict of interest *None of the authors has any potential conflict of interest.*

Funding *The work was carried out as part of the Governmental Project 1022041100465-8-3.2.10 "Structured titanium implants with controlled biological properties".*

Protocol of the Ethics Committee *No. 1(76) dated November 29, 2024.*

The patient's consent for publication of the findings was obtained and recorded in the patient's medical history.

REFERENCES

1. Feichtinger X, Kocijan R, Mittermayr R, et al. Fracture patterns in patients with multiple fractures: the probability of multiple fractures and the most frequently associated regions. *Eur J Trauma Emerg Surg*. 2020;46(5):1151-1158. doi: 10.1007/s00068-019-01087-4.
2. Shevtsov VI, Popkov AV. Distraction-Compression Osteosynthesis in Limb Elongation with the Ilizarov Apparatus. *Traumatology and Orthopedics of Russia*. 1995;(1):35-37. (In Russ.)
3. Dinah AF. Predicting duration of Ilizarov frame treatment for tibial lengthening. *Bone*. 2004;34(5):845-8. doi: 10.1016/j.bone.2004.01.026.
4. Kononovich NA, Popkov AV, Gorbach EN, Popkov DA. The effect of nanostructured hydroxyapatite coating on distraction osteogenesis. *Key Engineering Materials*. 2020;(854):216-222. doi: 10.4028/www.scientific.net/KEM.854.216.
5. Popkov AV, Gorbach ES, Mamedov UF, Stepanov RV. Tibial lengthening over a bioactive degradable intramedullary implant: a case report. *Genij Ortopedii*. 2023;29(6):645-649. doi: 10.18019/1028-4427-2023-29-6-645-649.
6. Stoddart JC, Dandridge O, Garner A, et al. The compartmental distribution of knee osteoarthritis - a systematic review and meta-analysis. *Osteoarthritis Cartilage*. 2021;29(4):445-455. doi: 10.1016/j.joca.2020.10.011.
7. Ogino T, Kumagai K, Yamada S, et al. Relationship between the bony correction angle and mechanical axis change and their differences between closed and open wedge high tibial osteotomy. *BMC Musculoskelet Disord*. 2020;21(1):675. doi: 10.1186/s12891-020-03703-6.
8. Kim JI, Kim BH, Han HS, Lee MC. Rotational Changes in the Tibia After High Tibial Valgus Osteotomy: A Comparative Study of Lateral Closing Versus Medial Opening Wedge Osteotomy. *Am J Sports Med*. 2020;48(14):3549-3556. doi: 10.1177/0363546520960114.
9. Schubert I, Ferner F, Dickschas J. The effect of open-wedge and closed-wedge high tibial osteotomies on the tibial posterior slope-a study of two hundred seventy-nine cases. *Int Orthop*. 2020;44(6):1077-1082. doi: 10.1007/s00264-020-04499-9.
10. Ji S, Gao Y, Zhang J, et al. High tibial lateral closing wedge and opening wedge valgus osteotomy produce different effects on posterior tibial slope and patellar height. *Front Surg*. 2023;10:1219614. doi: 10.3389/fsurg.2023.1219614.
11. Artemiev AA, Ivashkin AN, Kashoob AM, et al. Features of surgical treatment of posttraumatic lower limbs of different lengths in adult patients. *Russian Sklifosovsky Journal Emergency Medical Care*. 2020;9(4):573-579. doi: 10.23934/2223-9022-2020-9-4-573-579.
12. Feichtinger X, Kocijan R, Mittermayr R, et al. Fracture patterns in patients with multiple fractures: the probability of multiple fractures and the most frequently associated regions. *Eur J Trauma Emerg Surg*. 2020;46(5):1151-1158. doi: 10.1007/s00068-019-01087-4.
13. Shchepkina EA, Solomin LN, Sauta OI, Sabirov FK. Substantiation for the use of orthopedic hexapod for the femur lengthening over the nail. *Department of Traumatology and Orthopedics*. 2021;(3):27-36. (In Russ.) doi: 10.17238/issn2226-2016.2021.3.27-36.
14. Ilizarov GA, Predein AP, Bykov VM. *Automatic compression-distraction apparatus*. Patent US, no. 4,615,338. 1986. Available at: https://patentimages.storage.googleapis.com/df/60/66/d910996b4d41c8/US4615338.pdf. Accessed Oct 27, 2025.
15. Pursley JA, Holloway JM, Wakefield TL. *Automatic compression-distraction-torsion method and apparatus*. Patent US no. 4,973,331. 1990. Available at: https://patentimages.storage.googleapis.com/36/95/97/1622062a9a5d0b/US4973331.pdf. Accessed Oct 27, 2025.
16. Ilizarov GA, Ruts FYa, Nemkov VA, et al. Compression-distraction apparatus. Author's Certificate SU no. 1122308. 1984. Available at: https://patents.google.com/patent/SU1122308A1/en. Accessed Oct 27, 2025.
17. Shevtsov VI., Burlakov E.V., Nemkov V.A. *Transosseous device*. Patent RF for a utility model no. 30073. 2003. Available at: https://www.fips.ru/registers-doc-view/fips_servlet?DB=RUPM&DocNumber=30073&TypeFile=html. Accessed Oct 27, 2025. (In Russ.)
18. Shevtsov VI, Popkov AV, Popkov DA, Muradisinov SO. Elongation of lower limbs by an automatic mode. *Genij Ortopedii*. 1999;(3):20-24. (In Russ.)
19. Semkin AV, Piastro AE, Popkov AV, et al. *Systemforcontrollingprocessofdistractionosteosynthesisbasedonfeedba ck withdistractionforcesinautomatedtransosseouscompression-distraction apparatus*. Patent RF, no. 2833763, 2035. Available at: https://patentimages.storage.googleapis.com/c2/ac/2d/7c2820790e7a6f/RU2833763C1.pdf. Accessed Oct 27, 2025.
20. Popkov AV, Semkin AV, Popkov DA, et al. *Transosseous automated distraction device and automatic transfer unit*. Patent RF, no. 2763644 C1. 2021, Available at: https://www.fips.ru/registers-doc-view/fips_servlet?DB=RUPAT&DocNumber=2763644&TypeFile=html. Accessed Oct 27, 2025. (In Russ.)

21. Popkov AV, Popkov DA, Kononovich NA, et al. *Osteoperfusion of bioactive implants in the treatment of fractures of long tubular bones: a study guide*. Tomsk: Publ. House of Tomsk Polytechnic University; 2017:84-103. (In Russ.)
22. Popkov AV, Popkov DA. *Bioactive Implants in Traumatology and Orthopedics*. Irkutsk: NCRVH SO RAMS, 2012:127-177. (In Russ.)
23. Shevtsov VI, Popkov AV. *Operative Lengthening of the Lower Extremities*. Moscow: Meditsina Publ.; 1998:89-171. (In Russ.)
24. Popkov AV, Gorodtsov NA, Popkov DA, et al. Automation of Operative Limb Lengthening (Literature Review). *Medical Technology*. 2024; 348(6):49-53. (In Russ.)
25. Popkov AV, Popkov DA, Kononovich NA, et al. *Limb elongation under conditions of bioactive implantation in long tubular bones: a textbook*. Tomsk: Publ. House of Tomsk Polytechnic University; 2018:60-121. (In Russ.)

The article was submitted 04.04.2024; approved after reviewing 21.01.2025; accepted for publication 21.08.2025.

Information about the authors:

Arnold V. Popkov — Doctor of Medical Sciences, Professor, Chief Researcher, orthopaedic surgeon, apopkov.46@mail.ru;

Nikolai A. Gorodtsov — orthopaedic surgeon, postgraduate student, Junior Researcher, gorodcov17@gmail.com;

Pavel P. Buravtsov — Candidate of Medical Sciences, orthopaedic surgeon.

Original article
https://doi.org/10.18019/1028-4427-2025-31-6-813-821

Establishing boundaries of acetabular walls in total hip replacement

A.V. Tsybin[1], V.V. Lyubchak[1]✉, A.S. Falkovich[2], S.S. Bilyk[1], V.E. Baskov[3], I.V. Gayvoronskiy[4]

[1] Vreden Russian Scientific Research Institute of Traumatology and Orthopedics, Saint-Petersburg, Russian Federation
[2] Saratov State University, Saratov, Russian Federation
[3] Turner Russian Scientific Research Institute of pediatric Traumatology and Orthopedics, Saint-Petersburg, Russian Federation
[4] Kirov Military Medical Academy, Saint-Petersburg, Russian Federation

Corresponding author: Vyacheslav V. Lyubchak, drogbadider@mail.ru

Abstract

Introduction The term "acetabular walls" is used to describe the survival rate of total hip replacements (THR) and classifications of THR surgeries. With the experience accumulated in THR surgery, there is no information on establishing boundaries of the acetabular walls. ASPID is a classification system used to describe post-traumatic acetabular deformities with no technique for establishing boundaries of acetabular walls.

The **objective** was to demonstrate and provide a theoretical substantiation for a method establishing the boundaries of the acetabular walls in primary THR.

Material and methods Pelvic computed tomography scans of five children aged 10–12 years and 30 pelvic preparations of adult bones without signs of acetabular dysplasia were used.

Results Extraacetabular fixed anatomical landmarks were identified in 3D models from CT scans of pediatric pelvic bones with the planes dividing acetabulum into conditional walls separated by cartilage. The pelvic bones of 30 adults were scanned, and similar reconstructions performed to delineate boundaries of the acetabular walls. The proportional ratios and areas of each acetabular wall were determined in the pediatric and adult groups, and the results compared. The absence of statistical differences in the proportions of the superior, posterior and medial walls of the pediatric and adult acetabulum suggested high reliability of the method.

Discussion There were insignificant statistical differences in the anterior acetabular wall fraction of children and adults and could be associated with a small quantity of measurements. The absence of statistical differences in the proportions of the superior, posterior and medial walls of the pediatric and adult acetabulum suggested the reliability of the method. A larger number of measurements to be performed by several specialists, determination of the Cohen's Kappa coefficient and statistical analysis of the results are essential for the validity of the method.

Conclusion The method offered for establishing boundaries of the acetabular walls can be practical for scientific research, but cannot be used in routine practice due to its complexity and the need to use special software. The method can be recommended for describing post-traumatic deformities of the acetabular walls in cases where extraacetabular landmarks are not damaged or displaced.

Keywords: acetabulum, total hip replacement, posttraumatic deformity, walls, ASPID

For citation: Tsybin AV, Lyubchak VV, Falkovich AS, Bilyk SS, Baskov VE, Gayvoronskiy IV. Establishing boundaries of acetabular walls in total hip replacement. *Genij Ortopedii*. 2025;31(6):813-821. doi: 10.18019/1028-4427-2025-31-6-813-821.

INTRODUCTION

Hip replacement surgery is a treatment option for hip injuries and diseases and aims to relieve pain, restore function and improve quality of life. Hip replacement surgery was first performed in 1960 [1]. Short- and long-term outcomes, complications of the surgical procedure have been published in numerous articles since then [2, 3, 4].

The bone condition is one of the main factors for reliable primary implant fixation and survival of the artificial joint. The term "acetabular walls" was introduced to describe surgical technique, analyze long-term results and complications, and classify cases of primary and revision THR. The term can be encountered in publications reporting THR survival and in classifications of hip replacement surgeries [5–12]. This definition relies on the theoretical aspects of THR, but the use of the term “acetabular walls” provides no clarification regarding their boundaries. Anisimova et al. reported parameters of the acetabulum in details to include the thickness of the walls, without specifying the boundaries of the latter [13]. AO classification of acetabular fractures grades injury to the columns and to the walls of the acetabulum with the boundaries of the walls being not defined within the fracture assessment system [14]. There are a large number of works reporting the AO classification, the causes, treatment and consequences of pelvic and acetabular fractures, injury to the columns and acetabular walls with no information on the boundaries of the acetabular walls to be determined [15–22].

The authors of the Russian patent dated December 28, 2020 "A method for selecting surgical strategy depending on the degree of acetabular deformity and the integrity of the pelvic ring in patients with post-traumatic coxarthrosis," offered an original classification of post-traumatic acetabular deformities ASPID based on three criteria, including the deformity localization (anterior, superior, posterior, and medial walls of the acetabulum). The classification had no description of the method for determining the boundaries of the above walls [23, 24].

Outcomes of THR performed for stage 3 post-traumatic hip arthritis with acetabular wall deformities are significantly worse than those resulting from other causes. These cases are not classified according to acetabular wall defects due to the lack of a specific classification, making it difficult to accurately analyze the causes of failures [25, 26]. Although the method for determining the boundaries of the acetabular walls and localization of the boundaries during THR has not been described, the concept of “acetabular walls” exists and is widely used.

The **objective** was to demonstrate and provide a theoretical substantiation for a method establishing the boundaries of the acetabular walls in primary THR.

MATERIAL AND METHODS

Pelvic computed tomography scans of five children aged 10–12 years and 30 pelvic preparations of adult bones without signs of acetabular dysplasia were used.

Special computer programs: Materialise Mimics Research 21.0 and Materialise 3-matic Research 13.0 were used to create 3D models and analyze them, identify necessary landmarks, construct planes and divide the acetabulum into walls.

The landmarks were defined so that the lines drawn through them during 3D modeling based on CT scans in adults were close to the lines of incomplete osteogenesis dividing the walls of the acetabulum in children (Fig. 1).

The first stage of the study included analysis of pediatric CT scans of pelvic bones, construction of 3D models of the pelvic bones, and determination of extraacetabular fixed anatomical landmarks

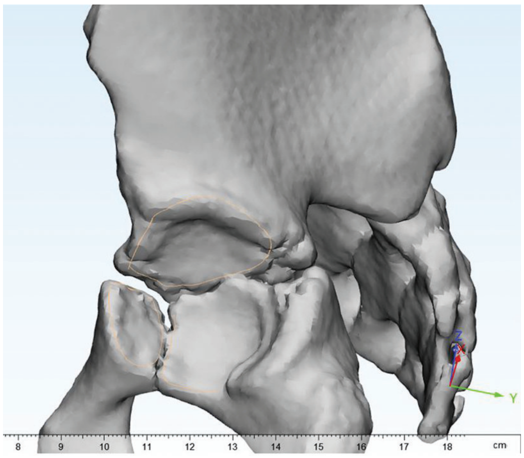

Fig. 1 An instance of a 3D model of a pediatric pelvis

to draw planes and divide the pediatric acetabulum into conditional walls separated by cartilage.

Based on computed tomography of the pelvic bones, a high-precision three-dimensional surface was formed with the points to be marked: the most prominent point of the pubic tubercle (1); the most prominent point on the pubic crest (2); the most prominent point of the ischial tuberosity (3) and the most prominent point of the anterior inferior iliac spine (4). The acetabular outlet plane was formed: the two most prominent points of the acetabular notch (5, 6) and a point on the superior wall of the acetabulum (7), obtained by drawing a perpendicular from the midpoint of the transverse ligament line to the superior wall. Next, the center point of the acetabulum was determined on the plane of the exit (9), — the maximum transverse diameter of the acetabulum and the distance, divided in half. Further construction of planes was performed relative to the plane of the acetabulum exit and the point (the center of the acetabulum) obtained by drawing a line through the center of the acetabulum, perpendicular to the plane of the acetabulum exiting to the medial wall (8) (Fig. 2).

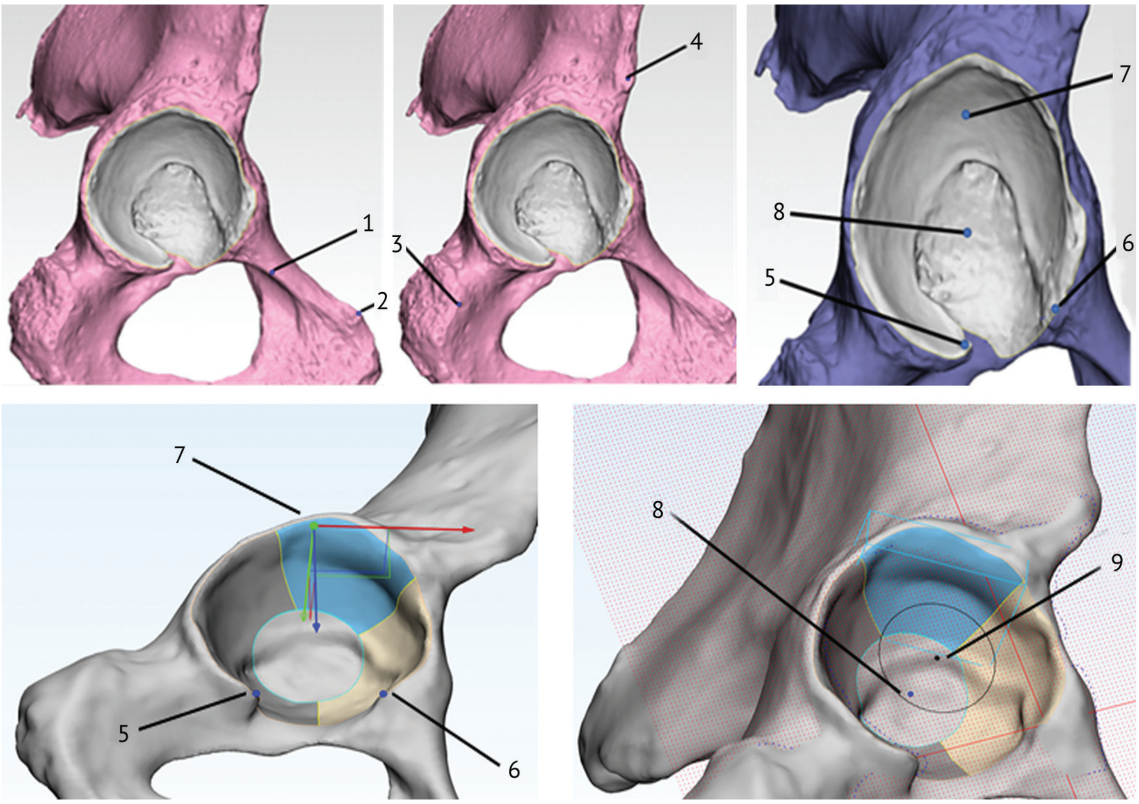

Fig. 2 Marking points on a 3D model of the acetabulum

The planes were constructed using points located directly on the triangular mesh of the computer model and freely in the 3D coordinate system. Materialise 3-matic Research 13.0, a 3D modeling application with reverse engineering functionality, was used to construct the planes (three points are the minimum necessary and sufficient number to construct a plane in a three-dimensional coordinate system). The projection of a circle (Fig. 2 shows a diagram with a plane and a circle) onto the wall of the acetabulum was constructed using the planar drawing function with the projection lines being superimposed on the surface of the triangulation model at the required angle (the function is included in the computer program). The acetabular boundaries were defined using a tool for dividing the main mesh into individual surfaces by specifying a series of points that were subsequently connected into a single closed line.

The first plane was formed by the center of the acetabulum, the most prominent point of the pubic tubercle and the most prominent point on the pubic crest (Fig. 3, plane 1). The second plane was formed by the center of the acetabulum, the most protruding point of the ischial tuberosity and the most protruding point of the anterior inferior iliac spine (Fig. 3, pl. 2).

A circle with a radius equal to ¼ of the maximum transverse diameter was formed From the center of the acetabulum parallel to the plane of the exit (this is how the medial wall was projected). A line segment connecting the two most prominent points of the acetabular notch was constructed. A point was placed in the middle, which was projected parallel to the plane of the acetabulum exit onto the medial wall (Fig. 3, point 10). Using an additional third point, a plane was obtained (Fig. 3, plane 3) dividing the fragment of the lower part of the acetabulum into anterior and posterior sections, which finally allowed formation of the anterior, posterior, superior and medial walls (Fig. 4).

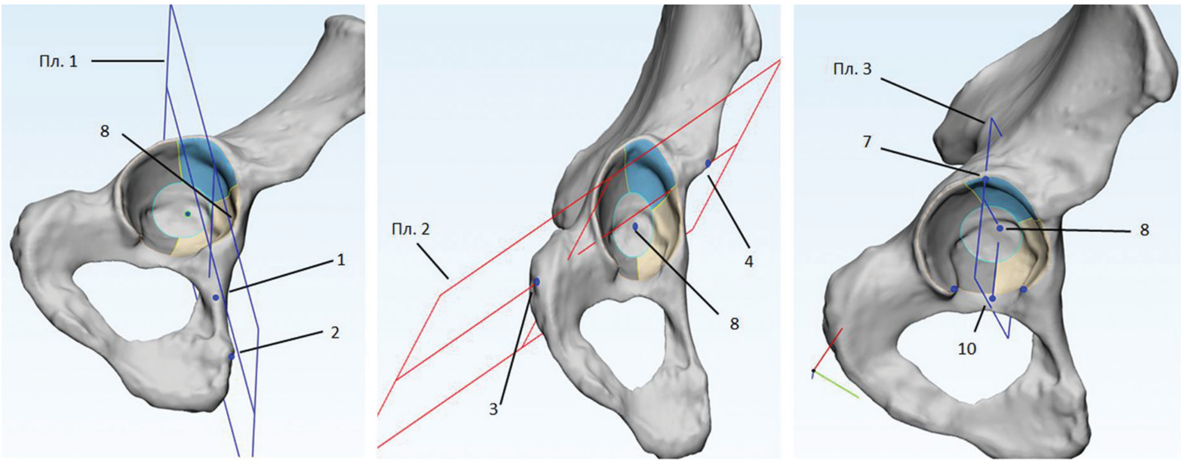

Fig. 3 Division of the acetabulum using planes

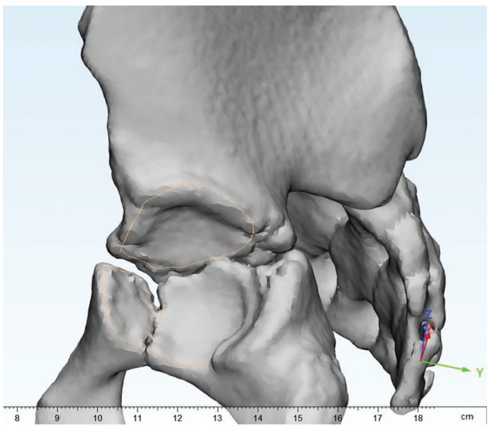

Fig. 4 The acetabulum divided into anterior, superior, posterior and medial walls following analysis of a 3D model of the pelvis

Scanning of the adult pelvis and conducting similar constructions was performed at the second stage to draw the boundaries of the acetabulum walls.

The proportional ratio and area of each wall of the acetabulum was determined in groups of children and adults at the third stage comparing the results and identifying measurement errors with a subsequent conclusion on the possible validity of the method. The total area of the acetabulum (mm), the areas of each acetabular wall, and their proportions relative to the total area were calculated in the cases using Materialise 3-matic Research 13.0. The results are tabulated for comparison of the data to determine the validity of the original method of dividing the acetabulum into "walls" in THR.

One-way analysis of variance, a nonparametric evaluation method, the Mann – Whitney rank test (U-test, Wilcoxon – Mann – Whitney test) were used for statistical analysis for testing the hypothesis about the difference between two samples, U-statistics U_1 and U_2 according to the formulas:

$$U_1 = n_1 \cdot n_2 + \frac{n_1(n_1 + 1)}{2} - R_1;$$

$$U_2 = n_1 \cdot n_2 + \frac{n_2(n_2 + 1)}{2} - R_2,$$

where n_1 and n_3 are the number of adults and children examined, respectively

RESULTS

One-way analysis of variance showed no statistical differences in the ratios of the percentage shares of the superior, posterior and medial walls relative to the total surface area of the acetabulum in adults and children (Table 1) confirming the validity of the method. There were slight differences in the parameters for the anterior wall due to the small number of measurements in the samples.

Table 1

One-way analysis of variance (comparison of the means in two samples)

Description	A (%)	S (%)	P (%)	I (%)
Adults (30 measurements)				
The mean	25.79	24.54	35.31	14.38
Standard deviation	2.63	3.55	3.21	1.01
Error of the mean	0.48	0.65	0.59	0.18
Children (5 measurements)				
The mean	30.08	23.02	32.10	14.80
Standard deviation	3.10	4.51	5.46	2.73
Error of the mean	1.39	2.01	2.44	1.22
Difference between means	4.30	1.52	3.20	0.41
Difference error	1.47	2.12	2.51	1.23
The ratio of the difference to the error of the difference	2.93	0.72	1.27	0.33

Note: A, anterior wall; S, superior wall; P, posterior wall; I, medial wall.

The data in the last row (the ratio of the difference to the error of the difference) were compared with the table value of the Student's t-distribution at a significance level of 0.05 with 32 (30 + 5 – 3) degrees of freedom, which was equal to 2.037. If the number obtained was greater than the table value (2.037) it was considered that the data in the two samples differed, as at wall "A". In the remaining three cases (S, P, I) the numbers obtained were less than 2.037 with no differences between the adult and child samples.

A similar result was obtained using a nonparametric evaluation method the Mann – Whitney U-test (Wilcoxon – Mann – Whitney test). The percentages of each acetabular wall were compared separately in the samples. The data from both samples were combined and sorted (ranked) in ascending order for each percentage (A, S, P, I). A sequential number ("rank") was assigned for each subject. Then, the sums of the ranks (R1 for the adult group, R2 for the child group) and the U-statistics U_1 and U_2 were calculated separately for adults and children (Table 2). The smallest of the two numbers obtained $U_e = \min(U_1, U_2)$ was chosen as the Mann – Whitney U statistic.

Table 2

Application of a nonparametric evaluation method the Mann – Whitney rank test

Description	A (%)	S (%)	P (%)	I (%)
Adults (n_1 = 30 measurements)				
Sum of ranks R_1	483	561	569	542
U_1	132	54	46	73
Children (n_2 = 5 measurements)				
Sum of ranks R_2	147	69	61	88
U_2	18	96	104	77
Table value of the Mann–Whitney statistic at a confidence level of 0.05	39			

Note: A, anterior wall; S, superior wall; P, posterior wall; I, medial wall.

If the statistic Mann – Whitney value of Ue was less than the table value (for example, when measuring the percentage of the "A" wall), the null hypothesis of no difference between the two samples was rejected and the alternative hypothesis was accepted, that is, the difference between the two samples was considered statistically significant. There were no differences in the percentages of walls S, P, and I did not differ between the adult and child samples in the remaining three cases. However, the interval diagram below (Fig. 5) shows that the difference in the percentages of wall A between adults and children was not very significant with no difference for walls S, P, and I.

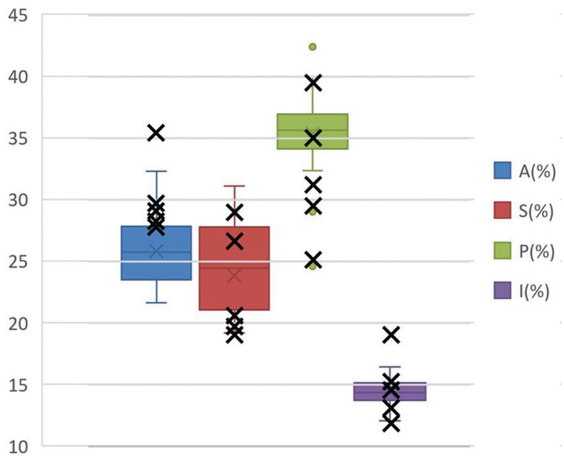

Fig. 5 Interval diagram. Colored elements represent adult data, black diagonal crosses represent children's data. Filled rectangles represent the second and third quartiles, horizontal lines in the middle of the rectangles are the medians, and T-shaped extension lines ("whiskers") indicate maxima and minima, excluding outliers, individual colored dots (on the diagram only for P) are outliers (values that deviate from the main sample array by more than 1.5 interquartile ranges from the nearest quartile)

DISCUSSION

Literature review on various aspects of THR confronts researchers with the concept of "acetabular walls." Given the absence of such a concept in normal anatomy, novice practitioners may encounter a number of contradictions when learning hip arthroplasty techniques and implanting the acetabular component. The problem is not associated with standard primary joint replacement procedures for minor acetabular changes and not related to post-traumatic conditions or congenital pathology with no changes in the bone structure or deformities.

CT scans of the pelvis of 10– to 12–year-old children without signs of hip dysplasia were used to devise the method for the following reason: tt is known that at birth, the acetabular cartilage complex is located between the ilium superiorly, the ischium inferiorly, and the pubic bone anteriorly.

The outer two thirds of the structure form the so-called acetabular cartilage, and its medial third belongs to the medial wall. At puberty (10–12 years), the depth of the acetabulum increases due to the development of three secondary ossification centers. Connolly and Weinstein suggested that the "acetabular bone" (os acetabulum) is a secondary epiphysis of the pubic bone and contributes to the development of the anterior wall of the acetabulum [27]. The epiphysis of the acetabulum is the secondary growth center of the ilium and forms the main part of the superior wall of the acetabulum. The ischium contains a small, innominate secondary growth center, which is involved in the formation of the posterior wall of the acetabulum [28]. Therefore, the walls of the pediatric acetabulum are formed from four ossification centers (one primary and three secondary) at the age of 10–12 years. The walls have not yet fully formed at this age, a clear boundary can be seen between them on CT scans. The observation served the basis for this study to determine the boundaries of the acetabular walls using extraacetabular landmarks.

In cases of traumatic origin, the anatomy of the acetabulum would acquire a unique configuration, which is difficult to describe and systematize due to the lack of a generally accepted assessment system [29]. There is a paucity of publications on THR performed for patients with post-traumatic acetabulum, reporting very small groups of patients with no practical role due to the lack of a generally accepted systemic approach. Primary THR is sometimes used for acute acetabular fractures and implant survival is difficult to evaluate. With no method for determining the acetabular wall boundaries, it is difficult to develop recommendations for the choice of strategy in the patients. Kirkeboe et al. reported 48 patients (mean age 68 years) with acetabular fractures treated with ORIF and acute THR, stabilizing both columns and the acetabular shell with no boundaries and sizes of defects of each acetabular wall during implantation of the acetabular component [30].

Our study is unique and can serve as the basis for a more comprehensive investigation of the acetabulum in congenital and post-traumatic deformities. The statistical results showed high reliability of this method. There were insignificant statistical differences in the fraction of the anterior acetabular wall of the pediatric and adult groups due to the small number of measurements produced in the groups. No statistical differences were found in superior, posterior, and medial acetabular wall fractions between the pediatric and adult groups confirmed the validity of the method. Requires a greater number of measurements to be performed by several specialists, measurement of the Cohen's Kappa coefficient and statistical analysis of the results are required for further evaluation of the validity of the method.

Our work is part of a larger study exploring outcomes of primary THR in patients with stage 3 post-traumatic hip arthritis and post-traumatic acetabular wall deformities. An original acetabular classification system called ASPID was developed for post-traumatic conditions at the Vreden National Medical Research Center for Trauma and Orthopedics by analogy with the TNM system used in oncology. The ASPID system used the walls of the acetabulum as the basis for classification with the concept of acetabular boundaries to be introduced, including theoretical aspects confirming the need to implement an original system for assessing acetabulum after acetabular fractures. An algorithm for selecting surgical strategy is to be developed based on this classification and to be tested on a larger group of patients as part of a multicenter study.

CONCLUSION

The method offered for determining the boundaries of the acetabular walls is theoretically substantiated and has no analogues in the world. The technique is difficult to use in routine diagnosis of post-traumatic deformities of the acetabulum as it is complex and specialized software to be employed. However, the technique may be practical for preoperative planning of challenging cases of primary THR and for scientific analysis of surgical outcomes. The technique is very important for accurate preoperative planning of primary THR in the presence of severe post-traumatic deformities of the acetabular walls, for the selection of the acetabular component and additional constructs for the reliable fixation. Therefore, the results of primary THR can be improved with the technique used for patients with stage 3 post-traumatic hip arthritis.

Conflict of interest *None of the authors has any potential conflict of interest..*

Funding*: No additional funds were used.*

Ethical Approval *Not required.*

Informed Consent *Not required.*

REFERENCES

1. Charnley J. Arthroplasty of the hip. A new operation. *Lancet*. 1961;1(7187):1129-1132. doi: 10.1016/s0140-6736(61)92063-3.
2. Mesbahi SAR, Ghaemmaghami A, Ghaemmaghami S, Farhadi P. Outcome after Surgical Management of Acetabular Fractures: A 7-Year Experience. *Bull Emerg Trauma*. 2018;6(1):37-44. doi: 10.29252/beat-060106.
3. Salama W, Ditto P, Mousa S, et al. Cementless total hip arthroplasty in the treatment after acetabular fractures. *Eur J Orthop Surg Traumatol*. 2018;28(1):59-64. doi: 10.1007/s00590-017-2021-x.
4. Stibolt Jr. RD, Patel HA, Huntley SR, et al. Total hip arthroplasty for posttraumatic osteoarthritis following acetabular fracture: A systematic review of characteristics, outcomes, and complications. *Chin J Traumatol*. 2018;21(3):176-181. doi: 10.1016/j.cjtee.2018.02.004.
5. Tikhilov RM, Shubnyakov II, Chiladze IT, et al. Choice of surgical approach for acetabular component's implantation using current classification for arthritis following acetabular fracture. *Traumatology and Orthopedics of Russia*. 2011;17(2):37-43. (In Russ.) doi: 10.21823/2311-2905-2011-0-2-37-43.
6. D'Antonio JA. Periprosthetic bone loss of the acetabulum: classification and management. *Orthop Clin North Am*. 1992;23(2):279-90.
7. Paprosky WG, Perona PG, Lawrence JM. Acetabular defect classification and surgical reconstruction in revision arthroplasty. A 6-year follow-up evaluation. *J Arthroplasty*. 1994;9(1):33-44. doi: 10.1016/0883-5403(94)90135-x.
8. Firoozabadi R, Hamilton B, Toogood P, et al. Risk factors for conversion to total hip arthroplasty after acetabular fractures involving the posterior wall. *J Orthop Trauma*. 2018;32(12):607-611. doi: 10.1097/BOT.0000000000001327.
9. Williams HLM, Bartlett GE, Norton MR, Middleton RG. The posterior acetabular wall (PAW): an aid to acetabular orientation at primary THA. *Hip Int*. 2018;28(1):29-32. doi: 10.5301/hipint.5000531.
10. Nikolaev NS, Malyuchenko LI, Preobrazhenskaia EV, et al. Use of customized acetabular components for hip joint arthroplasty in posttraumatic coxarthrosis. *Genij Ortopedii*. 2019;25(2):207-213. doi: 10.18019/1028-4427-2019-25-2-207-213.
11. Zagorodny NV, Kolesnik AI, Lazarev AF, et al. Current trends in the surgical treatment of patients with pelvic and acetabular injuries (literature review). *Genij Ortopedii*. 2020;26(2):266-274. doi: 10.18019/1028-4427-2020-26-2-266-274.
12. Beaule PE, Dorey FJ, Matta JM. Letournal classification of acetabular fractures. *J Bone Joint Surg Am*. 2003;85(9):1704-1709.
13. Anisimova EA, Yusupov KS, Anisimov DI, Bondareva EV. Morphology of bone structures of acetabulum and femoral component of hip joint. *Saratov Journal of Medical Scientific Research*. 2014; 10(1):32-38. (In Russ.)
14. Kellam JF, Meinberg EG, Agel J., et al. Fracture and Dislocation Classification Compendium-2018. *J Orthop Trauma*. 2018;32(1 Suppl):S1-S170. doi: 10.1097/BOT.0000000000001063.
15. Laird A, Keating JF. Acetabular fractures: a 16-year prospective epidemiological study. *J Bone Joint Surg Br*. 2005;87(7):969-973. doi: 10.1302/0301-620X.87B7.16017.
16. Olson SA. Diagnosis and Treatment of Acetabular Fractures: Historic Review. In: Smith WR, Ziran BH, Morgan SJ. (eds.) *Fractures of the Pelvis and Acetabulum* (1st ed.). CRC Press; 2007:127-140. doi:10.3109/9781420016383-8.
17. Bircher M. Pelvic and acetabular fractures past, present and future. *AO Dialogue*. 2007;1(07):36-39.
18. Moed BR, McMichael JC. Outcomes of posterior wall fractures of the acetabulum. *J Bone Joint Surg Am*. 2007;89(6):1170-1176. doi: 10.2106/JBJS.F.00473.
19. Manson T, Schmidt AH. Acetabular fractures in elderly: a critical analysis review. *JBJS Rev*. 2016;4(10):e1. doi: 10.2106/JBJS.RVW.15.00090.
20. Pesantez R, Ziran BH. Anatomy of Pelvis. In: Smith WR, Ziran BH, Morgan SJ. (eds.) *Fractures of the Pelvis and Acetabulum* (1st ed.). CRC Press; 2007:1-9. doi: 10.3109/9781420016383-2.
21. Lawrence DA, Menn K, Baumgaertner M, Haims AH. Acetabular fractures: anatomic and clinical considerations. *AJR Am J Roentgenol*. 2013;201(3):W425- W436. doi: 10.2214/AJR.12.10470.
22. Pierannunzii L, Fisher F, Tagliabue L, et al Acetabular both column fractures: essentials of operative management. *Injury*. 2010;41(11):1145-9. doi: 10.1016/j.injury.2010.08.011.
23. Tsybin AV, Tikhilov RM, Denisov AO, et al. *Method for choosing surgical tactics depending on the degree of deformation of the acetabulum and the state of the integrity of the pelvic ring in patients with post-traumatic coxarthrosis*. Patent RF, no. 2739674, 2020. Available at: https://www.fips.ru/registers-doc-view/fips_servlet?DB=RUPAT&DocNumber=2739674&TypeFile=html. Accessed Aug 25, 2025.. (In Russ.)

24. Tsybin AV, Lubchak VV, Sivkov VS, et al. Rationale for the use of the original classification of posttraumatic acetabular deformities in primary total hip replacement. *Genij Ortopedii*. 2021;27(5):508-513. doi: 10.18019/1028-4427-2021-27-5-508-513.
25. Makridis KG, Obakponovwe O, Bobak P, Giannoudis PV. Total hip arthroplasty after acetabular fracture: incidence of complications, reoperation rates and functional outcomes: evidence today. *J Arthroplasty*. 2014;29(10):1983-1990. doi: 10.1016/j.arth.2014.06.001.
26. Morison CZ, Moojen DJ, Nauth A, et al. Total Hip Arthroplasty After Acetabular Fracture Is Associated With Lower Survivorship and More Complications. *Clin Orthop Relat Res*. 2016;474(2):392-398. doi: 10.1007/s11999-015-4509-1.
27. Connolly P, Weinstein SL. The natural history of acetabular development in developmental dysplasia of the hip. *Acta Orthop Traumatol Turc*. 2007;41 Suppl 1:1-5. (In Turkish)
28. Pozdnikin IYu, Baskov VE, Voloshin SYu, et al. Errors of diagnosis and the initiation of conservative treatment in children with congenital hip dislocation. *Pediatric Traumatology, Orthopaedics and Reconstructive Surgery*. 2017;5(2):42-51. doi: 10.17816/PTORS5242-51.
29. Tikhilov R.M., Shubnyakov I.I., Denisov A.O. Classifications of acetabular defects: do they provide an objective evidence for complexity of revision hip joint arthroplasty? (critical literature review and own cases). *Traumatology and orthopedics of Russia*. 2019;25(1):122-141. doi: 10.21823/2311-2905-2019-25-1-122-141.
30. Kirkeboe RL, Madsen JE, Nordsletten L, Clarke-Jenssen J. Acute treatment of elderly patients with acetabular fractures by open reduction, internal fixation, and total hip arthroplasty: a 1-10-year follow-up of 48 patients. *Acta Orthop*. 2024;95:661-666. doi: 10.2340/17453674.2024.42113.

The article was submitted 06.09.2024; approved after reviewing 25.08.2025; accepted for publication 14.10.2025.

Information about the authors:

Alexander V. Tsybin — Candidate of Medical Sciences, Junior Researcher, alex_tsybin@mail.ru;

Vyacheslav V. Lyubchak — orthopaedic surgeon, drogbadider@mail.ru, https://orcid.org/0000-0001-7343-4529;

Alexander S. Falkovich — Doctor of Technical Sciences, Lecturer, falkovichas@yandex.ru;

Stanislav S. Bilyk — Candidate of Medical Sciences, Research Lab Assistant, bss0413@gmail.com;

Vladimir E. Baskov — Candidate of Medical Sciences, Head of Regional Interaction Department;

Ivan V. Gaivoronsky — Doctor of Medical Sciences, Professor, Head of Department.

Clinical case
https://doi.org/10.18019/1028-4427-2025-31-6-822-830

Treatment of infectious nonspecific coxitis in HIV-positive patients using an antibiotic-loaded spacer for the hip joint

E.O. Peretsmanas✉**, V.S. Zubikov, I.A. Gerasimov, Ya.A. Rukin**

National Medical Research Center of Phthisiopulmonology and Infectious Diseases, Moscow, Russian Federation

Corresponding author: Evgeniy O. Peretsmanas, peretsmanas58@mail.ru

Abstract

Introduction The fight with nonspecific infection in immunodeficient HIV-infected patients is challenging. There are no standardized treatment protocols yet. The most effective treatment method of purulent coxitis remains two-stage total hip arthroplasty with the first stage of joint resection and implantation of an antibiotic-loaded cement spacer, and the second stage of total hip replacement. One of the ways to reduce poor results and revision interventions is the development of new types of spacers for treatment of coxitis in patients with HIV infection.

The **aim** of the work is to demonstrate the effectiveness of a new method of surgical treatment of infectious coxitis in HIV-infected patients using an original design of an antibiotic-loaded articulating spacer in two clinical cases.

Materials and methods The treatment results of two HIV-positive patients with infectious coxitis, in whom an original two-layer design of an antibiotic-loaded cement spacer based on the individual bacterial sensitivity was applied at the first stage of treatment, were retrospectively evaluated. To study the effectiveness of this method we used the results of the dynamics of pain evaluation according to Visual Analogue Scale (VAS), the functional state of the affected joint using Harris Hip Score (HSS), Western Ontario and McMaster University osteoarthritis Index (WOMAC) scale and radiological data of patients in the early postoperative period and after 12-month follow-up.

Results Clinical cases demonstrate positive results of treatment of infectious coxitis associated with HIV infection. Application of the developed spacer design allowed eradication of bacterial infection. As a result of using of the new spacer model with an antimicrobial effect in the first clinical case it was possible to restore the joint function from 35 to 89 HHS points, from 79 to 14 WOMAC points, to reduce the pain syndrome from 7 to 1 VAS point; in the second patient from 32 to 91 HHS points, from 84 to 11 WOMAC points, to reduce the pain syndrome from 6 to 0 VAS points.

Discussion Based on scientific reports and our own clinical cases, we hypothesize that in HIV-associated purulent coxitis, one of the main reasons for poor results after two-stage arthroplasty is insufficient local concentration of antimicrobial agents, caused by the imperfect design of traditional cemented spacers. The original spacer design allows for a higher concentration and may become an effective alternative to traditional treatment methods.

Conclusion Application of the developed technology of surgical treatment of infectious coxitis in HIV-positive patients resulted in eradication of infection, reduction of pain syndrome, restoration of the hip joint functionality.

Keywords: infectious coxitis, HIV infection, two-stage arthroplasty, spacer, antimicrobial agents

For citation: Peretsmanas EO, Zubikov VS, Gerasimov IA, Rukin YaA. Treatment of infectious nonspecific coxitis in HIV-positive patients using an antibiotic-loaded spacer for the hip joint. *Genij Ortopedii*. 2025;31(6):822-830. doi: 10.18019/1028-4427-2025-31-6-822-830.

INTRODUCTION

The incidence of infectious coxitis worldwide ranges from 4 to 10 subjects per 100,000 of population [1]. The problem of providing medical care to patients with infectious coxitis remains relevant due to the lack of effective treatment protocols [2, 3, 4]. If treatment is not timely, the infectious process results in destructive changes in the bone structures of the joint, a significant decrease in the patient's quality of life, and sometimes in sepsis and death [5]. Treating patients with infectious coxitis associated with HIV infection is a particularly challenging task. The prevalence of inflammatory joint diseases among patients with HIV infection varies from 3 to 71 % [6, 7]. At the same time, the available literature lacks statistically significant data on the treatment outcomes in this cohort of patients. The studies report a small number of treated cases and high percentage of poor results [8].

The authors of the studies provide data on the effectiveness of two-stage hip arthroplasty in infectious coxitis as a technology that allows for the eradication of the infectious process and restoration of lost joint function [9, 10, 11, 12]. It is logical to assume that this technique may be the technology of choice for HIV-associated coxitis. The advantage of using a cement spacer impregnated with antimicrobial agents at the first stage is preserved anatomical relationships between the resected joint ends that ensures functional activity and a satisfactory quality of life for the patient until the permanent implant is installed. It creates a depot of antimicrobial agents, providing a local effect on pathogenic microflora in the joint area [13, 14, 15, 16]. Focal bactericidal concentration is one of the main functions of the spacer and allows for a reduction in the duration and an increase in the effectiveness of systemic antibacterial therapy [13, 14, 15, 16].

However, a number of studies have shown that high concentrations of drug-loaded cement mixture during spacer fabrication results in a significant reduction in its strength characteristics [17, 18, 19]. It is known that the maximum release of antibiotics occurs from the surface of the spacer, while antimicrobial agents from the internal parts of the spacer, due to the density of the bone cement, are practically not eluted into the joint medium [20, 21, 22]. Thus, not the entire spacer, but only its surface layer, performs the deposition function. In this regard, saturating the entire cement spacer with antimicrobial agents during spacer fabrication is impractical. Saturation of only the surface layers of the spacer with antimicrobial drugs does not affect its strength characteristics and increases its medicinal effectiveness, enables to achieve a high local antimicrobial concentration even of such drugs such rifampicin, known for its inhibitory effect on the process of polymerization of bone cement [23].

Purpose The aim of the work is to demonstrate on two clinical cases the effectiveness of a new method of surgical treatment of infectious coxitis in HIV-infected patients using an original design of an antibiotic-loaded articulating spacer.

MATERIAL AND METHODS

The results of treatment of two patients with infectious coxitis suffering from HIV infection were retrospectively evaluated. At the first stage of treatment, an original design of a two-layer cement spacer saturated with antimicrobial drugs based on their individual sensitivity to the microbial agents was used.

To achieve this goal, the design solution was to create a hip joint spacer with a two-component head. The internal component is made of standard cement with known strength characteristics, while the external component is made of a cement mantle containing antimicrobial agents in the required concentrations, including high ones, depending on the individual sensitivity of the microbial agent. The device has been granted Russian patent RU 212287 U1, "Antimicrobial Hip Joint Spacer" [24].

Surgical technique

Through the standard approach to the hip joint, the femoral head is dislocated and resected, and the joint capsule, purulent contents, and necrotic tissue are removed. The femoral head diameter is measured with calipers. The resected joint cavity is mechanically and antiseptically treated. A small rasp is used to create a bed in the femur for spacer insertion. The spacer is then fabricated on a separate table. First, the spacer stem is cast using bone cement in a sterile plastic mold. A metal reinforcement is positioned along the stem axis to ensure flexural strength. At the top of the stem, the proximal end of the 40 mm metal reinforcement is temporarily left uncovered by the cement mantle until bending. The size of the plastic mold and, accordingly, the stem corresponds to the zero rasp size of the ESI system, similar to the endoprosthesis installation technique. The second step is to fabricate the spacer head.

The first (internal) component of the hemispherical head is fabricated entirely from bone cement by immersing the proximal end of the metal stem reinforcement in a special plastic mold available in several sizes (44 mm, 46 mm, 48 mm, 50 mm, 52 mm, 54 mm, 56 mm, and 58 mm in diameter) filled with liquid cement during the polymerization stage. The size of the internal component of the head is selected to be 2 mm smaller than the dimensions of the removed femoral head and acetabulum. After the first component has partially hardened, 4–6 minutes after the start of polymerization, it is removed from the plastic mold. The second (external) component of the head is then fabricated. Initially, powdered antimicrobial agents in the required concentration are added to the powdered bone cement polymer and mixed mechanically. Next, liquid monomer is added to the powdered polymer-antimicrobial mixture, and the mixture is placed in a plastic mold 2 mm larger than the internal component. The internal component of the head is immersed in the mold filled with the cement-antimicrobial compound until it hardens for 8-10 minutes after mixing. The specimen is then removed from the plastic mold.

Thus, the head of the spacer, manufactured using this technology, consists of two components: the first (internal) is made of cement and possesses the necessary strength characteristics and capable of bearing functional load; the second (external) component is 2 mm thick and is produced of a mixture of cement and an antimicrobial agent and has an antimicrobial effect. Accordingly, in addition to its musculoskeletal function, the manufactured spacer also functions as a depot for the gradual release of antimicrobial agents. The manufactured spacer is inserted into the femoral canal. The head of the spacer is repositioned into the acetabulum. The wound is sutured layer by layer. Walking with gradual increase of load is allowed on days 2–4 after surgery.

To study the effectiveness of the method, the results of a dynamic assessment of the severity of pain syndrome using the VAS scale, the functional state of the affected joint using the HSS (Harris Hip Score), WOMAC (Western Ontario and McMaster Universities osteoarthritis Index) and radiological data of patients in the early postoperative period and after 12-month follow-up were used.

Case 1

Patient Sh., 42, with left-sided coxitis diagnosed in 2021, and established by infectious disease specialists stage 3 HIV infection had subclinical stage and took antiretroviral drugs (ART). According to the patient, the route of infection was sexual transmission. His medical history includes surgery for left varicocele in 1994.

Hip pain was persistent since November 2021. In July 2022, he received a course of intra-articular hyaluronic acid injections with a short-term positive effect. From December 2022, the pain has sharply worsened, and he started walking with crutches. He did not have antibiotic therapy as an outpatient.

The patient was admitted to the NMIC FPI complaining of pain in the left hip joint and walked with crutches. Joint functional scores were 35 HHS points, 79 WOMAC points, and 7 VAS points for pain severity. CT scans of the left hip joint revealed destruction of the upper fragment of the left femoral head without signs of contact destruction of the acetabulum and narrowing of the joint space (Fig. 1). Immunological studies: CD-4 = 551 cells/μL, VL in the blood < 20 copies/ml. Laboratory tests with deviation from reference values: ESR = 36 mm/hour, leukocytes = $2.41{\times}10^9$, C-reactive protein = 4.5 mg/L.

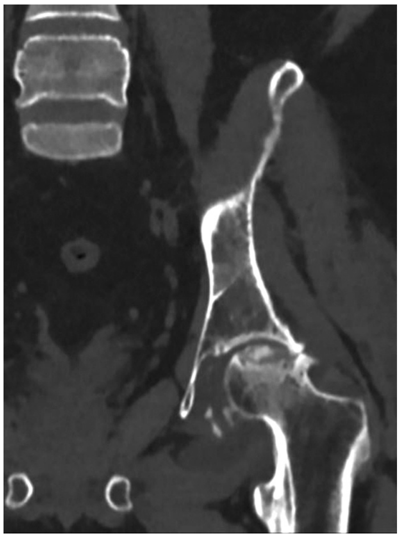

Fig. 1 Left hip CT scan of patient SH. at admission

On March 7, 2023, a trephine biopsy of the bone destruction focus in the femoral head was performed under radiological guidance. Microbiological examination of the biomaterial revealed a culture of *Acinetobacter baumanii* (susceptible to gentamicin) and *Staphylococcus capitis* (sensitive to the wide-range antibiotics). Pathohistological findings revealed signs of chronic nonspecific coxitis. The patient was diagnosed with nonspecific coxitis on the left associated with HIV infection. Before surgery, a course of combination antibacterial therapy was administered as prescribed by a clinical pharmacologist: meropenem 2000 mg 3 times a day intravenously, amikacin 1000 mg once a day intravenously for 15 days. On March 27, 2023, a left femoral head was resected, and an articulating two-layer spacer with gentamicin (4 g) was inserted (Fig. 2). PCR testing of the surgical material on March 28, 2023, revealed no Mycobacterium tuberculosis (MBT) DNA. The postoperative period was uneventful.

During a readmission seven months later to the National Medical Research Center for Pediatric Orthopedics and Pedagogical Research, a triple peri-implant puncture of the left hip joint was performed. No microbial growth was detected. Before the second stage of the arthroplasty, the functional indices of the joint were 64 HHS points, 32 WOMAC points, and 2 VAS points for pain. On November 17, 2023, the second stage of the arthroplasty was performed: removal of the articulating spacer and total cementless arthroplasty of the left hip joint using a Beijing Montagne Medical device/Zimmer (Fig. 3).

Fig. 2 X-ray of the left hip joint of patient Sh. on the first day after installation of an articulating cement spacer with a two-layer head. The outer cement mantle contained 4 g of gentamicin

Fig. 3 X-ray of the left hip joint of patient Sh. on the first day after the operation of total cementless arthroplasty with Beijing Montagne Medical device / Zimmer

Case 2

Patient K., 47, with a history of right-side coxitis, developed bilateral exudative pleurisy and tuberculous spondylitis at the level of T8-T10 before admission. The infectious disease specialist's report states: HIV 4B, in remission while receiving ART. Chronic hepatitis C is biochemically inactive. HIV was detected in 2020. The route of infection was sexual. ART has been administered since 2020 in the following regimen: tenofovir, lamivudine, and dolutegravir. Upon admission, the phthisiatrician's report stated: clinical cure of bilateral exudative pleurisy and tuberculous spondylitis at T8-T10. In 2021, treatment was administered according to regimen 3 of anti-tuberculosis chemotherapy, with 324 doses administered.

The patient reported that he was sick since June 2022 when pain and swelling developed in the right hip joint. He received antibacterial therapy with lincomycin for three weeks at a local hospital, with a temporary positive effect. In August 2022, he began walking with the additional support of crutches and with graduated weight-bearing on his right lower limb. Pain intensified again with weight-bearing, and he was given another two-week course of antibacterial therapy (lincomycin) that had a positive effect.

The patient was admitted to the NMIC FPI clinic. He complained of pain and severe limitation of motion in the right hip joint. His functional indices were 25 HHS points, 84 WOMAC points, and a pain severity VAS score of 6.

The radiograph of the right hip joint showed contact destruction of the articular ends and narrowing of the joint space (Fig. 4).

A trephine biopsy of the right femoral head was performed under radiological guidance.

Biological material analysis: MBT DNA was not detected. Human immunodeficiency virus (HIV) RNA was detected in the biopsy sample using real-time PCR (RT-PCR) at 6.7×10^4 c/ml. Microscopy of the surgical sample was negative. Microbiological study of the surgical sample: no microbial growth was detected. Histological examination revealed signs of nonspecific coxitis. Blood immunoassay: CD4 — 19 % — 654 cells/μl; HIV RNA — 120 c/ml. Based on the medical history and histological examination, a diagnosis of right-sided nonspecific coxitis was established.

On March 7, 2023, an operation was performed involving resection of the femoral head and placement of an articulating spacer made of bone cement with clindamycin (4.5 g) (Fig. 5). Clindomycin was chosen due to its mechanism of action and antimicrobial spectrum, which are similar to lincomycin (the patient's medical history indicates a positive effect of lincomycin administration), as well as the high elution capacity of the drug [25]. Microbiological study of tissues harvested intraoperatively did not reveal any pathogen.

No postoperative complications were noted; the patient resumed walking with additional support on the second postoperative day. He was discharged to be followed up by an orthopedic and an infectious disease specialists.

He was readmitted six months later. Local status: there was no shortening of the right lower limb. The postoperative scar showed no signs of inflammation. Joint functional scores were 77 HHS points, 24 WOMAC points, and 2 VAS points. Palpation revealed mild local tenderness over the right hip joint (2 points on the VAS scale). The radiograph is shown in Figure 6.

Peri-implant space punctures were performed at three points. Microbiological examination of the surgical biomaterial revealed no microbial growth.

On October 10, 2023, the surgery included removal of the articulating spacer and total cementless right hip arthroplasty with the ESI system (Fig. 7).

Fig. 4 X-ray of the right hip joint of patient K. upon admission

Fig. 5 X-ray of the right hip joint of patient K. on the first day after the installation of an articulating cement two-layer head spacer. The outer cement mantle contains 4 g of clindamycin

Fig. 6 X-ray of the right hip joint of patient K. 6 months after installation of an articulating cement two-layer head spacer

Fig. 7 X-ray of patient K.'s right hip joint on the first day after total cementless right hip arthroplasty with the ESI system

The postoperative period was uneventful; he began walking with additional support one day after surgery.

FOLLOW-UPS AND RESULTS

Case 1

Twelve months after the second stage involving removal of the articulating spacer and total cementless hip arthroplasty of the left hip joint with the Beijing Montagne Medical / Zimmer implant, the functional ratings of the joint were 89 HHS points, 14 WOMAC points and 1 VAS point for pain. The radiograph is shown in Figure 8.

Case 2

Twelve months after total cementless hip arthroplasty of the right hip joint with the ESI implant, the functional ratings of the joint were 91 HHS points, 11 WOMAC points and 0 VAS points for pain. The radiograph is shown in Figure 9.

Fig. 8 X-ray of the left hip joint of patient Sh. 12 months after total hip arthroplasty of the left hip joint

Fig. 9 X-ray of the right hip joint of patient K. 12 months after total hip arthroplasty of the right hip joint

DISCUSSION

The literature does not provide treatment results in patients with infectious coxitis associated with HIV infection. Some authors published data on a roughly equal number of poor results after total hip arthroplasty due to degenerative joint diseases in patients with normal and reduced immunodeficiency [25]. Other authors report a significantly decreased effectiveness of two-stage treatment, even with the use of an antibacterial spacer, in the presence of an implant-associated infection [26]. Primary purulent arthritis associated with HIV infection represents an extremely complex clinical group. Our clinical experience with this cohort of patients shows a high rate of poor results, manifested by infection recurrence.

The technical merit of using the technology developed by us is a prolonged high local concentration of antimicrobial agents in bone cement, which increases treatment effectiveness [27, 28, 29, 30] and maintains the strength properties of the spacer. The known spacer designs exhibit satisfactory mechanical properties; however, they do not create the necessary inhibitory concentrations of antimicrobial agents that affect the strength properties of bone cement, such as rifampicin.

The spacer design we proposed was originally developed for the use in surgery for tuberculous coxitis, a common comorbidity in HIV-infected patients. This design has also proven effective in patients with non-specific conditions. A significant improvement in the functional state of the affected joint was noted after the first stage of surgical treatment. At follow-up after 12 months, the patients expressed satisfaction with the treatment results. We believe this original design could become an effective alternative to traditional treatment methods.

CONCLUSION

Application of the developed technology of an antimicrobial two-layer head articulating spacer for surgical treatment of infectious coxitis in HIV-positive patients resulted in eradication of infection, reduction of pain syndrome, and restoration of the hip joint functionality.

Conflict of Interest *The authors declare no conflicts of interest.*

Source of Funding *Patients were treated under the state program of guaranteed free medical care for RF citizens. The study was conducted without sponsorship.*

***Compliance with Ethical Standards** The authors confirm that the rights of the patients participating in the study were respected, informed consent for participation in the study and the publication of medical data and images of the radiological examinations was obtained. The study was approved by the institutional ethics committee of the National Medical Research Center for Pediatrics and Pedagogical Research of the Ministry of Health of the Russian Federation, Protocol No. 17 dated August 25, 2022.*

REFERENCES

1. D'Angelo F, Monestier L, Zagra L. Active septic arthritis of the hip in adults: what's new in the treatment? A systematic review. *EFORT Open Rev*. 2021;6(3):164-172. doi: 10.1302/2058-5241.6.200082.
2. Astakhov DI, Artyukh VA. Pathogenesis and Modern Methods for Treatment of Hip Infectious Arthritis: A Review. *Traumatology and Orthopedics of Russia*. 2024;30(2):192-205. (In Russ.). doi: 10.17816/2311-2905-17497.
3. Balato G, de Matteo V, Ascione T, et ak. Management of septic arthritis of the hip joint in adults. A systematic review of the literature. *BMC Musculoskelet Disord*. 2021;22(Suppl 2):1006. doi: 10.1186/s12891-021-04843-z.
4. Anagnostakos K, Duchow L, Koch K. Two-stage protocol and spacer implantation in the treatment of destructive septic arthritis of the hip joint. *Arch Orthop Trauma Surg*. 2016;136(7):899-906. doi: 10.1007/s00402-016-2455-3.
5. Mathews CJ, Weston VC, Jones A, et al. Bacterial septic arthritis in adults. *Lancet*. 2010;375(9717):846-855. doi: 10.1016/S0140-6736(09)61595-6.
6. Biviji AA, Paiement GD, Steinbach LS. Musculoskeletal manifestations of human immunodeficiency virus infection. *J Am Acad Orthop Surg*. 2002;10(5):312-320. doi: 10.5435/00124635-200209000-00003.
7. Bukhanova DV, Belov BS. Joint damage in HIV positive patients. *Medical Council*. 2018;(9):82-87. (In Russ.) doi: 10.21518/2079-701X-2018-9-82-87.
8. ubikov VS, Peretsmanas EO, Gerasimov IA. The experience of surgical treatment of tuberculosis and non-specific arthritis with two-stage arthroplasty using articulating cement spacers saturated with antibiotics. *Tuberculosis and Lung Diseases*. 2019;97(11):25-32. (In Russ.) doi: 10.21292/2075-1230-2019-97-11-25-32.
9. Nikolaev NS, Karpukhin AS, Maksimov AL, et al. Experience in the treatment of patients with nonspecific coxitis using two-stage endoprosthetics. *The Department of Traumatology and Orthopedics*. 2020;4(42):5-13. (In Russ.) doi: 10.17238/issn2226-2016.2020.4.5-13.
10. Luo H, He C, Zhao Y, et al. Outcomes of single- vs two-stage primary joint arthroplasty for septic arthritis: a systematic review and meta-analysis. *EFORT Open Rev*. 2023;8(9):672-679. doi: 10.1530/EOR-22-0142.
11. Russo A, Migliorini F, Giustra F, et al. Two-stage total joint replacement for hip or knee septic arthritis: post-traumatic etiology and difficult-to-treat infections predict poor outcomes. *Arch Orthop Trauma Surg*. 2024;144(12):5111-5119. doi: 10.1007/s00402-024-05249-x.
12. Chen CY, Lin CP, Tsai CH, et al. Medullary-Sparing Antibiotic Cement Articulating Spacer Reduces the Rate of Mechanical Complications in Advanced Septic Hip Arthritis: A Retrospective Cohort Study. *J Pers Med*. 2024;14(2):162. doi: 10.3390/jpm14020162.
13. D'Angelo F, Monestier L, Zagra L. Active septic arthritis of the hip in adults: what's new in the treatment? A systematic review. *EFFORT Open Rev*. 2021;6(3):164-172. doi: 10.1302/2058-5241.6.200082.
14. Dudareva M, Kümin M, Vach W, et al. Short or Long Antibiotic Regimes in Orthopaedics (SOLARIO): a randomised controlled open-label non-inferiority trial of duration of systemic antibiotics in adults with orthopaedic infection treated operatively with local antibiotic therapy. *Trials*. 2019;20(1):693. doi: 10.1186/s13063-019-3832-3.
15. Lin TL, Tsai CH, Fong YC, et al. Posterior-Stabilized Antibiotic Cement Articulating Spacer With Endoskeleton-Reinforced Cam Reduces Rate of Post-Cam Mechanical Complications in Prosthetic Knee Infection: A Preliminary Study. *J Arthroplasty*. 2022;37(6):1180-1188.e2. doi: 10.1016/j.arth.2022.01.094.
16. Ayre WN, Birchall JC, Evans SL, Denyer SP. A novel liposomal drug delivery system for PMMA bone cements. *J Biomed Mater Res B Appl Biomater*. 2016;104(8):1510-1524. doi: 10.1002/jbm.b.33488.
17. Gálvez-López R, Peña-Monje A, Antelo-Lorenzo R, et al. Elution kinetics, antimicrobial activity, and mechanical properties of 11 different antibiotic loaded acrylic bone cement. *Diagn Microbiol Infect Dis*. 2014;78(1):70-74. doi: 10.1016/j.diagmicrobio.2013.09.014.
18. Paz E, Sanz-Ruiz P, Abenojar J, et al. Evaluation of Elution and Mechanical Properties of High-Dose Antibiotic-Loaded Bone Cement: Comparative "In Vitro" Study of the Influence of Vancomycin and Cefazolin. *J Arthroplasty*. 2015;30(8):1423-1429. doi: 10.1016/j.arth.2015.02.040.
19. Pithankuakul K, Samranvedhya W, Visutipol B, Rojviroj S. The effects of different mixing speeds on the elution and strength of high-dose antibiotic-loaded bone cement created with the hand-mixed technique. *J Arthroplasty*. 2015;30(5):858-863. doi: 10.1016/j.arth.2014.12.003.
20. Bistolfi A, Massazza G, Verné E, et al. Antibiotic-loaded cement in orthopedic surgery: a review. *ISRN Orthop*. 2011;2011:290851. doi: 10.5402/2011/290851.
21. Anagnostakos K, Meyer C. Antibiotic Elution from Hip and Knee Acrylic Bone Cement Spacers: A Systematic Review. *Biomed Res Int*. 2017;2017:4657874. doi: 10.1155/2017/4657874.
22. Athans V, Veve MP, Davis SL. Trowels and Tribulations: Review of Antimicrobial-Impregnated Bone Cements in Prosthetic Joint Surgery. *Pharmacotherapy*. 2017;37(12):1565-1577. doi: 10.1002/phar.2040.
23. Peretsmanas E.O., Artyukhov A.A., Shtilman M.I., Esin I.V., Zubikov V.S., Gerasimov I.A. Study of elution characteristics of anti-tuberculosis drugs mixed with bone cement. *Tuberculosis and Lung Diseases*. 2021;99(4):30-35. (In Russ.) doi: 10.21292/2075-1230-2021-99-4-3.

24. Peretsmanas EO, Tyulkova TE, Zubikov VS, et al. *Antimicrobial spacer for the hip joint*. Patent RF, no. No. 212287. 2022. Available at: https://www.fips.ru/registers-doc-view/fips_servlet?DB=RUPM&rn=8561&DocNumber=212287&TypeFile=html. Accessed Feb 21, 2025. (In Russ.)
25. Zhao CS, Li X, Zhang Q, et al Early Outcomes of Primary Total Hip Arthroplasty for Osteonecrosis of the Femoral Head in Patients with Human Immunodeficiency Virus in China. *Chin Med J (Engl)*. 2015;128(15):2059-64. doi: 10.4103/0366-6999.161364.
26. Tryapichnikov AS, Ermakov AM, Klyushin NV, et al. Treatment Outcomes of Periprosthetic Joint Infection in HIV-Positive Patients. *Traumatology and orthopedics of Russia*. 2019;25(4):117-125. doi: 10.21823/2311-2905-2019-25-4-117-125.
27. Kilmetov TA, Akhtyamov IF, Gilmutdinov IS, et al. Local antibiotic therapy in infection of arteficial joints. *Kazan medical journal*. 2014;95(3):405-411. (In Russ.) doi: 10.17816/KMJ1526.
28. Shevchenko YuL, Stoiko YuM, Gritsuk AA, et al. Local antibiotic prophylaxis in endoprosthesis replacement of major joints (publications overview). *Bulletin of Pirogov National Medical and Surgical Center*. 2010;5(3):44-56. (In Russ.)
29. Masri BA, Duncan CP, Beauchamp CP. Long-term elution of antibiotics from bone-cement: an in vivo study using the prosthesis of antibiotic-loaded acrylic cement (PROSTALAC) system. *J Arthroplasty*. 1998;13(3):331-338. doi: 10.1016/s0883-5403(98)90179-6.
30. Wall V, Nguyen TH, Nguyen N, Tran PA. Controlling Antibiotic Release from Polymethylmethacrylate Bone Cement. *Biomedicines*. 2021;9(1):26. doi: 10.3390/biomedicines9010026.

The article was submitted 09.12.2024; approved after reviewing 05.02.2025; accepted for publication 14.10.2025.

Information about the authors:

Evgeny O. Peretsmanas — Doctor of Medical Sciences, Head of Department,
peretsmanas58@mail.ru, https://orcid.org/0000-0001-7140-3200;

Vladimir S. Zubikov — Doctor of Medical Sciences, Professor, Leading Researcher,
zubikovladimir@gmail.com, https://orcid.org/0000-0002-2211-8400;

Ilia A. Gerasimov — orthopaedic surgeon, gerial36@yandex.ru, https://orcid.org/0000-0003-4388-155X;

Yaroslav A. Rukin — Doctor of Medical Sciences, Professor, Leading Researcher,
yar.rukin@gmail.com, https://orcid.org/0000-0001-7355-8556.

Clinical case
https://doi.org/10.18019/1028-4427-2025-31-6-831-838

Spinopelvic dissociation in an adolescent with severe combined injury complicated by cauda equina

P.V. Iskusov[1]✉, S.V. Bragina[1,2], I.M. Kornyakov[1], I.V. Nikitina[1], A.V. Fomin[1], A.S. Zvorykin[1], D.N. Medvedev[1], A.V. Agapitov[1], V.N. Anisimov[1]

[1] Arkhangelsk Regional Clinical Hospital, Arkhangelsk, Russian Federation
[2] Northern State Medical University, Arkhangelsk, Russian Federation

Corresponding author: Pavel V. Iskusov, iskusoffpawel@yandex.ru

Abstract

Introduction The clinical case demonstrated low prevalence and complexity of spinopelvic dissociation. Up-to-date diagnostic and modern osteosynthesis techniques were used for unstable injuries of the pelvic ring and the sacrum.

The **objective** was to report a rare clinical case of spinopelvic dissociation in an adolescent with severe combined injury complicated by cauda equina that resulted in a positive treatment outcome.

Material and methods An adolescent patient with spinopelvic dissociation as part of a severe multi-trauma injury complicated by cauda equina was reported. Cauda equina root decompression surgery, triangular osteosynthesis and minimally invasive fixation of anterior pelvic ring fractures were performed after four days of injury because of unstable hemodynamics in the patient.

Results A positive treatment outcome was achieved in the form of life-saving, restored musculoskeletal function of the pelvis and lower limbs and complete regression of neurological dysfunction of the pelvic organs demonstrated by the Majeed pelvic score at six months and at one year of injury.

Discussion Spinopelvic dissociation as part of a severe combined injury was caused by a fall from a height in the case. A ISS score of over 25 points is classified as profound and very severe with a high risk of mortality and is often accompanied by traumatic shock. There is a high risk of neurological disorders and damage to other locations in spinopelvic dissociation. The patient suffered damage to the cauda equina roots and disturbed pelvic functions, adjacent pelvic fractures (fractures of the left acetabulum, right pubic and ischial bones), visceral injuries including contusion to the right lung and the brain. Triangular osteosynthesis is considered the method of choice for spinopelvic dissociation providing stable and biomechanically reasonable fixation system for the vertical, rotation and angulation loading on the pelvic ring. Although the risk of postoperative complications is very high and can reach 50 % with open techniques according to international literature the patient developed no postoperative complications. The treatment strategy was adequate for the teenager with spinopelvic dissociation and severe combined trauma and resulted in consolidated pelvic ring fractures and positive long-term functional outcome.

Conclusion Despite the complexity of the injury, high risk of postoperative complications and the lack of experienced specialists the teenager could survive, avoid postoperative complications and restore pelvic and lower limb function due to the coordinated work of a multidisciplinary team, timely diagnosis and modern osteosynthesis techniques used for unstable pelvic injuries.

Keywords: spinopelvic dissociation, combined trauma, unstable pelvic injury, sacral fractures, triangular osteosynthesis

For citation: Iskusov PV, Bragina SV, Kornyakov IM, Nikitina IV, Fomin AV, Zvorykin AS, Medvedev DN, Agapitov AV, Anisimov VN. Spinopelvic dissociation in an adolescent with severe combined injury complicated by cauda equina. *Genij Ortopedii*. 2025;31(6):831-838. doi: 10.18019/1028-4427-2025-31-6-831-838.

INTRODUCTION

Spinopelvic dissociation (SPD) is a severe injury characterized by an anatomical separation between the spine and the pelvis. The condition can be caused by a horizontal sacral fracture and bilateral longitudinal fractures, resulting in SPD [1–7]. Due to the rarity, complexity of this injury and the high frequency of postoperative complications, there are not enough experienced specialists to diagnose and treat this pathology [4, 5]. The uniqueness of this clinical observation is associated with the low incidence, severity of the pathology, timely diagnosis and up-to-date methods of osteosynthesis used for unstable injuries of the pelvic ring and sacrum: open bilateral transpedicular spinal-pelvic fixation in combination with iliosacral screws (triangular osteosynthesis) and with retrograde minimally invasive osteosynthesis of the anterior pelvic half-ring. The treatment could save the teenager's life, avoid postoperative complications, and restore functions of the pelvis and lower extremities in the shortest possible time.

The **objective** was to report an uncommon clinical case of SPD in an adolescent with severe combined injury complicated by cauda equina that resulted in a positive treatment outcome.

MATERIAL AND METHODS

A 16-year-old girl was injured in a fall from the fifth floor. She was transported in critical condition by ambulance within 30 minutes to a specialized hospital at the Arkhangelsk Regional Clinical Hospital. Blood pressure was 100×60 mmHg, she was provided with artificial ventilation, inotropic support and neck immobilization with a Shants collar. Anti-shock treatment and diagnostic procedures were performed in the hospital. The patient was examined by a multidisciplinary team including a trauma surgeon, a neurosurgeon, general surgeon, a maxillofacial surgeon, and a resuscitation specialist. A computed tomography (CT) scan of the head, chest, abdomen, and pelvis was performed.

The patient was examined and diagnosed with combined trauma, catatrauma. closed craniocerebral injury, severe brain contusion, closed chest trauma, right lung contusion, unstable pelvic ring injury, comminuted unstable sacral fracture (DENIS type 3, ROY-CAMILL subtype 2), displacement and compression of the cauda equina roots, displaced fractures of the right pubic and ischial bones and the left acetabulum, neurogenic pelvic dysfunction, first-degree traumatic shock, contusions and abrasions of the soft tissues of the right side of the face and external nose, contused, penetrating wound of the lower lip, complete dislocation of teeth 1.1 and 2.1, partial dislocation and fracture of the crown of tooth 1.2, fracture of the nasal bones.

The Injury Severity Score (ISS) was 48, scored as an extremely severe injury. Mortality for injuries with an ISS score ⩾ 40 points is the highest, amounting to 65 % [8].

Preoperative CT scan of the pelvis revealed a comminuted unstable fracture of the sacrum with displacement; fractures of the right pubic and ischial bones and the left acetabulum with displacement (Fig. 1).

Blood tests upon admission showed erythrocytes measuring 2.5×1012/l, hemoglobin 72 g/l, total protein 50 g/l, CPK 2072 U/l, CPK MB 135 U/l.

Urgent surgery performed for the patient at the first stage included stabilization of the pelvic ring fractures using an external fixator (EF) (Fig. 2). Postoperative treatment was provided in the intensive care unit.

With the traumatic shock relieved and the patient's condition stabilized, a surgery performed four days later included removal of the EFD from the pelvis, decompression of the spinal nerve roots (cauda equina) at the level of the S2 vertebra, bilateral lumboiliac triangular fixation of the pelvis (transpedicular lumbar iliac fixation of the posterior pelvis at the level of L4, L5 and transcutaneous iliosacral fixation of sacral fractures with cannulated screws); minimally invasive retrograde metal osteosynthesis of fractures of the right pubic bone and left acetabulum with cannulated screws.

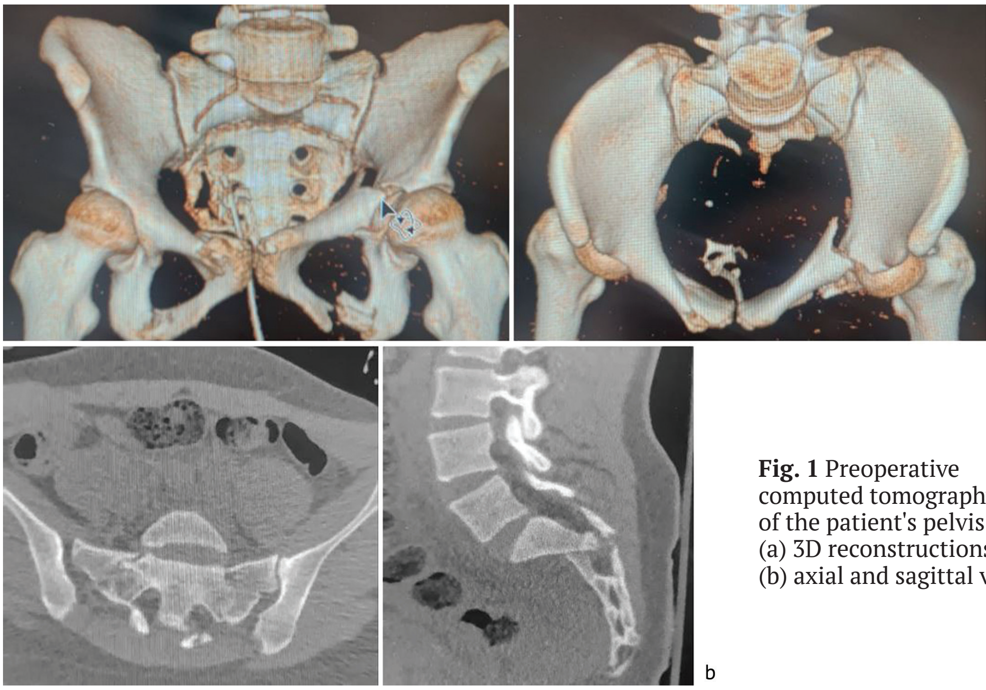

Fig. 1 Preoperative computed tomography scans of the patient's pelvis showing (a) 3D reconstructions; (b) axial and sagittal views

Fig. 2 Postoperative radiograph of the pelvis

The operating team included three trauma surgeons, a neurosurgeon, an anesthesiologist-resuscitator, and an operating nurse.

The EFD was removed from the pelvis under endotracheal anesthesia. With the patient prone, a 22-cm linear midline incision was made at the L5–S3 level in the sacral region. The soft tissues were separated, and the comminuted sacral fracture site was exposed. Hemostasis was achieved. The comminuted fracture plane and angular deformity were visualized at the S2 level. *Spina bifida* was identified at the S2 fracture plane. A laminectomy of S2 and partially S3 was performed. No visible bruising or morphological damage to the dura mater of the spinal cord or roots was detected. Decompression of the roots compressed by bone fragments was performed. Some small bone fragments were removed. The soft tissues were separated, and the arches and facet joints of L4/L5 and L5/S1 were skeletonized. Transpedicular screws were inserted into the roots of the L4 and L5 vertebrae on both sides under image intensifier (II) guidance. The screws were then secured into the iliac wings under II guidance. The sacral fracture dislocation was addressed under visual and radiological control. Transpedicular lumboiliac system was installed after modeling the connecting rods. Radiological examination revealed satisfactory positioning of the fragments. Two 1-cm skin incisions were made in the iliac wings. A cannulated screw was minimally invasively inserted into the body of the S1 vertebra through the longitudinal planes of the sacral fracture using guide wires (90 mm and 80 mm long, 7.3 mm in diameter) under II guidance. Iliosacral fixation of the sacral fractures was performed. A multislice radiograph revealed satisfactory bone position. The treatment performed included hemostasis, vacuum drainage to the fracture site, layered wound sutures and an antiseptic dressing.

In the supine position, retrograde minimally invasive metal osteosynthesis of the fracture of the right pubic bone was performed using two 0.5 cm skin incisions in the area of the pubic symphysis and cannulated screw with a diameter of 5 mm and a length of 40 mm and the fracture of the left acetabulum was fixed with a 110 mm screw with a diameter of 6.5 mm. The skin was sutured and aseptic dressings applied. Multislice radiograph of the pelvis and sacrum revealed satisfactory bone positioning (Fig. 3). The surgery lasted 4 hours 20 minutes, with blood loss of 700 ml.

Fig. 3 Plain radiographs of the pelvis after final osteosynthesis: medial oblique and AP; lateral oblique

RESULTS

The early postoperative period was uneventful. The treatments administered in the intensive care unit (ICU) included respiratory therapy, analgesics, prokinetics, lower extremity thrombosis prophylaxis, stress ulcer prophylaxis, antibacterial therapy, infusion/transfusion therapy, sedation, and enteral nutrition, physical therapy, nursing care, dressings, laboratory monitoring, 1162 ml of packed red blood cells, and 180 ml of cryoprecipitate. The drains were removed after two days. The patient was transferred from the ICU to the trauma and orthopedics department after three days. The patient's condition improved due to the treatment and she was able to walk with crutches without bearing weight on her left leg. The sutures were removed 21 days after surgery. Wound healing occurred by primary intention. Pelvic neurological impairments regressed. Neither vascular nor neurological disorders of the lower extremities were detected. Blood tests at discharge revealed: red blood cells 4.1×10^{12}/L, hemoglobin 125 g/L, total protein 74 g/L.

The patient was discharged for outpatient treatment after 33 days of injury with recommendations to continue treatment with a trauma surgeon and pediatrician, neurologist at the local clinic, walking with no weight on the left leg for three postoperative months, CT scan of the pelvis at six and 12 months of surgery, anticoagulants (Eliquis 2.5 mg 2 times a day for 11/2 months), elastic compression of the lower extremities, exercise therapy, massage, physiotherapy, analgesics, chondroprotectors, vitamins. A combination of minimally invasive osteosynthesis and open surgical techniques was used for the case for treating pelvic injuries. The patient's life was saved, lower limb function restored, and pelvic neurological disorders regressed. The treatment outcome was excellent.

The patient was examined by an orthopedic and trauma surgeon at the Arkhangelsk Regional Clinical Hospital at 6 and 12 months of surgery. She was satisfied with the treatment results, could walk with full weight-bearing on both lower extremities, and did not limp. Neither swelling nor deformities were detected in the extremities. Squats were painless, knee and hip movements unrestricted and pain free (Fig. 4). No signs of infection in postoperative scars in the pelvic area. Loading the iliac wings was painless. Sensation and movement of the toes were not impaired. Pelvic organ function was normal.

Fig. 4 Photo of the patient at six months of surgery

The patient demonstrated an excellent score of over 85 on the Majeed scale (an international scale for the long-term outcome of surgical treatment of unstable pelvic and sacral injuries) and the metal constructs to be removed. Computed tomography scans of the pelvis (Fig. 5) showed consolidated pelvic and sacral fractures at six and at 12 months of surgery (Fig. 6) with the metal constructs being stable.

a

b

Fig. 5 Computed tomography scans of the pelvis at six months of surgery showing (a) 3D reconstruction; (b) scans in frontal and sagittal planes

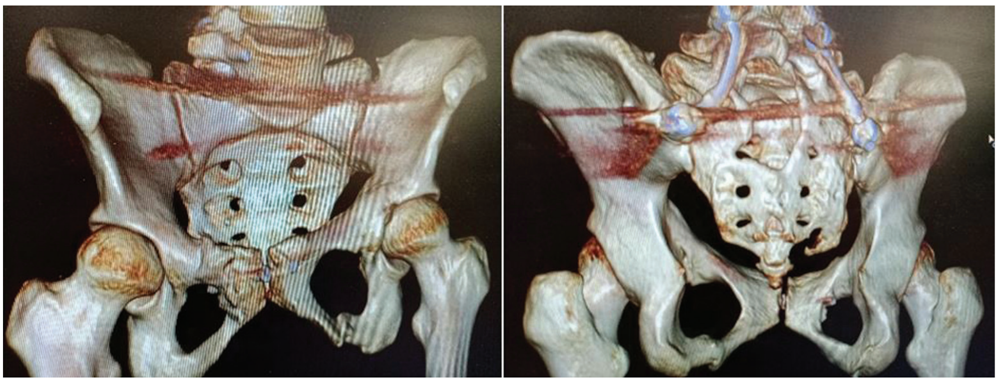

a

Fig. 6 Computed tomography scans of the pelvis at 12 months of surgery showing (a) 3D reconstruction

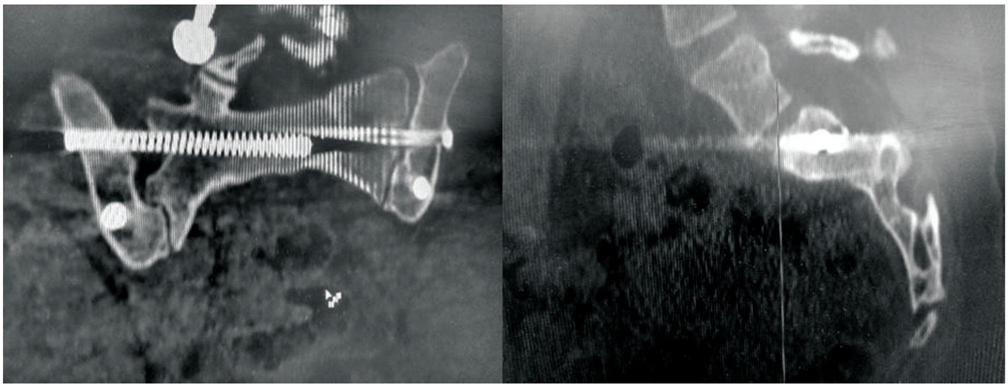

b

Fig. 6 (continuation) Computed tomography scans of the pelvis at 12 months of surgery (b) scans in frontal and sagittal planes

DISCUSSION

With technological advances in traumatology, treatment of patients with unstable pelvic ring injuries as part of severe combined trauma is challenging and requires an interdisciplinary approach. SPD is a rare injury that may occur in 2–3 % of cases with transverse sacral fractures and in 3 % of cases with sacral fractures associated with pelvic ring injuries. The diagnosis may be difficult or neglected in 25–70 % of cases depending on the diagnostic method used [9, 10].

In our clinical observation, the of high-energy severe combined injury in a teenager was caused by a fall from a height which is the main cause of such injuries along with road traffic accidents [7]. Multislice CT with a sensitivity of 88 % is the "gold standard" for diagnosing lumbopelvic dissociation [1, 7]. Upon admission to a Level 1 trauma center, the patient underwent diagnostic and treatment procedures including a CT scan of the head, chest, abdomen and pelvis to combat shock. This case was classified as extremely severe, with an ISS score of 48 since the mortality rate of 65 % for injuries with an ISS score ⩾ 40 [8]. The patient underwent urgent pelvic ring stabilization using an external fixator to be followed by treatment in the ICU.

According to a meta-analysis, neurological deficit is present in 68.1 % of cases, of which 65.1 % show improvement after surgical treatment. There is a high risk of neurological injury when the fracture presents a kyphosis of ⩾ 20° [5]. In our clinical case, the patient had a neurological deficit (cauda equina syndrome), that regressed after surgical treatment. This type of injury is commonly associated with injuries to other locations with the incidence of 87.5 % associated spinal fractures, 71 % of lower extremity fractures, adjacent pelvic fractures 66.7 % and visceral injuries 28.6 %. The association with soft tissue injuries, such as Morrel-Lavallé syndrome may complicate the treatment of this cohort of patients [5]. The presence of severe traumatic brain injury or other bone and internal organ damage usually complicates neurological examination and early surgical treatment. This means that definitive surgical treatment must often be delayed until hemodynamic stability is achieved, although it is recommended within 72 hours. Some authors set a limit of 14 days after injury. Surgery should be performed as soon as possible for patients with neurological symptoms, preferably within the first 24 hours [5]. According to the literature, in case of SPD is commonly associated with injuries to other localizations, which is confirmed by our clinical case: damage to the roots of the cauda equina with disruption of pelvic functions, adjacent pelvic fractures (fractures of the left acetabulum, right pubic and ischial bones), visceral injuries with contusion of the right lung and contusion of the brain.

Spinal-pelvic fixation combined with iliosacral screws or a plate (triangular osteosynthesis) is considered the method of choice [10–13]. A triangle created is usually formed by two systems: horizontal transverse fixation using iliosacral screws and a vertical lumbopelvic transpedicular system providing optimal conditions for fracture consolidation [14–16]. Open reduction of the sacral fracture with triangular spinopelvic fixation would be required for neurologically complicated SPD [1, 2, 5]. In our case, decompression of the cauda equina nerve roots, triangular osteosynthesis, and minimally invasive fixation of the anterior pelvic ring fractures were performed after four days of the injury due to unstable hemodynamics. The fractures of the right pubic bone and left acetabulum were fixed using a minimally invasive technique to restore the integrity of the pelvic ring, increasing stability and reducing the risk of failure of the posterior pelvic half-ring. The Association of Osteosynthesis / Orthopedic Trauma Association (AO / OTA) classification, modified by Tile and Young-Burgess, is widely used to describe sacral fractures in the context of the whole pelvic ring [1]. Several classifications have been established for sacral fractures by Denis supplemented by Roy – Camille and later by Strange – Vognsen and Lebech, B. Isler, but they cannot be considered separately from the entire pelvic ring, because the sacrum is a part of the pelvis, and not just one of the sections of the spine [1].

In 2012, A new classification system called lumbosacral injury classification system (LSICS) was devised and fractures with LSICS 4 or greater should be treated operatively [1, 5]. The Letournel – Judet classification system remains the most widely accepted framework for describing these fractures based on which anatomical component of the acetabulum is affected and the subsequent patterns [17, 18]. Several classifications were used for the clinical case to identify adequate treatment strategy for the injury to the pelvic ring and an associated pelvic injury (unstable pelvic ring damage, unstable sacral fracture, SPD, left acetabulum fracture with displacement). There are few experienced specialists for the diagnosis and treatment of this pathology due to the rarity, severity of this injury and high frequency of postoperative complications, which is a limitation of this treatment method [1, 2, 4, 5].

Further study of this pathology and the implementation of strategies with the use of minimally invasive approaches, preoperative planning employing 3D systems, intraoperative navigation or the use of sacroiliac screws are essential to minimize postoperative complications that occur in 30–50 % of cases [19–22]. Most common complications include discomfort due to the metal structure for osteosynthesis (95 %), infections (36–50 %, higher with open surgical approaches), implant instability (11–17 %), nonunion (9.3 %), implant malposition (15 %), root damage (2–15 %), deep vein thrombosis, progression of sacral kyphosis (independent of fixation of the anterior ring), cerebrospinal fluid leakage, ureteral and bladder injury [1, 5]. In our case, we managed to avoid postoperative complications, although, according to world literature, their probability is very high and reaches 50 % with open techniques. Triangular osteosynthesis is considered the method of choice for SPD, as the most stable, biomechanically sound fixation system providing optimal conditions for fracture consolidation and allows the patient to ambulate. Analyzing this clinical case, it can be stated that the treatment strategy for SPD in an adolescent with severe combined injury appeared to be adequate, which was confirmed by the consolidated pelvic ring fractures and positive long-term functional results.

CONCLUSION

The coordinated work of the multidisciplinary team, timely diagnosis, and up-to-date osteosynthesis techniques used for the pelvic ring injuries (triangular osteosynthesis and minimally invasive techniques) saved the life of the patient, helped to avoid postoperative complication, and facilitated quick restoration of the pelvic and lower extremity function in an adolescent with SPD as part of a severe combined injury.

Conflicting Interests *The authors declared no potential conflicts of interest with respect to the authorship and/or publication of this article.*

Funding *The authors received no financial support for the research and/or authorship of this article.*

Written informed consent *for the participation in the research project was obtained from the subject's parent/legally acceptable representative.*

REFERENCES

1. Aganesov NA, Lazarev AF, Kuleshov AA, et al. Posterior pelvic ring injuries: classification, diagnosis, methods of treatment. *N.N. Priorov Journal of Traumatology and Orthopedics*. 2022;29(2):205-220. (In Russ.) doi: 10.17816/vto109172.
2. Altwaijri NA, Abdulaziz M, Bhat R, et al. Spinopelvic Dissociation Case Report and Literature Review. *Cureus*. 2023;15(5):e39750. doi: 10.7759/cureus.39750.
3. Kim DH, Vaccaro AR, Diekman KA, et al. Spine. *Surgical anatomy and operative technique*. Russ. ed.: Yu.A. Shcherbuk. Moscow: Panfilov Publishing House; 2016:848. (In Russ.)
4. Sevillano-Perez E, Prado-Novoa M, Postigo-Pozo S, et al. L4 fixation is not necessary in L5-Iliac spinopelvic fixation after trauma, but coadjutant transilio-transsacral fixation is. *Injury*. 2024;55(3):111378. doi: 10.1016/j.injury.2024.111378.
5. Hirschfeld M, Pascual-Lopez FJ, Guerado E. Spinopelvic dissociation: Current concepts. *Rev Esp Cir Ortop Traumatol*. 2024;68(4):T398-T408. doi: 10.1016/j.recot.2024.01.025.
6. Liu ZJ, Hu YC, Tian W, et al. Robot-Aided Minimally Invasive Lumbopelvic Fixation in Treatment of Traumatic Spinopelvic Dissociation. *Orthop Surg*. 2021;13(2):563-572. doi: 10.1111/os.12908.
7. Santolini E, Kanakaris NK, Giannoudis PV. Sacral fractures: issues, challenges, solutions. EFORT Open Rev. 2020;5(5):299-311. doi: 10.1302/2058-5241.5.190064.
8. Seliverstov PA, Shapkin YG. Assessment of severity and prognosis of polytrauma outcome: the current state of the problem (review). *Modern technologies in medicine*. 2017;9(2):207-218. doi: 10.17691/stm2017.9.2.25.
9. 3Zakirov RI, Akhtyamov IF, Fayzrakhmanova GM. Successful treatment of a patient with multiple trauma including dislocated sacral fracture complicated with caudopathy. *Genij ortopedii*. 2022;28(6):837-841. doi: 10.18019/1028-4427-2022-28-6-837-841.
10. Kuleshov AA, Aganesov NA, Vetrile MS, et al. Biomechanical analysis of variants of spinopelvic fixation of longitudinal sacral fractures by the finite element method. *Russian Journal of Spine Surgery*. 023;20(1):28-35. doi: 10.14531/ss2023.1.28-35.
11. Petryla G, Bobina R, Uvarovas V, et al. Functional outcomes and quality of life after surgical treatment of spinopelvic dissociation: a case series with one-year follow-up. *BMC Musculoskelet Disord*. 2021;22(1):795. doi: 10.1186/s12891-021-04676-w.
12. Mohd Asihin MA, Bajuri MY, Ahmad AR, et al. Spinopelvic Fixation Supplemented With Gullwing Plate for Multiplanar Sacral Fracture With Spinopelvic Dissociation: A Case Series With Short Term Follow Up. *Front Surg*. 2019;6:42. doi: 10.3389/fsurg.2019.00042.
13. Shi B, Peng Y, Zhang G, et al. Spinopelvic dissociation: extended definition, physical examination, classification, and therapy. *J Orthop Surg Res*. 2023;18(1):56. doi: 10.1186/s13018-023-03523-z.
14. Su PH, Huang YH, Yeh CW, et al. What Are the Key Factors of Functional Outcomes in Patients with Spinopelvic Dissociation Treated with Triangular Osteosynthesis? *J Clin Med*. 2022;11(22):6715. doi: 10.3390/jcm11226715.
15. Shetty AP, Renjith KR, Perumal R, et al. Posterior Stabilization of Unstable Sacral Fractures: A Single-Center Experience of Percutaneous Sacroiliac Screw and Lumbopelvic Fixation in 67 Cases. *Asian Spine J*. 2021;15(5):575-583. doi: 10.31616/asj.2020.0337.
16. Petryla G, Bobina R, Uvarovas V, et al. Functional outcomes and quality of life after surgical treatment of spinopelvic dissociation: a case series with one-year follow-up. BMC Musculoskelet Disord. 2021;22(1):795. doi: 10.1186/s12891-021-04676-w.
17. Lazarev AF, Akhtyamov IF, Azizov MZh,et al. *Surgical treatment of acetabulum fractures*. Kazan: OOO "World without borders"; 2019:319. (In Russ.)
18. Kolesnik AI, Borozda IV, Gnetetskiy SF, et al. *Surgical treatment of acetabular fractures: international approaches*. Moscow: GEOTAR-Media; 2021:160. (In Russ.) doi:10.33029/9704-6408-3-STC-2021-1-160.
19. Bagheri H, Govsa F. Anatomical considerations of safe drilling corridor upper sacral segment screw insertion. *J Orthop*. 2019;16(6):543-551. doi: 10.1016/j.jor.2019.04.010.
20. Mohd Asihin MA, Bajuri MY, Ahmad AR, et al. Spinopelvic Fixation Supplemented With Gullwing Plate for Multiplanar Sacral Fracture With Spinopelvic Dissociation: A Case Series With Short Term Follow Up. *Front Surg*. 2019;6:42. doi: 10.3389/fsurg.2019.00042.
21. Wu C, Deng J, Pan J, et al. Anatomical conditions and patient-specific locked navigation templates for transverse sacroiliac screw placement: a retrospective study. *J Orthop Surg Res*. 2020;15(1):260. doi: 10.1186/s13018-020-01752-0.
22. Alshehri A, Alrehaili H, Batayyib S, et al. Spinopelvic in situ fixation and early mobilization: a case report and literature review. *Cureus*. 2023;15(3):e36454. doi: 10.7759/cureus.36454.

The article was submitted 19.02.2025; approved after reviewing 09.04.2025; accepted for publication 14.10.2025.

Information about the authors:

Pavel V. Iskusov — orthopaedic surgeon, iskusoffpawel@yandex.ru, https://orcid.org/0000-0001-7170-8194;

Svetlana V. Bragina — Candidate of Medical Sciences, associate professor of the department, svetabragina69@mail.ru, https://orcid.org/0000-0002-0900-4572;

Igor M. Kornyakov — neurosurgeon, arhiigor@mail.ru, https://orcid.org/0009-0009-3849-1646;

Irina V. Nikitina — anesthesiologist-resuscitator, nikitina.i.1984@mail.ru, https://orcid.org/0009-0005-0692-2369;

Alexander S. Zvorykin — orthopaedic surgeon, dasterrast@mail.ru, https://orcid.org/0000-0002-0869-0208;

Alexander V. Fomin — orthopaedic surgeon, oma111169@gmail.com, https://orcid.org/0009-0005-0654-9736;

Dmitry N. Medvedev — orthopaedic surgeon, medved29russia@yandex.ru, https://orcid.org/0009-0005-0525-4936;

Viktor N. Anisimov — radiologist, viknik.2010@yandex.ru, https://orcid.org/0009-0003-7497-3534;

Andrey V. Agapitov — radiologist, doctoragapitov@mail.ru, https://orcid.org/0009-0006-9074-135.

Review article
https://doi.org/10.18019/1028-4427-2025-31-6-839-849

CT navigation in spinal deformity surgery

O.G. Prudnikova✉, E.A. Matveev, M.S. Strebkova, A.V. Evsyukov

Ilizarov National Medical Research Centre for Traumatology and Orthopedics, Kurgan, Russian Federation

Corresponding author: Oksana G. Prudnikova, pog6070@gmail.com

Introduction One of the most challenges in spinal deformity surgery is screw placement, which utilizes various methods and options for radiographic guidance, particularly computed tomography-based navigation (CT navigation). Discussions about the advantages and disadvantages of the technologies used determined the relevance of this study.

The **aim** of this study was to evaluate the effectiveness of intraoperative CT navigation in the surgical treatment of patients with spinal deformities using systematic data from the scientific literature.

Materials and Methods A literature search for studies evaluating the parameters of surgical interventions using CT navigation in spinal deformity surgery was conducted in Pubmed, EMBASE, ELibrary, and Google. The article type was a systematic review and meta-analysis, with a search depth of 10 years. The study was conducted in accordance with the PRISMA international guidelines for systematic reviews and meta-analyses. Levels of evidence and strength of recommendations were assessed using the ACCO protocol. A total of 40 articles were found in the databases, with 11 more articles in their reference lists, 48 of which were full-text articles. Eight studies met the inclusion criteria, and two more were added in the sample by agreement of the authors. The following parameters were determined for analysis: screw placement accuracy, malposition rate and complications, operative time, blood loss, reoperation rate, reference frame positioning, and radiation exposure.

Results and discussion The analysis revealed the advantages of using intraoperative CT navigation for screw placement. CT navigation improves screw placement accuracy, does not increase surgical time, and does not reduce the effectiveness of deformity correction. Surgery time, blood loss, and radiation exposure with CT navigation are comparable to other methods. Positioning of one reference frame significantly reduces surgical time, does not affect screw placement accuracy, and does not require additional CT scanning, thereby reducing radiation exposure. To reduce radiation exposure, it is recommended to set a scanning mode with a reduced radiation dose.

Conclusion CT navigation offers advantages in terms of screw placement accuracy, lower malposition rates and associated complications, and reduced reoperation rates. The high safety profile of the navigation system is due not only to the increased accuracy of screw placement but also to lower complication rates.

Keywords: computer navigation for scoliosis, computer navigation scoliosis

For citation: Prudnikova OG, Matveev EA, Strebkova MS, Evsyukov AV. CT navigation in spinal deformity surgery. *Genij Ortopedii*. 2025;31(6):839-849. doi: 10.18019/1028-4427-2025-31-6-839-849.

INTRODUCTION

Scoliosis is one of the most common pathological conditions for which instrumental spinal fixation is performed surgically. Regardless of the etiologic factor, scoliotic deformities are accompanied not only by a deviation of the spinal axis but also by changes in the shape and size of the vertebral structures, including rotation and torsion. The goal of surgery is to correct the deformity to achieve a balanced spinal position and prevent scoliosis curvature progression [1, 2]. Screw placement is one of the most challenging problems of spinal surgery due to the risk of improper placement, resulting in injuries to the spinal cord, nerve roots, and adjacent internal organs, as well as subsequent implant migration or break [3].

According to postoperative computed tomography (CT) data, the incidence of screw malposition during surgical interventions to correct spinal deformities may rise up to 57.8 %. Complications associated with the position of the screws are observed in 0.64–1.1 % of cases, and neurological deficit in 0.3–0.8 % [2, 4, 5].

Malposition of transpedicular screws and long duration of surgery are two major problems that affect final results of scoliosis surgery [1, 4].

During installation of screws, surgeons use both different implantation methods and X-ray control options:

— Fluoroscopically guided (FS) insertion;

— Free-hand (FH) technique with or without radiographic guidance after placement;

— Fluoroscopic navigation using a C-arm, providing two-dimensional fluoroscopic images;

— Robotic navigation and computer navigation using an O-arm (CT navigation), providing three-dimensional visualization.

CT navigation allows for intraoperative CT monitoring of screw positioning and their repositioning in the event of malposition. CT navigation has become the preferred option in many spinal surgery centers, as it provides three-dimensional visualization, real-time definition of spinal anatomy, and assists the surgeon in implant placement. Proponents of this method claim that it allows for consistent, precise screw placement during vertebral fixation, while opponents argue that it increases surgical time, blood loss, and radiation exposure, negating the value of CT navigation [1, 6, 7, 8].

The **aim** of this study was to evaluate the effectiveness of intraoperative CT navigation in the surgical treatment of patients with spinal deformities using systematic data from the scientific literature.

MATERIALS AND METHODS

Strategy for searching and selecting literature data

The search for literature data evaluating the parameters of surgical interventions using CT navigation in patients with spinal deformities was conducted in the Pubmed, EMBASE, ELibrary, and Google databases.

The study was conducted in accordance with the international PRISMA protocol. The inclusion and exclusion criteria are presented in Table 1. As part of the protocol, the first stage involved a literature search using the keywords "computer navigation for scoliosis." The search depth was 10 years. In the second stage, studies that did not meet the inclusion criteria were excluded. In the third stage, the full texts of the selected articles were analyzed for inclusion criteria and the reference lists were reviewed for relevant studies. The search was conducted by three researchers: the initial data extraction was performed by one author and subsequently verified by another author. The three authors then screened the publications according to the exclusion criteria and conducted a final analysis.

A total of 40 articles published from 2014 throughout 2024 were found in the search databases, another 11 were found in the reference lists of these articles; 48 of those 51 studies were full-text. Eight studies met the inclusion criteria (Table 1, Fig. 1).

Table 1

Selection criteria and inclusion/exclusion of publications according to the PRISMA protocol

PRISMA parameters	Selection criteria	
Intervention	Posterior instrumental fixation using intraoperative CT navigation	
Comparison	Study groups in selected publications	
Result	Advantages and Shortcomings of using intraoperative CT navigation in surgical treatment of patients with spinal deformities	
	Inclusion criteria	Exclusion criteria
Participants	Patients who underwent surgical treatment for scoliosis with intraoperative CT navigation	Patients who underwent surgical treatment with intraoperative CT navigation for reasons other than scoliosis
Study design	Systematic review	Randomized and non-randomized, retrospective, and prospective studies. Clinical cases and case series.
Publications	In English, Russian; Full text	Other languages; Access to full text is not available

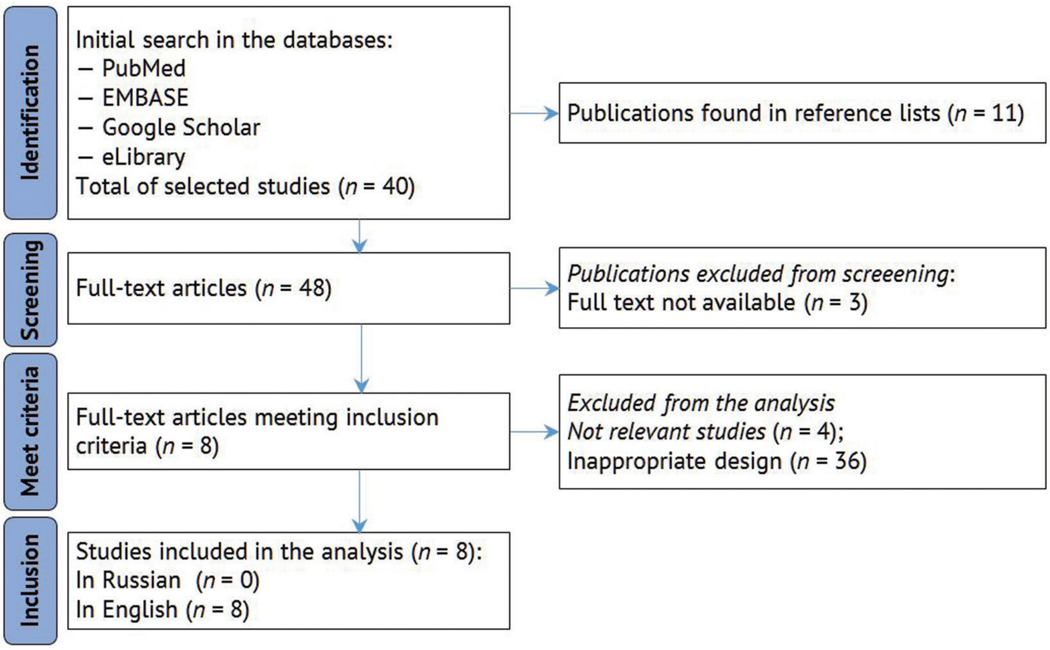

Fig. 1 Schematic algorithm for selecting thematic publications in accordance with the PRISMA protocol

To analyze the works, the main research questions were formulated:

1. Screw position accuracy, rate of malposition
2. Complications of malposition
3. Intervention and screw placement time
4. Blood loss
5. Rates of reoperation
6. Positioning of the reference frame
7. Radiation exposure

By agreement of the authors of this present study, two more articles were included: a review article by Ansorge et al. [9], which did not meet the criteria for a systematic review but contained a comparative analysis of radiation exposure in different types of interventions, and an original article by Kapoor et al. [10], which presented the rationale for a low-dose radiation study protocol. Thus, the study included 10 articles (Table 2).

The main design of the articles is a comparative analysis of different screw placement techniques according to the parameters selected by the authors. Odds ratios (OR) and 95 % confidence intervals (CI) were most frequently used. Pooled OR estimates for all studies were obtained using a fixed-effects model. Due to heterogeneity of the samples, the ORs were combined using a random-effects model [11, 12, 13]. It should be noted that for conducting a comparative analysis, the authors used heterogeneous combined statistical parameters, so it is impossible to interpret the results using a single numerical indicator.

Table 2

List of studies that meet inclusion criteria for the analysis

Authors, reference	Study design	Number of included studies	Search strategy	Patients characteristics	Study characteristics	Evaluation parameters	System for evaluation of screw position accuracy
Kapoor S. et al., 2021 [10]	Original study	–	–	Phantoms, 4 children	Development of a low-dose CT navigation protocol, calculations and models	Analysis of images taken at different radiation doses	–
Ansorge A. et al., 2023 [9]	Review	51	No data	–	Comparative analysis of surgical interventions with CT navigation and other visualization methods	Selected: radiation exposure	–
Tian W. et al., 2016 [11]	Systematic review	8	PRISMA	321 patients, 3821 screws, under CT navigation 1920 screws, without CT navigation 1901 screws, idiopathic scolyosis	Comparative analysis of surgical interventions with and without CT navigation	Screw placement accuracy, malposition rate, correction of deformities, duration of surgery, radiation exposure	Proposed option based on medial/lateral displacement 0–2 mm, 2–4 mm, more than 4 mm
Feng W. et al., 2020 [14]	Systematic review	8	PRISMA	850 patients, 10 cadavers, 5522 screws, thoracic and lumbar deformities of various etiologies	Comparative analysis of the effectiveness of O-Arm and C-Arm fluoroscopy	Screw placement accuracy, preparation time for screw placement, screw placement time, surgery duration	Scale rating from 0 to 3, Layne classification; scale system from 1 to 10
Chan A. et al., 2017 [13]	Systematic review	79	PROSPERO	4795 patients, 5923 screws; age 12.1–19.6 years; idiopathic scoliosis	Comparative analysis of surgical interventions with CT navigation, fluoroscopy and the free-hand (FH) method	Duration of surgery, volume of blood loss, frequency of malpositions, complications of malpositions, reoperations, postoperative complications	Various options, based on medial/lateral displacement 0–2 mm, 2–4 mm, more than 4 mm
Baldwin K.D. et al., 2022 [8]	Systematic review and meta-analysis	13	PRISMA	5578 patients, CT navigation — 485; idiopathic scoliosis (6), neurofibromatosis (1), spinal deformities (1), mixed groups (5)	Comparative analysis of surgical interventions with and without CT navigation	Duration of surgery, volume of blood loss, number of malpositions, complications of malpositions, reoperations, postoperative complications, radiation exposure	Gerzbein classification or its derivatives

Table 2 (continued)

List of studies that meet inclusion criteria for the analysis

Authors, reference	Study design	Number of included studies	Search strategy	Patients characteristics	Study characteristics	Evaluation parameters	System for evaluation of screw position accuracy
Oba H. et al., 2023 [15]	Systematic review	20	PRISMA	6209 patients; children; idiopathic scoliosis (381), neuromuscular scoliosis (44), neurofibromatosis (9), congenital scoliosis (8), systemic scoliosis (14), other diseases (7)	Comparative analysis of surgical interventions with and without CT navigation	Accuracy of placement, malposition, radiation dose, duration of surgery, volume of blood loss, reoperations, screw support, complications	Classifications of Rao (3), Neo (4), Gerzbein (4), Jeswani (1), Tanikawa (1). A unified classification was presented
Aoude A.A. et al., 2015 [16]	Systematic review	68	No data	3,442 patients, 60 cadavers; 43,305 screws	Comparative analysis of surgical interventions with CT navigation and the free-hand (FH) method	Accuracy of screw placement	Analysis of main classifications
Meng X.T. et al., 2017 [12]	Meta-nalysis	14	PRISMA	1723 patients, 9019 screws	Comparative analysis of surgical interventions with CT navigation and fluoroscopy	Accuracy of installation, malposition rate, duration of surgery, volume of intraoperative blood loss, time of transpedicular screw installation, complication rate	No data
Chan A. et al., 2020 [2]	Systematic review and meta-analysis	94	PRISMA	–	Comparative analysis of surgical interventions with and without CT navigation	Accuracy of installation, frequency of malpositions, duration of surgery, frequency of complications	Gerzbein classification

RESULTS

Accuracy of screw placement, rates of malposition

The key parameters for the comparative analysis in all the studies that were analyzed are screw placement accuracy and malposition rate. Depending on the selected statistical parameter, screw placement accuracy with CT navigation was higher in all studies and was assessed as *moderately higher, higher, or significantly higher*, ranging from 75.6 % to 97.3 % (Table 3). Screw placement accuracy without CT navigation was characterized as lower, *moderately lower, or significantly lower*, ranging from 58.5 % (FS) to 91.4 % (FH).

The analysis by Baldwin et al. showed that the probability of optimal screw placement in the pedicle is almost twice as high with the use of CT navigation, the probability of acceptable placement is three times higher, and the probability of potentially unsafe placement is one third of the probability if only manual techniques or fluoroscopy are used [8].

The malposition rate is also lower with the use of CT navigation and ranges from 7.2 % to 15.4 %. If screws are placed without CT navigation, malposition is detected more frequently: from 11.8–26.5–66.8 % (FH) to 50.7 % (FS) [2, 11, 12, 14, 15]. According to Baldwin et al., unsafe malposition with CT navigation is diagnosed in 1.9 % of cases, while with screw placement without CT navigation it rises up to 7 % of cases [8]. The analysis of spinal levels with the most frequent malposition is presented in the review by Oba et al. By using CT navigation, a greater number of reports show malposition in the upper thoracic and mid-thoracic spine, and with the freehand method in the mid-thoracic and lower thoracic regions. The use of CT navigation reduces the incidence of medial displacements to a greater extent than the incidence of lateral ones [15]. Ansorge et al. and Aoude et al. show that the problem in assessing the accuracy of screw positioning and determining malposition is the lack of a standard method of assessment and classification which would consider clinical manifestations and further tactics [9, 16].

Complications of malposition

The analysis of complications due to screw malposition was conducted in five studies. Baldwin et al. and Oba et al. note the absence of screw malposition complications if CT navigation is used [8, 15]. Chan et al. point to conflicting data regarding complications associated with screw placement due to heterogeneity of samples. In a 2017 study, the complication rate with CT navigation was 1.8 %, with fluoroscopy 25.8 %, with the freehand method 28.7 % [2]. In the subsequent 2020-study, complications with CT navigation were 0-1.6 % and 0-1.7 % without CT navigation [13]. In a study by Meng et al., the analysis using a fixed-effect model showed a significant difference between the groups with CT navigation and fluoroscopy: the complication rate with CT navigation was lower [12].

Duration of surgery and screw placement time

The main debatable issue in the comparative analysis of surgical interventions with CT navigation and without it, is the duration of the surgical procedure. Preparatory stages (installation of the reference frame, CT scanning of the vertebrae, instrument calibration) take a certain amount of time, the reduction of which depends on the surgeon's experience and the techniques used. However, it is important to remember that fluoroscopy in cases of spinal deformity also requires time.

The analysis of the duration of operations was conducted in seven studies. According to six reviews, the duration of surgery with CT navigation does not differ from other methods of intraoperative imaging: 446 min with navigation versus 412 min without navigation 8], 257 min and 227 min, respectively [13], 310 min and 136–380 min [2]. These data are confirmed by other studies [11, 12, 14]. Surgical interventions in 362 patients averaged 309 min using CT navigation, according to Oba et al. [15]. Some authors note that the time for preparing for screw installation is longer with navigation [12, 14].

Thus, most researchers indicate that there is no significant difference in the duration of surgery with and without CT navigation.

Blood loss

The authors of four reviews discuss the volume of blood loss if CT navigation is used; all studies show that the volume of blood loss in such interventions is no greater than with the use of fluoroscopy or the freehand method.

According to Baldwin et al., blood loss in the groups with and without CT navigation does not differ significantly (1131.0 ml versus 1077.0 ml) [8]. Meng et al., using a random effects model, prove that the volume of blood loss in surgeries with CT navigation is less than in surgeries with fluoroscopy [12]. In the review by Chan et al., some studies show that with CT navigation, the volume of blood loss is 1138 ml, with fluoroscopy 523-860 ml, with the freehand method 305–1813 ml [2]. According to Oba et al., the average blood loss in 347 patients during operations using CT navigation was 675 ml [15].

Rates of reoperation

Data on reoperations are reflected in four reviews, and all noted their absence by using CT navigation. Baldwin et al. describe six cases of reoperations in the group without CT navigation ($n = 465$), while no reoperations were recorded in the group with CT navigation [8]. Thus, it can be concluded that there are no cases of critical malposition with the use of intraoperative CT navigation, which indirectly confirms its high safety.

Positioning of reference frame

One of the factors that determines duration of the operation and radiation exposure is the preparatory stage: installation of a reference frame and CT scanning of the vertebrae in the fixation zone. The classic option is to place the frame for scanning and navigation of six vertebrae (three above and three below), followed by repositioning the frame and repeating scanning if more extensive implantation is necessary. This approach increases both the operating time and radiation exposure. Only Oba et al. discuss the issue of reference frame positioning options and the associated malposition rate. The data they present demonstrate the accuracy of screw placement for six to nine vertebrae from the reference frame, which eliminates the need for repeated frame positioning and CT scanning, significantly reducing the operating time and radiation exposure [15].

Radiation exposure

Another controversial issue with CT navigation is the radiation exposure to the patient and surgeon during surgery. Opponents of the method cite high radiation exposure, which poses a risk to the patient and surgical staff. Proponents believe that radiation exposure is reduced by using a special low-dose protocol, adhering to safety measures, and optimal surgical planning, including reducing scanning time by positioning the reference frame. The radiation exposure received during intraoperative CT navigation is fixed and depends on the number of scans and the imaging protocol used [15].

The authors of only two systematic reviews analyzed radiation exposure by using CT navigation and other methods. According to Baldwin et al., although radiation exposure in the navigation group was higher than in the non-navigation group, the difference was not statistically significant due to a high degree of variance. An additional sensitivity analysis revealed an insignificant difference in patient and surgeon radiation exposure between navigation and non-navigation techniques [8].

Oba et al. point out the heterogeneity of the results due to the lack of statistically significant values. However, the authors specify that the radiation dose during intraoperative fluoroscopy is 20 mSv/min which is twice as high as that during a CT study from T1 to L5 is approximately 10 mSv. This suggests that the total radiation dose during preoperative CT navigation and postoperative CT assessment of screw position is almost equal to the dose during intraoperative fluoroscopy for 1 min. Thus, the radiation dose during basic radiographic examinations within this procedure is reasonable [15].

Ansorge et al. analyzed the intraoperative radiation exposure in four publications. During screw placement with freehand technique and conventional fluoroscopy, the average fluoroscopy time was 24 to 35 seconds, which corresponds to an effective radiation dose of 0.17 to 0.34 mSv. In CT navigation, the effective radiation dose to the patient was 1.11 to 1.48 mSv. Using a low-dose protocol in two case-control series, the effective radiation dose was 0.65 mSv for each examination, which is equivalent to 85 sec of conventional fluoroscopy and allows visualization of 6–8 vertebrae [9].

In a consensus study by Kapoor et al., an analysis and justification of a low-dose protocol for the study are presented. The cadaveric portion of the study includes the development of an imaging protocol sufficient for reliable image evaluation, while the clinical portion (4 patients) involves testing it in humans during scoliosis surgeries. The low-dose protocol (reducing the X-ray tube current to 10 mA while maintaining the potential at 90 kV) allows for obtaining images of acceptable quality, while the radiation dose is only 14 % of the recommended radiation dose according to the protocol. The total radiation dose received according to this protocol is approximately 0.8 mSv per rotation. This effective dose is less than 1/3 of the average radiation level in the UK and less than 1/6 of the average radiation level in the USA per year. No neurological complications or complications associated with screw placement were observed in the patients [10]. The presented protocol is recommended for surgical treatment of patients with scoliosis. However, it is important to understand that the use of intraoperative navigation after X-ray scanning eliminates the need for the surgical team to remain in the operating room during the examination, and subsequent procedures are performed without radiation exposure, further reducing radiation exposure for the operating room staff.

Table 3 presents the main parameters of the comparative analysis of surgical interventions using CT navigation and other methods.

Table 3

Comparative analysis of surgical interventions for scoliosis using CT navigation and other methods

Criteria	Tian W et al., 2016 [11]	Baldwin KD et al., 2022 [8]	Chan A et al., 2020 [13]	Feng W et al., 2020 [14]	Oba H et al., 2023 [15]	Aoude AA et al., 2015 [16]	Meng XT et al, 2017 [12]	Chan A et al., 2017 [2]
	CTN / no CTN			**O-Arm / C-Arm**	**CTN / FH**		**CTN / FS**	**CTN / FS / FH**
Accuracy of screw placement	higher / lower	75.6 % / 58.5 %	moderately higher / moderately lower	higher / lower	–	97.3 % / 91.4 %	significantly higher / significantly lower	–
Malposition rate	3.7 % / 11.9 %	Unsafe malposition 1.9 % / 7 %	13 % / 20 %	lower / greater	7.2–11.5 % / 11.8–26.5 %	–	lower / greater	15.4 % / 50.7 % / 66.8 %
Complcation rate	–	0 / 12 persons	0–1.6 % / 0–1.7 %	–	0 / –	–	lower / greater	1.8 % / 25.8 % / 28.7 %
Time to prepare for screw placement	–	–	–	twice as longer / less	–	–	longer /shorter	–
Time of screw placement	–	–	–	no difference	–	–	–	–
Duration of surgery, min	no difference	446 / 412	257 / 227	no difference	309 / –	–	shorter/ lomger	310 / 274 / 136–380
Blood loss, ml	–	1131 / 1077	–	–	675 / –	–	lower / greater	1138 / 523–860 / 305–1813
Reoperations	0/1	0 / 6 persons	–		0 / –	–	–	0 / 0 / 4 %
Infectious complications	–	–	–		–	–	–	0 / 0 / 14.1 %
Screw break, pseudarthrosis	–	–	–		–	–	–	0 / 0 / 6.7 %
Deformity correction	no difference							
Radiation exposure	–	no difference	–	–	heterogeneous data	–	–	–

Notes: CTN — CT navigation; FS — fluoroscopy; FH — free hand

DISCUSSION

Spinal deformity surgery is one of the most complex areas of spinal surgery and is associated with a high complication rate. Screw placement in a deformed spine and altered vertebral bone structures requires careful monitoring of their position to prevent damage to neural structures, adjacent anatomical structures, and implant instability [17]. Vascular and neurological complications associated with screw malposition are a major concern in spinal deformity correction [18, 19].

The accuracy of screw placement is of paramount importance and is a vital component of a successful intervention. To improve screw positioning, instruments as well as new visualization and navigation methods have been developed and perfected [16, 17, 19]. The free-hand method is predominant for screw placement, despite the fact that the intraoperative use of three-dimensional images improves the accuracy of their placement [1, 2, 4, 5, 7, 13, 19]. The main discussed issues of intraoperative CT navigation are the accuracy of screw placement, the rate and complications of malposition, the duration of surgery, the volume of blood loss and, most importantly, the radiation exposure to the patient and staff [6, 20, 21]. The conducted analysis of the literature data shows the advantages of using CT navigation in surgical interventions in patients with scoliosis in terms of the accuracy of screw placement, a lower rate of malposition and associated complications and, accordingly, the rate of re-operations.

Duration of surgery is also comparable between CT-navigated surgery and other methods of intraoperative screw visualization. As surgeons become more proficient with navigation systems, the registration process becomes more accurate, screw placement time reduces, and data comparison between devices improves, leading to shorter duration of placement procedure [12, 22, 23].

The systematic reviews discussed above do not show increased blood loss or longer surgical times during CT navigation, although preparation for screw placement requires additional time.

Since screw placement is only a step in surgical intervention for spinal deformities, the use of CT navigation and other methods does not determine the degree of correction [1, 11, 17, 20].

Minimizing radiation exposure for patients with scoliosis is of paramount importance. Perioperative radiation exposure can be influenced by the type and settings of the imaging modality used (conventional fluoroscopy, 3D fluoroscopy, CT navigation, CT control) [20, 21]. To reduce radiation exposure, it is recommended to set a scanning mode with a reduced radiation dose, as well as to use special techniques during surgery [10]. Single positioning of the reference frame significantly reduces the duration of the operation, does not affect the accuracy of screw placement, and does not require additional CT scanning, thereby reducing the radiation dose [24, 25, 26].

The absence of a unified system for assessing and classifying screw displacements determines the need to develop it based on clinical manifestations and treatment tactics [16, 25, 26].

CONCLUSION

The present analysis demonstrates that intraoperative CT navigation during screw placement improves the accuracy of screw placement, does not prolong the duration of the surgery, and does not decrease the effectiveness of deformity correction. The improved surgical safety achieved with the navigation system is due not only to a greater accuracy of screw placement but also to the reduced incidence of complications.

Conflict of interests *None*

Source of funding *None*

REFERENCES

1. Cammarata G, Scalia G, Costanzo R, et al. Fluoroscopy-Assisted Freehand Versus 3D-Navigated Imaging-Assisted Pedicle Screw Insertion: A Multicenter Study. *Acta Neurochir Suppl*. 2023;135:425-430. doi: 10.1007/978-3-031-36084-8_65.
2. Chan A, Parent E, Narvacan K, et al. Intraoperative image guidance compared with free-hand methods in adolescent idiopathic scoliosis posterior spinal surgery: a systematic review on screw-related complications and breach rates. *Spine J*. 2017;17(9):1215-1229. doi: 10.1016/j.spinee.2017.04.001.
3. Rivkin MA, Yocom SS. Thoracolumbar instrumentation with CT-guided navigation (O-arm) in 270 consecutive patients: accuracy rates and lessons learned. *Neurosurg Focus*. 2014;36(3):E7. doi: 10.3171/2014.1.FOCUS13499.
4. Zhao Z, Liu Z, Hu Z, et al. Improved accuracy of screw implantation could decrease the incidence of post-operative hydrothorax? O-arm navigation vs. free-hand in thoracic spinal deformity correction surgery. *Int Orthop*. 2018;42(9):2141-2146. doi: 10.1007/s00264-018-3889-8.
5. Zhang W, Takigawa T, Wu Y, et al. Accuracy of pedicle screw insertion in posterior scoliosis surgery: a comparison between intraoperative navigation and preoperative navigation techniques. *Eur Spine J*. 2017;26(6):1756-1764. doi: 10.1007/s00586-016-4930-5.
6. Berlin C, Quante M, Thomsen B, et al. Intraoperative Radiation Exposure for Patients with Double-Curve Idiopathic Scoliosis in Freehand-Technique in Comparison to Fluoroscopic- and CT-Based Navigation. *Z Orthop Unfall*. 2021;159(4):412-420. doi: 10.1055/a-1121-8033.
7. Singh A, Kotzur T, Peterson B, et al. Computer Assisted Navigation Does Not Improve Outcomes in Posterior Fusion for Adolescent Idiopathic Scoliosis. *Global Spine J*. 2024:21925682241274373. doi: 10.1177/21925682241274373.
8. Baldwin KD, Kadiyala M, Talwar D, et al. Does intraoperative CT navigation increase the accuracy of pedicle screw placement in pediatric spinal deformity surgery? A systematic review and meta-analysis. *Spine Deform*. 2022;10(1):19-29. doi: 10.1007/s43390-021-00385-5.
9. Ansorge A, Sarwahi V, Bazin L, et al. Accuracy and Safety of Pedicle Screw Placement for Treating Adolescent Idiopathic Scoliosis: A Narrative Review Comparing Available Techniques. *Diagnostics (Basel)*. 2023;13(14):2402. doi: 10.3390/diagnostics13142402.
10. Kapoor S, O'Dowd K, Hilis A, Quraishi N. The Nottingham radiation protocol for O-arm navigation in paediatric deformity patients: a feasibility study. *Eur Spine J*. 2021;30(7):1920-1927. doi: 10.1007/s00586-021-06762-y.
11. Tian W, Zeng C, An Y, et al. Accuracy and postoperative assessment of pedicle screw placement during scoliosis surgery with computer-assisted navigation: a meta-analysis. *Int J Med Robot*. 2017;13(1). doi: 10.1002/rcs.1732.
12. Meng XT, Guan XF, Zhang HL, He SS. Computer navigation versus fluoroscopy-guided navigation for thoracic pedicle screw placement: a meta-analysis. *Neurosurg Rev*. 2016;39(3):385-391. doi: 10.1007/s10143-015-0679-2.
13. Chan A, Parent E, Wong J, et al. Does image guidance decrease pedicle screw-related complications in surgical treatment of adolescent idiopathic scoliosis: a systematic review update and meta-analysis. *Eur Spine J*. 2020;29(4):694-716. doi: 10.1007/s00586-019-06219-3.
14. Feng W, Wang W, Chen S, et al. O-arm navigation versus C-arm guidance for pedicle screw placement in spine surgery: a systematic review and meta-analysis. *Int Orthop*. 2020;44(5):919-926. doi: 10.1007/s00264-019-04470-3.
15. Oba H, Uehara M, Ikegami S, et al. Tips and pitfalls to improve accuracy and reduce radiation exposure in intraoperative CT navigation for pediatric scoliosis: a systematic review. *Spine J*. 2023;23(2):183-196. doi: 10.1016/j.spinee.2022.09.004.
16. Aoude AA, Fortin M, Figueiredo R, et al. Methods to determine pedicle screw placement accuracy in spine surgery: a systematic review. *Eur Spine J*. 2015;24(5):990-1004. doi: 10.1007/s00586-015-3853-x.
17. Kwan MK, Loh KW, Chung WH, et al. Perioperative outcome and complications following single-staged Posterior Spinal Fusion (PSF) using pedicle screw instrumentation in Adolescent Idiopathic Scoliosis (AIS): a review of 1057 cases from a single centre. *BMC Musculoskelet Disord*. 2021;22(1):413. doi: 10.1186/s12891-021-04225-5.
18. Zhang W, Takigawa T, Wu Y, et al. Accuracy of pedicle screw insertion in posterior scoliosis surgery: a comparison between intraoperative navigation and preoperative navigation techniques. *Eur Spine J*. 2017;26(6):1756-1764. doi: 10.1007/s00586-016-4930-5.
19. Kothari AR, Katkade SM, Bhilare PD, et al. "Critical pedicle wall" breaches analysis in complex spinal deformity using O-arm navigation. *Surg Neurol Int*. 2023;14:306. doi: 10.25259/SNI_437_2023.
20. Urbanski W, Jurasz W, Wolanczyk M, et al. Increased Radiation but No Benefits in Pedicle Screw Accuracy With Navigation versus a Freehand Technique in Scoliosis Surgery. *Clin Orthop Relat Res*. 2018;476(5):1020-1027. doi: 10.1007/s11999.0000000000000204.
21. Obid P, Zahnreich S, Frodl A, et al. Freehand Technique for Pedicle Screw Placement during Surgery for Adolescent Idiopathic Scoliosis Is Associated with Less Ionizing Radiation Compared to Intraoperative Navigation. *J Pers Med*. 2024;14(2):142. doi: 10.3390/jpm14020142.
22. Shin MH, Hur JW, Ryu KS, Park CK. Prospective Comparison Study Between the Fluoroscopy-guided and Navigation Coupled With O-arm-guided Pedicle Screw Placement in the Thoracic and Lumbosacral Spines. *J Spinal Disord Tech*. 2015;28(6):E347-E351. doi: 10.1097/BSD.0b013e31829047a7.
23. Jin M, Liu Z, Qiu Y, et al. Incidence and risk factors for the misplacement of pedicle screws in scoliosis surgery assisted by O-arm navigation-analysis of a large series of one thousand, one hundred and forty five screws. *Int Orthop*. 2017;41(4):773-780. doi: 10.1007/s00264-016-3353-6.

24. Uehara M, Takahashi J, Ikegami S, et al. Are pedicle screw perforation rates influenced by distance from the reference frame in multilevel registration using a computed tomography-based navigation system in the setting of scoliosis? *Spine J*. 2017;17(4):499-504. doi: 10.1016/j.spinee.2016.10.019.
25. Oba H, Ikegami S, Uehara M, et al. Reduction in CT scan number with the reference frame middle attachment method in intraoperative CT navigation for adolescent idiopathic scoliosis. *Eur Spine J*. 2023;32(9):3133-3139. doi: 10.1007/s00586-023-07842-x.
26. Shimizu M, Takahashi J, Ikegami S, et al. Are pedicle screw perforation rates influenced by registered or unregistered vertebrae in multilevel registration using a CT-based navigation system in the setting of scoliosis? *Eur Spine J*. 2014;23(10):2211-2217. doi: 10.1007/s00586-014-3512-7.

The article was submitted 10.04.2025; approved after reviewing 14.04.2025; accepted for publication 14.10.2025.

Information about the authors:

Oksana G. Prudnikova — Doctor of Medical Sciences, Senior Researcher, Head of Department, pog6070@gmail.com, https://orcid.org/0000-0003-1432-1377, Author ID: 416145, Scopus AuthorID: 57094937500;

Evgeny A. Matveev — neurosurgeon, matveevea@mail.ru, https://orcid.org/0009-0003-6055-4013;

Margarita S. Strebkova — postgraduate student, Strebkovams@mail.ru, https://orcid.org/0009-0007-2618-6164;

Alexey V. Evsyukov — Candidate of Medical Sciences, Head of the Clinic, alexevsukov@mail.ru, https://orcid.org/0000-0001-8583-0270, Author ID: 615954, Scopus AuthorID: 57196004386.

Главный редактор А.В. Бурцев

Компьютерная верстка М.А. Беляева

Журнал зарегистрирован Федеральной службой по надзору в сфере связи,
информационных технологий и массовых коммуникаций
ПИ № ФС77-68207 от 30 декабря 2016 года

Территория распространения: Российская Федерация, зарубежные страны

Подписано в печать 10.12.2025. Дата выхода 24.12.2025
Формат 60 × 84 1/8. Усл. печ. л. 18.6
Тираж 75 экз. Заказ № 18168. Свободная цена

Адрес издателя, редакции журнала «Гений ортопедии»
640014, Россия, г. Курган, ул. М. Ульяновой, 6
http://ilizarov-journal.com

Отпечатано в Типографии «Эталон». 198097, г. Санкт-Петербург, ул. Трефолева, 2 литера БН, помещение 3-Н, офис 1